

University of Alberta

**Polymer by Anionic Polymerization of ϵ -Caprolactam with the Presence of
Bisphenol-A Polycarbonate: Characterization and Properties**

by

Jiang Bai



A thesis submitted to the Faculty of Graduate Studies and Research in partial fulfillment
of the requirements for the degree of

Doctor of Philosophy

in

Chemical Engineering

Department of Chemical and Materials Engineering

Edmonton, Alberta

Fall 2002



National Library
of Canada

Acquisitions and
Bibliographic Services

395 Wellington Street
Ottawa ON K1A 0N4
Canada

Bibliothèque nationale
du Canada

Acquisitions et
services bibliographiques

395, rue Wellington
Ottawa ON K1A 0N4
Canada

Your file Votre référence

Our file Notre référence

The author has granted a non-exclusive licence allowing the National Library of Canada to reproduce, loan, distribute or sell copies of this thesis in microform, paper or electronic formats.

The author retains ownership of the copyright in this thesis. Neither the thesis nor substantial extracts from it may be printed or otherwise reproduced without the author's permission.

L'auteur a accordé une licence non exclusive permettant à la Bibliothèque nationale du Canada de reproduire, prêter, distribuer ou vendre des copies de cette thèse sous la forme de microfiche/film, de reproduction sur papier ou sur format électronique.

L'auteur conserve la propriété du droit d'auteur qui protège cette thèse. Ni la thèse ni des extraits substantiels de celle-ci ne doivent être imprimés ou autrement reproduits sans son autorisation.

0-612-81160-3

Canada

University of Alberta

Library Release Form

Name of Author: Jiang Bai

Title of Thesis: Polymer by Anionic Polymerization of ϵ -Caprolactam with the Presence
of Bisphenol-A Polycarbonate: Characterization and Properties

Degree: Doctor of Philosophy

Year this Degree Granted: 2002

Permission is hereby granted to the University of Alberta Library to reproduce single copies of this thesis and to lend or sell such copies for private, scholarly or scientific research purposes only.

The author reserves all other publication and other rights in association with the copyright in the thesis, and except as herein before provided, neither the thesis nor any substantial portion thereof may be printed or otherwise reproduced in any material form whatever without the author's prior written permission.



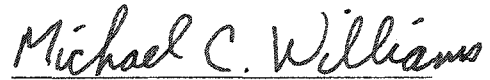
1111 Twin Brooks Point,
Edmonton, Alberta
Canada T6J 7G5

Date: August 27, 2002

University of Alberta

Faculty of Graduate Studies and Research

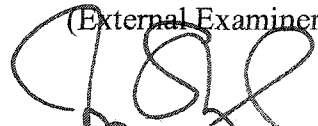
The undersigned certify that they have read, and recommend to the Faculty of Graduate Studies and Research for acceptance, a thesis entitled **Polymer by Anionic Polymerization of ϵ -Caprolactam with the Presence of Bisphenol-A Polycarbonate: Characterization and Properties** submitted by **Jiang Bai** in partial fulfillment of the requirements for the degree of **Doctor of Philosophy in Chemical Engineering**.



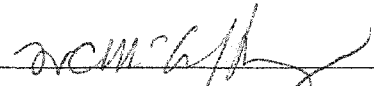
Professor Michael C. Williams
(Thesis Supervisor)



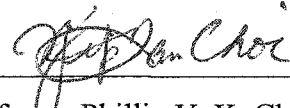
Professor Donald R. Paul
(External Examiner)



Professor Jeffrey M. Stryker
(Member of Supervisory Committee)



Professor William C. McCaffrey
(Member of Supervisory Committee)



Professor Phillip Y. K. Choi
(Examiner)

Professor Janet A.W. Elliott
(Chair)

August 26, 2002

Abstract

This thesis deals with the anionic polymerization of ϵ -caprolactam in the presence of polycarbonate by using a Grignard reagent as initiator. Previously a “liquid-solid” method was used and the so-formed polymer was found to have strong tensile properties and good adhesion to glass fiber. In this research a change has been made to a “liquid-liquid” system; comparison between the two methods on the basis of tensile properties showed that the “liquid-liquid” method was preferred.

To investigate the possible reaction route, model reactions were conducted and evidence has shown that the activating specie came from the interaction between polycarbonate and caprolactamate anion. GPC, FTIR and NMR spectroscopic results were used to support the proposed reaction route. The final material was also characterized by SEM to show its single-phase morphology; solubility properties were investigated in various solvents and thermal stability examined by TGA results. Diphenyl carbonate (DPC) was used to synthesize pure nylon 6 to be used as a comparison polymer. The polymer made from polycarbonate has better thermal stability than pure nylon 6 in both dry and wet conditions.

The effect of environmental (i.e. oil bath) temperature during polymerization (T_{oil}) was studied in the range of 95°C-160°C. The original reactive mixture contained 75g ϵ -caprolactam /0.75g polycarbonate (SPP)/10mmol iso-Bu-MgCl. Various properties of the nascent polymers were measured and compared. Monomer conversion changed little (over 95%) with different T_{oil} 's while intrinsic viscosity data in 90% formic acid was higher for polymers made at higher T_{oil} 's. In the polymers made at T_{oil} 's above 147°C there was gel formation. Melt viscosity data showed the same trend as intrinsic viscosity

with the polymer made at 160°C showing the highest value. There was a decrease in degree of crystallinity for polymers when T_{oil} increased. Both DSC and X-ray showed the same trend. The α crystal structure was the major form in this series of polymers while the one made at 160°C contained more γ structure than the others. It has been found that at lower T_{oil} 's, there were more voids formed in the nascent materials. This led to the poorer tensile properties and higher moisture absorption for polymers made at lower T_{oil} 's (under both “dry” and “wet” test conditions).

The influence of the type and amount of polycarbonate and Grignard reagent was also studied. An optimal ratio between polycarbonate and Grignard reagent has been found in order to have higher monomer conversion and rate of polymerization, i.e. *8 mmol initiator/g polycarbonate*. Results have shown that more polycarbonate in the reaction system led to faster rate of polymerization and lower intrinsic viscosity. Melt complex viscosity was used to show the reinforcement of final polymer by the existence of polycarbonate blocks. There was a decreasing trend in melting temperature and degree of crystallinity as the concentration of polycarbonate increased while the ones using DPC showed the reverse trend due to the existence of γ form in the nascent polymers. The difference between iso-Bu-MgBr and iso-Bu-MgCl and the difference between two polycarbonates with different MW on various final properties were also evaluated.

Acknowledgements

First and foremost, I would like to express my sincere thanks to my supervisor, Prof. Michael C. Williams who brought this project to me in my first year at University of Alberta and since then has always been there to show support both academically and in life. Without his patience, encouragement and guidance, I would not be able to complete this thesis. I feel fortunate to be one of his students and maybe the last one. His tremendous knowledge in the area of polymer science, hard-working ethics and positive attitude will never be forgotten.

I would like to thank my present and previous colleagues in the Polymer and Rheology group for all kinds of help during the past years. I owe special thanks to Dr. Nai-Hong Li for so many intellectually stimulating discussions and valuable suggestions throughout the whole project. Thanks to Dr. Wei-Yan Wang for demonstration on how to use DSC and RMS 800, and to Dr. Ibnelwaleed Hussein for discussion on the use of densitometer.

Financial support from Natural Sciences and Engineering Research Council of Canada is greatly appreciated.

Thanks are also due to Ms. Naiyu Bu for helping me on GPC analysis, Dr. Ah-Dong Leu for helping on TGA and X-Ray measurements, Mingqian Zhang for discussion of X-ray data treatment, and Ms. Tina Barker for help with the SEM analysis.

I wish to acknowledge and appreciate the help provided by Walter Boddez and Richard Cooper for all the instrumentation assistance, and Bob Scott and other machinists from the Machine Shop for cutting tensile specimens for me. Special thanks to Bob Konzuk for much help on tensile tests and the operation of the Instron machine.

I acknowledge with gratitude my thesis committee members: Prof. J. M. Stryker, Prof. P. Choi, Prof. W. C. McCaffrey for their criticism, advice and time spent on reviewing this thesis. I feel grateful to have Prof. Donald Paul to be the external committee member whose profound knowledge and valuable advice would greatly benefit this project. I also owe thanks to Prof. Z. Xu and Prof. U. Sundararaj for their advice in my candidacy report, Prof. J. Elliot for being Chairman in both my candidacy exam and my thesis defense exam.

Special thanks to DSM Chemicals North America, Inc. for generously providing anhydrous ϵ -caprolactam , and Prof. U. Sundararaj and GE Plastics for the help with supplying polycarbonate resins.

I would like to extend my appreciation to Dr. Y. Maham for help with the solution viscosity measurements and DSC analysis, and most importantly for encouraging me to enjoy life even under stress. Thanks are also due to all my friends whose support has carried me through my time here and made it enjoyable.

I am indebted to my parents, brother and my husband for their encouragement, patience and sacrifice. Without them, I could not have come this far.

Table of Contents

Chapter 1 Introduction

| | |
|--------------------------|---|
| 1.1 The Background | 1 |
| 1.2 The Objectives | 4 |

Chapter 2 Literature Review

| | |
|--|----|
| 2.1 History of Nylon 6 and Polycarbonate..... | 6 |
| 2.1.1 Nylon 6..... | 6 |
| 2.1.2 Polycarbonate..... | 8 |
| 2.2 Polymerization of Nylon 6 Homopolymer..... | 9 |
| 2.2.1 Hydrolytic Polymerization..... | 10 |
| 2.2.2 Anionic Method..... | 12 |
| 2.2.2.1 Reaction Mechanism | 12 |
| 2.2.2.2 Advantages of Anionic Method | 16 |
| 2.2.2.3 Industrial Applications of Anionic Method | 18 |
| 2.3 Anionic Copolymerization of ϵ -Caprolactam | 19 |
| 2.3.1 Introduction to Copolymer | 19 |
| 2.3.2 Synthesis of Copolymer of Nylon 6..... | 21 |
| 2.4 Nylon 6 Blends..... | 23 |
| 2.4.1 Introduction to Polymer Blends..... | 23 |
| 2.4.2 Miscibility | 24 |
| 2.4.3 Compatibilization of Polymer Blends | 25 |
| 2.4.4 Processing of Nylon 6 Blends and Their Compatibilization | 26 |

| | |
|--|----|
| 2.4.5 Blends of Nylon 6 and Polycarbonate | 27 |
| 2.4.5.1 Experimental Observations | 28 |
| 2.4.5.2 Compatibilization of Nylon 6/Polycarbonate Blends..... | 30 |

Chapter 3 Experimental

| | |
|---|----|
| 3.1 Instruments and Procedures | 33 |
| 3.2 Materials..... | 38 |
| 3.2.1 Chemical Reagents | 38 |
| 3.2.2 Polymers | 40 |
| 3.3 Synthesis of Nylon 6 Homopolymer..... | 45 |
| 3.3.1 Synthesis of Nylon 6 by Using N-Acetylcaprolactam as Activator..... | 45 |
| 3.3.2 Synthesis of Nylon 6 by Using Diphenyl Carbonate as Activator | 45 |
| 3.4 Synthesis of Nylon 6–Polycarbonate Copolymer | 46 |

Chapter 4 Synthesis and Characterization

| | |
|--|----|
| 4.1 Comparison between “Liquid-Liquid” and “Liquid-Solid” Methods..... | 47 |
| 4.1.1 Reaction System of Liquid-Solid Method (L-S)..... | 47 |
| 4.1.2 Reaction System of Liquid-Liquid Method (L-L) | 48 |
| 4.1.3 Effect of Polycarbonate Particle Size | 48 |
| 4.2 Possible Reaction Mechanism..... | 54 |
| 4.2.1 The Role of Polycarbonate | 54 |
| 4.2.2 The Role of Grignard Reagent..... | 55 |
| 4.2.3 Model Reaction-1..... | 58 |
| 4.2.4 Model Reaction–2 | 60 |
| 4.2.5 Possible Reaction Route | 65 |
| 4.3 Characterization of the Copolymer Mixture | 67 |

| | |
|---|----|
| 4.3.1 Solubility..... | 67 |
| 4.3.2 Thermal Gravimetric Analysis..... | 69 |
| 4.3.3 Morphology Studies..... | 71 |
| 4.3.3.1 Morphology of Nylon 6/Polystyrene in-situ Reactive Blend..... | 71 |
| 4.3.3.2 Morphology of Nylon 6/Polycarbonate Melt Blend..... | 74 |
| 4.3.3.3 Morphology of Copolymer..... | 77 |
| 4.3.4 ^{13}C and ^1H NMR..... | 79 |

Chapter 5 The Effect of Reaction Temperature

| | |
|--|-----|
| 5.1 Why is the Temperature Important?..... | 82 |
| 5.1.1 Monomer Conversion and Molecular Weight..... | 82 |
| 5.1.2 The Process of Crystallization..... | 83 |
| 5.2 Temperature Profile..... | 85 |
| 5.3 Polymer Homogeneity Analysis..... | 88 |
| 5.3.1 Tensile Properties for "Scale-Up" Sample..... | 88 |
| 5.3.2 Intrinsic Viscosity Difference..... | 91 |
| 5.4 Results..... | 94 |
| 5.4.1 Monomer Conversion..... | 95 |
| 5.4.1.1 Water-Extraction Method..... | 95 |
| 5.4.1.2 GC-MS Method..... | 97 |
| 5.4.2 Intrinsic Viscosity..... | 100 |
| 5.4.3 Rheological Measurements..... | 105 |
| 5.4.3.1 Parameter Setup..... | 105 |
| 5.4.3.2 Rheological Properties for Samples Made at Different Temperatures..... | 110 |

| | |
|---------------------------------------|-----|
| 5.4.4 Degree of Crystallinity | 115 |
| 5.4.4.1 DSC Method | 115 |
| 5.4.4.2 X-Ray Diffraction Method..... | 118 |
| 5.4.5 Tensile Properties | 122 |
| 5.4.6 Moisture Absorption | 127 |
| 5.4.7 Bulk Density Measurement | 129 |

Chapter 6 The Effect of Initiator and Activator

| | |
|--|-----|
| 6.1 Why is It Important to Study the Effects of Initiator and Activator? | 134 |
| 6.2 The Effect of Initiator..... | 135 |
| 6.2.1 The Use of Grignard Reagents | 135 |
| 6.2.2 The Amount of Initiator | 137 |
| 6.2.2.1 Rate of Polymerization | 137 |
| 6.2.2.2 Monomer Conversion..... | 140 |
| 6.2.2.3 Intrinsic Viscosity [η]..... | 142 |
| 6.2.3 Comparison between <i>iso-Bu-MgBr</i> and <i>iso-Bu-MgCl</i> | 147 |
| 6.3 The Effect of Activator | 149 |
| 6.3.1 Rate of Polymerization | 151 |
| 6.3.2 Monomer Conversion | 153 |
| 6.3.3 Intrinsic Viscosity | 155 |
| 6.3.4 Complex Melt Viscosity | 158 |
| 6.3.5 Melting Temperature and Degree of Crystallization..... | 165 |
| 6.3.5.1 DSC Results..... | 165 |
| 6.3.5.2 X-ray Results | 170 |

Chapter 7 Conclusions and Future Work

| | |
|----------------------|-----|
| 7.1 Conclusions..... | 174 |
| 7.2 Future work..... | 182 |

| | |
|------------------------|------------|
| References..... | 184 |
|------------------------|------------|

Appendices

| | |
|---|-----|
| Appendix A Supplement to Chapter 4..... | 194 |
| Appendix B Supplement to Chapter 5..... | 220 |
| Appendix C Supplement to Chapter 6..... | 252 |
| Appendix D Supplement to Chapter 7..... | 270 |

List of Tables

| | |
|--|-----|
| Table 2.1: Nylons: Pattern of Consumption (in US and Canada)..... | 7 |
| Table 3.1: GPC Result Summary for 3 Polycarbonate Samples..... | 40 |
| Table 4.1: DSC Results for "Liquid-Solid" Samples (First Heating, 10 °C/min) | 53 |
| Table 4.2: GPC Result Summary (HDPE for calibration)..... | 59 |
| Table 4.3: Solubility of ϵ -Caprolactam, Nylon 6, Polycarbonate and Copolymerin in Some Solvents | 68 |
| Table 5.1: Intrinsic Viscosity Data at 3 Various Locations of Two Samples | 92 |
| Table 5.2: Water Soluble Content Data for Samples Made at Different Environmental Temperatures (75 g ϵ -caprolactam, 0.75g polycarbonate and 10mmol isobutyl magnesium chloride)..... | 96 |
| Table 5.3: Calibration Constant K for GC-MS Method | 99 |
| Table 5.4: Comparison of the Results on Monomer Conversion from Two Methods (Weight-loss Method and GC-MS Method)..... | 100 |
| Table 5.5: X-Ray Results for Polymers Made at Different Oil Bath Temperatures..... | 121 |
| Table 5.6: Moisture Absorption Data form Samples Made at Different Oil Bath Temperatures (from dry to 50%R.H., room temperature) | 128 |
| Table 5.7: Bulk Density, Estimated Density and Void Content for Samples Made at Different Oil Bath Temperatures..... | 133 |
| Table 6.1: Amount of Initiators Used for Various Concentrations of Activators..... | 150 |
| Table 6.2: X-Ray Results for Polymers Made from DPC and PCs at Various Concentrations with Different Initiators..... | 171 |
| Table A-1a: Tensile Test Results for Copolymer with 1% PC by "L-L" Method..... | 195 |
| Table A-1b: Tensile Test Results for Copolymer with 1% PC (<80 μ m) by "L-S" Method..... | 196 |

| | |
|---|-----|
| Table A-1c: Tensile Test Results for Copolymer with 1% PC (80-200 μm) by "L-S" Method | 197 |
| Table A-1d: Tensile Test Results for Copolymer with 1% PC (200-400 μm) by "L-S" Method | 198 |

List of Figures

| | |
|---|----|
| Figure 2.1: Equilibrium Monomer Concentration in Caprolactam-Nylon 6s at Different Temperatures | 17 |
| Figure 3.1: Dimension of Tensile Specimens (in mm) | 36 |
| Figure 3.2: GPC Analysis for 3 Polycarbonate Samples | 41 |
| Figure 3.3: DSC Thermograms of Polycarbonate Pellet and Powder (First heating at 10°C/min, Nitrogen)..... | 43 |
| Figure 3.4: X-Ray Diffraction Patterns for SPP Polycarbonate Powder & Pellet | 44 |
| Figure 4.1: Tensile Properties of Samples Made by “L-L” Method and “L-S” Method with Different Particle Size of Polycarbonate Powder. (a). Young’s modulus; (b). Tensile strength at break; (c). Tensile strain at break; (d). Toughness..... | 50 |
| Figure 4.2: GPC Results of Original PC and IBMB Treated PC..... | 59 |
| Figure 4.3: FTIR Spectra of Three Polymer Samples..... | 64 |
| Figure 4.4: TGA Results for Polymers: Nylon 6 Made from Diphenyl Carbonate (1% wt) and Nylon 6 Copolymer Made from Polycarbonate (1%wt). (a) Dry samples. (b). Conditioned samples..... | 70 |
| Figure 4.5: SEM Analysis of Nylon 6/PS (2%wt) in-situ Reactive Blend. (a) & (b). Major morphology at low and high magnification respectively; (c). Second morphology | 73 |
| Figure 4.6: SEM Pictures of Nylon 6 /Polycarbonate Melt Blends (with 2% wt of Polycarbonate) after Mixing for (a). 5 minutes; (b). 10 minutes and (c). 15 minutes..... | 75 |
| Figure 4.7: SEM Pictures of Nylon 6 /Polycarbonate Melt Blends (with 10% wt of Polycarbonate) after Mixing for (a). 5 minutes; (b). 10 minutes and (c). 15 minutes..... | 76 |
| Figure 4.8: SEM Picture of Nylon 6/PC Copolymer (with 2% wt PC) | 78 |
| Figure 4.9: ¹³ C NMR for a Trifluoroacetylated Copolymer (containing 2% Polycarbonate) | 81 |

| | |
|--|-----|
| Figure 5.1: Spherulitic Crystallization Rates vs. Isothermal Temperature for Nylon 6 ($\overline{M}_n=24,700$, stayed at 270 °C for 0.5 hr prior to crystallization, Magill, 1965)..... | 84 |
| Figure 5.2: Temperature Profiles of the Center Point in the Reactive Mixture under Different Oil Bath Temperatures (75g ϵ -capro-lactam/0.75g polycarbonate/12 mmol isobutyl magnesium bromide)..... | 87 |
| Figure 5.3: Tensile Properties of Specimens Taken from Various Locations of a “Scale-Up” Cylindrical Sample (250g ϵ -capro-lactam/2.5g polycarbonate/40 mmol iso-butyl magnesium bromide, 120°C)..... | 90 |
| Figure 5.4: Water Soluble Content for Samples Made at Different Oil Bath Temperatures | 96 |
| Figure 5.5: An Example of GC-MS Result..... | 98 |
| Figure 5.6: η_{sp}/C vs. C Plots for Samples Made at Different Oil Bath Temperatures..... | 104 |
| Figure 5.7: Time Sweep Test for Nylon 6 Made from 0.5%DPC ($T_{\text{measurement}}=250$ °C, Frequency =0.1 rad/s, Strain $\gamma^0=0.5\%$) | 106 |
| Figure 5.8: Strain Sweep Test for Nylon 6 Made from 0.5% DPC ($T_{\text{measurement}}=250$ °C, Frequency =0.1 rad/s) | 108 |
| Figure 5.9: Dynamic Frequency Sweep Tests in Both Ascending & Descending Order of Frequency for Nylon 6 Made from 0.5% DPC ($T_{\text{measurement}}=250$ °C, Disk and Plate, $\gamma^0=1\%$) | 109 |
| Figure 5.10(a): Complex Viscosity Data in Dynamic Frequency Sweep Tests for Samples Made at Different Oil Bath Temperatures ($T_{\text{measurement}}=250$ °C, Disk and Plate, $\gamma^0=1\%$) | 111 |
| Figure 5.10(b): Complex Modulus Data in Dynamic Frequency Sweep Tests for Samples Made at Different Oil Bath Temperatures. ($T_{\text{measurement}}=250$ °C, Disk and Plate, $\gamma^0=1\%$) | 112 |
| Figure 5.11: Dynamic Frequency Sweep Tests in Both Ascending and Descending Order of Frequency for Copolymer Made at Oil Bath Temperature of 160 °C. ($T_{\text{measurement}}=250$ °C, Disk and Plate, $\gamma^0=1\%$) | 114 |
| Figure 5.12: Melting Temperatures (\square) and Degree of Crystallinity (Δ) for Samples Made at Different Oil Bath Temperatures. (Data taken from the first heating scan in DSC) | 116 |

| | |
|--|-----|
| Figure 5.13(a): Schematic X-ray diffraction pattern with amorphous halo in shaded area..... | 119 |
| Figure 5.13(b): Schematic X-ray diffraction pattern with fitted curves | 119 |
| Figure 5.14: Comparison of x_C Data from X-ray and DSC Methods | 121 |
| Figure 5.15: Results from Tensile Tests under “Dry” and “Wet” Conditions for Samples Made at Different Oil Bath Temperatures. (a). Young’s modulus. (b). Tensile stress at break. (c). Tensile strain at break. (d). Toughness | 123 |
| Figure 5.16: Tensile Test Results for Dry Samples Made at Different Oil Bath Temperatures (Composition: 75g ϵ -caprolactam, 0.75 poly-carbonate, 12 mmol isobutyl magnesium bromide) | 126 |
| Figure 5.17: Bulk Densities of Samples Made at Different Oil Bath Temperatures (Measured at room temperature)..... | 130 |
| Figure 6.1: The Effect of Amount of Initiators on Rate of Polymerization. [Composition: 100 g ϵ -caprolactam/1%(w/w) or 2% (w/w) GE-S11AP/various amounts of iso-BuMgCl or iso-BuMgBr; Temperature: 130°C]..... | 139 |
| Figure 6.2: The Effect of Amount of Initiators on Monomer Conversion. [Composition: 100 g ϵ -caprolactam/1%(w/w) or 2% (w/w) GE-S11AP/various amounts of iso-BuMgCl or iso-BuMgBr; Temperature: 130°C]..... | 141 |
| Figure 6.3: Comparison of $[\eta]$ Values from Two Different Methods | 144 |
| Figure 6.4: The Effect of Amount of Initiators on Intrinsic Viscosity [Composition: 100 g ϵ -caprolactam/1%(w/w) or 2% (w/w) GE-S11AP/various amounts of iso-BuMgCl or iso-BuMgBr; Temperature: 130°C]..... | 146 |
| Figure 6.5: Plot on Rate of Polymerization vs. Activator Concentration. (a). with DPC (iso-Bu-MgBr), GE-S11AP (both iso-Bu-MgBr and iso-Bu-MgCl); (b) with GE-S11AP and GE-S3G100 (iso-Bu-MgCl)..... | 152 |
| Figure 6.6: Results of Monomer Conversion vs. Concentration of Various Activators (DPC or PCs with two initiators) | 154 |

| | |
|--|-----|
| Figure 6.7: Plot of Intrinsic Viscosity $[\eta]$ vs. Activator Concentration. (a). with DPC (iso-Bu-MgBr), polycarbonate GE-S11AP (both iso-Bu-MgBr and iso-Bu-MgCl); (b). with the two polycarbonates GE-S11AP and GE-S3G100 (iso-Bu-MgCl)..... | 156 |
| Figure 6.8: Plot of η^* versus $[\eta]$ for Nylon 6s Made from Various Concentrations of DPC | 160 |
| Figure 6.9: Plot of η^* versus $[\eta]$ for All Samples at Various Concentrations of DPC or polycarbonates | 162 |
| Figure 6.10: Plots of η^* versus Polycarbonate Concentrations. (a). for GE-S3G100 polycarbonate and iso-Bu-MgCl; (b). for GE-S11AP polycarbonate and iso-Bu-MgCl; (c). for GE-S11AP polycarbonate and iso-Bu-MgBr | 163 |
| Figure 6.11: Data of Degree of Crystallinity x_C and Melting Temperatures T_m s versus Concentration of Polycarbonates with Different Initiators. (a). GE-S11AP/iso-Bu-MgBr; (b). GE-S11AP/iso-Bu-MgCl; (c). GE-S3G100/iso-Bu-MgCl..... | 166 |
| Figure 6.11(d): Data of Degree of Crystallinity x_C and Melting Temperatures T_m s versus Concentration of DPC (DPC/iso-Bu-MgBr)..... | 168 |
| Figure 6.12: X-ray Diffraction Patterns for Nylon 6s Made with DPC at Various Concentrations | 173 |
| Figure A.1a: Stress-Strain Curves for DD (polymer with 1% PC by "L-L" method) | 199 |
| Figure A.1b: Stress-Strain Curves for AA [polymer by "L-S" method with 1% PC (<80 μ m)]..... | 199 |
| Figure A.1c: Stress-Strain Curves for CC [polymer by "L-S" method with 1% PC (80-200 μ m)]..... | 200 |
| Figure A.1d: Stress-Strain Curves for GG [polymer by "L-S" method with 1% PC (200-400 μ m)]..... | 200 |
| Figure A.2: DSC Heating and Cooling Curves for "L-S" Sample with "<80 micron" PC (Scan rate: 10 $^\circ$ C/min, nitrogen) | 201 |
| Figure A.3: DSC Heating and Cooling Curves for "L-S" Sample with "80-200 micron" PC (Scan rate: 10 $^\circ$ C/min, nitrogen) | 202 |

| | |
|--|-----|
| Figure A.4: DSC Heating and Cooling Curves for “L-S” Sample with “200-400 micron” PC (Scan rate: 10°C/min, nitrogen) | 203 |
| Figure A.5: DSC Heating and Cooling Curves for Pure Nylon 6 Pellets (Scan rate: 10°C/min, nitrogen)..... | 204 |
| Figure A.6: FTIR Spectrum of Polycarbonate Powder..... | 205 |
| Figure A.7: FTIR Spectrum of Nylon 6 Made form 0.1% Diphenyl Carbonate | 206 |
| Figure A.8: SEM Image of Nylon 6/PS (2%wt) <i>in-situ</i> Reactive Blend | 207 |
| Figure A.9: SEM Images of Nylon 6/Polycarbonate Melt Blend (with 2% Polycarbonate) after Mixing for 5 minutes (at different magnifications)..... | 208 |
| Figure A.10: SEM Images of Nylon 6/Polycarbonate Melt Blend (with 2% Polycarbonate) after Mixing for 10 minutes (at different magnifications)..... | 209 |
| Figure A.11: SEM Images of Nylon 6/Polycarbonate Melt Blend (with 2% Polycarbonate) after Mixing for 15 minutes (at different magnifications)..... | 210 |
| Figure A.12: SEM Image of Nylon 6/Polycarbonate Melt Blend (with 10% Polycarbonate) after Mixing for 5 minutes..... | 211 |
| Figure A.13: SEM Image of Nylon 6/Polycarbonate Melt Blend (with 10% Polycarbonate) after Mixing for 10 minutes..... | 212 |
| Figure A.14: SEM Pictures of Nylon 6/Polycarbonate Melt Blend (with 10% Polycarbonate) after Mixing for 15 minutes (at different magnifications) | 213 |
| Figure A.15: SEM Image of Copolymer with 2%wt Polycarbonate | 214 |
| Figure A.16: ¹³ C NMR Spectrum of Polycarbonate in CDCl ₃ | 215 |
| Figure A.17: ¹³ C NMR Spectrum of Trifluoroacylated Nylon 6 in CDCl ₃ | 216 |
| Figure A.18: ¹ H NMR Spectrum of Polycarbonate in CDCl ₃ | 217 |
| Figure A.19: ¹ H NMR Spectrum of Trifluoroacylated Nylon 6 in CDCl ₃ | 218 |
| Figure A.20: ¹ H NMR Spectrum of Trifluoroacylated Copolymer (with 2% PC) in CDCl ₃ | 219 |

| | |
|--|-----|
| Figure B.1: Stress-Strain Curves for Specimens from the "Scale-Up" Sample | 221 |
| Figure B.2: Plots of $\ln \eta_{rel}/C$ versus C for 2 Samples.(a). Nylon 6 made by using Red-Al as initiator (100 g ϵ -caprolactam/1ml N-acetyl caprolactam /3 mmol Red-Al); (b). Nylon 6 made by using isobutyl magnesium chloride as initiator (100 g ϵ -caprolactam/1ml N-acetyl caprolactam /3 mmol isobutyl magnesium chloride)..... | 222 |
| Figure B.3-(a1)&(a2): GC-MS Results for 0.0523g/100mL Standard Solution . (a1: run 1; a2: run 2) | 223 |
| Figure B.3-(b1)&(b2): GC-MS Results for 0.1028g/100mL Standard Solution. (b1: run 1; b2: run 2)..... | 225 |
| Figure B.3-(c1)&(c2): GC-MS Results for 0.2162g/100mL Standard Solution. (c1: run 1; c2: run 2) | 227 |
| Figure B.4-(a1)&(a2): GC-MS Results for Sample #1. (a1: run 1; a2: run 2)..... | 229 |
| Figure B.4-(b1)&(b2): GC-MS Results for Sample #2. (b1: run 1; b2: run 2)..... | 231 |
| Figure B.4-(c1)&(c2): GC-MS Results for Sample #3. (c1: run 1; c2: run 2)..... | 233 |
| Figure B.5-(a)-(f). DSC Thermogram for Samples Made at Different Oil Bath Temperatures (10°C/min, first heating scan, nitrogen). (a). 95°C; (b). 110°C; (c). 120°C; (d). 134°C; (e). 147°C; (f). 160°C..... | 235 |
| Figure B.6-(a)-(f). X-Ray Diffraction Patterns for Samples Made at Different Oil Bath Temperatures. (a). 95°C; (b). 110°C; (c). 120°C; (d). 134°C; (e). 147°C; (f). 160°C. | 241 |
| Figure B.7-(a)-(f). Tensile Test Results for "Dry" Specimens from Samples Made at Different Oil Bath Temperatures (75 g ϵ -caprolactam /0.75 g polycarbonate (SPP) /10 mmol isobutyl magnesium chloride). (a). 95°C; (b). 110°C; (c). 120°C; (d). 134°C; (e). 147°C; (f). 160°C. | 244 |
| Figure B.8-(a)-(f).Tensile Test Results for "Wet" Specimens from Samples Made at Different Oil Bath Temperatures (75 g ϵ -caprolactam /0.75 g polycarbonate (SPP) /10 mmol isobutyl magnesium chloride). (a). 95°C; (b). 110°C; (c). 120°C; (d). 134°C; (e). 147°C; (f). 160°C. | 247 |
| Figure B.9-(a)-(d). Tensile Test Results for "Dry" Specimens from Samples Made at Different Oil Bath Temperatures (75 g ϵ -caprolactam/0.75 g polycarbonate (SPP) /12 mmol isobutyl magnesium bromide). (a). 106°C; (b). 126°C; (c). 146°C; (d). 164°C. | 250 |

| | |
|---|-----|
| Figure C.1-(a)-(c). DSC Thermograms for Pure Nylon 6s Made from DPC(10°C/min, nitrogen). (a). 0.2%wt; (b). 1% wt; (c). 2% wt. | 253 |
| Figure C.1-(d)-(f). DSC Thermograms for Copolymers Made from GE-S11AP (with iso-Bu-MgBr). (10°C/min, nitrogen). (d). 0.2%wt; (e). 1% wt; (f). 2% wt. | 256 |
| Figure C.1-(g)-(I). DSC Thermograms for Copolymers Made from GE-S11AP (with iso-Bu-MgCl). (10°C/min, nitrogen). (g). 0.2%wt; (h). 1% wt; (i). 2% wt. | 259 |
| Figure C.1-(j)-(i). DSC Thermograms for Copolymers Made from GE-S3G100 (with iso-Bu-MgCl). (10°C/min, nitrogen). (j). 0.2%wt; (k). 1%wt; (i). 2% wt. | 262 |
| Figure C.2-(a)-(c). X-Ray Diffraction Patterns for Copolymers Made from GE-S11AP (with iso-Bu-MgBr). (a). 0.2%wt; (b). 1%wt; (c). 2% wt. | 265 |
| Figure C.2-(d)-(f). X-Ray Diffraction Patterns for Copolymers Made from GE-S11AP (with iso-Bu-MgCl). (d). 0.2%wt; (e). 1%wt; (f). 2%wt. | 266 |
| Figure C.2-(g)-(i). X-Ray Diffraction Patterns for Copolymers Made from GE-S3G100 (with iso-Bu-MgCl). (g). 0.2%wt; (h). 1%wt; (i). 2%wt. | 268 |
| Figure D.1 SEM Image of Bare Glass Fibre. | 271 |
| Figure D.2 SEM Images of Fractured Surface for Glass-fiber Reinforced Composite Made at 100 °C Oil Bath Temperature (at different magnifications) (containing 1% polycarbonate (SPP)) | 272 |
| Figure D.3 SEM Images of Fractured Surface for Glass-fiber Reinforced Composite Made at 117 °C Oil Bath Temperature (at different magnifications) (containing 1% polycarbonate (SPP)) | 273 |
| Figure D.4 SEM Images of Fractured Surface for Glass-fiber Reinforced Composite Made at 133 °C Oil Bath Temperature (at different magnifications) (containing 1% polycarbonate (SPP)) | 274 |
| Figure D.5 SEM Images of Glass-fiber Reinforced Composites Containing Polycarbonate (SPP) at Concentration of: (a). 0.1%; (b). 1%. (Both were made at environmental temperature 170°C) | 275 |

Nomenclature

| | |
|---------------------------|---|
| <i>a</i> | amorphous phase |
| A_a | area corresponding to the amorphous halo |
| A_c | area corresponding to the crystalline peak |
| <i>ABS</i> | acrylonitrile-butadiene-styrene triblock copolymer |
| <i>ATBN</i> | amine-terminated butadiene-acrylonitrile copolymer |
| <i>c</i> | crystalline phase (subscript) |
| <i>C</i> | concentration of solution (g/dL) |
| <i>DPC</i> | diphenyl carbonate |
| <i>E</i> | Young's modulus (Mpa) |
| <i>EVA</i> | ethylene-vinyl acetate copolymer |
| <i>est</i> | estimated |
| <i>G</i> | shear modulus (Pa), or Gibbs free energy (J/mol) |
| G' | storage modulus in shear (Pa) |
| G'' | loss modulus in shear (Pa) |
| G^* | complex modulus in shear (Pa), = $G' + iG''$ (Pa) |
| ΔG_{mix} | Gibbs free energy of mixing (J/mol) |
| <i>HDPE</i> | high density polyethylene |
| ΔH_f | heat of fusion for a semicrystalline polymer (J/g) |
| ΔH_f° | heat of fusion for 100% crystalline structure (J/g) |
| ΔH_{mix} | enthalpy of mixing (J/mol) |
| <i>K</i> | empirical constant in Mark-Houwink equation (dL/g), or calibration constant in GC-MS method |
| <i>L</i> | liquid |
| <i>MW</i> | molecular weight (g/mol) |
| <i>MWD</i> | molecular weight distribution |
| M_n or \overline{M}_n | number average molecular weight (g/mol) |
| M_v or \overline{M}_v | viscosity average molecular weight |

| | |
|---------------------------|--|
| M_w or \overline{M}_w | weight average molecular weight (g/mol) |
| M_z | z-average molecular weight (g/mol) |
| <i>PC</i> | polycarbonate |
| <i>PDMS</i> | poly(dimethylsiloxane) |
| <i>PP</i> | polypropylene |
| <i>PPE</i> | polyphenylene ether |
| <i>PS</i> | polystyrene |
| <i>PVPh</i> | poly(vinyl phenol) |
| <i>S</i> | solid |
| <i>SEBS-gMA</i> | styrene-(ethylene- <i>co</i> -butylene)-styrene triblock copolymer functionalized by maleic anhydride |
| <i>S.D.</i> | standard deviation |
| ΔS_{mix} | entropy of mixing (J/mol.K) |
| <i>t</i> | time (second or minute) |
| t_o | flow time for solvent (second or minute) |
| t_s | solidification time (minute) |
| <i>T</i> | temperature (°C or K) |
| T_g | glass transition temperature (°C or K) |
| $T_{initial}$ | initial temperature of center point in reactive mixture (°C) |
| T_m | melting temperature (°C or K) |
| $T_{measurement}$ | temperature for rheology measurement (°C or K) |
| T_{oil} | oil bath temperature (°C or K) |
| <i>V</i> | void content (%) |
| <i>VAc</i> | vinyl acetate |
| W_{air} | weight of sample in air (g) |
| W_{oil} | weight of sample in oil (g) |
| x_c | degree of crystallinity (%) |
| ϵ_b | tensile strain at break (%) |
| γ | shear strain (%) |
| γ° | dynamic (shear) strain amplitude (%) |

| | |
|--------------|---|
| η | non-Newtonian viscosity (Pa.s) |
| $[\eta]$ | intrinsic viscosity (dL/g) |
| η' | dynamic viscosity (Pa.s) |
| η'' | elastic component in complex viscosity (Pa.s) |
| η^* | complex viscosity, = $\eta' - i\eta''$ (Pa.s) |
| η_0 | zero shear rate limiting Newtonian viscosity (Pa.s) |
| η_{sp} | specific viscosity, = $t/t_0 - 1$ |
| η_{rel} | relative viscosity, = t/t_0 |
| 2θ | Bragg angle (degree) |
| ρ | density (g/cm ³) |
| ρ_{oil} | density of oil (g/cm ³) |
| ρ_s | bulk density of sample (g/cm ³) |
| τ | toughness (MPa) |
| τ_b | tensile stress at break (MPa) |
| ω | frequency (rad/s) |

Chapter 1 Introduction

1.1. The background

Nowadays engineering thermoplastics materials are used everywhere, from daily life to hi-tech. Among them, nylon 6 and Bisphenol-A polycarbonate are two of the very popular ones. Based on their chemical natures, each of them has advantages and disadvantages. Nylon 6 has strong chemical resistance, excellent wear and abrasion resistance etc.; but its affinity to moisture makes it difficult to maintain dimensional stability and causes poor mechanical properties under a humid environment. Polycarbonate has outstanding rigidity and toughness but it is weak under the attack of organic chemicals. A blend or copolymer of these two polymers might show promise for compensating the weaknesses of the two pure homopolymers.

During the past several decades, the physical blending of existing polymers has experienced fast growth due to economic consideration and possible synergistic properties above the original polymers. However it has been shown that melt-blending nylon 6 and polycarbonate is not successful (Gattiglia et al., 1989, 1990). Many types of copolymers were chosen to compatibilize the melt blend of these two (Kim et al., 1996; Horiuchi et al., 1996 and 1997). In our group, a nylon 6–polycarbonate copolymer was synthesized upon the ring-opening copolymerization of ϵ -caprolactam (monomer of nylon 6) and a cyclic carbonate oligomer (Li and Williams, 1995). This copolymer was

later used to compatibilize the melt blended nylon 6 and polycarbonate over a wide range of compositions. Finer morphology was found for the blend of nylon 6 and polycarbonate with the copolymer compared with the one containing no copolymer.

One other approach to making a polymer-polymer blend is as following: firstly polymer B is dissolved into the molten monomer of polymer A; then by polymerizing the monomer in this solution, a new polymer (i.e. polymer A) is synthesized and a polymer-polymer blend (of A and B) is thus formed. Some examples of this process include high impact polystyrene, rubber toughened epoxy (Levita, 1987) and PPE/nylon 6 blend (Chorvath et al., 1998).

Among three polymerization methods to produce nylon 6 from its monomer ϵ -caprolactam, the anionic one becomes more and more attractive because of its mild reaction requirements, absence of by-product, high degree of conversion and highly crystalline nature. All these advantages make the processes of reactive injection molding (RIM) and reactive extrusion possible in industrial applications. Much research has been done by first adding a second polymer either with or without an end-functional group which can be used as activating species into the monomer ϵ -caprolactam melt, then polymerizing ϵ -caprolactam anionically. In this way either a block-copolymer of nylon 6 or a blend of nylon 6 can be formed respectively.

Previously in our group, nylon 6 and nylon 6-glass fiber composites have been successfully made through the in-situ anionic polymerization route at temperatures much lower than the melting temperature of nylon 6 (Duangchan, 1994; Shah, 1996). Sodium hydride and phenyl isocyanate were used as initiator and activator respectively. An attempt was made to make a copolymer by using a polymerization route similar to that of making nylon 6, while mixing a certain amount of polycarbonate powder directly into molten ϵ -caprolactam containing initiator for anionic polymerization (Sankholkar, 1996). The so-produced material showed a higher tensile strength than pure nylon 6, and possible better adhesion between the polymer and glass fibre in the glass-fibre reinforced composites.

In the above-mentioned method, polycarbonate was introduced into the system in the form of solid powder. Since normally the anionic polymerization has very fast kinetics (sometimes in terms of few minutes), it was possible that polycarbonate may not be completely dissolved in the molten monomer before the final product was solidified. Therefore in this study, changes were made in the reaction procedure as follows: in the first stream polycarbonate was completely dissolved into molten ϵ -caprolactam to form a homogeneous melt solution while the second stream contained molten ϵ -caprolactam with initiator (Grignard reagent); upon mixing the two streams anionic polymerization of ϵ -caprolactam was conducted. The final polymer did not show two-phase morphology as normally expected for a blend of two immiscible polymers (e.g. nylon 6 and polycarbonate).

1.2 The objectives

The first goal in this research was to try to find the roles of polycarbonate and Grignard reagents. Unlike the classical roles of them as activator and initiator respectively, there might be an interaction between the two of them. To prove this hypothesis, Gel Permeation Chromatography (GPC) was used to show the change of MW before and after the interaction of initiator (a Grignard reagent) and polycarbonate. A small molecule carbonate (diphenyl carbonate) was used as activator for a model polymerization system. Finally, a possible route of reaction was proposed to show that a copolymer might be formed.

The second goal was to find the influence of reaction temperature on various properties of the final product. As it is well known that the performance of a polymer product is directly related to its molecular information such as molecular weight, degree of crystallinity and so on. In this part, several temperatures were studied to see the effect of temperature; solution viscosity and zero-shear melt viscosity were used to characterize these polymers; degree of crystallinity was obtained by both DSC method (Differential Scanning Calorimetry) and X-ray method. Also tensile properties under dry and wet conditions were measured and compared to show the influence of moisture absorption.

The third goal of this research was to study the influence of initiator and activator. In this part, the amount and type of the initiator and the amount of polycarbonate with different molecular weights were investigated. For various concentrations of

polycarbonate, the use of different amount of initiator was studied. Monomer conversion was measured by water-extraction method. Solution viscosity and zero-shear melt viscosity of polymers under different conditions were used to characterize molecular weight and the reinforcement of the copolymer melt due to the existence of polycarbonate chain block. Also DSC and X-Ray diffraction were used to get the information on degree of crystallinity for each sample.

One interesting property of this copolymer was its adhesion to glass. In producing glass fiber-reinforced composites it was imperative to have a strong adhesive bonding at the interface of glass fiber and polymer matrix. Generally, nylon 6 and glass fiber showed very poor adhesion because (1) intrinsic incompatibility between the inorganic glass fiber and the organic nylon 6; (2) volumetric change arose from the crystallization of nylon 6 during the production; (3) the affinity of nylon 6 to moisture in which moisture disrupts the weak adhesive bond formed during dry conditions. Various treatments on the glass fiber had been tried to improve the bonding at the interface of glass fiber and nylon 6 matrix (Duangchan, 1994; Shah, 1996). It was found that the new polymer showed some adhesion to untreated glass fiber, which was promising for making a composite by using the new polymer as matrix. Scanning Electron Microscopy (SEM) was used to check the bonding between glass fiber and polymer matrix.

Chapter 2 Literature Review

2.1 History of Nylon 6 and Polycarbonate

2.1.1 Nylon 6

Nylon is the general name for a series of synthetic linear aliphatic polyamides, which have functional group of amide --CONH-- in the repeating molecule. Nylon is the first plastic with crystalline structure which gave rise to high service temperature. It also provides a combination of toughness, rigidity, excellent abrasion, chemical and heat resistance which leads to particular utility in performing a mechanical function that traditionally would have been performed by a metal part. In this way, nylon was also called an engineering thermoplastic, and it was one of the oldest engineering plastics (Kohan, 1973).

A large amount of commercial nylon resin is used in making synthetic fibers, while the market for molded nylon plastics in automotive parts, electrical and electronic parts, film and cable is experiencing good growth. A substantial and increasing amount of nylon resin is consumed in compounded form with reinforcements and other additives. Table 2.1 gives an estimate for nylon consumption pattern in the U.S. and Canada in 1999 and 2000 ("Resin 2001", 2001).

Among various polyamides, nylon 6 and nylon 66 are two of the most popularly used ones, contributing around 80-90% consumption of polyamide produced in major regions (United States, Western Europe and Japan) in 1996 (Davenport, 1998). There are not many differences in performance characteristics between nylon 6 and nylon 66.

Generally nylon 66 tends to exhibit higher tensile strength and greater hardness and stiffness but lower impact strength, while nylon 6 has better surface appearance and flow characteristics and can be more easily colored.

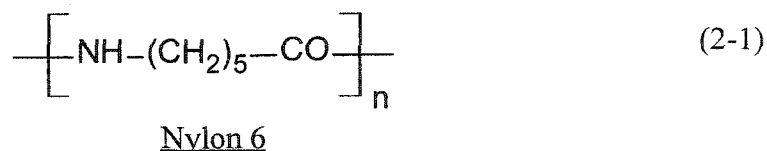
**Table 2.1 Nylons^a: Pattern of Consumption
(in US and Canada)**

| Market | Million | Lb. |
|------------------------|--------------|------------|
| | 1999 | 2000 |
| Filaments | 28.6 | 29.1 |
| Film | 71.5 | 73.5 |
| Wire & Cable | 33.9 | 35 |
| Appliances/power tools | 16 | 17 |
| Consumer products | 36 | 36.7 |
| Electrical/electronics | 44.9 | 47.7 |
| Industrial | 45.6 | 46.6 |
| Transportation | 223 | 232.1 |
| Other ^b | 88.9 | 78.3 |
| Total | 588.5 | 596 |

a: All types

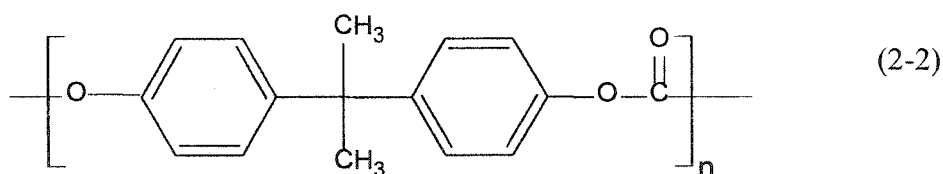
b: Includes materials sold by independent compounders and traders, powder coatings, hot melts, grades for blow molding, monomer casting etc.

Nylon 6 has a repeating unit of five $-\text{CH}_2-$ groups linked to an amide $-\text{CONH}-$ group. It was discovered in 1938 (Shlack, 1938). The earliest commercial production of nylon 6 started in I.G. Farben's Berlin-Lichtenberg factory in 1939.



2.1.2 Polycarbonate

Bisphenol-A polycarbonate was separately discovered by Farben-fabriken Bayer Company A. G. in Germany and General Electric Company in U.S. A. in late 1950s. It can be manufactured by condensation polymerizations either through direct reaction between bisphenol A and phosgene in presence of a base, or by an ester exchange between bisphenol A and a carbonate precursors such as carbonyl halide, carbonate ester or haloformate etc. (Hall and Humphrey, 1980). The molecular structure of Bisphenol A polycarbonate is shown below:



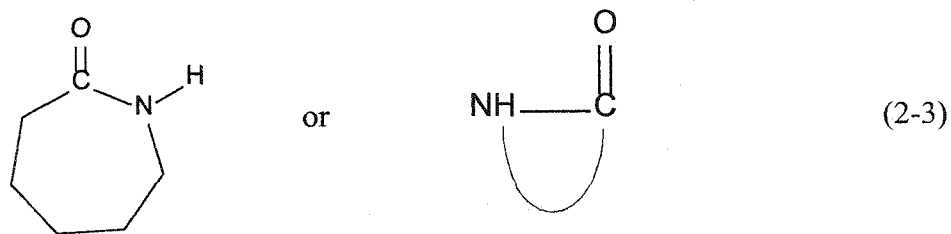
Bisphenol-A Polycarbonate

Polycarbonate is well known for its rigidity and toughness at both low and high temperatures while its maximum permissible service temperature is 135 °C. Being an amorphous material, its transparency to light and high impact strength lead to its use for laboratory safety shields and for automobile windows.

The largest application field is in electronics and electrical engineering. For example covers for time switches and relays utilize the good electrical insulation properties together with transparency, flame resistance and durability. Other applications include compact discs, medical devices and domestic appliance housing.

2.2 Polymerization of Nylon 6 Homopolymer

The monomer used in manufacturing nylon 6 is ϵ -caprolactam. It is a cyclic molecule shown below.



ϵ -caprolactam

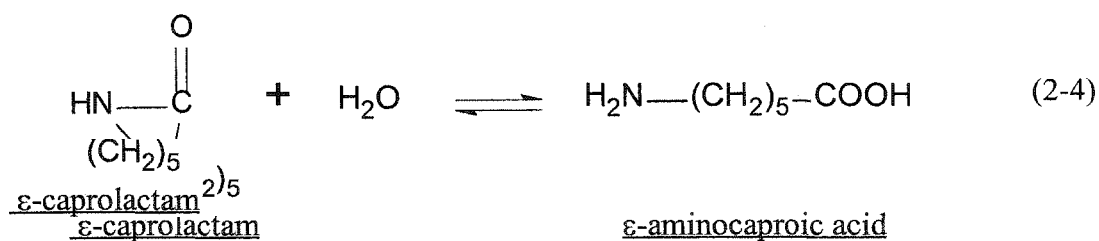
Generally, there are 3 polymerization methods for making nylon 6. They are hydrolytic, anionic and cationic methods. All the polymerization involves the ring-opening reaction of ϵ -caprolactam. Among them, the cationic process using strong acids as catalysts is not commercialized due to its limited monomer conversion and low

molecular weight of final product. Therefore only the hydrolytic and anionic methods are to be discussed here.

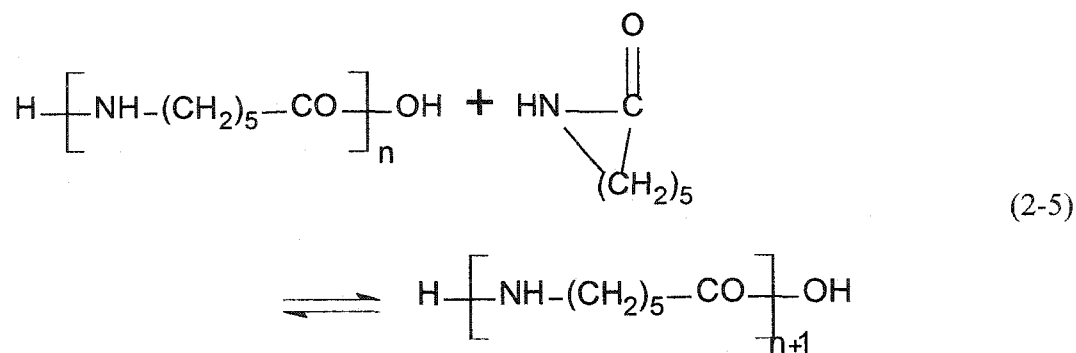
2.2.1 Hydrolytic Polymerization

Most commercial nylon 6 is made through the hydrolytic mechanism. In this process, water is used to initiate polymerization (Reimschuessel, 1977). A well-accepted mechanism consists of the following steps (Nelson, 1976):

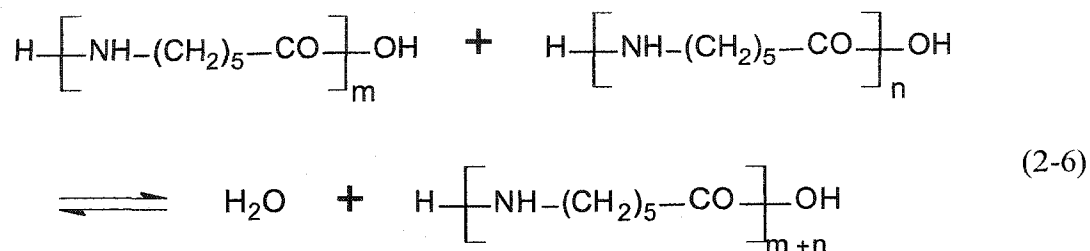
(1) Ring Opening, i.e. hydrolysis of ϵ -caprolactam to give an ϵ -aminocaproic acid:



(2) Addition, a direct coupling of an ϵ -caprolactam molecule to polymer chain.



(3) Condensation, the reaction between a carboxyl end group and an amino end group to form an amide group plus a molecule of water:



A general hydrolytic polymerization in a batch reactor is as follows: a mixture of ϵ -caprolactam, water or water releasing substance (5-10% by weight) is fed into a reactor which has been purged with nitrogen. The mixture is heated at a temperature in the range from 250°C - 270°C for about 12 hours to more than 24 hours, and a pressure of about 15 atmospheres is maintained by venting off steam.

The polymerization does not result in complete conversion of monomer caprolactam but an equilibrium. Normally in industry about 8-9% caprolactam and about 3% low molecular-weight oligomers remain in the polymer because there exists a monomer-oligomer-polymer equilibrium. Subsequent leaching by hot water or vacuum evaporation is essential to remove monomer and oligomers from the final product.

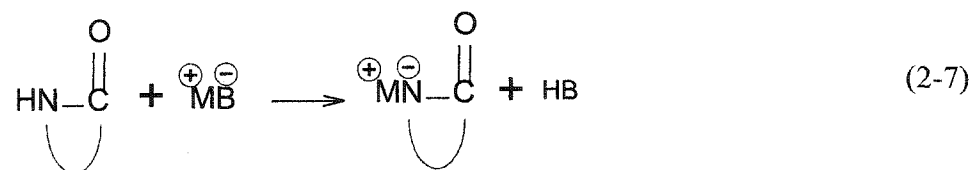
2.2.2 Anionic Method

The anionic method to synthesize nylon 6 was first described by Joyce and Ritter (1941). In their patent, Joyce and Ritter found that by introducing metal sodium, calcium or lithium into ϵ -caprolactam melt held at a temperature of 100-150 °C and then raising to about 230-250 °C, ϵ -caprolactam could be converted into polyamide much faster than the hydrolytic method.

2.2.2.1 Reaction Mechanism

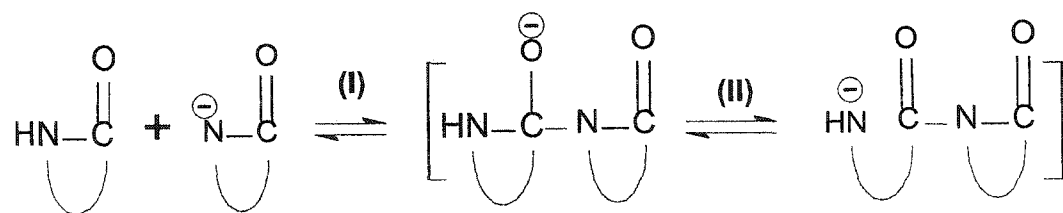
The anionic mechanism of ring opening polymerization of ϵ -caprolactam has been extensively studied (Reimschuessel, 1977; Šebenda, 1989). The free ion mechanism was usually used to demonstrate the polymerization route:

(1). Generation of ϵ -caprolactam anion, i.e. reaction of ϵ -caprolactam with a strong base such as hydrides, amides, alcoholates, carbonates and hydroxides of alkali and alkaline earth metals or metal organic compounds and Grignard reagents.

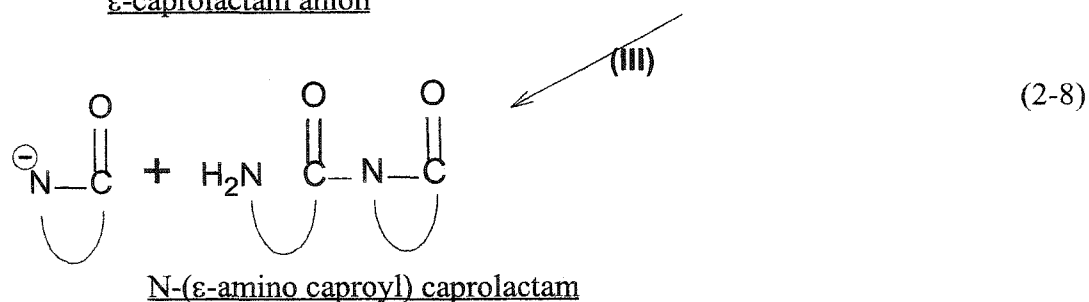


Where M stands for metal and B for base.

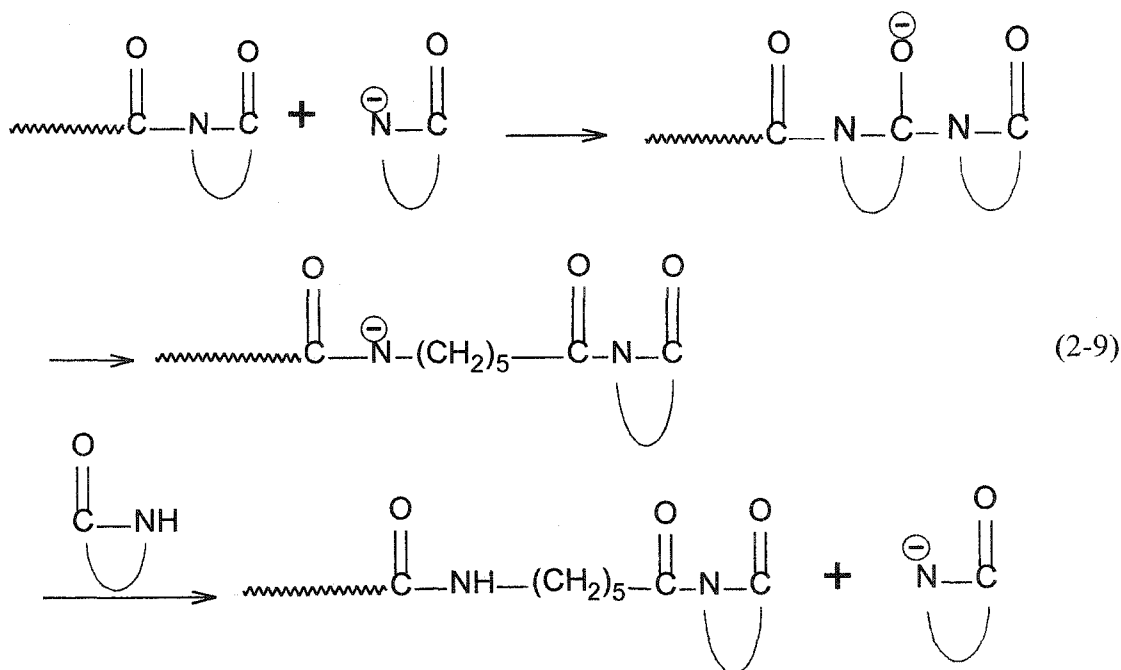
(2). Initiation, N-(ϵ -amino caproyl) caprolactam is formed through a disproportionation (I), forming of a conjugated primary amine anion (II) and a rapid proton exchange (III).



ϵ -caprolactam anion

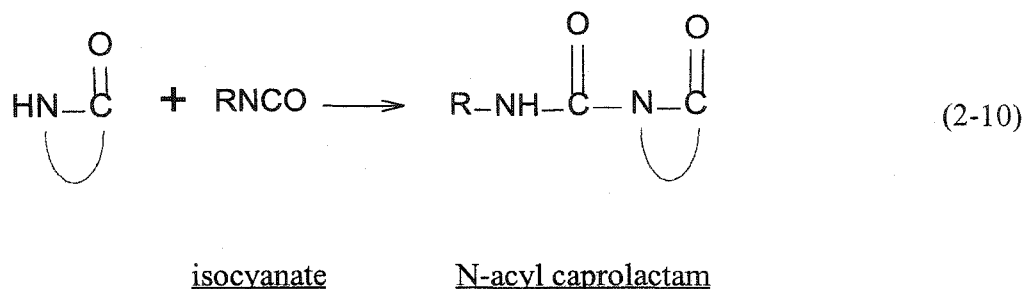


(3). Propagation: The N-carbonyl moiety constitutes the center for subsequent propagation by the attack of ϵ -caprolactam anion at its endocyclic carbonyl group and subsequent ring opening in the penultimate position.



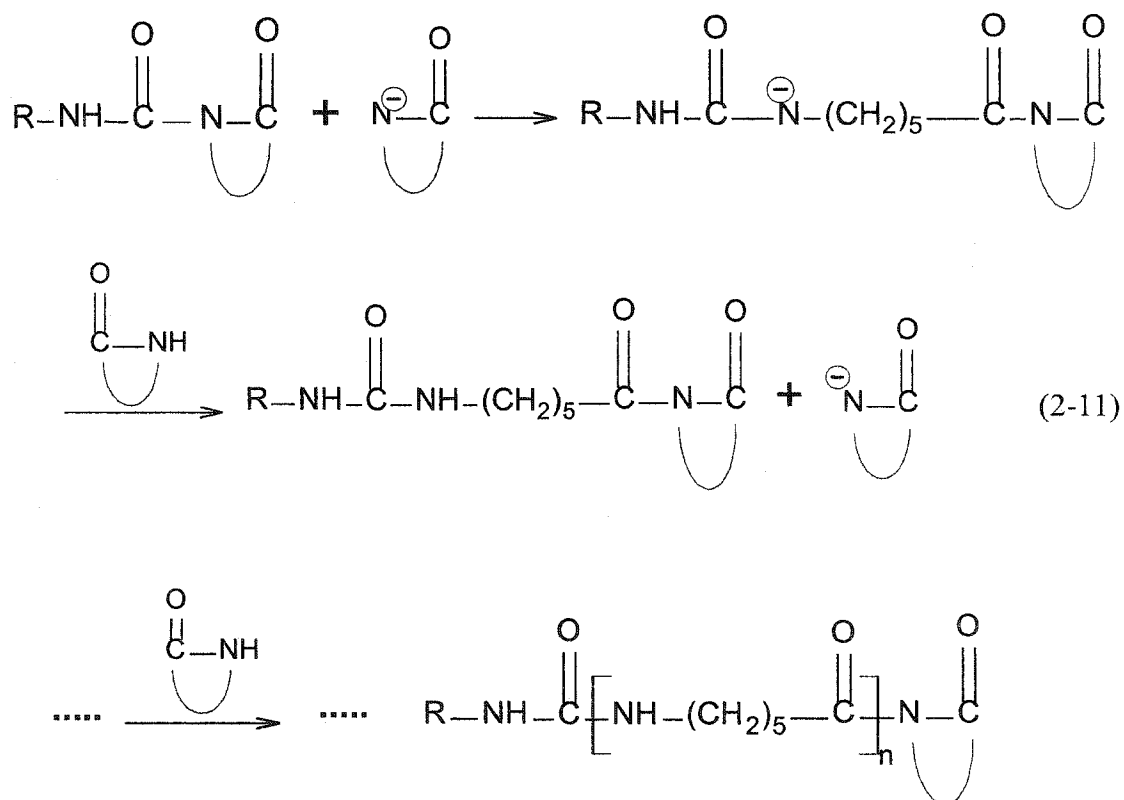
The lactam ring opening step in initiation involves a much higher activation energy than for propagation, causing a slow rate of induction and high reaction temperature. Therefore, a certain amount of N-substituted lactams with electronegative substituents such as N-acyl lactam are either added directly or formed *in situ* by a fast reaction to act as activators (or called chain initiator by Šebenda (1989)). The reaction route for this so-called activated anionic polymerization is demonstrated as follows by using an isocyanate as activator:

Firstly, formation of N-acyl caprolactam:



With the presence of isocyanate, ϵ -caprolactam can be rapidly converted to an N-acyl caprolactam. Therefore the induction period in the non-activated route can be eliminated, and polymerization can proceed at a much lower temperature between the melting temperature of monomer caprolactam (72°C) and that of nylon 6 (around 220°C).

Then, the reactions for the formation of caprolactam anion and propagation follow the same routes as the non-activated ones with the propagation shown below:



Compared with other anionic polymerization such as polystyrene and polybutadiene, anionic ring-opening polymerization of ϵ -caprolactam is different in that its growth center at chain end is neutral while the monomer forms anionically active specie.

2.2.2.2 Advantages of Anionic Method

Compared with hydrolytic polymerization, the anionic method has several advantages (Reimschuessel, 1977): (1). absence (or very small amount) of by-products; (2). low reaction temperature (below the melting temperature of nylon 6, i.e. 220 °C); (3). high crystalline nature of final polymers because the temperature for the maximum rate of polymer crystallization coincides within the range of reaction temperature; (4). high degree of conversion (content of unconverted monomer can be less than 2%).

Figure 2.1 shows monomer content in a caprolactam-nylon 6 equilibrium at different temperatures (Wichterle ,1959). At temperatures below the melting temperature of nylon 6, the amount of remaining monomer is much less than the extrapolated values (the dotted line) from those at higher temperatures. It is explained that monomer in the equilibrium polymerizate only exists within the amorphous part of the polymer, while the crystalline part does not contain any monomer . Since in the low-temperature reaction system, polymerization and crystallization happen at the same time, the crystalline fraction of the polymer is then excluded from the monomer-polymer equilibrium.

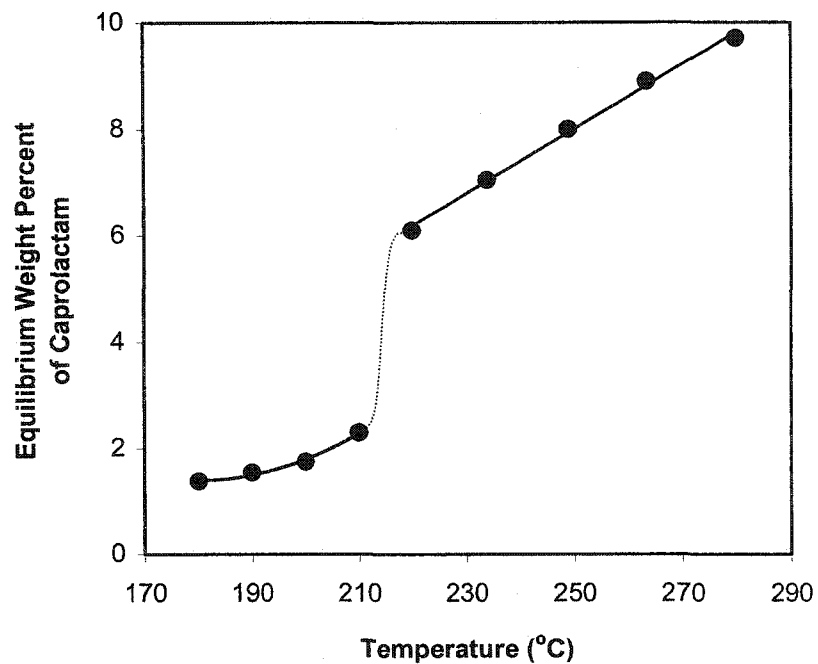


Figure 2.1 Equilibrium Monomer Concentration in Caprolactam-Nylon 6s
at Different Temperatures (data taken from Kohan, 1973)

2.2.2.3 Industrial Applications of Anionic Method

Due to the special feature of this anionic method, it can be used for several industrial applications (Udipi, 1998). Among them, reactive extrusion and reactive thermoplastic pultrusion of nylon 6 are two of the continuous process. Reactive extrusion makes use of single (Reinking, 1972; Blazen and Potin, 1978) or twin screw extruders (Hornsby, 1994; Kye and White, 1994), while reactive thermoplastic pultrusion is for manufacturing nylon 6 composites having unidirectional fibers and constant cross-sectional areas (Udipi, 1998). Reactive injection molding (RIM or monomer casting) of nylon 6 is a batch process in which the reactive liquid component (molten monomer caprolactam, initiator and activator) are mixed and injected into molds of certain shapes, and fast polymerized into molded solid parts.

Compared with other processes, RIM has several advantages especially in making large molded parts suitable for applications such as automotive parts. Various types of modifiers can be added to the RIM nylon 6 process in order to achieve different property enhancements, such as glass fiber-reinforced nylon 6 (Duangchan, 1994; Shah, 1996; Hodek and Seiner, 1985) for rigidity and strength improvement, and rubber-toughened nylon 6 (Baer, 1981; Gaitskell et al., 1984; Ning and Ishida, 1991; Udipi, 1991) for notched impact strength enhancement. Various nylon 6 block copolymers were also produced in RIM processes. By introducing blocks such as polyols (Van Geenen and Kerssemakers, 1994; Iobst and Garner, 1992) or one of polyurethane, polyurea and

polyisocyanurate polymers (Frisch et al., 1986) into nylon 6 copolymers, better impact resistance and elastic deformation were obtained.

2.3 Anionic Copolymerization of ϵ -Caprolactam

2.3.1 Introduction to Copolymer

Copolymers, normally made of two or more monomers, have chemical structures containing two or more species of repeating units. Based on the way that these repeating units are chemically linked, there are four types of copolymers: random copolymers, alternating copolymers, block copolymers and graft copolymers. This is schematically illustrated below with A and B being two of the monomer units:

Random copolymer:

-A-B-A-A-B-A-B-B-B-A-A-B-A-B-B-B-B-A-A-

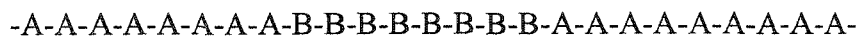
Alternating copolymer:

-A-B-A-B-A-B-A-B-A-B-A-B-A-B-A-B-A-B-

Graft copolymer:

-A-
B B B
B B B
B B B
B B B

Block copolymer:



ABA triblock copolymer



AB diblock copolymer



(A-B)_n multiblock copolymer

When a block copolymer is made of low- T_g and high- T_g (or high- T_m) blocks, the low- T_g blocks are designated as the “soft segment” or “soft phase” if phase separated; while the high- T_g (or high- T_m) blocks are called the “hard segment” or “hard phase” if phase separated (Turi, 1997).

Block copolymers contain at least two distinctive sequences, they tend not to mix well (immiscible) (similar to the thermodynamics of polymer-polymer blends which will be discussed later). Therefore, they usually exhibit two-phase morphology. However, the restriction of the covalent bonds holds the different blocks together, in this way there is no macroscopic phase separation; segregation only takes place at a local

scale, i.e. microscopic separation. The strong interphase adhesion and small domain size can result in a good balance of mechanical properties. Many other properties can also be improved depending on the various block types of the copolymer.

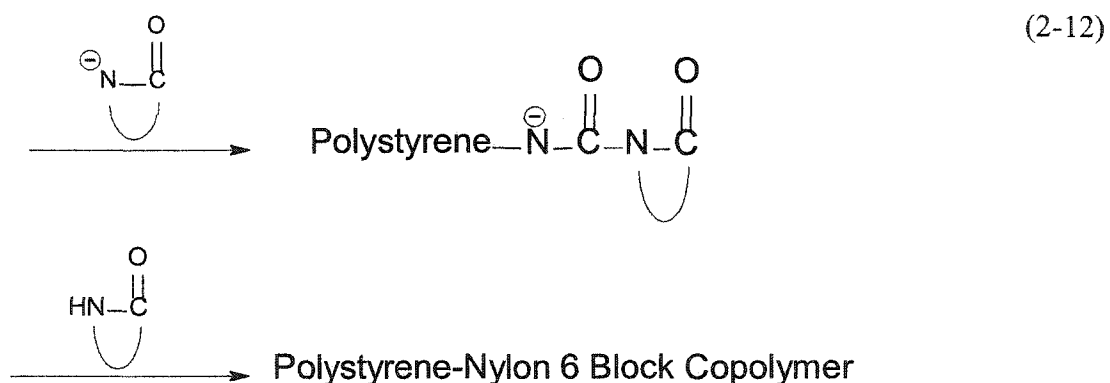
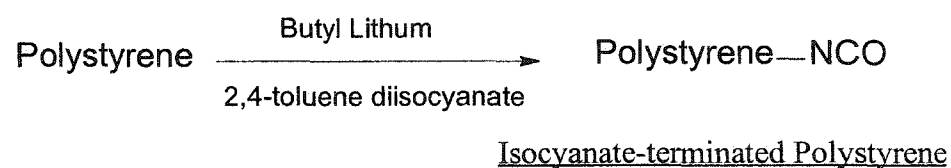
2.3.2 Synthesis of Copolymer of Nylon 6

There has been a large number of nylon 6 block copolymers produced for industrial applications. Generally nylon 6 blocks in a copolymer act as the “hard phase”, while many polymeric chains have been chosen for “soft phase” such as rubbers to improve its impact strength. On the other hand, a block such as aromatic polyamides (i.e. aramids) was introduced into its nylon 6 copolymer as molecular reinforcement so that better tensile properties could be achieved (Zhang, 1998).

Based on the anionic polymerization mechanism of ϵ -caprolactam, an activator is added to the reaction system not only to accelerate polymerization, but also to join the reaction and behave as the starting point of chain growth. The final product will have an end group featuring the chemical structure of the activator.

Generally an activator has functional group of N-acyl caprolactam in its structure directly or can be formed indirectly. It can be deduced that, a polymer whose end or ends are capped with N-acyl caprolactam can act as a macroactivator. In this way, a chain of nylon 6 will start growing at the end of the macroactivator, and thus a di-block or tri-block copolymer can be formed through anionic route similar to that for homopolymer nylon 6.

Petit et al. (1979) synthesized prepolymers: ester-terminated polystyrene and α,ω -isocyanate-terminated polybutadiene, then used them as macroactivators respectively in the anionic polymerization of ϵ -caprolactam to make nylon 6 – polystyrene or polydiene block copolymer with catalyst sodium hydride. The following scheme shows the reaction route for synthesizing a polystyrene-nylon 6 block copolymer by using an isocyanate-terminated polystyrene as macroactivator (Hergenrother and Ambrose, 1974):



Gardlund and Bator (1990) synthesized a carbamyl caprolactam terminated polyurea by reacting caprolactam, 1,6-hexamethylene diisocyanate and amine-terminated poly(propylene oxide) in tetrahydrofuran (THF), then anionically copolymerized

caprolactam by using the modified polyether as activator and sodium hydride as initiator. Similar systems were also studied by other groups (Stehlicek and Šebenda, 1982; Gabbert et al., 1986; Coutinho and Sobrinho, 1991; Akkapeddi et al., 1986; Iobst and Garner, 1992; Chen and Chen, 1993; Seo and Ha, 1993).

Gonzalez-de los Santos et al. (2001) further increased the functionality of the poly(ether urethane) prepolymer. By carrying a reaction between isocyanate-terminated poly(ether urethane) and glycerol, a starlike activator was formed. Then it was used in anionic copolymerization of ϵ -caprolactam with caprolactam magnesium bromide being catalyst through a RIM process.

Yn and Ma (1994) synthesized block copolymer of poly(ϵ -caprolactam) – poly(butadiene-co-acrylonitrile). They first treated the amine end group of ATBN (amine-terminated butadiene acrylonitrile copolymer) with terephthaloyl biscaprolactam to form a polymeric activator. With caprolactam magnesium bromide being used as initiator, a block copolymer was formed which showed great improvement on notched Izod impact strength.

2.4 Nylon 6 Blends

2.4.1 Introduction to Polymer Blends

The approach of physically blending different polymers has seen an explosive growth during the past two decades (Turi, 1997). The purposes of blending the already-existing polymers instead of synthesizing new ones are based on consideration of cost saving and desired properties. The most attractive blends are those in which synergistic

behavior can be obtained, so that the properties of the blend are superior to those of individual polymers.

Polymer blends can be miscible (homogeneous) or immiscible (phase separated). Whether the properties of the blends are better than those of the individual components, or worse, or intermediate will be greatly determined by the miscibility of the blend.

2.4.2 Miscibility

For miscible blending of two or more polymers to happen, the necessary (though not sufficient) condition is that the Gibbs free energy of mixing ΔG_{mix} be negative or zero (Turi, 1997). ΔG_{mix} can be defined as:

$$\Delta G_{\text{mix}} = \Delta H_{\text{mix}} - T\Delta S_{\text{mix}} \quad (2-13)$$

where ΔH_{mix} and ΔS_{mix} are the enthalpy and entropy of mixing respectively, and T is the temperature. For ΔS_{mix} , there is always an increase in combinatorial entropy associated with mixing two substances. However, for a polymeric system with restrictions along the long chains, the entropy of mixing is small. Since the heat of mixing is generally positive, and larger than the $T\Delta S_{\text{mix}}$ term, the sign of ΔG_{mix} is very likely to be positive. That is why most polymer blends are immiscible.

In order for the ΔG_{mix} to be negative, a negative enthalpy of mixing is usually required, which means that specific intermolecular interactions are needed to produce exothermic heat upon mixing. The interactions can range from relatively weak forces (e.g. dipole-dipole) to relatively strong forces (e.g. hydrogen bonding). Therefore, it is

possible to produce a miscible polymer blend by selecting suitable polymers which contain interaction bonds to each other. For example, poly (vinyl phenol) (PVPh) was found to be miscible with ethylene-*co*-vinyl acetate (EVA) when the weight percentage of vinyl acetate (VAc) content in EVA is 70% (high density of hydrogen bonding between PVPh and VAc), but immiscible when the weight percentage of VAc is 25% (low density of hydrogen bonding between PVPh and VAc) (Coleman et al., 1989; Moskala et al., 1984 and 1985).

2.4.3 Compatibilization of Polymer Blends

Based on the thermodynamic study of miscibility, polymer blends tend to be immiscible which normally leads to either a two-phase morphology with one phase dispersed in the other continuous phase, or a morphology of co-continuous phases when the two components are present in similar concentrations. The interface between individual phases is a critical factor in determining the final morphology of the blend. The typical situation is that the interfacial tension between the two is very high which results in large dispersed particle sizes (i.e. to minimize total surface area for a given volume of polymer) and poor adhesion (due to small surface area) (Paul and Newman, 1978). In practice, a compatibilizer, also called “interfacial emulsifier”, which is often a block or graft copolymer is added or generated in situ during blending. The functions of the compatibilizer are to reduce the interfacial tension, produce finer dispersion, improve adhesion and more importantly stabilize the system by preventing the particles from coalescing (Hu et al., 1999).

2.4.4 Processing of Nylon 6 Blends and Their Compatibilization

Polymer blends can be processed in different ways such as extrusion, injection molding etc. For blending nylon 6 with other polymers, generally there are two major methods: extrusion or reactive extrusion and reactive casting. Since mid-1980s, a number of nylon blends have been developed. Polymers that have been blended with nylon 6 in commercial uses are: polyphenylene ether (PPE, for high temperature resistance, good melt flow and reduced water absorption); poly(acrylonitrile-*co*-butadiene-*co*-styrene) (ABS, for superior toughness and weatherability); polyolefin including polyethylene and polypropylene (for greater dimensional stability) and so on. However, the future growth of nylon 6 blends is limited due to the cost of making compatibilized blends (Davenport et al., 1998).

Hornsby and Tung (1995) used a twin-screw extruder to polymerize ϵ -caprolactam in the presence of polypropylene (with sodium caprolactamate catalyst and bis-acyllactam hexmethylenediamine activator). The so-called "reaction blends" were produced from simultaneous formation of nylon 6 and homogenization with secondary modifying polymer phase. When compared with the blends of nylon 6 and polypropylene (PP) by conventional melt blending, the reactive extruded blends showed unusual microstructures which exhibited greatly increased phase miscibility. The authors attributed the differences to the in-situ formation of a nylon 6-g-PP copolymer during the reactive extrusion.

Nanoblends (the size scale of one polymer dispersed in the other is below 100 nm) of polypropylene and polyamide-6 were developed in a co-rotating twin screw extruder by Hu (1999). The process consisted of anionically polymerizing ϵ -caprolactam in the matrix of polypropylene which was partially modified to act as growing center to initiate the nylon 6 chain. In this way, formation of nylon 6 and a graft copolymer of polypropylene and nylon 6 took place simultaneously in the continuous phase of PP, leading to compatibilized PP/nylon 6 blends.

Polyamide 6 and poly (2,6-dimethyl-1,4-phenylene ether) (PPE) blend (Chorvath et al., 1998) were prepared below melting point of polyamide-6 by using lactam magnesium bromide catalyst and ϵ -caprolactam blocked hexamethylene diisocyanate activator. Different amount of PPE was first dissolved into ϵ -caprolactam melt forming PPE/ ϵ -caprolactam solutions. By polymerization of caprolactam in the solution, PPE-polyamide-6 blends were formed with either the morphology of a continuous PPE and dispersed nylon 6 phase or vice versa, depending on the concentration of PPE in the blends.

2.4.5 Blends of Nylon 6 and Polycarbonate

Nylon 6 and polycarbonate are both popular engineering plastics with outstanding properties. Nevertheless, each of them has weaknesses that in some way might be compensated for by the other polymer. For example, nylon 6 has strong chemical resistance to most organic solvents while polycarbonate is very sensitive to solvent attack; nylon 6 has affinity to moisture which makes it difficult to maintain dimensional

stability, while the moisture absorption value for polycarbonate is very low. Therefore, it is attractive to see if any promising results could appear after combining these two polymers together by mechanical blending.

2.4.5.1 Experimental Observations

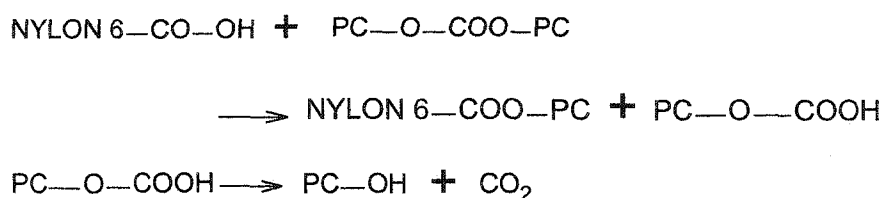
Gattiglia et al. (1989, 1990) investigated the melt blends of polyamide 6 and polycarbonate over the full range of compositions by using a single screw extruder at 260 °C. Their SEM characterization showed domains of clearly segregated homophases and voids between the two polymers which indicated no adhesion at the interface. DSC and Dynamic Mechanical Analysis (DMA) results indicated the existence of two glass transition temperatures corresponding to two separated phases. It was concluded that nylon 6 and polycarbonate are substantially immiscible in cases where polycarbonate constitutes the matrix (when its concentration is higher than 35% wt). The incompatibility was also shown by the mechanical properties (Young's modulus and breaking stress) which were much weaker than those of both of the pure polymers. However, the blend with 90% nylon 6 behaved differently from others which was reflected by the improved impact properties, this was attributed to the chemical interactions between the two polymers.

The above-mentioned chemical interchange reaction was studied by Cortazar et al.(1989) on the 50/50 mixture (by solution casting) of nylon 6 and polycarbonate by the use of a calorimetric technique. They found that, as the thermal treatment time of the sample at 250 °C became longer, the crystallization exotherm for pure nylon 6 became

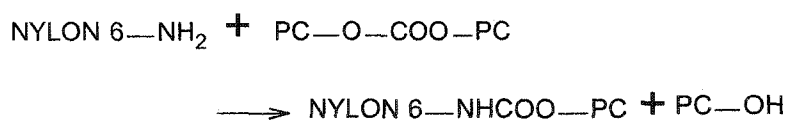
smaller and finally disappeared, and a single glass transition temperature was found after 57 minutes. This suggests the possible existence of copolymer formed by the reaction of nylon 6 and polycarbonate.

Gattiglia et al. (1992) and Valenza et al. (1994) prepared blends of nylon 6 and polycarbonate in a Brabender mixer at 240°C for different time intervals. Gattiglia et al. first proposed the possible interactions of nylon 6 with polycarbonate (shown in 2-14), i.e. acidolysis of the acidic terminals of nylon 6 on the carbonate group to form ester bonds; aminolysis of the amine terminals of nylon 6 on the carbonate group to form urethane bonds; amidolysis of the amide group of nylon 6. Their results suggested that the aminolysis is the main reaction.

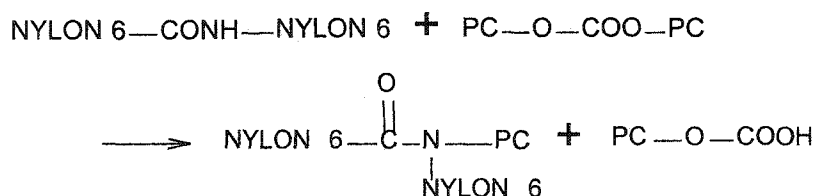
Acidolysis:



Aminolysis:



Amidolysis:



(2-14)

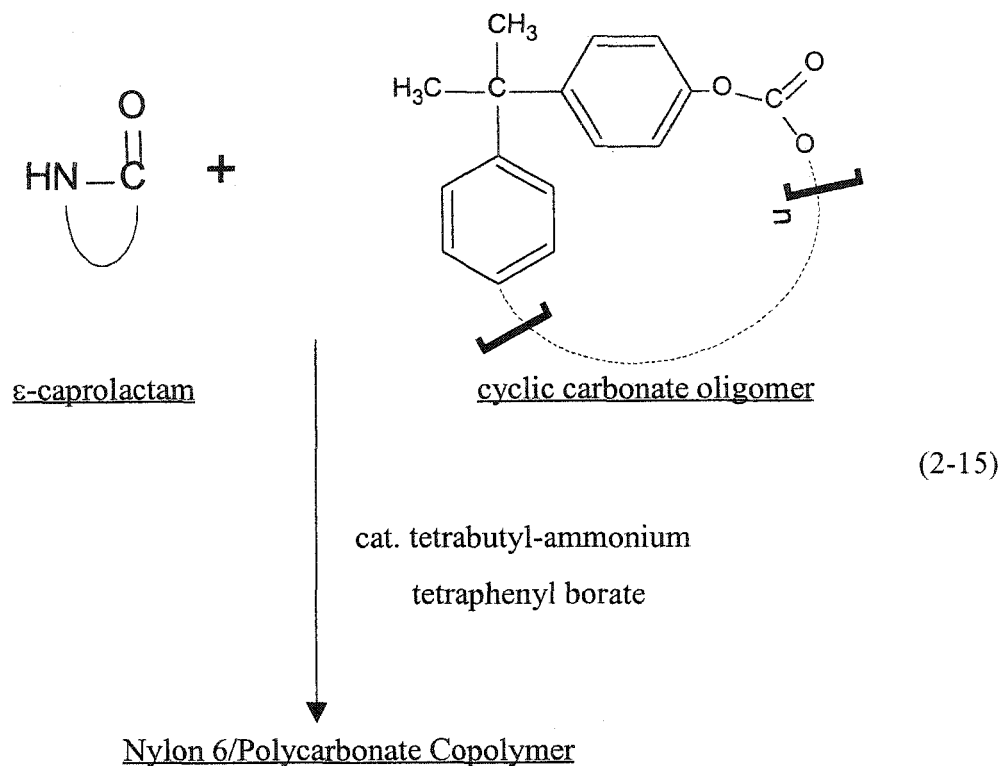
Valenza et al. (1994) further confirmed the above reaction by selecting nylon 6 samples with different concentration of the $-NH_2$ terminal group. Results showed that, as the $-NH_2$ concentration increased, the kinetics of the reactions increased. Montaudo et al. (1994) detected the urethane group interconnecting polycarbonate and nylon 6 by NMR and found that the amount of urethane units increased with mixing time.

2.4.5.2 Compatibilization of Nylon 6/Polycarbonate Blends

Because of the above mentioned problems, people have been looking for a suitable compatibilizer for nylon 6/polycarbonate blends. A block or graft copolymer of the two pure homopolymers could act as compatibilizing agents since they could migrate to the blend interface, thus decreasing the interfacial energy between the two phases and inducing compatibilization in the system.

Montaudo et al. (1996) synthesized ABA and AB nylon 6/polycarbonate copolymers by using diamino- and monoamino- terminated nylon 6 respectively. After that, they melt-mixed 2% of each individual copolymer with 75/25 (mol/mol) nylon 6/polycarbonate blend at 240 °C in a Brabender mixer. From SEM analysis, it was shown that the sizes of polycarbonate particles became smaller and more adherent to nylon 6 matrix when compared with the non-compatibilized control samples.

Li and Williams (1995) synthesized a multiblock compatibilizer for the blends of polycarbonate and nylon 6 by ring-opening polymerization of two cyclic chemicals: one is ϵ -caprolactam, the other is cyclic Bisphenol A-carbonate.



Then the copolymer was used to compatibilize the melt blends of nylon 6/polycarbonate, and a very fine morphology was found in SEM analysis.

A poly [styrene-*b*-(ethylene-*co*-butylene)-*b*-styrene] triblock copolymer functionalized by maleic anhydride (SEBS-gMA) was used by Horiuchi et al. (1996, 1997) as reactive compatibilizer in nylon 6/polycarbonate blends. It was known that compatibilizers with anhydride would form a chemical linkage through the reaction of anhydride group with the amine end group of polyamide 6. Thus during the melt processing, the functionalized copolymer reacted with polyamide 6 to produce chemical coupling of the phases and reduce the dispersed rubber (ethylene-*co*-butylene) particle

size. Their results showed that, the SEBS-gMA phase was formed at the interface of nylon 6-polycarbonate and there were no voids on the domain boundary.

Other compatibilizers used in nylon 6/polycarbonate blends include: poly(allyl-co-maleic anhydride) (Kim et al., 1996); nylon 6-polycarbonate block copolymer (Hathaway et al., 1988).

Chapter 3 Experimental

3.1 Instruments and Procedures

^{13}C Nuclear Magnetic Resonance (^{13}C NMR) spectra were recorded on a UNITY 500 spectrometer by VARIAN at 125 MHz under room temperature. Deuteriochloroform was used as solvent and internal standard.

Infrared (IR) spectra were obtained using a Magna IR 750 by Nicolet Instruments under Nic-Plam microscope. All spectra were recorded at room temperature with resolution of 4 cm^{-1} wavenumber.

Dilute solution viscosity was measured at $30\text{ }^{\circ}\text{C}$ by using Ubbelohde Viscometer based on ASTM method D 2857-95. Temperature of water bath was controlled by a thermoregulator. The solvent used was 90% formic acid. Four concentrations of polymer in solution ranging from $C = 0.04\text{g/dL}$ to $C = 0.15\text{g/dL}$ were prepared and filtered. For each sample, at least three measurements were taken to make sure data were reproducible within 0.5 second. Data were used to obtain intrinsic viscosity $[\eta]$ by extrapolation of $(\eta - \eta_s)/C\eta_s$ to $C \rightarrow 0$.

Scanning Electron Microscopy (SEM) was used to determine both the morphologies of the fracture surfaces of polymers and the extent of adhesion at the interface between

glass fibers and polymer matrix for glass-fiber reinforced polymers. Samples were first quenched in liquid nitrogen, followed by fracturing with a hammer; then the fresh surfaces were coated with evaporated carbon from a Hitachi HUS-4 Vacuum Evaporator; finally a Hitachi S-2700 SEM equipped with a PGT(Princeton Gamma-Tech) Imix Imaging system was used for SEM analysis.

Differential Scanning Calorimetry (DSC) data were obtained from a TA Instruments DSC 2910 equipped with Thermal Analyst 2200. A Liquid Nitrogen Cooling Accessory (LNCA) was connected to the system in order to achieve automatic and continuous temperature control. Nitrogen (Extra Dry grade) was used as purging gas. Generally, a sample weighing about 5-10 mg was pressed into a pair of nonhermetic aluminum pans by using a Sample Encapsulating Press. The temperature program was usually set as follows: sample was first equilibrated at 25 °C, then the temperature was increased at 10 °C/min to 280 °C. After staying isothermal for 3 minutes, the temperature was decreased at 10 °C/min to 20 °C. Sometimes another run of heating at 10 °C/min to 280 °C was done. Data of heat flow versus temperature was recorded. The melting temperature (T_m) corresponded to the temperature at the endotherm peak. The heat of fusion from the crystalline structure of nylon 6 part corresponded to the peak area between a linear baseline and the melting peak.

Gel Permeation Chromatography (GPC) was used by Mrs. N. Bu of the Wanke/Lynch lab in Chemical and Materials Engineering Building at the University of

Ablerta to determine the molecular weight and molecular weight distribution of different polycarbonate samples. GPC (Waters, GPCV 200) equipped with Refractive Index detector was run at 145 °C with trichlorobenzene as eluent at flow rate of 1.0 ml/min. Near-monodisperse HDPE was used as calibration standard.

Bulk density of the polymer samples at room temperature was measured by a method based on Archimedes' Law. A sample was cut into rectangular shape with dimension of 10mm × 1mm × 4mm. For each sample, at least two specimens were tested and averaged. The set-up of experiment was: an electronic balance, a beaker containing silicone oil of known density ρ_{oil} (here Dow Corning 710 Fluid was used), a copper wire with one end hanging from the bottom of the balance and the other end being hooked to a sample. Weights of sample in the air (W_{air}) and after immersing into the oil (W_{oil}) were measured. The bulk density of sample ρ_s was calculated as following:

$$\rho_s = \frac{\rho_{oil}}{1 - \frac{W_{oil}}{W_{air}}}$$

Tensile Properties for polymers were obtained at room temperature on a MTS (50,000 lb frame) equipped with Instron 8500 plus controller and Series IX software. An Instron loadcell of 2000 lbs. is used. The measurement procedure followed ASTM

method D 638-95 with an actuator speed of 1 mm/min. Tensile samples were machined by the Chemical and Materials Engineering Department Machine Shop into dimensions shown in Figure 3.1. Before testing, all samples were pretreated and kept in sealed containers for 48 hours either under dry air or under “wet” condition with relative humidity controlled by mixing glycerol and water in a certain volumetric ratio.

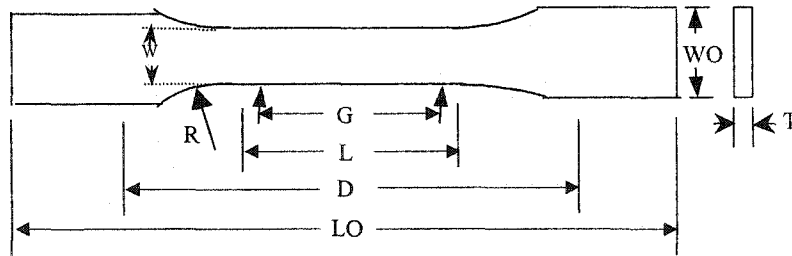


Figure 3.1 Dimension of Tensile Specimens (in mm)

| | |
|-----------------------------|----------------|
| W – Width of narrow section | 3.18 ± 0.5 |
| L-length of narrow section | 9.53 ± 0.5 |
| WO – Width overall | $9.53 + 3.18$ |
| LO – Length overall | 63.5 (no max) |
| G – Gage length | $7.62 + 0.25$ |
| D – Distance between grips | 25.4 ± 5 |
| R – Radius of fillet | 12.7 ± 1 |
| T – Thickness | 3.2 ± 0.4 |

Melt rheological properties were obtained from Rheometrics Mechanical Spectrometer 800 (RMS 800) with torque capacity of 2000 g.cm. Two parallel platens, a disk and plate with 25mm diameter were taken as the test geometry. To avoid the influence of moisture inside the polymers, all samples were dried in a vacuum oven at 70 °C for 24 hours before each measurement. In order to eliminate the possible degradation of samples in air during the compression molding process, about 1.2 g of bulk sample (original) was directly placed between the two platens, the top platen was lowered to reach the surface of sample, then the oven temperature was increased to 250 °C by nitrogen convection. The normal force was monitored to be within the permissible range while the top platen was being lowered. When the gap distance was reached, molten sample that was forced radially out of the edge of platens was wiped off quickly. All the measurements were conducted under nitrogen atmosphere. Dynamic shear mode was applied to molten samples at 240 °C or 250 °C so as to be above the melting temperature of nylon 6 (i.e. around 220 °C)

Thermal Gravimetric Analysis (TGA) was used to determine thermal stability of polymers. On a Dupont 950 TGA about 10-20 mg of polymer sample was heated at 5 °C /min from 30 °C to 500 °C under an extra-dry nitrogen atmosphere. Data of remaining weight versus temperature were recorded.

X-ray analysis was run on Philips X-ray Diffractometer (PW 1730, Holland Philips) at room temperature. An angle (2θ) of 10° to 35° was scanned at $0.1^\circ/\text{step}$ and retention time of $10 \text{ sec}/\text{step}$.

GC-MS analysis was conducted by using DB Wax capillary column (30 m-length and 0.24mm ID) in VISTA 6000 GC by VARIAN and VG7070E MS. Pre-purified helium was used as carrier gas. Column temperature was kept at 200°C . For each run $3 \mu\text{L}$ of sample was injected.

3.2 Materials

3.2.1 Chemical Reagents

Acetone (99+%, A.C.S. reagent) from Aldrich Chemical Company Ltd. was used as received.

N-acetylcaprolactam (99%, liquid) from Aldrich Chemical Company Ltd. was used as received.

ϵ -Caprolactam monomer is white hydrophilic flake. The anhydrous-grade ϵ -caprolactam was supplied generously by DSM Chemicals North America (in Augusta, GA). To prevent it from contacting with air moisture, ϵ -caprolactam was kept with Drierite (an indicating desiccant manufactured by W.A.Hammond Drierite Company

Ltd., generally containing 97% CaSO_4 and 3% CoCl_2) or phosphorous pentoxide (P_2O_5) in a vacuum environment before each use.

Chloroform-d (99.8+ atom % D) from Aldrich Chemical Company Ltd. was used as received.

Diphenyl carbonate (99%) from Aldrich Chemical Company Ltd. was used as received.

Formic acid (90% in water) from Fisher Scientific was used as received.

Grignard reagents isobutyl-magnesium bromide and isobutyl-magnesium chloride (both 2.0M in diethyl ether, from Aldrich Chemical Company Ltd.) were used as received.

Methylene chloride (99.6%, A.C.S. reagent) from Aldrich Chemical Company Ltd. was used as received.

Trifluoroacetic anhydride (99+%, liquid) from Aldrich Chemical Company Ltd. was used as received.

3.2.2 Polymers

Nylon 6 pellets from Scientific Polymer Products Inc. were dried at 70 °C under vacuum for 24 hours before each use. This grade has a M_w of approximately 10,000, density at 20 °C of 1.12 g/cm³, T_m and T_g at 221 °C and 62.5 °C respectively.

Three amorphous Bisphenol-A polycarbonate samples were obtained. The one (SPP) in pellet form was purchased from Scientific Polymer Product Inc.. It has a M_w of around 45,000, density at 20 °C of 1.2 g/cm³ and T_g of 149 °C. The other two samples (GE-S11AP and GE-S3G100) in the form of powder were supplied by GE Plastics (Burkville, AL) with no detailed characterization data. The GPC analysis results for these 3 samples are listed in Table 3.1 and shown in Figure 3.2.

Table 3.1 GPC Result Summary for 3 Polycarbonate Samples

| Sample | Retention Time (min) | M_n | M_w | M_z | M_w/M_n |
|-----------|----------------------|-------|-------|-------|-----------|
| SPP | 26.542 | 11000 | 21000 | 31500 | 1.91 |
| GE-S11AP | 26.854 | 7500 | 16500 | 25000 | 2.20 |
| GE-S3G100 | 26.32 | 13600 | 24400 | 36500 | 1.79 |

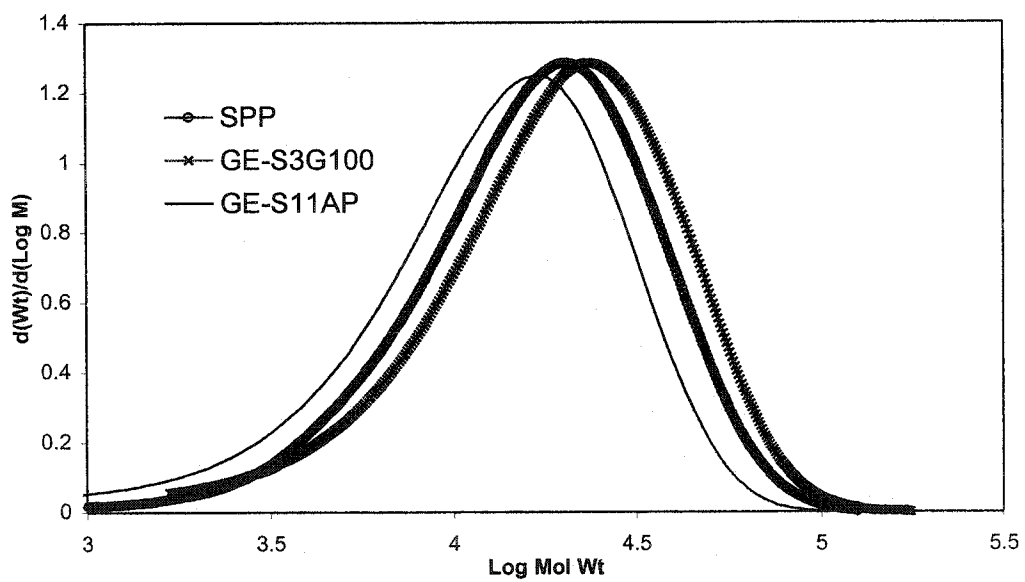


Figure 3.2 GPC Analysis for 3 Polycarbonate Samples

In order for polycarbonate to be dissolved into molten ϵ -caprolactam easily, amorphous polycarbonate samples went through the following pretreatment: (1). Dissolve desired amount of polycarbonate samples into methylene chloride; (2). Add the above-mentioned solution drop by drop into pure acetone in a glass flask to precipitate polycarbonate, while keep stirring the mixture vigorously; (3). Filter the solid formed in (2), then dry sample at 70°C under vacuum until constant weight. The so-produced powder has the same molecular weight as in its original form, while it has semi-crystalline structure with melting temperature at 223 °C. The DSC data for both polycarbonate pellet and powder of SPP product are shown in Figure 3.3, with both T_g and T_m (for SPP powder) visible. Another evidence of the existence of crystalline structure in SPP Polycarbonate powder was from X-ray analysis shown in Figure 3.4, where the diffraction pattern for polycarbonate pellet showed an amorphous halo while the one for SPP polycarbonate precipitated powder showed two sharp crystalline diffraction peaks around 2θ values of 17.1 and 25.3 degrees.

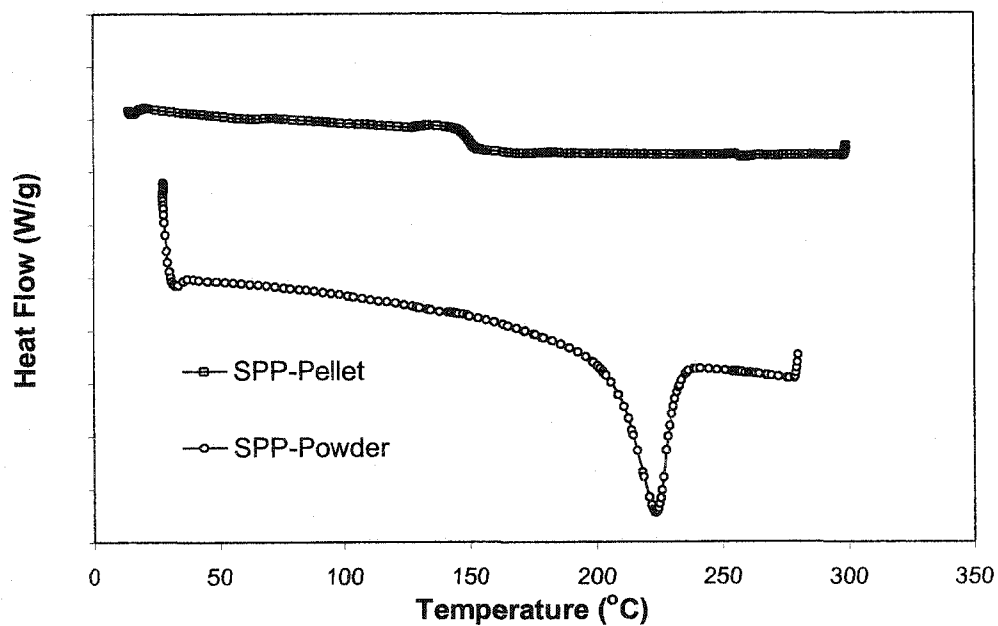


Figure 3.3 DSC Thermograms of Polycarbonate Pellet and Powder
(First heating at 10°C/min, Nitrogen)

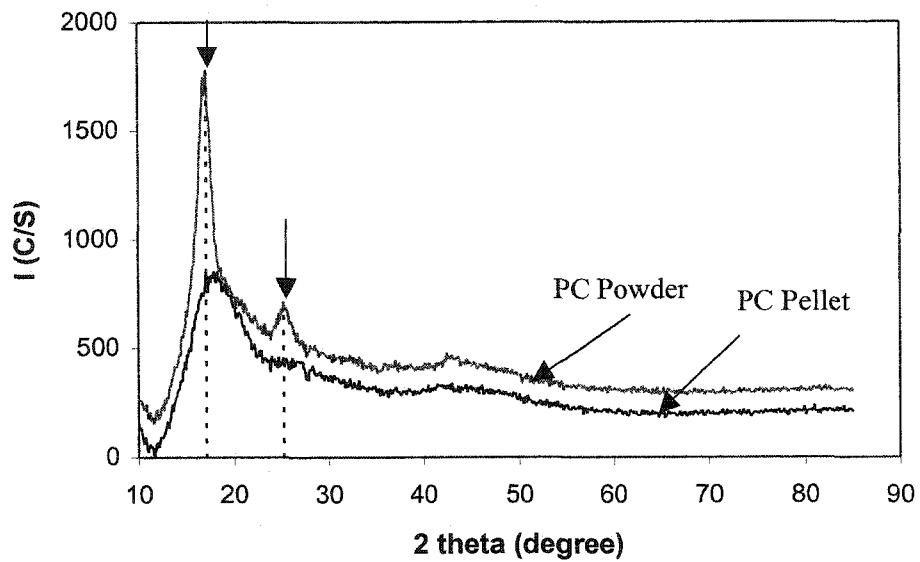


Figure 3.4 X-Ray Diffraction Pattern for SPP Polycarbonate Powder & Pellet

(Note: Vertical arrows designate the crystalline peaks of the precipitated PC powder)

3.3 Synthesis of Nylon 6 Homopolymer

3.3.1 Synthesis of Nylon 6 by Using N-Acetylcaprolactam as Activator

100 g of anhydrous ϵ -caprolactam was added to a 250 ml Erlenmeyer flask with a magnetic stirrer bar. A nitrogen blanket was introduced to the flask to purge air and maintain an inert atmosphere. Then the flask was put into an oil bath of 130 °C where the bath temperature was kept constant through a thermocouple connected to a digital readout and an on-off controller. After ϵ -caprolactam was melted ($T_m = 70$ °C), 3ml of 2.0M isobutyl-magnesium bromide solution in diethyl ether was introduced to the melt by syringe. The mixture was stirred until a homogenous solution was formed and there were no visible bubbles of released isobutane. Then 1ml of N-acetylcaprolactam was injected to the system while stirring the mixture vigorously for one minute. The mixture became opaque within 2 minutes. The viscosity of the mixture rapidly increased, and solidification occurred in 5-10 minutes. Finally the mixture was kept at the same temperature under the nitrogen purge for another 2 hours before it was taken out of the oil bath and cooled to room temperature.

3.3.2 Synthesis of Nylon 6 by Using Diphenyl Carbonate as Activator

Two 250 ml glass flasks were used, each containing 50 g of ϵ -caprolactam. Nitrogen gas was introduced to each flask to maintain an inert environment. The two flasks were put into a 150 °C oil bath. After ϵ -caprolactam melted, 3 ml of 2.0 M isobutyl-magnesium bromide solution in diethyl ether was introduced into one flask and 1

g of diphenyl carbonate was added to the other flask. After both mixtures became homogenous solutions, contents of the two flasks were mixed together with vigorous stirring for two minutes. Finally the mixture was kept at the same temperature and under nitrogen for another 2 hours to ensure complete reaction.

3.4 Synthesis of Nylon 6–Polycarbonate Copolymer

Two glass flasks each containing 50g of anhydrous-grade ϵ -caprolactam were put into a 130 °C oil bath. Nitrogen flow was introduced to both flasks to maintain an inert atmosphere. After ϵ -caprolactam was melted, 1 g of polycarbonate powder was added to one flask and 4 ml of 2.0M isobutyl-magnesium bromide solution in diethyl ether was added to the other flask. After two homogenous solutions were formed, they were mixed together with vigorous stirring for 2 minutes. The viscosity of the solution increased rapidly and the mixture solidified within 5 minutes. Finally, the mixture was kept at the same temperature for another 2 hours to ensure a complete reaction, while a nitrogen purge is maintained.

As will be discussed later, the above procedure was sometimes used with other oil-bath temperatures to observe the effect of this parameter.

Chapter 4 Synthesis and Characterization

4.1 Comparison between “Liquid-Liquid” and “Liquid-Solid” Methods

4.1.1 Reaction System of Liquid-Solid Method (L-S)

Previously in our research group, a polymer made from ϵ -caprolactam with polycarbonate (Sankholkar, 1996) showed better tensile properties than those for pure nylon 6, and there was good adhesion at the interface between the polymer and glass in the glass-fiber reinforced composites. Similar polymers were synthesized in my work for use in comparing polymers made differently with these.

The synthesis process was as following: firstly monomer ϵ -caprolactam and catalyst isobutyl magnesium bromide were heated up under nitrogen blanket above the melting temperature of ϵ -caprolactam, then polycarbonate powder was added directly into the molten caprolactam to make the solution. While the mixture was kept mixing at a constant temperature, the polymerization process progressed rapidly; and within several minutes the whole mixture solidified.

Since polycarbonate was added to the system in the form of solid powder, this method was labeled as “liquid-solid method”. The “L-S” method has certain disadvantages for commercial production, primarily because the handling of solid-state ingredients is inconvenient and also because the mixing cannot be done homogeneously.

4.1.2 Reaction System of Liquid-Liquid Method (L-L)

There are two factors that need to be considered in the “liquid-solid method”: firstly, due to the fast kinetics of the reaction system, the time from the addition of polycarbonate to the formation of final solid polymer is short; secondly, it takes time for polycarbonate powder to be completely dissolved into ϵ -caprolactam (on the molecular level). Therefore, in order to make sure there was a good dissolution of polycarbonate into ϵ -caprolactam, a “liquid-liquid” method is here proposed.

In this method, half the total amount of ϵ -caprolactam was melted and mixed with catalyst to form a compound while the other half was melted separately and used to dissolve polycarbonate. Both mixtures were kept above the melting temperature of ϵ -caprolactam (i.e. 70 °C) under nitrogen blanket until clear solutions were formed, indicating complete dissolution. Then the two solutions were poured together with continuous stirring at a desired temperature (95-160 °C) to form a homogeneous solution before it reacted and became more and more viscous and finally solidified.

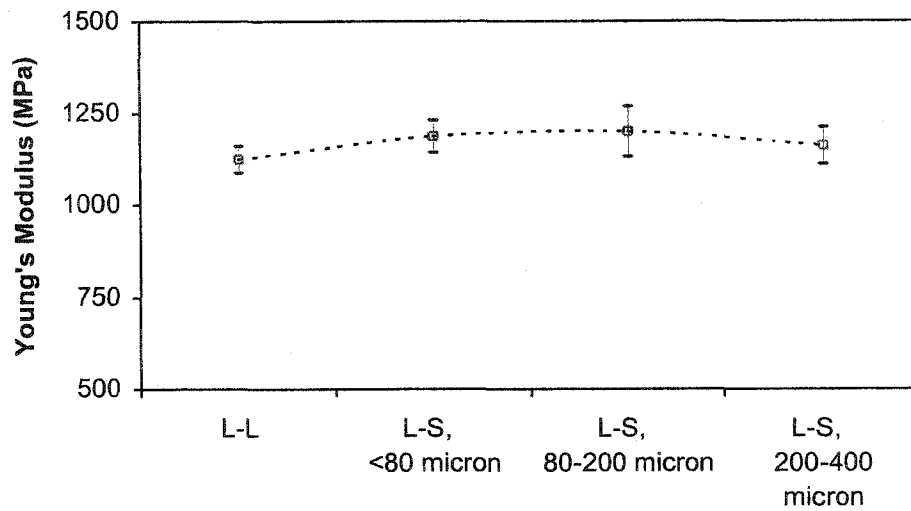
4.1.3 Effect of Polycarbonate Particle Size

To compare the “L-L” and “L-S” methods, the effect of particle size of the polycarbonate powder in “liquid-solid” system was considered. Polycarbonate powder (pellets from SPP, produced as described in 3.2.2) was sieved into three batches with different particle sizes, i.e. less than 80 micron, 80 to 200 micron, and 200 to 400 micron.

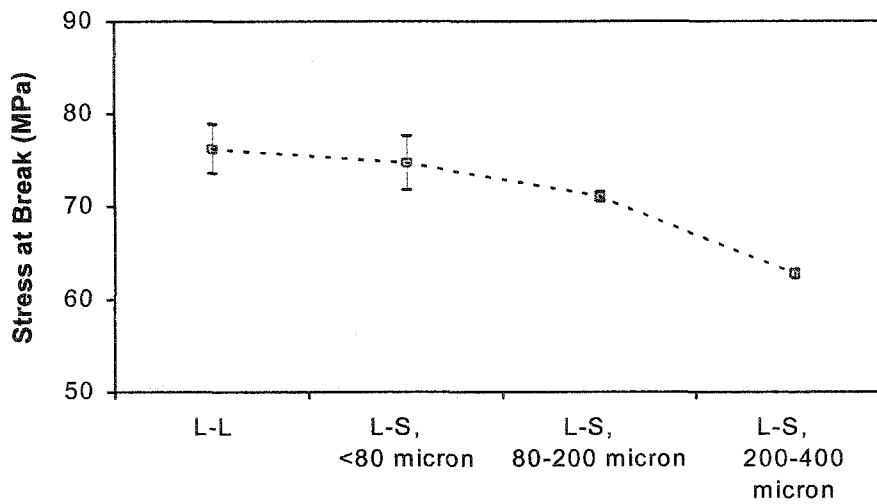
The same "L-S" reaction procedure was conducted for each of the three powder batches. The oil bath temperature was set at 140 °C (the effect of oil bath temperature will be discussed in the next chapter). Erlenmeyer flasks of 250 mL were used for each synthesis. The reactant composition included 75 g of ϵ -caprolactam (0.663mol), 0.75 g of SPP polycarbonate powder and 6 ml (12 mmol) of isobutyl-magnesium bromide (2M solution in diethyl ether). After polycarbonate powder was poured into the solution of ϵ -caprolactam and catalyst, the stirrer was kept moving vigorously for 1.5 minutes to ensure a good dispersion of polycarbonate powder. The whole mixture would become more and more viscous which indicated the chain growth of Nylon 6 part. After mixing, the flask containing the whole mixture was kept in the oil bath of same temperature for a total of 2 hours before being cooled in the air to room temperature.

A reaction of same composition as the above was conducted by "L-L" method. Then three "L-S" samples and one "L-L" sample were cut into dumbbell specimens for tensile testings. Each sample had three or four specimens and was kept in an environment of 44% RH (Relative Humidity) and 21.5 °C before the tensile test.

Tensile tests on the four samples were conducted at room temperature according to ASTM D638-95 at an extension speed of 1mm/min. Original results and stress-strain curves for each sample are presented in Tables A.1 (a)-(d) and Figures A.1 (a)-(d) in Appendix A). These results were averaged over three or four specimens, and are shown on the following pages in Figs. 4.1-(a) to (d). It is shown, for Young's Modulus in Fig.4.1-(a), that although the sample made by "L-L" method was slightly smaller than



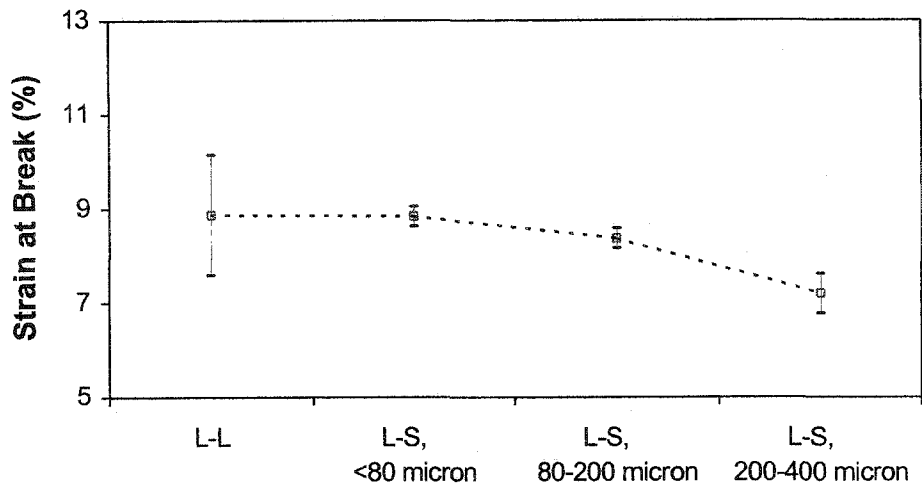
(a)



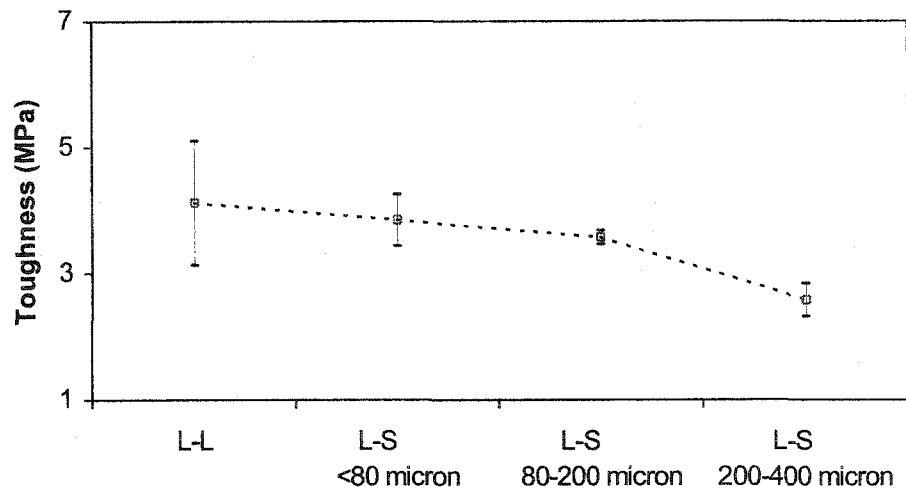
(b)

Fig. 4.1 Tensile Properties of Samples Made by “L-L” Method and “L-S” Method with Different Particle Size of Polycarbonate Powder. (a). Young’s modulus; (b). Tensile strength at break;

(Note: error bars correspond to average value \pm standard deviation)



(c)



(d)

Fig. 4.1 Tensile Properties of Samples Made by “L-L” Method and “L-S” Method with Different Particle Size of Polycarbonate Powder. (c). Tensile strain at break; (d). Toughness.

(Note: error bars correspond to average value \pm standard deviation)

the other three samples, there was not much difference in magnitude between the four of them. For the other tensile properties such as tensile stress at break, tensile strain at break and toughness, the “L-L” sample shows properties similar to or better than the “L-S” samples. It should be noted that, as the particle size in “L-S” samples decreased, the tensile stress at break increased greatly which is shown in Figure 4.1-(b). The sample with particles of “<80 micron” also tended to have higher values in tensile strain at break and toughness than the other, i.e. samples of “80-200 micron” and “200-400 micron” [see Fig.4.1-(c) and (d)]. The trends in Fig. 4 indicate a well-behaved effect of particle size, with the “L-L” data anchoring the trend in the imaginary limit of particle size $\rightarrow 0$.

To check if microscopic properties such as crystallinity play a role in making differences in tensile properties, DSC tests were run on the three “L-S” samples at rate of 10 °C/min under a nitrogen atmosphere. Table 4.1 shows values for the melting temperature and heat of fusion on first heating (detailed thermograms are shown in Appendix Figure A.2-A.4). As the particle size increased, the heat of fusion increased from 75.4 J/g (for “<80 micron”) to 81.5 J/g (for “200-400 micron”) while the melting temperature showed a slight increase of 2.25 °C from sample of “<80 micron” (213.70°C) to sample of “200-400 micron” (215.95°C). This might indicate that the degree of crystallinity for the produced polymer increased when larger size of polycarbonate powder was used in “L-S” method.

Table 4.1 DSC Results for “Liquid-Solid” Samples

(First Heating, 10 °C/min)

| | Melting Temperature (°C) | Heat of Fusion (J/g) |
|------------|-------------------------------------|---------------------------------|
| < 80 μm | 213.70 | 75.4 |
| 80-200 μm | 214.16 | 77.3 |
| 200-400 μm | 215.95 | 81.5 |

It is often assumed that, for semicrystalline polymers, modulus and strength increases and elongation at break decreases with increasing crystallinity (Kohan, 1973). Although the sample with “200-400 micron” has a higher crystallinity than the one with “<80 micron” (as suggested by Table 4.1), its tensile stress is much lower than that of “<80 micron”. This excludes the factor of the extent of crystallinity, but allows an explanation based on defects in the crystal structures formed from larger polycarbonate particles that may not have been distributed homogeneously, i.e. the influence of the particle size of polycarbonate powder in the “L-S” method.

As it was mentioned in 4.1.2, the two competing time factors for polycarbonate to be involved in the reaction of “L-S” method are the time for polycarbonate to be

dissolved into ϵ -caprolactam, and the time for the viscosity of reacting mixture to be built up. Although it is unclear what happens microscopically, it is positive to say that the smaller the particle size of polycarbonate in the melt of ϵ -caprolactam is, the better tensile properties it has. Therefore, the "L-L" method is preferred. *All the polymerizations reported hereafter were conducted by this method.*

4.2 Possible Reaction Mechanism

4.2.1 The Role of Polycarbonate

In the process of "L-L" polymerization, there are two solutions: one is catalyst (i.e. isobutyl magnesium bromide) dissolved in ϵ -caprolactam melt; the other is polycarbonate dissolved in ϵ -caprolactam melt. Since ϵ -caprolactam as monomer and Grignard reagent as catalyst have been used often in the anionic polymerization to produce nylon 6, it is important to learn what role polycarbonate plays in this process. There are three observations that need to be mentioned:

Firstly, a model experiment is done to show if only the mixture of monomer ϵ -caprolactam and catalyst can make the polymerization happen. 75 g of ϵ -caprolactam (0.663 mol) and 4 ml of 2M isobutyl magnesium bromide (8 mmol) solution in diethyl ether were mixed inside a glass flask under nitrogen blanket. The flask was then put into an oil bath maintained at 130 °C. After 8 hours of mixing, the whole solution was still clear and the magnetic stirrer in the solution was movable, showing the viscosity did not

build up quickly. This is in accordance with the slow induction step in the anionic mechanism which is stated in 2.2.2.1 (in Chapter 2).

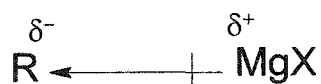
Secondly, when polycarbonate was dissolved into ϵ -caprolactam melt under nitrogen environment at 110 °C, its molecular weight (measured by vapor pressure osmometry) stayed constant, indicating that there was no reaction between polycarbonate and ϵ -caprolactam (Sankholkar, 1996).

Thirdly, when the solution of polycarbonate in ϵ -caprolactam was added into the above mentioned model polymerization system, even in a very small amount, the whole mixed solution becomes viscous very quickly.

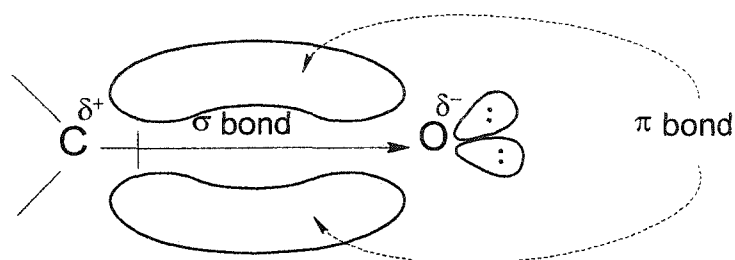
Based on the above observations, it is reasonable to deduce that there is chemical reaction between Grignard reagent and polycarbonate. The so-obtained product then acts as an activator to let the ϵ -caprolactam propagate at its end.

4.2.2 The Role of Grignard Reagent

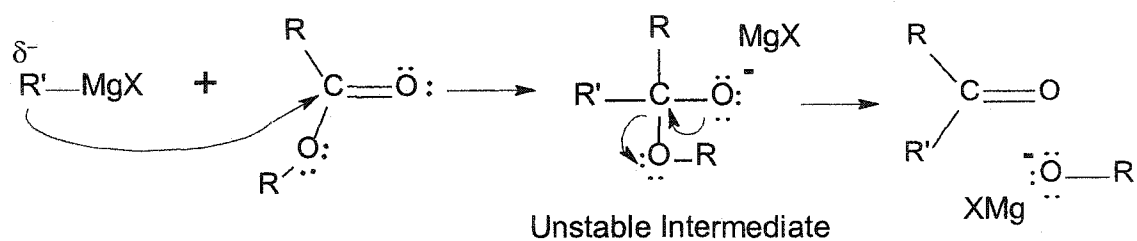
Grignard reagents, named in honor of the French chemist Victor Grignard, are a series of organomagnesium halides with general formula R-Mg-X (Wade, 1987) where R is alkyl, aryl, or other organic group, and X is halide. Due to the polarization of the carbon-metal bond, there is a partial negative charge on the carbon atom which is next to the metal compound.



On the other hand, the C = O double bond in the carbonate group -O-CO-O- is strongly polarized because oxygen is more electronegative than carbon. Therefore, there is a positive charge on its carbon atom.



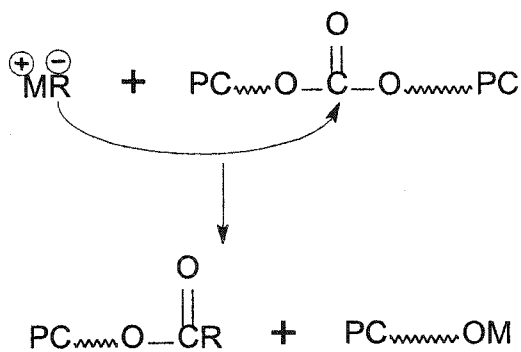
When the positive charged carbon in carbonyl group is attacked by a nucleophilic group from Grignard reagent, an addition reaction will happen. For example, when an ester is attacked by Grignard reagent,



Similar reaction applies to other organometallic reagents such as sodium borohydride (NaBH_4) and lithium aluminum hydride (LiAlH_4).

Mougin et al. (1992) discovered that, when synthesizing a di-block copolymer of poly(dimethylsiloxane) (PDMS) and nylon 6, the active lactamate anion from strong base (i.e. NaH or LiAlH_4) reacted aggressively with the electrophilic Si – O bond of PDMS, instead of propagating the chain of nylon 6. However, when they chose a catalyst with lower nucleophilicity such as alkali metal dialkoxyaluminum hydrides [$\text{LiAlH}_2(\text{OR})_2$], the so-formed anion was completely inert toward PDMS.

Wurm et al. (1992) also found that the active species of ϵ -caprolactam anion with alkali metal lithium or potassium as counterion (M^+) reacts with carbonate group of either monomer or polymer, as below:



Here, R is the ϵ -caprolactam anion. The first product has the structure of N-acylated caprolactam which is essential for activating the anionic ring-opening polymerization of ϵ -caprolactam.

4.2.3 Model Reaction-1

To prove our hypothesis that Grignard reagent may attack the polycarbonate chain, a model reaction was conducted. First, 0.8 g of polycarbonate (SPP) powder was dissolved into 30 ml of dichloromethane contained inside a glass flask at room temperature under nitrogen atmosphere. Then 5 ml of isobutyl magnesium bromide (2 M solution in diethyl ether) was introduced into the solution; after 3 hours of mixing, diluted hydrochloric acid (1N) was added to neutralize the mixture. Finally, the organic phase was separated and solvent dichloromethane was evaporated to dry the Grignard reagent-treated polycarbonate.

Both the original polycarbonate and the one after the above-mentioned treatment were sent for GPC analysis. Figure 4.2 showed the GPC results. It was clear that the polycarbonate chain had been scissored due to the nucleophilic attack of iso-butyl magnesium bromide. The corresponding molecular weight information is listed in Table 4.2. It should be noted that the values in Table 4.2 are not absolute ones because HDPE standards were used for calibration of the GPC column. Based on the information provided by the manufacturer, the actual weight-average molecular weight \overline{M}_w of the original polycarbonate (SPP) is about 45,000. Therefore, it can be deduced that the actual \overline{M}_w of the polycarbonate after treatment would be higher than the one shown in Table 4.2. However, the important fact that emerges is that molecular weight is reduced by Grignard reagent treatment. The treated PC also showed a narrower molecular weight

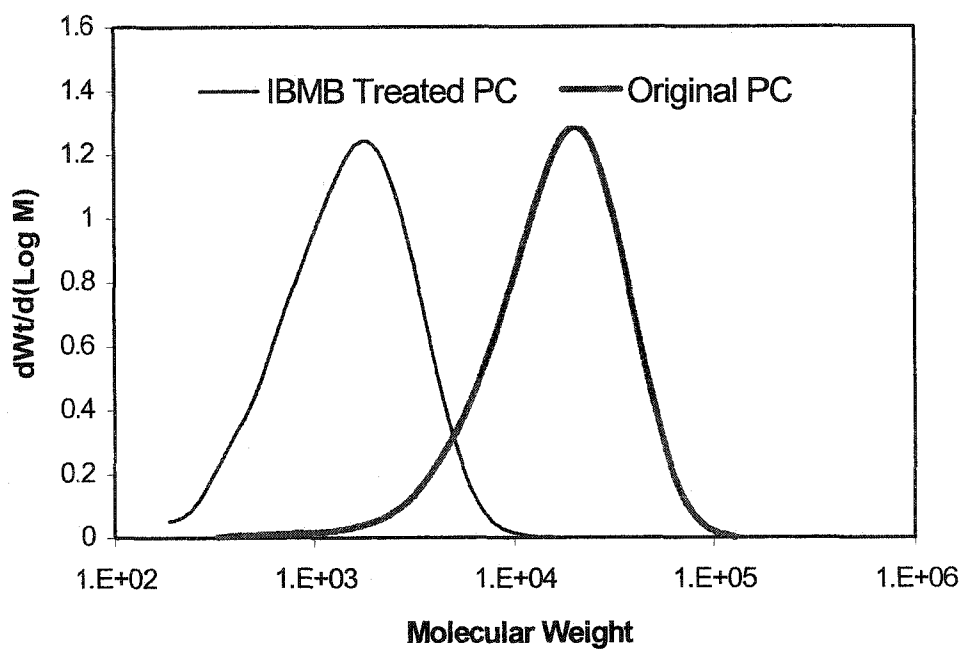


Figure 4.2 GPC Results of Original PC (SPP) and isobutyl magnesium bromide (IBMB) treated PC.

Table 4.2 GPC Result Summary (HDPE for calibration)

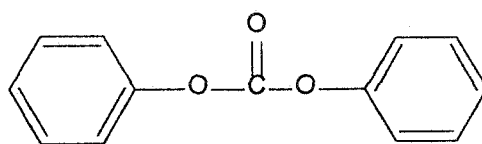
| Sample | M_w | M_n | M_w/M_n |
|-------------------|-------|-------|-----------|
| Original PC (SPP) | 21000 | 11000 | 1.91 |
| IBMB Treated PC | 1900 | 1100 | 1.69 |

distribution by a smaller value of M_w/M_n . This can be attributed to the fact that when there are random reactions (or attacks) along the polymer chain, the resulting product tends to have a "most probable" distribution of molecular weight. As shown in Figure 4.2, the mean value of molecular weight for the original polycarbonate shifted down to a lower mean value for the IBMB treated polycarbonate while the distribution of the molecular weight was even narrower for the treated one.

One might doubt that the caprolactam anion formed from the deprotonation of ϵ -caprolactam with Grignard reagent is more inclined to attack polycarbonate chains. If it is true, then the polycarbonate chain might be cut into very small pieces so that there would be no polycarbonate block in the product. In fact, this was not observed from the experiments. It was true that the polycarbonate chain was scissored to a certain extent; however, as soon as there was enough activator species produced, the polymerization of ϵ -caprolactam started and the viscosity of the whole mixture built up very fast which indicated the fast chain growth. Within minutes, the monomer conversion reached to a very high level (monomer conversion data will be shown in Chapters 5 and 6).

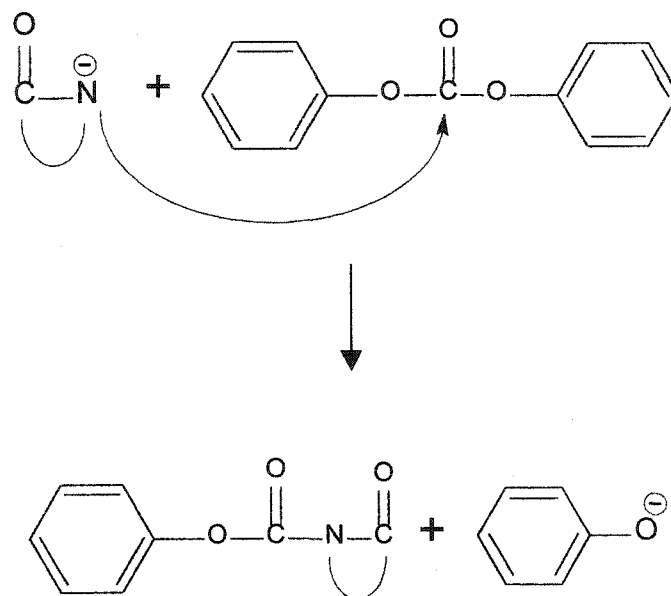
4.2.4 Model Reaction –2

A model polymerization was conducted by using diphenyl carbonate instead of polycarbonate in the reactive system. Diphenyl carbonate was chosen because it has a molecular structure similar to that of the repeating unit of Bisphenol-A polycarbonate.

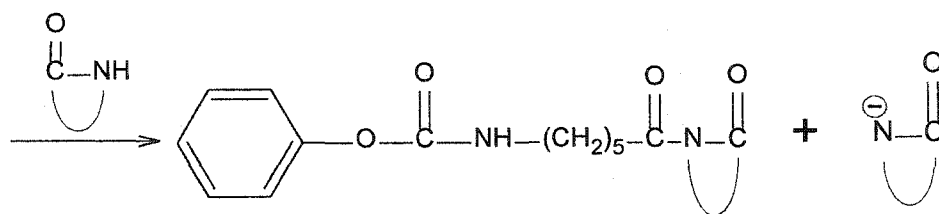
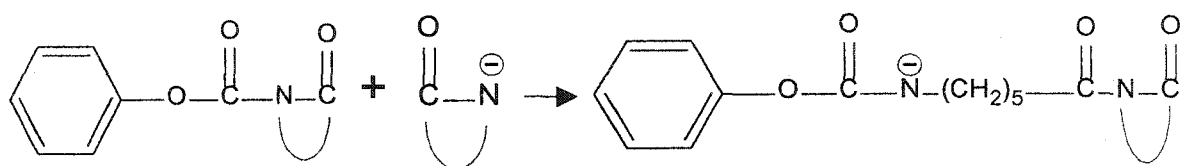


Diphenyl Carbonate (DPC)

As ϵ -caprolactam anion attacks diphenyl carbonate, the following reaction is expected:



The first product on the right side has the structure of an activator, the following polymerization is speculated as below:



⇒ ⇒ ⇒ Nylon 6

The polymer produced from the above model polymerization is basically *pure Nylon 6*. The DPC product was characterized by using FTIR, and both commercial nylon 6 and the polymer made with 1% (wt) polycarbonate were characterized for comparison. In Figure 4.3, all three samples show similar distinctive bands at wavenumber of around 1640 cm⁻¹, corresponding to the absorbance of carbonyl group, and two bands at 3300 cm⁻¹ and 1547 cm⁻¹ characteristic of the N-H group stretching and bending respectively. The only difference between the commercial nylon 6 and the two made in our lab is the intensity difference of N-H and C = O. The absorbance for both groups (N-H and C=O)

are at same intensity for the commercial one; while for the polymers made by polycarbonate and diphenyl carbonate (both through the anionic polymerization method), the absorbance for the C = O bond is stronger than that of the N-H bond. Other samples such as pure polycarbonate and nylon 6 with 0.1% DPC were also run. Those spectra were put into Figures A.6 and A.7 in Appendix A.

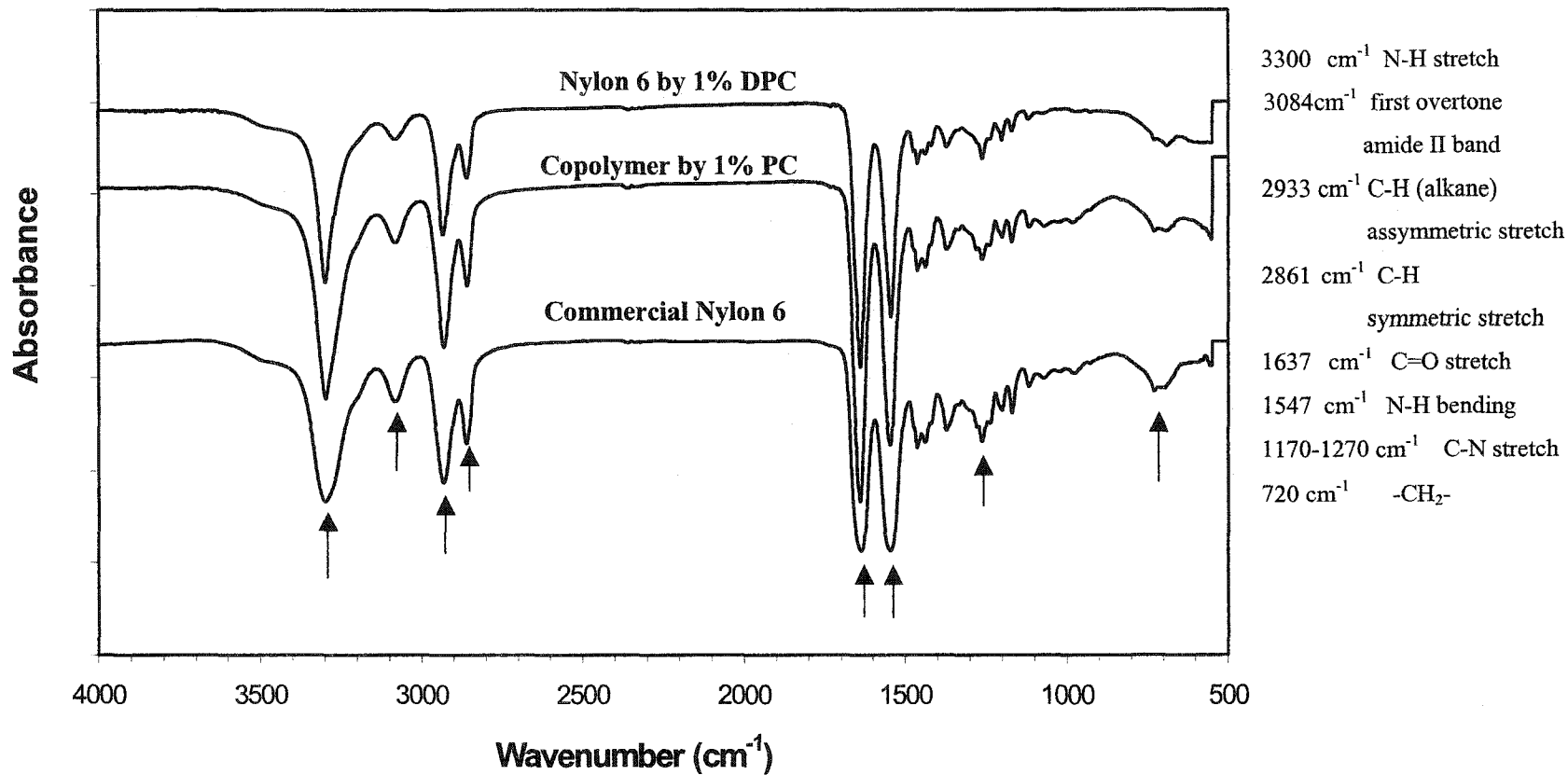
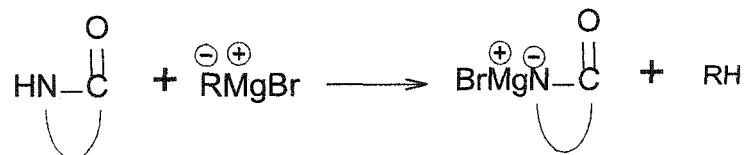


Figure 4.3 FTIR Spectra of Three Polymers
(Note: arrows show matching wavenumbers used to compare different polymers)

4.2.5 Possible Reaction Route

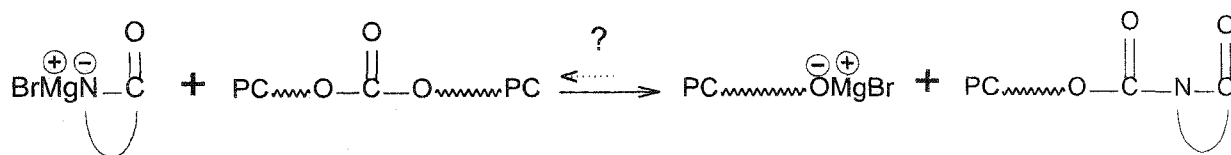
Based on the above evidence, the possible reaction route is proposed as follows:

Formation of anion:

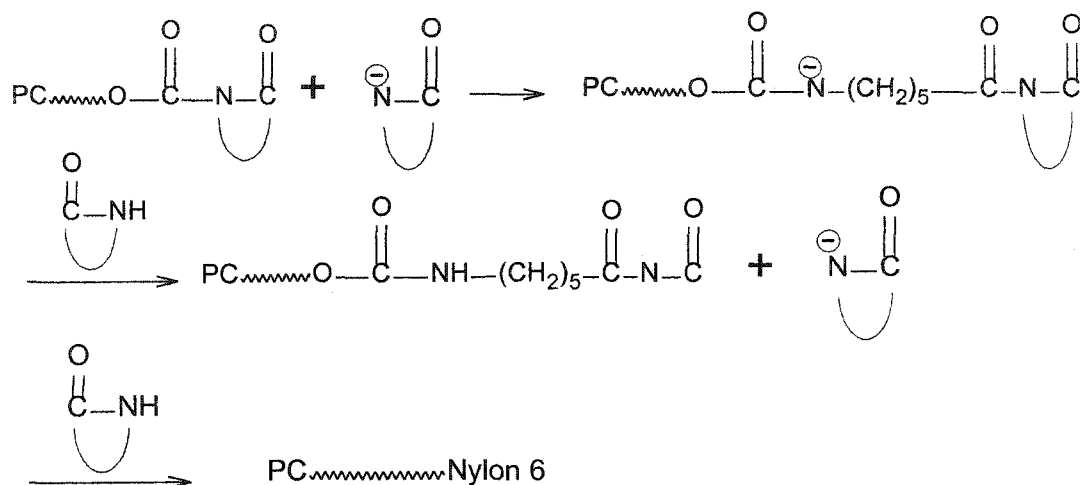


Where R: isobutyl

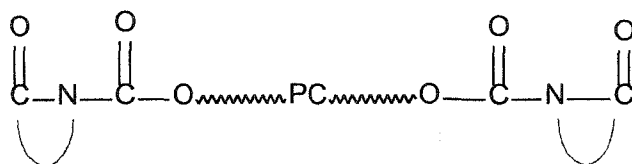
Formation of N-acylated caprolactam:



Propagation:



Possibly during the formation of activating species, a polycarbonate block with both ends capped with N-acylated caprolactam could be formed as:



Subsequent addition could lead to an ABA tri-block copolymer:



Therefore, the final solid product is a mixture of nylon 6/ polycarbonate block copolymer, polycarbonate and some unreacted monomer ϵ -caprolactam.

4.3 Characterization of the Copolymer Mixture

4.3.1 Solubility

Table 4.3 lists the common solvents for ϵ -caprolactam, nylon 6 and polycarbonate. The copolymer is soluble in the solvents for nylon 6, but not soluble in the solvents for polycarbonate. This indicates that the PC block in the copolymer is not very long. When the copolymer was placed into the solvents for nylon 6, the PC block can be “dragged” into the solvent along with the nylon 6 blocks. This can be used to explain the observation that it takes a longer time to dissolve the same amount of the copolymer than to dissolve the same amount of commercial nylon 6 and nylon 6 made from DPC. For example, 0.1 g of commercial nylon 6, nylon 6 made from DPC and copolymer made from polycarbonate were weighed and added into 20 ml of 90% formic acid at room temperature. Under stirring, commercial nylon 6 was the first to be completely dissolved (within 25 minutes); nylon 6 made from DPC was dissolved within 32 minutes; it took about 90 minutes to have the copolymer completely dissolved. It should also be noted here that the copolymers produced at high reaction temperature (e.g. 160 °C) tend not to be dissolved completely into solvents for nylon 6; instead, a solution with transparent gel-like materials was formed. This will be discussed in Chapter 5.

For comparison, when a nylon 6 blend with 2% polycarbonate was produced through melt-blending process (details in 4.3.2) was also added into 90% formic acid, a turbid emulsion-like solution was formed.

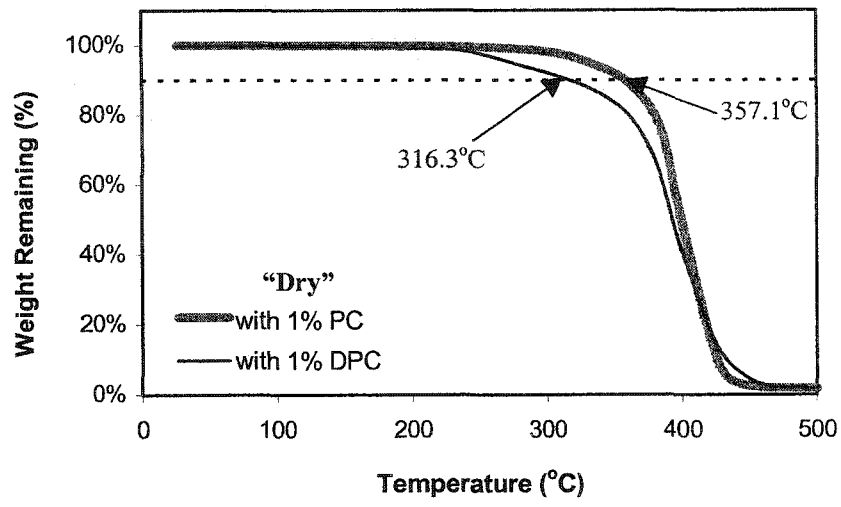
Table 4.3 Solubility of ϵ -Caprolactam, Nylon 6, Polycarbonate and Copolymer
in Some Solvents (where S stands for Soluble, I stands for Insoluble)

| | H ₂ O | Formic Acid (90%) | m-Cresol | Trifluoro- ethanol | Dichloro- methane |
|--|------------------|----------------------|----------|-----------------------|----------------------|
| ϵ-Caprolactam | S | S | S | S | S |
| Nylon 6 (Commercial) | I | S | S | S | I |
| Polycarbonate | I | I | I | I | S |
| Nylon 6 (by DPC) | I | S | S | S | I |
| Copolymer | I | S | S | S | I |

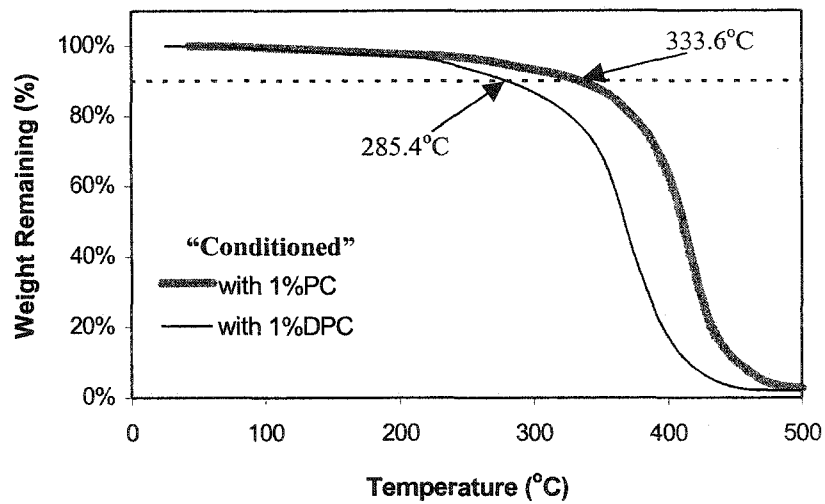
4.3.2 Thermal Gravimetric Analysis

Thermal gravimetric analysis was done on polymer samples made from polycarbonate and diphenyl carbonate of 1%wt composition. Both samples were first mixed with water at 60°C to extract the water-soluble content and then dried at 70°C under vacuum for 24 hours over P₂O₅. To see the effect of moisture on thermal degradation, samples were conditioned at room temperature and 44% Relative Humidity before being heated up to 500 °C at 5 °C/min under nitrogen atmosphere. Result is shown in Figure 4.4 (a) and (b). The temperatures at which samples lost 10% of original weights were marked with arrows on the figures.

It can be seen that the copolymer showed higher thermal stability than pure nylon 6 under both dry and moisture conditions. Pure polycarbonate had better thermal stability than nylon 6. Due to the existence of the polycarbonate chains, the dry copolymer (with 1% PC) in Figure 4.4-(a) showed a 10% weigh loss at 357.1 °C while the dry nylon 6 (with 1%DPC) had a 10% weight loss at 316.2°C. In Figure 4.4-(b) the conditioned copolymer (with 1% PC) showed a 10% weight loss at 333.6 °C while the conditioned nylon 6 (with 1% DPC) had a 10% weight loss at 285.4°C. For both samples there was a decrease for temperature corresponding to 10% weight loss from dry ones to conditioned ones. However, the temperature difference corresponding to 10% weight loss for the copolymer (between dry and conditioned) was about 13.4 °C while that for the nylon 6 (1% DPC) was 30.8 °C. There are two possible contributions for the weight loss of "wet" samples during the heating process in TGA. One is from the evaporation of moisture that has been absorbed inside the polymer; the other is from the thermal degradation caused



(a)



(b)

Figure 4.4 (a)-(b). TGA Results for Polymers: Nylon 6 Made from diphenyl carbonate (1%wt) and Nylon 6 Copolymer Made from Polycarbonate (1%wt). (a) Dry samples. (b). Conditioned samples.

(Note: Arrows designate temperatures at which 10% weight loss is achieved)

by hydrolysis or condensation (Nelson, 1976). Under "wet" condition the copolymer might contain less amount of equilibrium moisture because of the polycarbonate blocks, therefore the temperature corresponding to 10% weight loss for the copolymer would be higher than that for the pure nylon 6.

4.3.3 Morphology Studies

Scanning Electron Microscopy was used to study the internal morphology of the copolymer. To compare the difference of the copolymer from the blends of nylon 6 with other polymers, blends of nylon 6 with polystyrene and polycarbonate were made through different processing methods, and analyzed.

4.3.3.1 Morphology of Nylon 6/Polystyrene *in-situ* Reactive Blend

The blend of nylon 6 and polystyrene was made by using a similar anionic polymerization method for nylon 6. First, 2 g of polystyrene (PS) pellets (from Dow Chemicals) was introduced into 100 g of ϵ -caprolactam (0.884 mol) at 130 °C under nitrogen atmosphere. When polystyrene was completely dissolved, 3 ml of isobutyl magnesium bromide (2M solution in diethyl ether, 6 mmol) solution was injected into the solution. After the produced bubble stops releasing, 1 ml of N-acetyl caprolactam (7.05 mmol) was added to the solution. The viscosity of the solution increased very fast after the addition of activator. Within 5 minutes, the whole mixture became solid-like. Then it was kept in the oil bath of same temperature for another two hours before cooling in the air.

Since there is no interaction between polystyrene and isobutyl magnesium bromide, the so-produced polymer is in fact an in-situ reactive blend of nylon 6 and polystyrene. After cooling, the blend was quenched in liquid nitrogen, and fracture surfaces were created for SEM analysis (details in Chapter 3).

Figures 4.5 (a)-(c) show the SEM pictures of the nylon 6/polystyrene blend. Generally, there are two kinds of morphologies existing in the material. Polystyrene and nylon 6 are inherently incompatible; therefore, in the major morphology 2% polystyrene forms the dispersed phase (with particle sizes ranging from 3 μm to 30 μm) while nylon 6 forms the continuous matrix phase in Figure 4.5 (a) and (b). Another morphology is that in Figure 4.5 (c) polystyrene formed the continuous phase while nylon 6 formed dispersed phase with particle size around 6 μm (an image at higher magnification could be found in Figure A.8 in Appendix A).

It might seem surprising to observe the second morphology at PS concentration as low as 2%. However, when we check back the process of making this blend, it can be found that the whole mixture was kept at an oil bath of temperature at 130 $^{\circ}\text{C}$ for more than one hour after it solidified. It can be treated as a process of annealing (although temperature might not be isothermal which will be discussed in Chapter 5). It is known that polystyrene has a glass transition temperature of around 100 $^{\circ}\text{C}$, i.e. above 100 $^{\circ}\text{C}$ polystyrene segments have a certain mobility. Without the presence of a compatibilizer in the blend, polystyrene chains would tend to coalesce to form larger particles in order to reduce its interfacial tension.

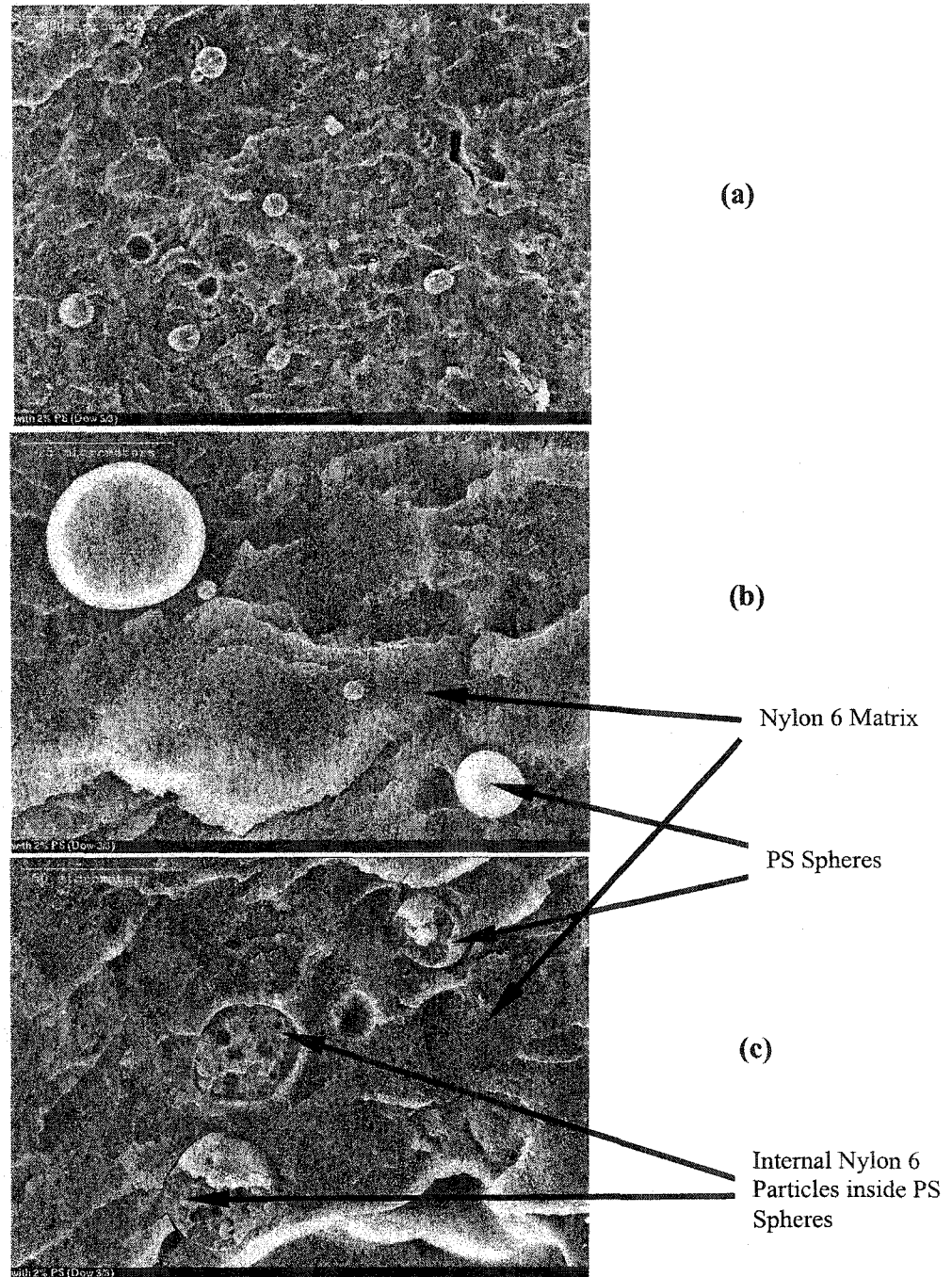


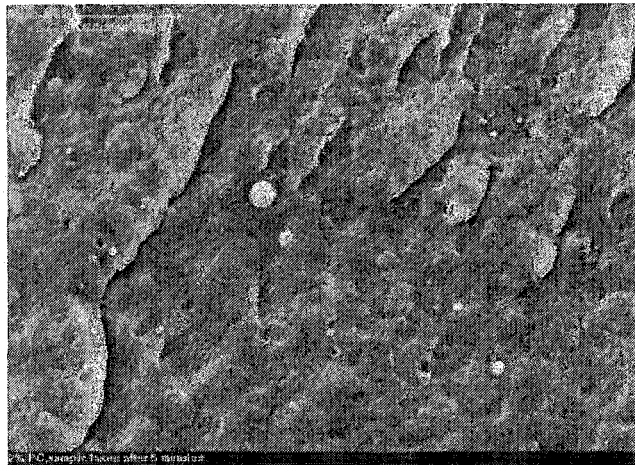
Figure 4.5 (a)-(c). SEM Analysis of Nylon 6/PS (2%wt) *in-situ* Reactive Blend. (a) & (b) Major morphology at low and high magnification respectively; (c) Second morphology (viewed at another location on the fracture surface showing that polystyrene spheres contain small internal cavities or particles of nylon 6).

4.3.3.2. Morphology of Nylon 6/Polycarbonate Melt Blend

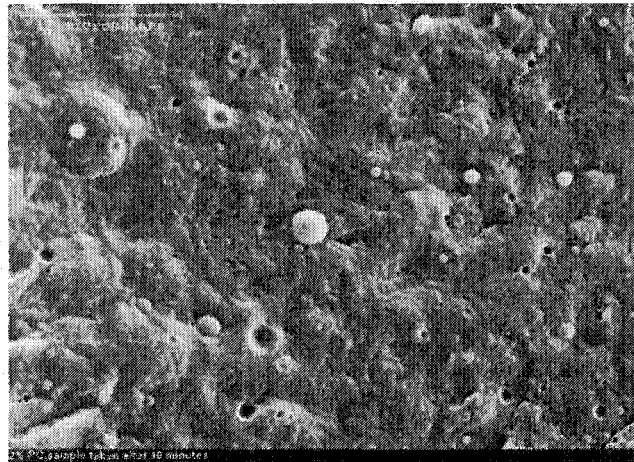
The blends of nylon 6 and polycarbonate were processed through melt blending. Both nylon 6 pellets ($\overline{M}_w \approx 10,000$, from Scientific Polymer Products, Inc.) with a melting point of 225 °C (DSC scan shown in Appendix Figure A.5) and polycarbonate powder ($\overline{M}_w \approx 45,000$) with a melting point of 225 °C were dried overnight at 100 °C under vacuum.

A Brabender mixer from C.W. Brabender Instruments Inc. was used. The blend procedures were as follows: first, the mixer was heated up to the set temperature (here, 240°C) while a nitrogen flow was maintained. Then the rotation of the blades was started and its speed was set at 30 rpm. Pre-weighed nylon 6 pellets (around 50 g) were quickly loaded into the mixer. After nylon 6 was completely melted, a certain amount of polycarbonate powder (2% and 10% in total weight for two separate batches) was added into the mixer. For each batch, three melt-blend samples were collected after mixing for 5 minutes, 10 minutes and 15 minutes respectively, then quickly quenched into liquid nitrogen. Fracture surfaces were created for SEM analysis.

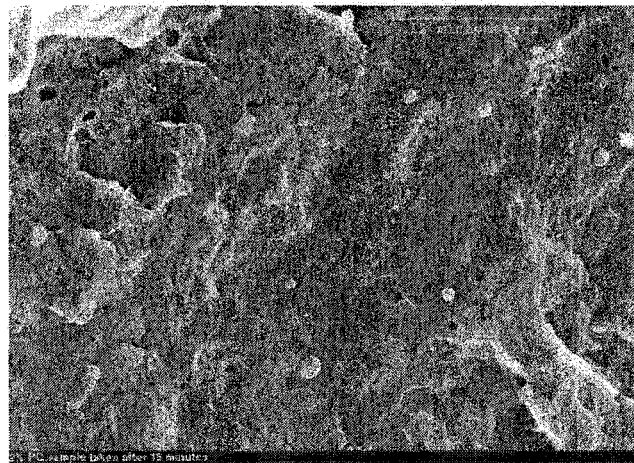
Figures 4.6 (a), (b) and (c) show the SEM pictures for the blends with 2% polycarbonate at 5, 10, 15 minutes respectively. All samples showed the morphology of polycarbonate particles dispersed into continuous nylon 6 phase. For the blends with 2% polycarbonate, the particle size of polycarbonate did not change much as the blending time got longer, ranging from 0.5 μm to 2.5 μm . On the other hand, for the blends with 10 % polycarbonate shown in Figures 4.7 (a) -(c), the particle size of polycarbonate



(a). Sample taken after 5 minutes of mixing



(b). Sample taken after 10 minutes of mixing

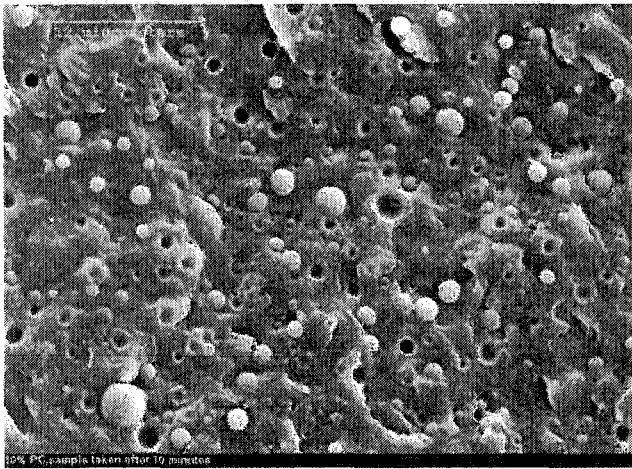


(c). Sample taken after 15 minutes of mixing

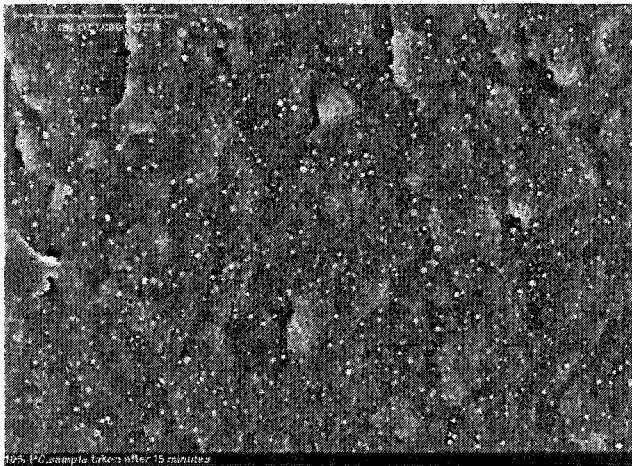
Figure 4.6 SEM Pictures of Nylon 6 /Polycarbonate Melt Blends (with 2% wt of Polycarbonate) after Mixing for (a). 5 minutes; (b). 10 minutes and (c). 15 minutes.



(a). Sample taken after 5 minutes of mixing



(b). Sample taken after 10 minutes of mixing



(c). Sample taken after 15 minutes of mixing

Figure 4.7 SEM Pictures of Nylon 6 /Polycarbonate Melt Blends (with 10% wt of Polycarbonate) after Mixing for (a). 5 minutes; (b). 10 minutes and (c). 15 minutes.

changed quite a lot. As the time of processing increased, the particle size of polycarbonate became smaller and more uniform. For the sample with 10% polycarbonate, after mixing for 15 minutes, the particle size was reduced to as little as 0.3 μm . The difference can be explained by the chemical interaction between nylon 6 and polycarbonate mentioned in 2.4.4.1. When there was more polycarbonate in the blend (i.e. higher concentration of -O-COO- group), the chemical interaction between the two pure polymers became more intense. More nylon 6-polycarbonate copolymer was formed which would act as compatibilizer in the blend. In this way the particle size of polycarbonate was reduced as more mixing (means more copolymer produced) was involved. On the other hand, the blend with 2%wt polycarbonate did not show a similar trend. This can be explained by the low concentration of polycarbonate. More SEM images at higher magnification are shown in Figures A.9-A.14 in Appendix A.

4.3.3.3 Morphology of Copolymer

As discussed before, the blends of two pure components made by two methods (with the same concentration of 2% wt for minor components) both show two-phase morphology. What about the morphology of the copolymer? Figure 4.8 shows the SEM pictures for the fracture surface of the copolymer made with 2%wt polycarbonate. The dispersed phase seen in Figure 4.6 and Figure 4.7 did not exist in this material. There is basically one phase which could consist of either the copolymer itself or a mutually miscible mixture of the copolymer and individual PC. An image taken at higher magnification is shown in Figure A.15 in Appendix A.

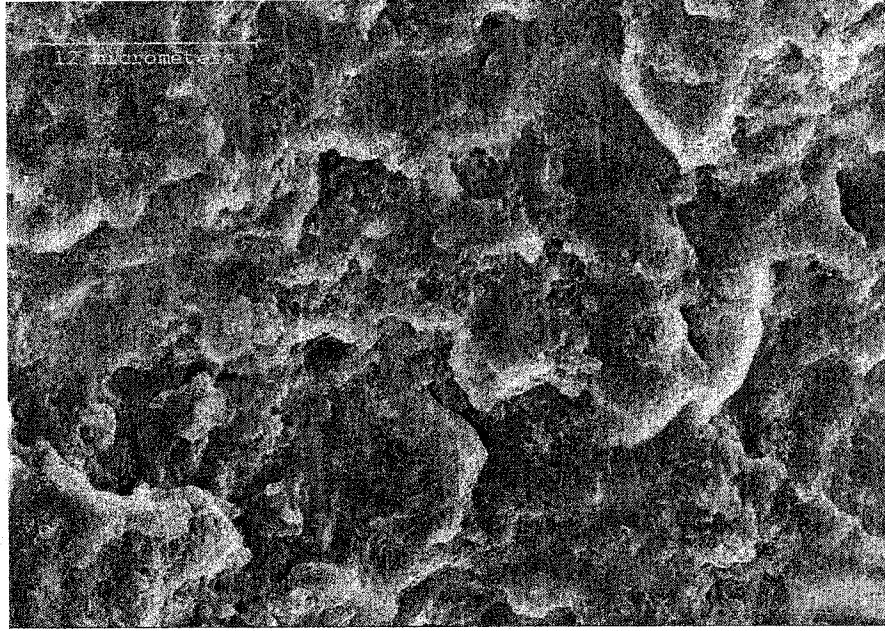
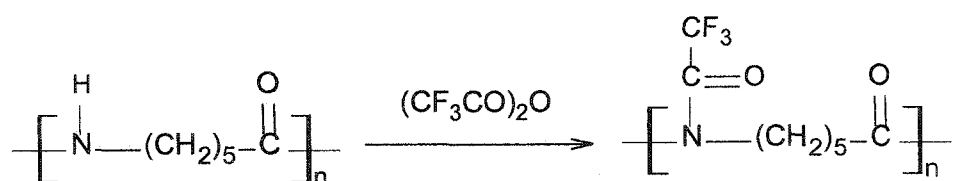


Figure 4.8 SEM Picture of Nylon 6/PC Copolymer
(with 2% wt PC).

4.3.4 ^{13}C and ^1H NMR

To characterize the chemical structure of the polymer, ^{13}C NMR analysis was done on a Bruker Spectrometer. Deuterated chloroform was used as solvent and internal standard. In order for the copolymer and Nylon 6 samples to be dissolvable into chloroform before the test, they had to be pretreated with trifluoroacetic anhydride (Jacobi et al., 1980).



Generally, around 0.1 g of sample was introduced into an Erlenmeyer flask containing dichloromethane. After stirring for 1 hour to dissolve the individual pure polycarbonate (which was not bonded with the copolymer), the sample was filtered and added to another flask containing dichloromethane. Then about 0.1 g of trifluoroacetic acid was added and vigorous stirring was started until the sample was completely dissolved. After that, stirring was continued for another hour to ensure all the polyamide units were trifluoroacetylated. Then the solvent, excess trifluoroacetic anhydride $[(\text{CF}_3\text{CO})_2\text{O}]$ and the produced trifluoroacid $[\text{CF}_3\text{COOH}]$ were evaporated under vacuum. The so-formed dry polymer sample was then dissolved into deuterated chloroform for NMR characterization.

The completion of this treatment can be proved by the disappearance of the peak corresponding to -NH- at chemical shift around 5.8 ppm in ^1H NMR for treated nylon 6 shown in Figure A 19 in Appendix A.

Figure 4.9 shows the ^{13}C NMR result for the trifluoroacetylated polymer made with 2% polycarbonate. The characteristic spectra for both nylon 6 and polycarbonate can be observed. This is an evidence that a copolymer of nylon 6 and polycarbonate was formed from the "L-L" process.

The ^{13}C NMR for pure Nylon 6 and polycarbonate were also run and they are attached in Figures A16 and 17 in Appendix A. ^1H NMR of polycarbonate and copolymer containing 2% polycarbonate are also shown in Figures A. 18 and 20 respectively.

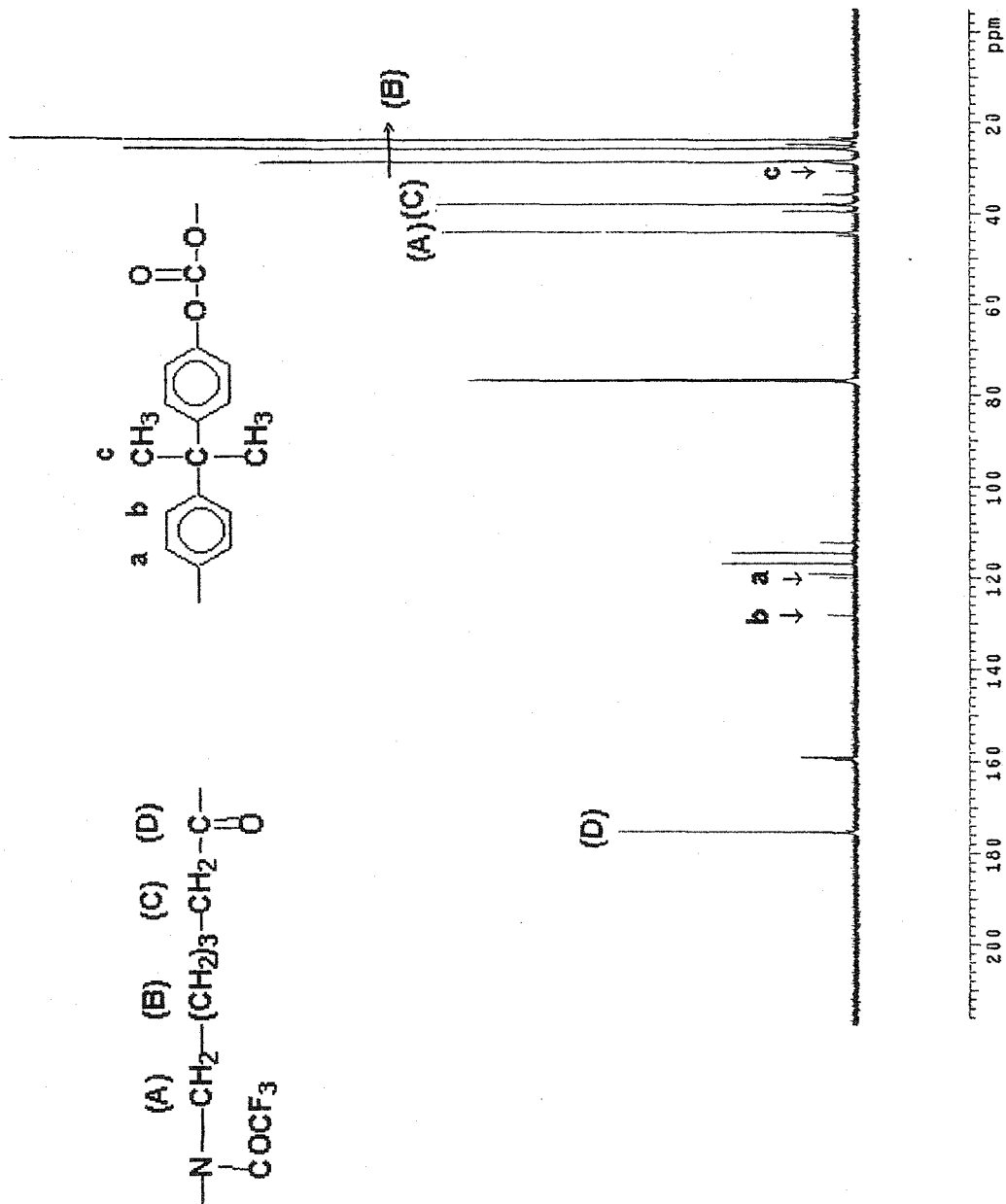


Figure 4.9 ¹³C NMR for a Trifluoroacetylated Copolymer (containing 2% Polycarbonate)

Chapter 5 The Effect of Reaction Temperature

5.1 Why is the Temperature Important?

In terms of reaction temperature, the anionic polymerization of ϵ -caprolactam can be categorized into two types: “high temperature”, featuring reactions above the melting point of nylon 6 (around 220 °C), and “low temperature”, also called “solid phase polymerization” (Kohan, 1995), with a reaction temperature between the melting point of ϵ -caprolactam (70 °C) and that of nylon 6. The process used in this study was the “low temperature” one. At the start of this process, the reactive mixture was in liquid phase containing the activator, catalyst and monomer melt. After nylon 6 chain of enough length was formed, the process of crystallization of nylon 6 or nylon 6 block in the copolymer started. At the end of this process, the mixture became solid phase containing the produced polymer and some unreacted monomer. The influence of reaction temperature can be manifested in several areas: monomer conversion, molecular weight, rate of polymerization and rate of crystallization etc.

5.1.1 Monomer Conversion and Molecular Weight

As was discussed in Chapter 2, one of the advantages of “solid phase polymerization” is its small amount of free monomer in the final product which does not need any further treatment for extracting monomer. It has been shown in Figure 2.1 that, as temperature decreases, the concentration of equilibrium monomer gets smaller.

However, the reaction temperature cannot be too low. The solid phase polymerization could not be successfully completed by Wichterle's system under 150 °C (Wichterle, 1959), because the solubility of nylon 6 in ϵ -caprolactam falls remarkably under 150 °C and the polymer begins to precipitate from the monomer melt with a relatively low molecular weight. Also, the active sites may be constrained by hydrogen bonds between the linear amides in the formed polymeric chain and thus the access of lactam anion in order for chain propagation is hindered (Sekiguchi, 1973).

5.1.2 The Process of Crystallization

It was reported (Khoury, 1957) that, in the cooling process of molten nylon 6, nylon 6 crystallized in a superstructure form of spherulites. The growth rate of the spherulites is temperature dependent, i.e., as temperature decreases, the growth rate of spherulites increases, reaching a maximum in the temperature range of 140 °C to 150 °C, and decreases upon further decrease of temperature (Reimschuessel, 1977). Figure 5.1 shows results (Magill, 1965) for isothermal spherulite growth rate on a nylon 6 sample ($\overline{M}_n = 24,700$) at different isothermal temperatures. It reached a maximum around 138 °C.

In the polymerization process used in this thesis, the way in which nylon 6 chain (block in the copolymer) crystallized was somewhat different from the crystallization process mentioned above. Frunze et al. (1980) studied the structure formation of nylon 6

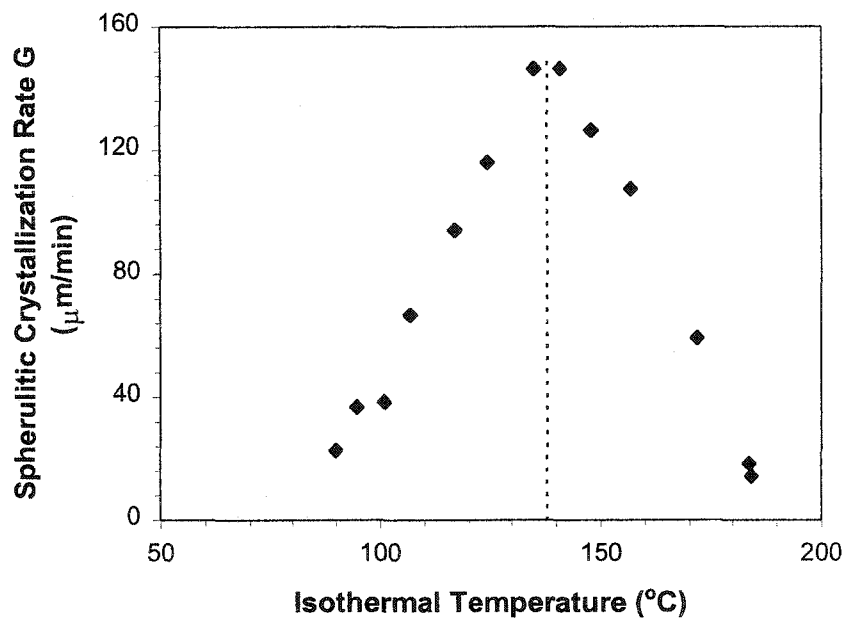


Figure 5.1 Spherulitic Crystallization Rates vs. Isothermal Temperature for Nylon 6

($\bar{M}_n=24,700$, held at 270 °C for 0.5 hr prior to crystallization, Magill, 1965)

during the anionic process under adiabatic conditions. It was found that the crystallization process comprised three successive stages: firstly, nylon 6 formed dendritelike structures with the space in between containing monomer; secondly, loose spherulites were formed under rapid crystallization with the dendritic structure serving as nuclei; the third step was slow secondary crystallization with a decrease in size and an increase in number for the spherulites. Frunze et al. (1981) also found that the initial temperature had a lot of influence on the three steps of crystallization, as well as the formation and size-changing of the spherulites.

5.2 Temperature Profile

It has been known that the process of anionic polymerization of ϵ -caprolactam would generate heat which comes from two sources: one is the heat evolved from the polymerization reaction; the other is heat of crystallization of nylon 6 chains (Frunze, 1981). Therefore, the temperature distribution inside the reaction mixture would not be uniform.

In the system used in this research, the reactive mixture was surrounded by an environment of constant temperature (i.e. oil bath temperature). While the center point of the mixture can be treated as an adiabatic point with the highest temperature, there would be a temperature gradient from the center point to the surfaces of the polymer. In this way the temperature profile is different for different locations inside the polymer.

To examine what happened to the "L-L" system, two flasks containing ϵ -caprolactam melt were prepared, one containing 35 g of ϵ -caprolactam and 12mmol isobutyl magnesium bromide and the other containing 40 g of ϵ -caprolactam with 0.75 g of polycarbonate powder (original pellets from Scientific Polymer Products, Inc.) dissolved into it. Both solutions were kept in the oil bath at the same temperature before being mixed together. The whole process was kept under extra-dry nitrogen environment. Right after the two solutions were mixed, a thermocouple was inserted into the mixture and the tip was placed at the center point of mixture. Meanwhile, the whole mixture was kept in an oil bath at the same initial temperature. The temperature of the center point was recorded as time went by. Four groups of temperature profiles were measured with different initial temperatures (i.e. oil bath temperatures). They are shown in Figure 5.2.

Generally, at the beginning, the temperature of the center point increased as time increased due to the generation of heat; after reaching a maximum, the temperature dropped gradually to the environmental temperature because of heat conduction caused by temperature difference. There are two factors that need to be noted: first, the difference of temperature (ΔT) from the initial to the maximum ranged from 40 °C for $T_{\text{initial}} = 160$ °C and $T_{\text{initial}} = 147$ °C to 56 °C for $T_{\text{initial}} = 104$ °C; secondly, the higher the initial temperature was, the faster the temperature reached to its maximum (i.e higher rate of reaction). For example, for $T_{\text{initial}} = 105$ °C, it took more than 12 minutes before the temperature reached its maximum, while for $T_{\text{initial}} = 160$ °C, less than 2 minutes was needed.

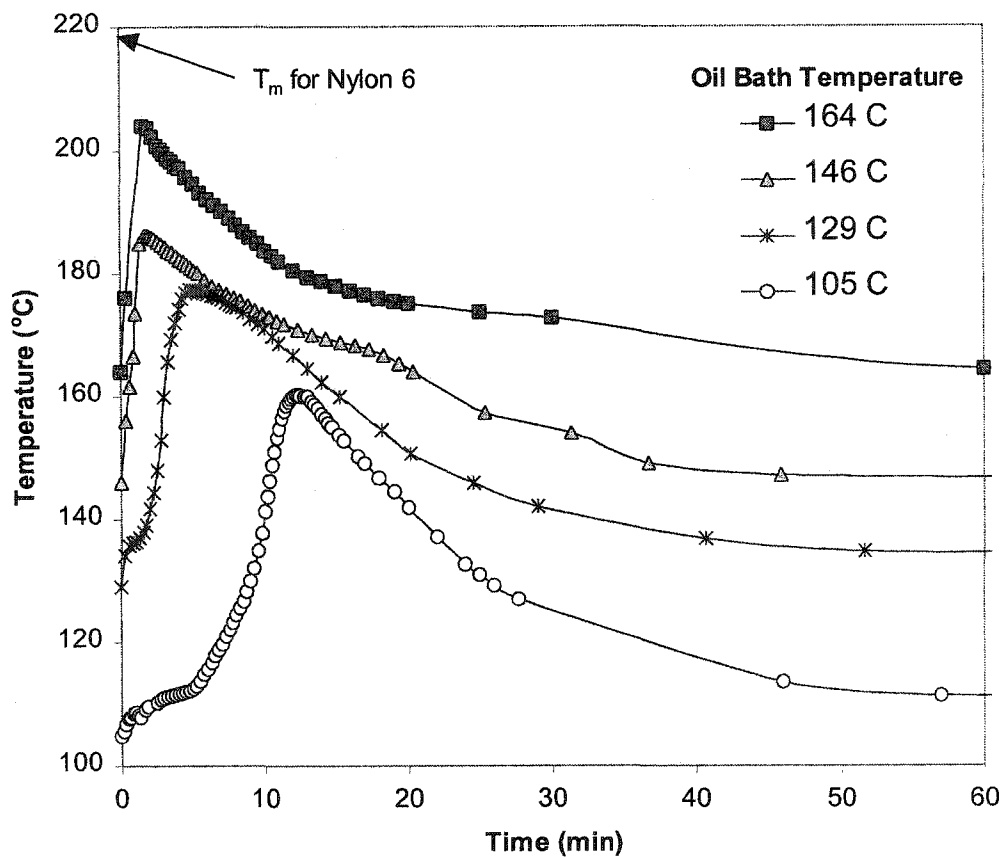


Figure 5.2 Temperature Profiles of the Center Point in the Reactive Mixture under Different Oil Bath Temperatures (75g ϵ -caprolactam/0.75g polycarbonate/12mmol isobutyl magnesium bromide)

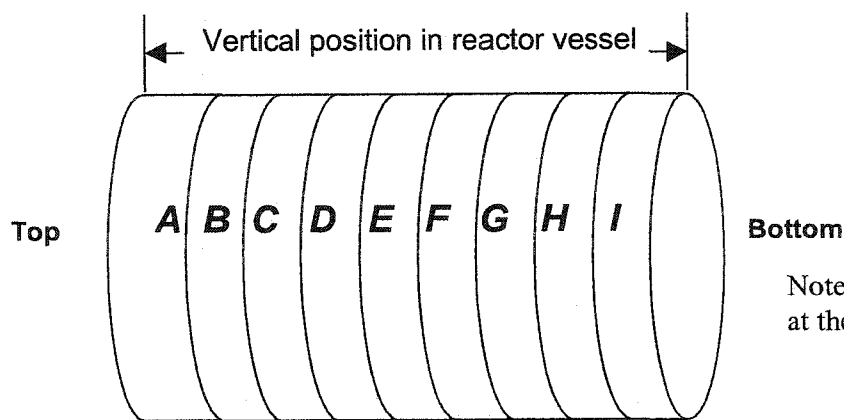
Although only the temperature profile of the center point was measured here, it showed us roughly how high the temperature of the reactive mixture could go. In fact, even for the edge point of the mixture, its temperature would not stay constant at the environmental temperature. This has been studied by Malkin et al. (1982). Under non-isothermal condition similar to ours, temperature profiles for two points (one in the center, the other at the edge of a sphere with radius of 4 cm (this distance is also similar to the dimensions used in our system)) were recorded. Basically both temperatures increased with time, and at the time when T_{\max} was observed, the difference between the center and the edge is only about 15 °C (for an initial temperature of 158 °C). Therefore, although the temperature distribution in the polymeric mixture was not uniform, there might not be much difference between the hottest point (i.e. center) and coolest point (i.e. edge).

5.3 Polymer Homogeneity Analysis

5.3.1 Tensile Properties for "Scale-Up" Sample

There are two purposes for making a larger sized sample. Firstly, it was interesting to see if the process used in small flasks could be scaled up. Two samples (both containing 1% wt Polycarbonate) were able to be synthesized successfully from 250 g and 1000 g of ϵ -caprolactam respectively by using cylindrical metal cans of diameter 10 cm and length 20 cm.

The other purpose is to see if the non-uniformity of temperature distribution could cause any property differences, specifically the tensile properties. The above-mentioned 250g sample in cylindrical shape was sliced horizontally into 9 pieces as shown in Figure 5.3. From each piece the center part was used to cut into one tensile specimen with dimension as Type IV described in ASTM standard D638-95 (details in Chapter 3). Extension speed was set at 0.8 mm/min. All specimens were pre-conditioned at 44% Relative Humidity at room temperature. The results for tensile properties such as Young's Modulus, Tensile Stress at Break and Tensile Strain at Break are shown in Figure 5.3. Dotted lines represent the averaged values for all eight specimens. There was generally not much difference for Young's Modulus and Tensile Stress at Break along the vertical direction of the sample, indicating both good uniformity of sample composition and success of scale-up procedure. Although for tensile strain at break the bottom specimen (I) did show a smaller value, there was still no significant tendency. The stress-strain curves were put in Figure B.1 in Appendix B.



Note: Specimen C failed at the start.

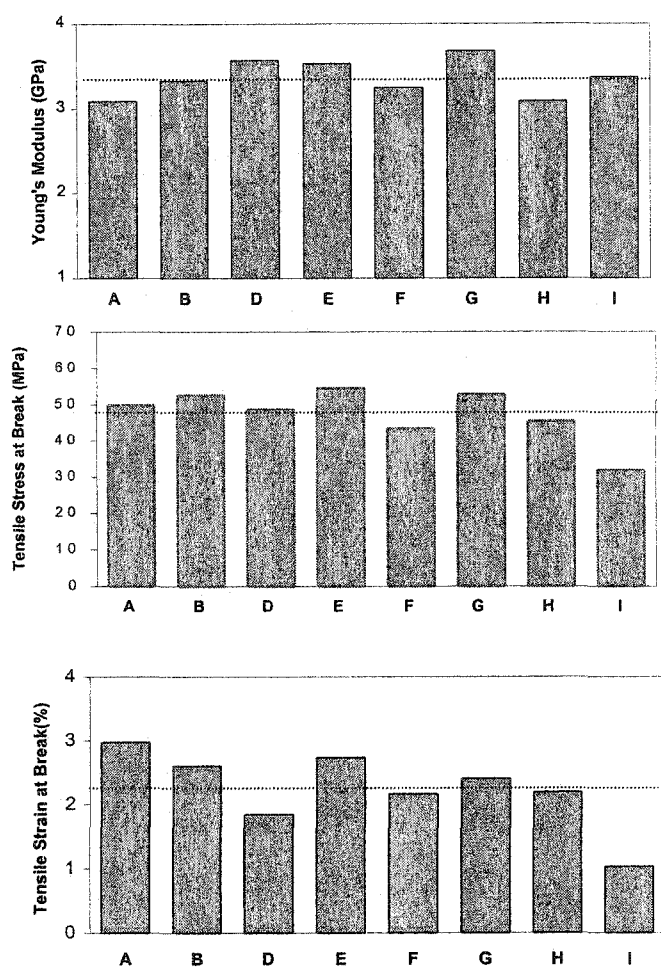


Figure 5.3 Tensile Properties of Specimens Taken from Various Locations of a “Scale-Up” Cylindrical Sample (250g ϵ -caprolactam/2.5g polycarbonate/40mmol iso-butyl magnesium bromide, 120°C).

5.3.2 Intrinsic Viscosity Difference

After checking the tensile properties of the bulk (scale-up system) product, specimens from the small samples made inside the Erlenmeyer flask were tested to see if there was any difference in intrinsic viscosity (i.e. molecular weight for pure nylon 6) from the center point to the edge.

Two samples were prepared in 250 ml Erlenmeyer flasks. First 100 g of ϵ -caprolactam was melted under nitrogen blanket at 130 °C, 3 mmol of initiator (isobutyl magnesium chloride for sample A, Red-Al for sample B) was then added to the monomer melt. Red-Al is a 65%(wt) solution of sodium bis(2-methoxyethoxy) aluminum hydride [i.e. $\text{NaAlH}_2(\text{OCH}_2\text{CH}_2\text{OMe})_2$] in toluene. The reason that Red-Al was chosen is that, compared with the traditional catalysts such as sodium hydride, the reactive species from $\text{NaAlH}_2(\text{OCH}_2\text{CH}_2\text{OMe})_2$ with ϵ -caprolactam showed reduced nucleophilicity (Mougin et al., 1993) which would be inert toward polymer like polydimethylsiloxane (PDMS) in synthesizing a block copolymer of PDMS-nylon 6. Further discussion of using Red-Al in the system of "L-L" method will be discussed in Chapter 6. After clear solution was formed, 1 ml of N-acetyl caprolactam as activator was added to the solution. The whole mixture was stirred until the viscosity was built up. Then the polymer was kept at the same oil bath temperature for another 2.5 hours before cooling in the air.

Each sample was first cut into three parts including the "center", the "edge" and the "middle" designating the area between the center and the edge. After the surfaces were scraped by fine sand papers to get rid of contaminants, each part of the samples was

ground (pulverized) into powder (after quenching in liquid nitrogen) and dried at 70 °C under vacuum for overnight.

For the intrinsic viscosity measurement, 90% formic acid was used as solvent. Water bath was used to keep a constant temperature at 30 °C. The detailed figures of η_{rel} (relative viscosity)/C versus C (concentration of solution) could be found in Figure B.2 (a) and (b).

Table 5.1 Intrinsic Viscosity Data at 3 Various Locations of Two Samples
(in 90% formic acid, at 30 °C)

| | [η] at different locations (dL/g) | | |
|---|--|--------------------|--------------------|
| | Edge | Middle | Center |
| Sample A | 1.087 (30,900)* | 1.077 (30,600)* | 1.150 (33,100)* |
| Sample B | 1.803 (57,300)* | 1.870 (59,900)* | 1.994 (64,800)* |
| Nylon 6 from Scientific Polymer Products | 1.153 (33,200)* | | |

*: Values of \bar{M}_v given in parentheses (see equation in next page)

Table 5.1 shows the results for both samples. The activator used in A and B was N-acetyl caprolactam; therefore, pure Nylon 6 was produced. For a linear polymer chain, the Mark-Houwink-Sakurada equation can be used to relate the intrinsic viscosity to viscosity-average molecular weight \overline{M}_v . The equation is as follows:

$$[\eta] = K \overline{M}_v^a$$

where K and a are empirical constants differing for different solvents and conditions. The value for a is related to the conformation of the macromolecules in the solution (e.g., random coil or extended ellipsoid, etc.). For nylon 6 in formic acid and m-cresol, a usually has values ranging from 0.5 to 1.0. Unfortunately, there are no reported data for K and a values for Nylon 6 in 90% formic acid at 30 °C. The closest I could find is (Brandrup and Immergut, 1989):

for Nylon 6 in 85% formic acid at 25 °C:(molecular weight range from 7, 000 to 120,000)

$$K = 22.6 \times 10^{-3} \text{ dl/g}$$

$$a = 0.82$$

By using these data some rough idea may be obtained on what range of the \overline{M}_v could have been reached and how the \overline{M}_v value changed along the radial direction in the small samples. \overline{M}_v values corresponding to the $[\eta]$ values were calculated and listed in parenthesis below $[\eta]$ in Table 5.1.

For each sample, the center part tended to show higher molecular weight while the edge had lower molecular weight. However, the difference in \overline{M}_v between the center and the edge was not significant. For example, sample A had \overline{M}_v ranging from 30.6k (middle) to 33.1k (center), while the \overline{M}_v of sample B ranged from 57.3k (edge) to 64.8k (center). Therefore, at different locations of polymer, the molecular weight did not vary much. Nevertheless, care was taken in the following viscosity studies where *only center parts of samples were used in measurements.*

5.4 Results

To examine the effect of temperature, six samples of the same compositions were prepared at six different temperatures. The temperatures chosen were: 95, 110, 120, 134, 147 and 160 °C. Here, to be specific, the temperature being controlled was the environmental temperature, i.e. oil bath temperature (T_{oil}). The composition was as following: 75 g of ϵ -caprolactam, 0.75 g of polycarbonate (from Scientific Polymer Products, Inc.), and 10 mmol of isobutyl magnesium chloride (2M solution in diethyl ether). The synthesis procedure was described in detail in Chapter 3. Various measurements were run on these six samples to obtain monomer conversion, degree of crystallinity, intrinsic viscosity and melt viscosity, water absorption and tensile properties under “dry” and “wet” conditions.

5.4.1 Monomer Conversion

5.4.1.1 Water-Extraction Method

For each sample, around 0.7-0.8 g of small pieces were cut from the center part of the sample and dried in the desiccator overnight. Then they were put into a flask containing 40 ml of hot water at a temperature of about 50 °C. After being stirred constantly for 18 hours, the sample was filtered and washed, and dried at 100 °C under vacuum overnight before cooling. The weights of the small pieces before and after the hot-water treatment were measured. The weight loss was considered to be the so-called “water-soluble content” which included mostly non-reacted monomer or oligomer.

Table 5.2 and Figure 5.4 show the data of water soluble content for six samples. Generally, the content of monomer and oligomer in the final product was very low, on the order of 2-4%. There was not much difference between the samples made at higher temperatures and lower temperatures. Although generally samples synthesized at higher temperatures showed slightly higher water-soluble content values than those made at lower temperatures, it may be due to the fact of faster kinetics at higher temperature. The viscosity of the reactive mixture built up so fast that some of the monomer ϵ -caprolactam was trapped and could not join the polymerization.

Table 5.2 Water Soluble Content Data for Samples Made at Different Oil Bath Temperatures

(75 g ϵ -caprolactam, 0.75g polycarbonate and 10mmol isobutyl magnesium chloride)

| Oil Bath Temperature ($^{\circ}$ C) | Water Soluble Content (%) |
|--------------------------------------|---------------------------|
| 95 | 2.02 |
| 110 | 1.76 |
| 120 | 2.61 |
| 134 | 3.37 |
| 147 | 3.27 |
| 160 | 3.07 |

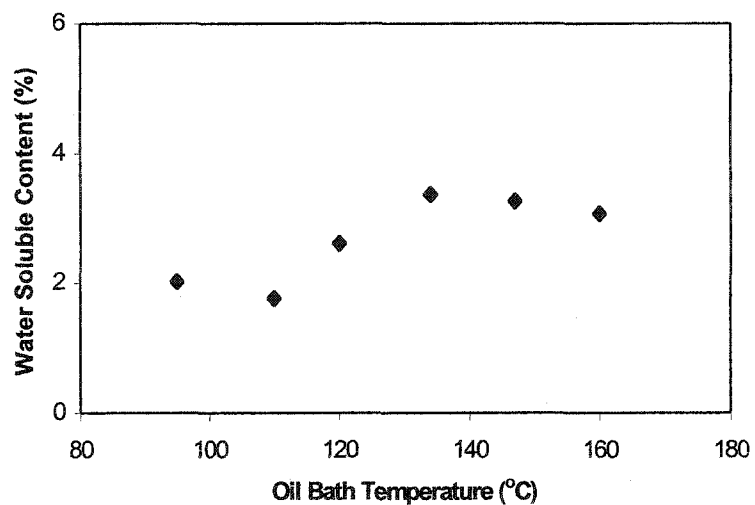


Figure 5.4 Water Soluble Content for Samples Made at Different Oil Bath Temperatures.

5.4.1.2 GC-MS Method

Another approach to obtain the information on monomer conversion is through GC-MS analysis on the solution in which water-soluble content was extracted. Based on the method described by Ongemach and Moody (1967), at first, a calibration curve was made by using four standard solutions of ϵ -caprolactam with bis-[2-(2-methoxyethoxy)ethyl ether] as internal standard. Figure 5.5 shows an example of GC-MS result (other GC-MS results can be found in Appendix B). The peak at residence time of 346 seconds is the one for caprolactam while peak at residence time of 272 seconds is for the internal standard.

The calibration constant K was calculated as following:

$$K = \frac{t_1 A_1 V_2 S}{V_1 A_2 t_2 C}$$

where t, A, V were residence time, peak area and volume of solution respectively, 1 and 2 represented for caprolactam peak and internal standard peak respectively, S is the concentration of internal standard (20.18mg/ml), C is the concentration of standard caprolactam solution.

For each set of standard solution of caprolactam, K value was calculated and averaged. Table 5.3 showed the K values over the concentration of caprolactam in the standard solution from 0.05g/dL to 0.2g/dL. The average K value is 1.4475.

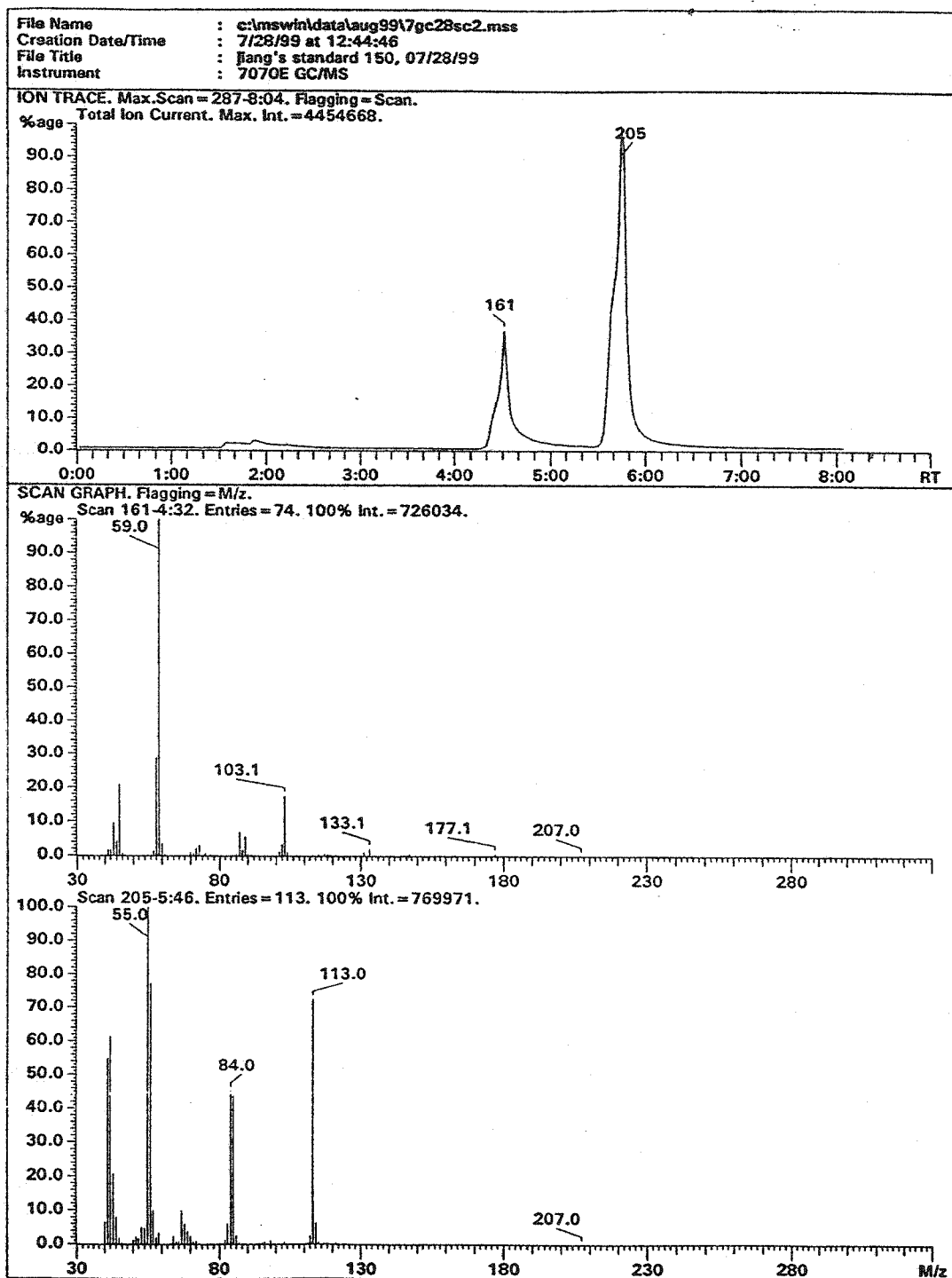


Figure 5.5 An Example of GC-MS Result

Table 5.3 Calibration Constant K

| Concentration of caprolactam in Standard Solution | K value |
|--|-----------------|
| 0.0523 g/100mL | 1.3666 |
| 0.1028 g/100mL | 1.3763 |
| 0.1550 g/100mL | 1.3653 |
| 0.2162 g/100mL | 1.6817 |
| | Average: 1.4475 |

After calibration constant K was obtained, several sample solutions (with addition of certain amount of internal standard) were analyzed to obtain the concentration of caprolactam $M\%$ through the following equation:

$$M\% = \frac{t_1 A_1 V_2 S(V_o)}{1000 t_2 A_2 V_1 W K} \times 100\%$$

where V_o is the total volume of sample solution, W is the original weight of polymer sample.

Table 5.4 lists the results from GC-MS analysis for three random samples (*I to III*) in the third column. The results from the weight loss in the first method were also listed in the second column for comparison. There was a good match between the two results. Although the ones from GC-MS were bit lower than those from weight-loss method, the difference might come from the water-soluble oligomer that was not counted

in GC-MS method. As it can be seen that the “weight-loss” method was easier and more economic, therefore *only this method was used for later study.*

Table 5.4 Comparison of the Results from Two Methods

| Samples | Water-Soluble Content (%) (Weight-loss Method) | Monomer Content (%) (GC-MS Method) |
|------------|---|---------------------------------------|
| <i>I</i> | 2.432 | 1.904 |
| <i>II</i> | 1.921 | 1.859 |
| <i>III</i> | 1.928 | 1.769 |

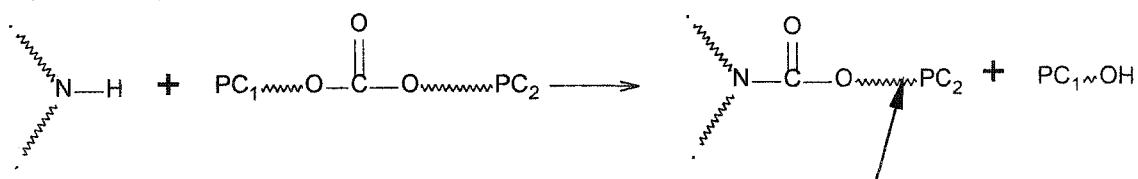
5.4.2 Intrinsic Viscosity

Intrinsic viscosity measurement was conducted for the six samples made at different oil bath temperatures. 90% formic acid was used as solvent, and the temperature of measurement was 30 °C.

However, during the preparation of solutions, it was found that samples made at 147°C and 160°C (i.e. the two highest temperatures) could not be completely dissolved into 90% formic acid, nor could they be dissolved completely in m-cresol at 60 °C. Instead, there were gel-like particles in the solutions. For example, a cube-shaped copolymer (made at 160°C) weighing 0.2744 g was put into about 50 mL of 90% formic acid. After four days, it became a transparent gel-like material which still held its cubic shape. The weight of the material was about 19.66 g , with a weight increase of about 70

times. After that, a solution with small gel particles was formed. Extended soaking (i.e. about 1 month) in the solvent caused the small gel particle to disappear, but somehow there was discoloration of the solution which might suggest degradation in the solution.

There have been reports on the formation of gel-structure during the synthesis of nylon 6. Ricco, L. et al. (1999) found in their study which four different activators were involved in an isothermal process, three activators showed “extensive cross-linking from a specific polymerization temperature on”. They attributed this to the formation of chain irregularities from side reactions at higher temperatures. Mateva and Delev (1995) showed the possible reaction to explain the large amount of gel formation when trialkylsilylcaprolactam was used as activator. Although the possible side reactions in the “L-L” system of this study were not studied, speculatively it could be related to: (1). The strong interaction between the active growing chain ends and the neighboring polymer chains at higher temperature; or (2). The secondary amines from the nylon 6 chains could react with carbonate group in the polycarbonate chains (Foldi and Campbell, 1962). This might lead to the formation of block or graft copolymers of the two. The possible scheme was shown below:



This reaction could continue if the -NH- group of another nylon 6 would attack the carbonate group of the above graft copolymer product (shown by the arrow). This would lead to a crosslinked structure in the final product.

For the other four samples (i.e. polymers made at 95°C, 110°C, 120°C and 134 °C), there was no difficulty in dissolving them into 90% formic acid at room temperature. The measurement of intrinsic viscosity generally followed the procedure described in ASTM D2857-95. For each sample, four solutions of different concentration (ranging from 0.04 g/100mL to 0.15 g/100mL) were prepared, and filtered before each measurement. An Ubbelohde tube was used in the measurement. Time t for the solution to flow from one end of the capillary to the other end was recorded. For each sample, values of η_{SP}/C vs. C were plotted where specific viscosity η_{SP} was calculated as below:

$$\eta_{SP} = \frac{t}{t_o} - 1$$

Here, t_o is the flow time for the pure solvent passing through the capillary. There is a semi-empirical form suggested by Huggins (1942) that as mass concentration C decreases to zero (i.e. infinitely diluted solution), the y-intercept of plot η_{SP}/C vs. C is the so-called *intrinsic viscosity*:

$$[\eta] = \left(\frac{\eta_{SP}}{C} \right)_{C \rightarrow 0}$$

Intrinsic viscosity describes the frictional property of polymer in solvent which is correlated to the “hydrodynamic volume” of polymer in the solvent. For linear homopolymers, there is the Mark-Houwink equation that relates the value of $[\eta]$ to the Viscosity-average molecular weight \overline{M}_v . Here the equation is not applicable due to the

fact that the polymer being tested is a copolymer instead of a linear homopolymer. However, the concept of intrinsic viscosity may still be used to inspect the size of polymer molecules in a certain solvent. In this way, some relative information on how the reaction temperature affects the molecular weight of the final product can be obtained.

Figure 5.6 shows the plots of η_{sp}/C vs. C for four samples. Clearly, $[\eta]$ increased monotonically with the temperature of reaction, and this implies that the molecular coil volume did also.

Theoretically, if a polymer is in a good solvent, it would tend to have a large hydrodynamic volume in that solvent; while if a polymer molecule is in a bad solvent, it would have a smaller hydrodynamic size. For a nylon 6 copolymer with polycarbonate, since 90% formic acid was not a good solvent for polycarbonate, therefore the polycarbonate block in the copolymer would have very little contribution to the hydrodynamic size of the copolymer in the solvent. This suggests that the measured value of intrinsic viscosity was mainly contributed by the nylon 6 block in the copolymer. In this way, some tentative conclusion could be made that at different reaction temperatures, the molecular weights of copolymers having the same compositions did show some difference. The reason can be speculated as following: at low temperature, chain propagation (viscosity build-up) was slower than those at higher temperature; also the solubility of nylon 6 in the ϵ -caprolactam melt was lower at lower temperature, therefore

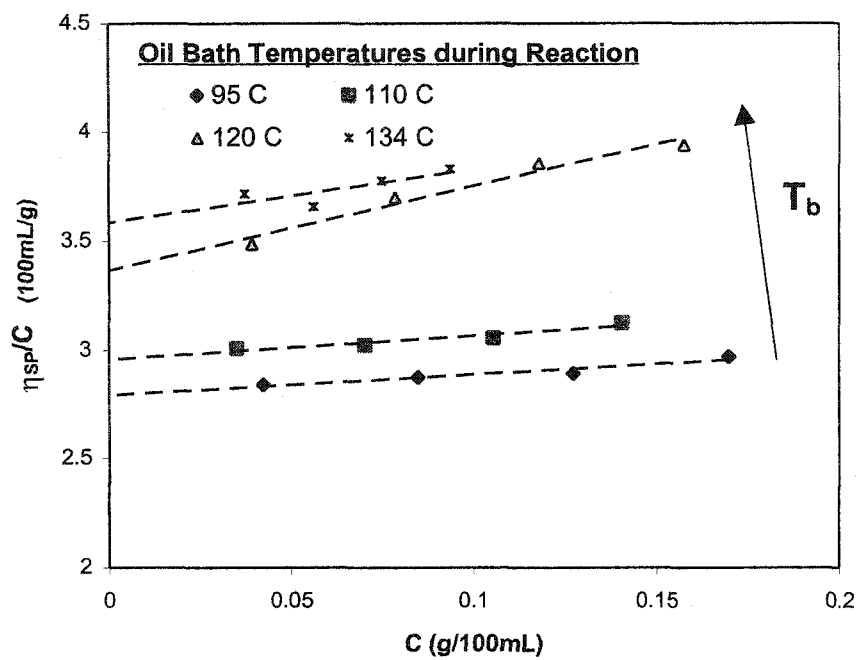


Figure 5.6 η_{sp}/C vs. C Plots for Samples Made at Different Oil Bath Temperatures.

polymer would precipitate with low molecular weight and the active center for chain propagation would be trapped and become unavailable.

5.4.3 Rheological Measurements

5.4.3.1 Parameter Setup

Melt rheological properties of the six samples were measured on the RMS 800. A fixture of disk and plate with radius of 12.5mm was used. Temperature of measurement was 250 °C (the melting temperature for all samples was around 220°C). Sample used for setting up experimental parameters was nylon 6 made from 0.5% diphenyl carbonate (with iso-butyl magnesium chloride as initiator).

Pretreatment of sample was done by heating up at 70 °C under vacuum for at least 24 hours. It had been studied that the existence of moisture would decrease the zero-shear melt viscosity of nylon 6 dramatically (Khanna et al., 1996).

At the beginning, a dynamic time sweep was run with a shear strain amplitude of 0.5% and frequency of 0.1 rad/s. The result is shown in Figure 5.7. Generally, there was not much change for complex viscosity η^* , dynamic viscosity η' and loss modulus G'' . This suggests that there was no thermal relaxation needed after the sample was loaded between the two platens and that sample degradation at 250°C does not occur within 30 minutes. However, for further measurement, samples would have five minutes of thermal relaxation time before each measurement.

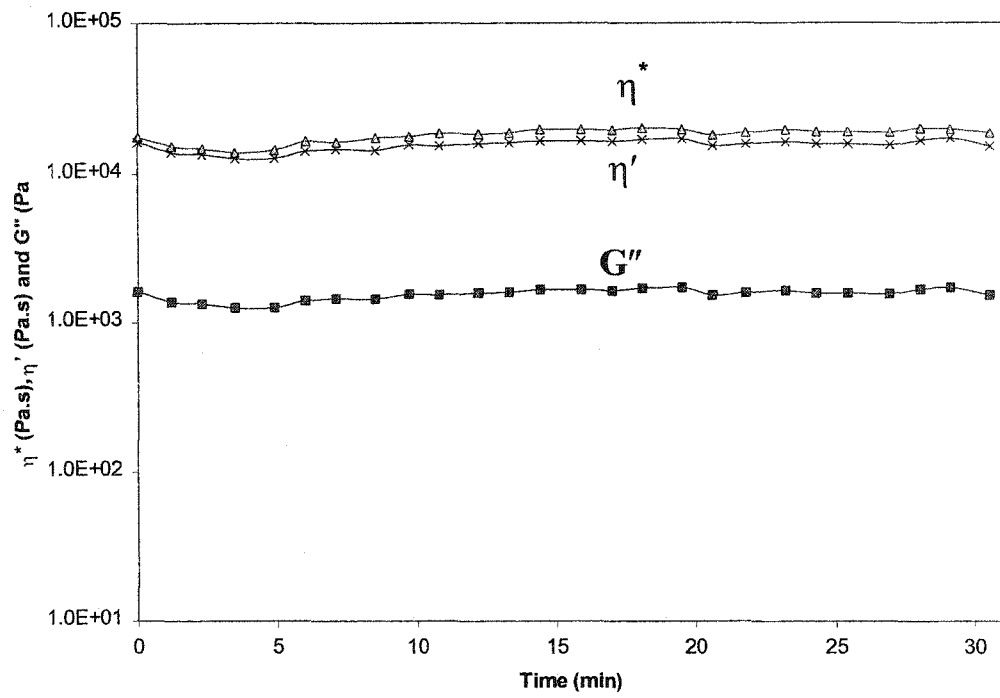


Figure 5.7. Time Sweep Test for Nylon 6 Made from 0.5%DPC
 ($T_{\text{measurement}} = 250 \text{ }^\circ\text{C}$, Frequency = 0.1 rad/s, Strain $\gamma^0 = 0.5\%$)

To select a strain amplitude γ^0 that is in the linear viscoelastic range of samples being tested, a strain sweep was conducted at constant frequency of 0.1 rad/s and constant temperature of 250°C. The range of γ^0 was from 0.1% up to 30%. Results are shown in Figure 5. 8. It can be found that the complex viscosity η^* , dynamic viscosity η' and storage (elastic) modulus G' were all linear up to $\gamma^0=30\%$. Generally γ^0 of 1% was chosen for further measurement, and the RMS 800 transducer was easily able to detect and measure accurately stresses generated by the sample even at such a low γ^0 .

To examine whether there was any degradation happening to the polymer melt during the measurement, dynamic frequency sweep tests were conducted both in the ascending order of frequency (0.05 rad/s to 100 rad/s) and descending order of frequency (100 rad/s to 0.05 rad/s) on same polymer melt specimen. The other parameters were kept exactly the same. If there are some degradation or any interactions happening during the measurement, then the two runs would show some difference. The results are shown in Figure 5.9. It was found that the two run overlapped quite well, indicating that negligible degradation was occurring and also that the data were reproducible.

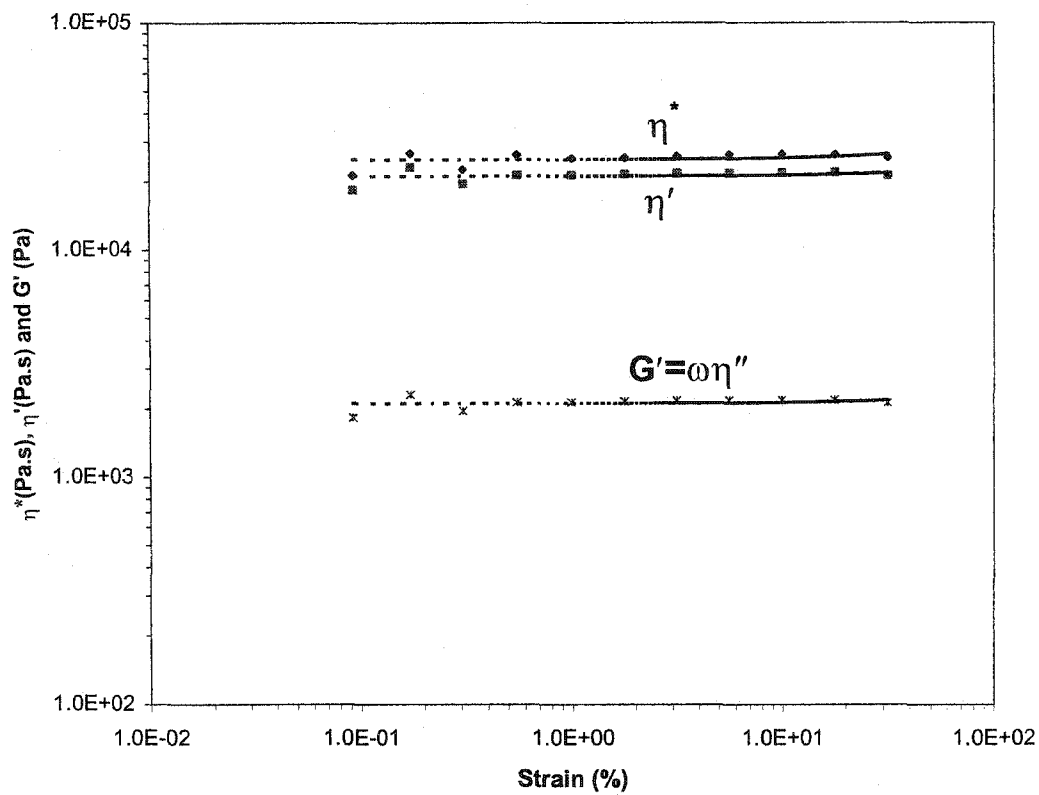


Figure 5.8 Strain Sweep Test for Nylon 6 Made from 0.5% DPC
 ($T_{\text{measurement}} = 250 \text{ }^\circ\text{C}$, Frequency = 0.1 rad/s)

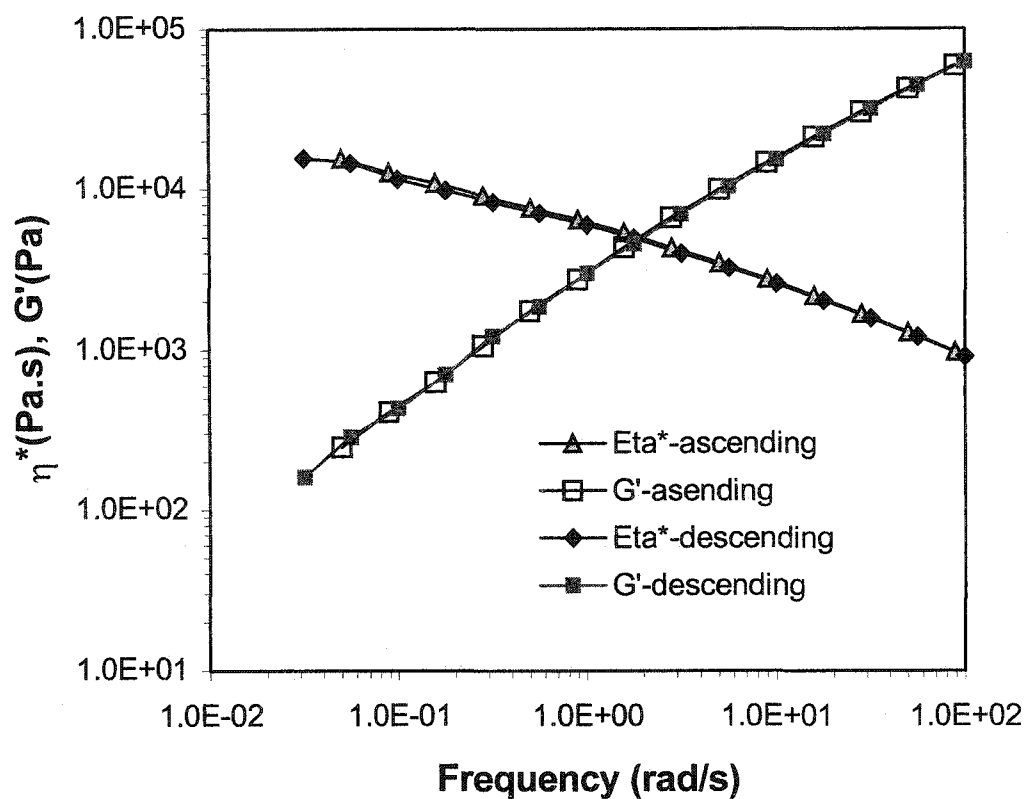


Figure 5.9. Dynamic Frequency Sweep Tests in Both Ascending and Descending Order of Frequency for Nylon 6 Made from 0.5% DPC.

($T_{\text{measurement}}=250\text{ }^{\circ}\text{C}$, Disk and Plate, $\gamma^{\circ}=1\%$)

5.4.3.2. Rheological Properties for Samples Made at Different Temperatures

Dynamic frequency sweep tests were conducted on five samples made at different reaction temperatures. The temperature of measurement was at 250°C, and $\gamma^0 = 1\%$ was used. Each sample was maintained at 250°C for 5 minutes before the test started.

The results of complex viscosity η^* and modulus G^* with respect to frequency for five samples are shown in Figure 5.10 (a) and (b) respectively. In the range of low frequency, the values of η^* and G^* for the five polymer melts were quite different, ranging from 4×10^3 Pa.s to 7.5×10^4 Pa.s for η^* (at frequency of 0.05 rad/s) and 200 Pa to 3700 Pa for G^* (at frequency of 0.05 rad/s). There is a tendency that for polymers made at higher temperatures, shear viscosity and modulus would tend to be higher.

For samples made at low reaction temperatures (110°C up to 134 °C), as mentioned in 5.4.2, different reaction temperatures would lead to different molecular weights of copolymers, therefore the difference in zero shear viscosity might come from the different molecular weights of copolymer. On the other hand, for samples made at higher reaction temperature (147 °C and 160 °C), it was suspected that there might be cross-linking structure formed, and the resulting gel structure would contribute to the higher zero shear viscosity and higher modulus.

At higher frequency, the differences in η^* and G^* between various melts were getting smaller than those at low frequency. This indicated that under extensive shearing, there was little dependence of melt viscosity and modulus on molecular weight.

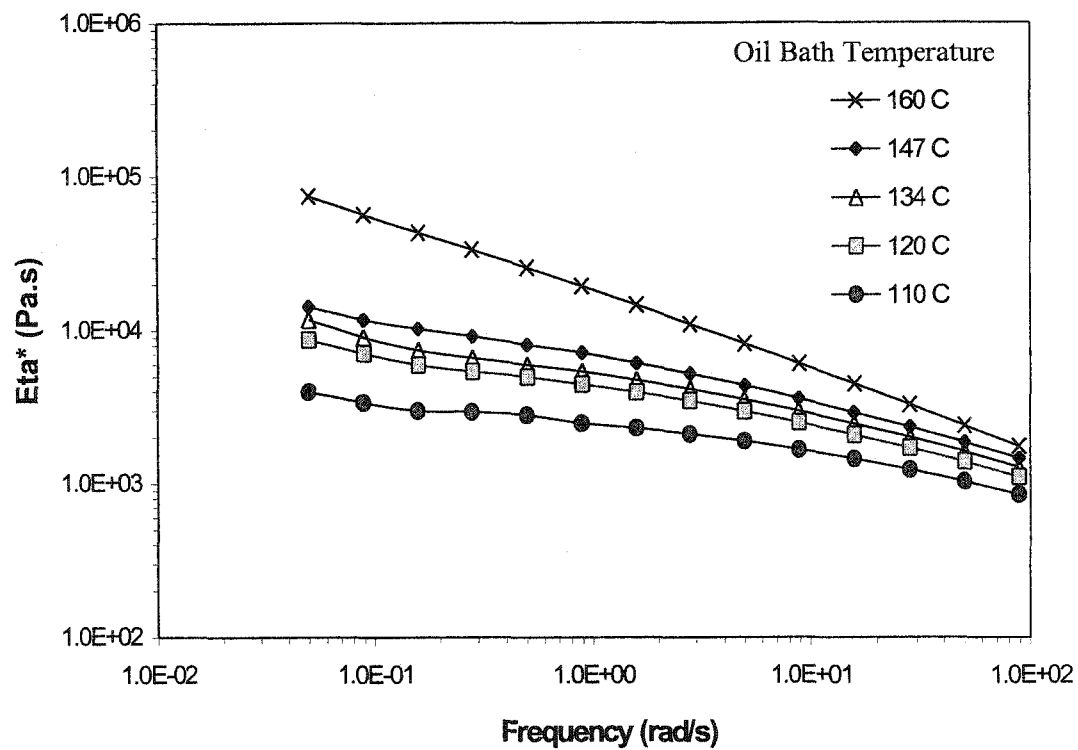


Figure 5.10 (a). Complex Viscosity Data in Dynamic Frequency Sweep Tests for Samples Made at Different Oil Bath Temperatures.

($T_{\text{measurement}}=250\text{ }^{\circ}\text{C}$, Disk and Plate, $\gamma^{\circ}=1\%$)

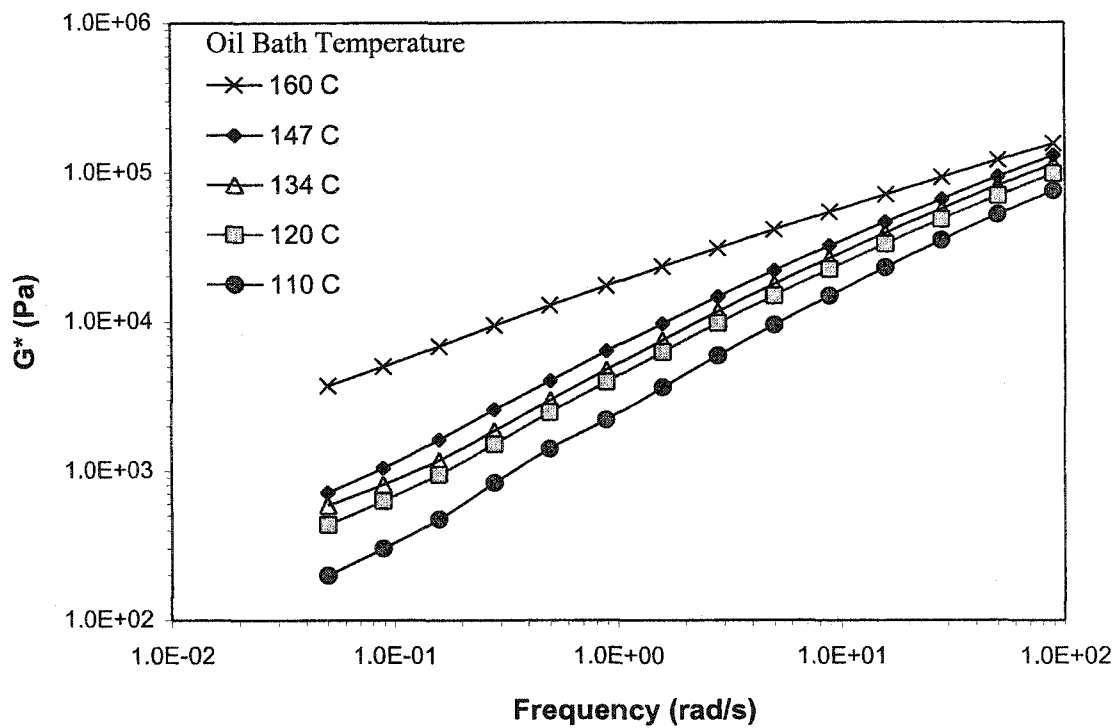


Figure 5.10 (b). Complex Modulus Data in Dynamic Frequency Sweep Tests for Samples Made at Different Oil Bath Temperatures.

($T_{\text{measurement}}=250\text{ }^{\circ}\text{C}$, Disk and Plate, $\gamma^0=1\%$)

It is important to know if samples with gel-like structure behaved differently after being sheared at high frequency, which would imply that mechanical degradation was taking place. The sample made at oil bath temperature of 160 °C was used to conduct dynamic frequency sweep tests in both ascending and descending order of frequency. The polymer melt specimen was rerun in descending order of frequency after first being tested in the ascending order. As shown in Figure 5.11, there was still a good match between the two runs although the “descending” data lie below the ascending data slightly. This suggests that some small amount of degradation may have taken place during the first run (ascending), and the gel structure may be destroyed a little bit by the extensive shear.

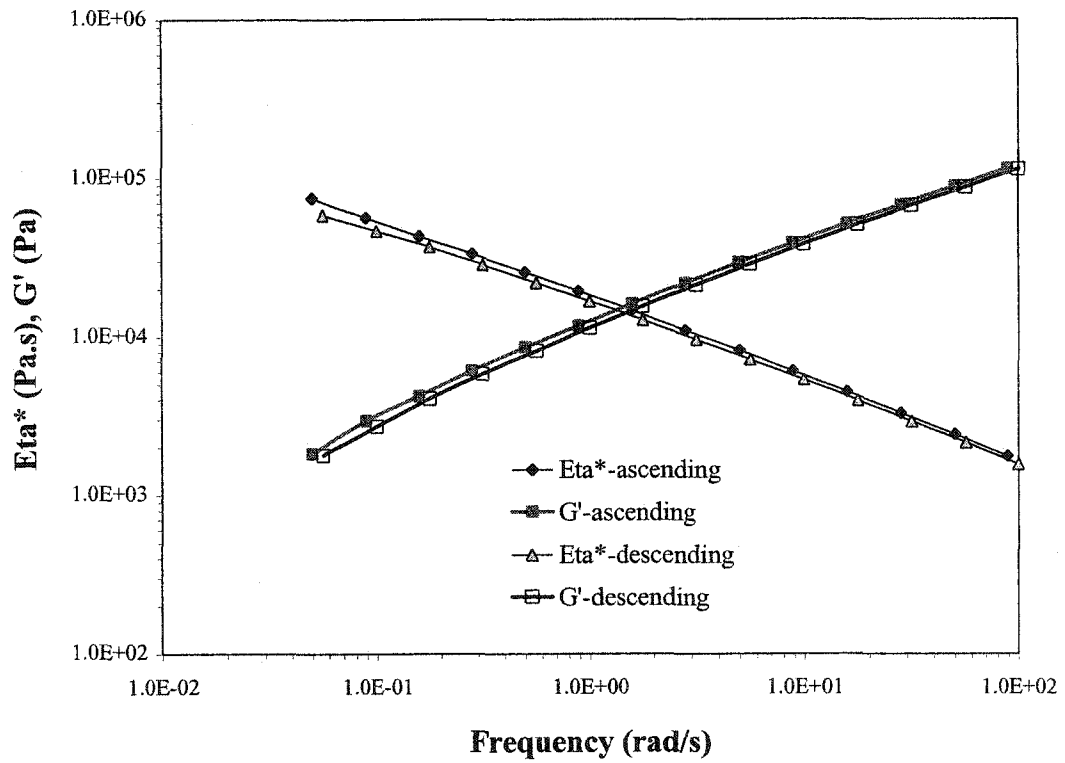


Figure 5.11 Dynamic Frequency Sweep Tests in both Ascending and Descending Order of Frequency for Copolymer Made at Oil Bath Temperature of 160 °C .

($T_{\text{measurement}}=250\text{ }^{\circ}\text{C}$, Disk and Plate, $\gamma^{\circ}=1\%$)

5.4.4 Degree of Crystallinity

5.4.4.1 DSC Method

After each copolymer sample had its water-soluble content extracted and was dried at 70°C under vacuum for overnight, DSC (Differential Scanning Chlorimetry) was used to obtain information on the melting point and degree of crystallinity for the six samples of semi-crystalline nature. For each run about 10 mg of sample was used. Scan rate was set at 10°C/min under nitrogen blanket. The melting point was taken as the temperature corresponding to the one where the endothermic peak was; while the degree of crystallinity (x_c , expressed as percentage crystals by weight) was calculated as following:

$$x_c = \frac{\Delta H_f}{w\Delta H_f^0} \times 100\%$$

where ΔH_f was the heat of fusion per unit mass for the copolymers which could be obtained from calculating the area of endothermic peak; w was the weight percentage of nylon 6 content in the copolymer (here is about 99%); ΔH_f^0 was the heat of fusion for nylon 6 with 100% crystalline structure; it has a value of 190 J/g (Brandrup and Immergut, 1989). Figure 5.12 shows the values for melting temperature and degree of crystallinity. The data for melting temperature were distributed randomly, ranging from

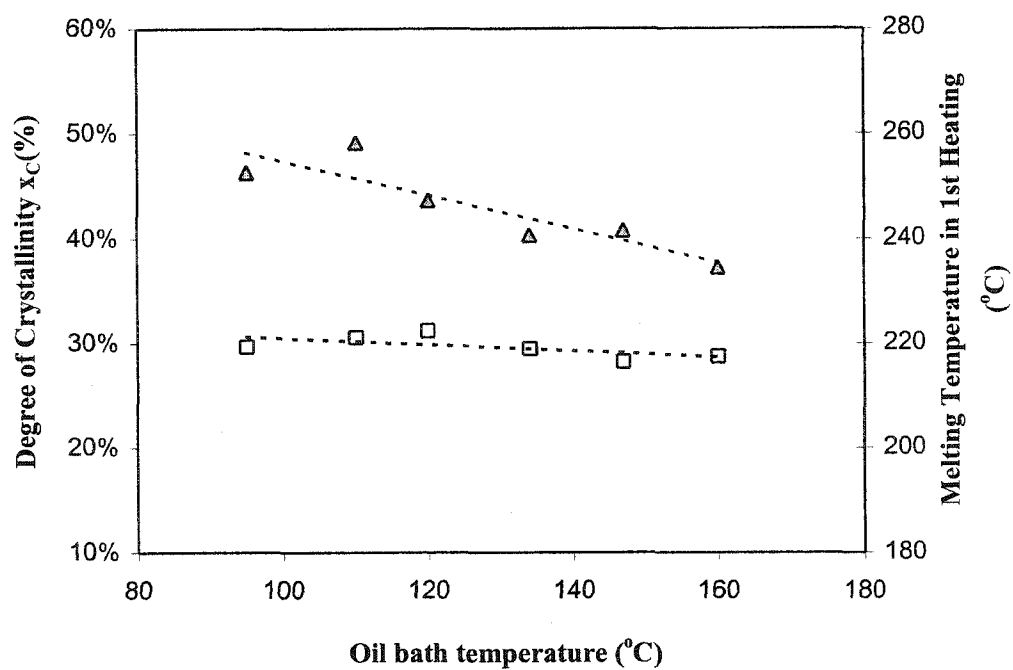


Figure 5.12. Melting Temperatures (\square) and Degree of Crystallinity (Δ) for Copolymer Samples Made at Different Oil Bath Temperatures. (Data taken from the first heating scan in DSC)

216 °C to 222.4 °C. For the data on crystallinity, there was a decrease as reaction temperature increased within the range of oil bath temperature of 110°C-160°C, while the one at 95°C did not follow the same trend. The original DSC thermodiagram for the six samples are available in Appendix B.5-(a)-(f).

The decreasing tendency in x_C may be explained by the thermal history that the sample experienced. For example, when we compared polymers made at oil bath temperatures of 120°C and 160°C, due to exothermic heat of reaction, the true local temperature of reactive mixture would increase during the whole process. The core temperature of reactive mixture with original oil-bath temperature of 120°C would pass 160°C during the polymerization; while the core temperature of reactive mixture with original temperature of 160°C would reach as high as 200°C and stay above 170 °C for more than half an hour (shown in Figure 5.2). As mentioned in 5.1, the rate of crystallization for nylon 6 reached maximum around 140°C, and decreased fast in both directions from the maximum (i.e at temperatures higher or lower than the maximum). Therefore, the crystallization process for polymer made in oil bath of 160 °C would be slower and less perfect than that for polymer made at oil bath of 120 °C. This might lead to the lower value of crystallinity for polymer made at high reaction temperature. The other reason might come from the possible gel-structure formed at higher reaction temperature (e.g. 160°C), which would hinder the crystallization process.

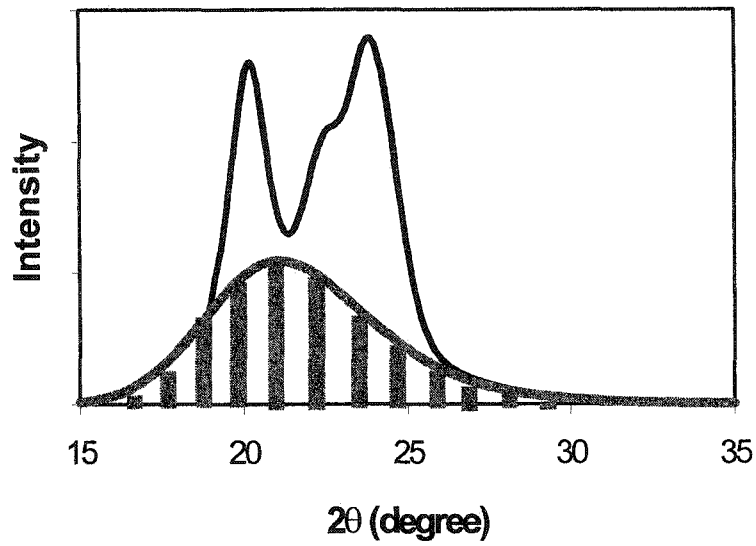
5.4.4.2 X-ray Diffraction Method

The degree of crystallinity for a semi-crystalline polymer can also be obtained through an X-ray diffraction method in which diffracted intensity versus 2θ (θ is the diffraction angle) was measured. Generally the diffraction pattern for the amorphous phase is more like a broadened halo while the diffraction pattern for the crystalline phase shows sharp peaks at certain angles. Degree of crystallinity x_C can be calculated by:

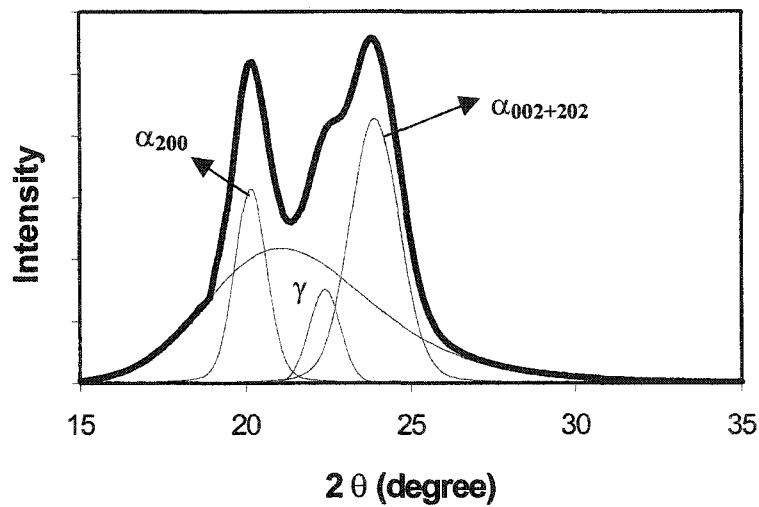
$$x_C = \frac{A_C}{A_a + A_C} \times 100\%$$

here A_a is the enclosed area corresponding to the amorphous halo, and A_C is the area corresponding to the crystalline peaks.

An amorphous sample was obtained by first heating up a nylon 6 copolymer (with 1% polycarbonate) melt at 250°C for 5 minutes in nitrogen atmosphere to destroy all the crystalline structures, then quenching the melt into liquid nitrogen. Figure 5.13 (a) shows a general diffraction pattern of copolymer, with the amorphous halo shown in shaded area. The crystalline peaks were located at about $2\theta = 20^\circ, 23.6^\circ, 22.4^\circ$ which are characteristic peaks for nylon 6. The experimental scans were fitted with a software called Peakfit. In the curve-fitting, a linear baseline was used; the amorphous halo was fitted as 5-parameter function EMG(Exponentially Modified Gaussian) + GMG (half Gaussian Modified Gaussian); and the three crystalline peaks were fitted with Gaussian



(a)



(b)

Figure 5.13 (a). Schematic Diffraction Pattern with Amorphous Halo in Shaded Area. (b). Schematic Diffraction Pattern with Fitted Curves.

and Lorentzian functions. Figure 5.13 (b) showed an example of the original pattern and the fitted curves.

When a nylon 6 melt is cooled, its crystalline state is characterized by polymorphism (Reimschuessel, 1977) which contains α and γ structure. The monoclinic α form involves fully extended zig-zag conformation because of the antiparallel packing of adjacent hydrogen-bonded polymer chains; the γ form involves a pseudohexagonal conformation which is less stable than the α form. The relative content of each structure depends on the thermal history and the constitution of the macromolecules. On the X-ray profile, the peaks at $2\theta=20^\circ$ and 23.6° correspond to the α structure with the reflections of crystalline (200) and (002)+(202) respectively; while the γ structure can be found at $2\theta=22.4^\circ$.

The six copolymer samples were evaluated by using the above-mentioned method. The calculated values for x_C are listed in Table 5.5. It can be seen that the major crystalline form in the six polymers was α structure, while the content of γ structure was very little except the one made at 160°C which contains about 9% of γ crystal structure. The original X-ray diffraction patterns for the six samples are available in Appendix B.6-(a) to (f).

When the values of degree of crystallinity by both methods (i.e. DSC and X-Ray) were compared, it was found in Figure 5.14 that the data from X-ray were generally higher than that from DSC method. This discrepancy had also been found by other researchers (Ricco, L. et al., 1999; Mateva, R. et al., 2000) which was due to the different

Table 5.5 X-Ray Results for Polymers Made at Different Oil Bath Temperatures

| Oil Bath Temperature (°C) | Crystalline Peak Area (%) | | | | Amorphous Area (%) |
|---------------------------|---------------------------|------------------------------|--------------------|-------|--------------------|
| | α structure (200) | α structure (002+202) | γ structure | Total | |
| 95 | 13.27 | 35.59 | 3.50 | 52.36 | 47.64 |
| 110 | 12.83 | 36.78 | 5.23 | 54.84 | 45.16 |
| 120 | 15.35 | 35.35 | 4.02 | 54.71 | 45.29 |
| 134 | 17.79 | 29.92 | 4.70 | 52.41 | 47.59 |
| 147 | 16.09 | 24.93 | 5.22 | 46.24 | 53.76 |
| 160 | 11.71 | 25.43 | 9.54 | 46.69 | 53.31 |

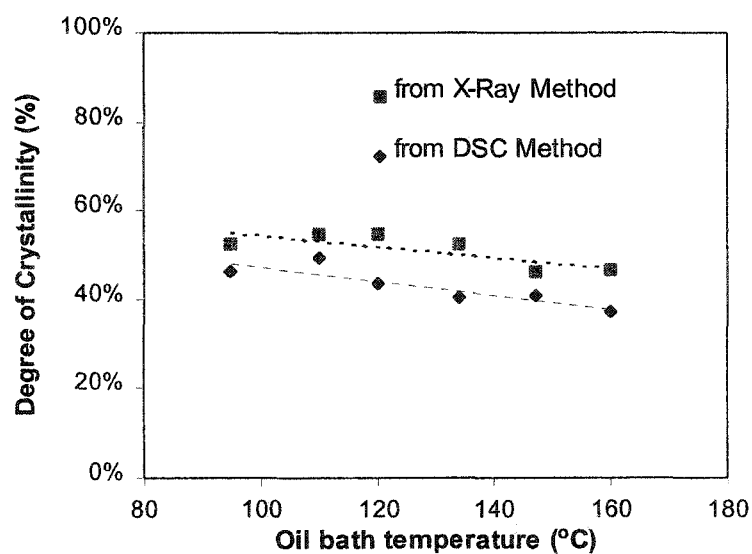


Figure 5.14 Comparison of x_C Data from X-ray and DSC Methods

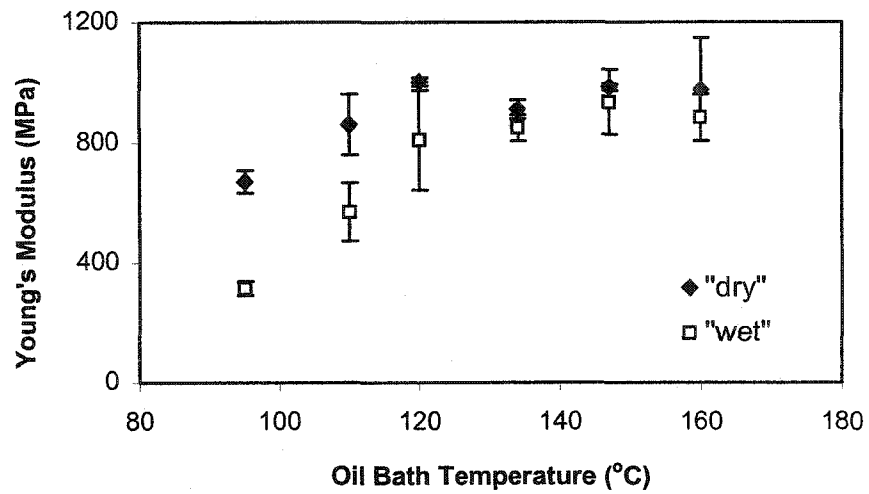
sensitivity of these two techniques. Careful examination of the data from X-ray method would lead to the same conclusion as from DSC method, i.e. the copolymer made at higher reaction temperature tended to have lower crystallinity.

5.4.5 Tensile Properties

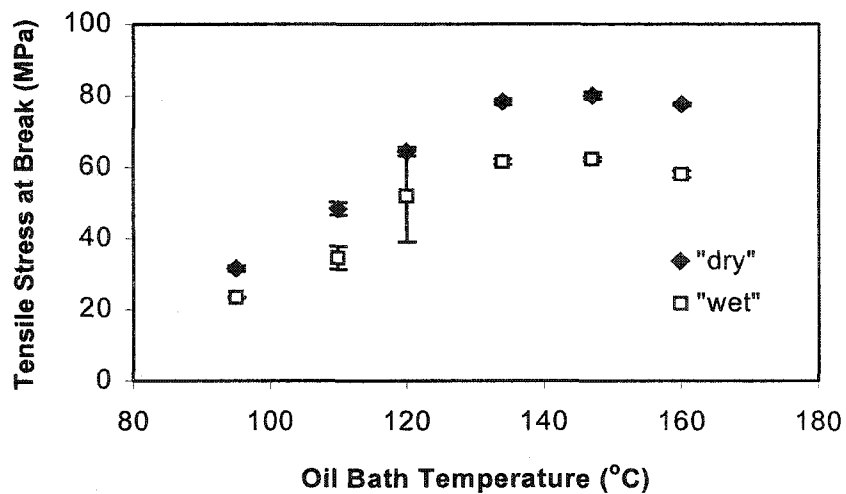
With the differences in molecular weight, molecular structure and degree of crystallinity for polymers made at different reaction temperatures, one could expect that their mechanical properties would behave differently too. Tensile tests were run for the six samples made at six different oil bath temperatures. It is well known that pure nylon 6 is a hydrophilic polymer and will absorb moisture which may play a role in determining tensile properties. Therefore, after specimens for each sample were cut, half of them were kept in “dry” condition over P_2O_5 in a desiccator while the other half were put into a “wet” condition, i.e. an environment of nominally 50% R.H.. The 50% R.H environment was achieved by mixing glycerol and water at volume ratio (glycerol/water) of 3.5 and putting into a desiccator with the test specimens, with RH monitored by a humidity meter also enclosed.

All specimens were kept either in “dry” or “wet” condition before being loaded into the testing machine. The tests were done at room temperature with lab humidity at 42% R.H.. The dimension of specimen was based on ASTM standard D638-95 and was described in Chapter 3. The speed of extension was 1mm/min.

Figures 5.15 (a)-(d) show the results of tensile tests for six samples made at different temperatures under both “dry” and “wet” conditions. When the data for all dry



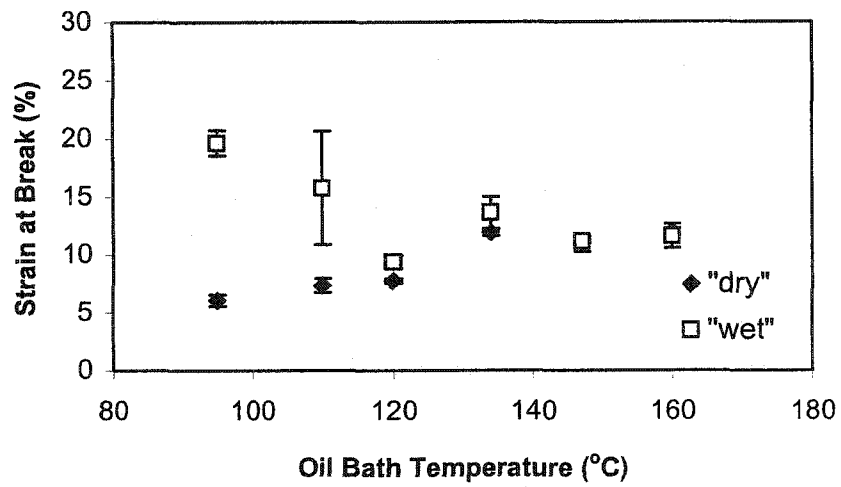
(a)



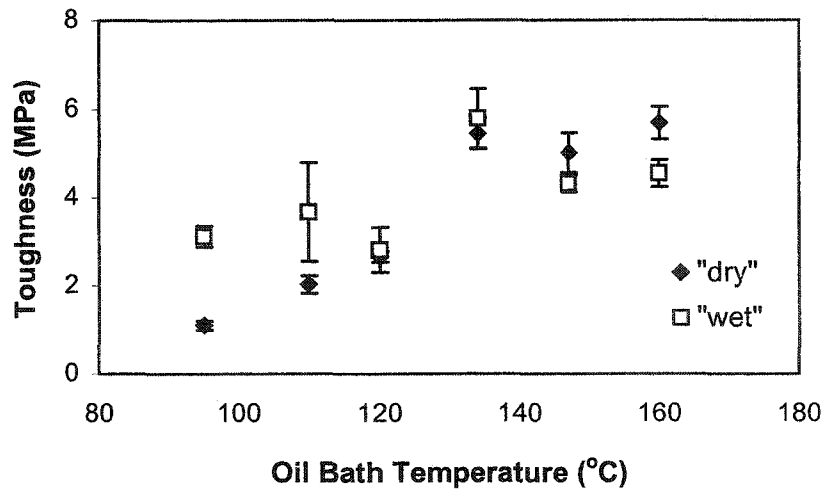
(b)

Figure 5.15 Results from Tensile Tests under “Dry” and “Wet” Conditions for Samples Made at Different Oil Bath Temperatures. (a). Young’s Modulus. (b). Tensile Stress at Break

(Note: error bars designate the range of average \pm standard deviation)



(c)



(d)

Figure 5.15 Results from Tensile Tests under “Dry” and “Wet” Conditions for Samples Made at Different Oil Bath Temperatures. (c). Tensile Strain at Break. (d). Toughness.

(Note: error bars designate the range of average \pm standard deviation)

samples (shown as black diamond in all figures) were compared, the following could be found: as oil bath temperature increased, Young's Modulus in Figure 5.15(a) increased up to 120 °C and then leveled off; while the tensile strength at break in (b), tensile strain at break in (c) and toughness in (d) all leveled off at 134°C.

When moisture was involved in the semi-crystalline polymers, it acted as a plasticizer. All data for wet samples are designated by square symbols. Both Young's Modulus and tensile strength at break were decreased to some extent while the tensile strain at break increased. In fact the tensile strain at break for polymers made at lower oil bath temperatures shows quite a difference between "dry" and "wet" samples, but the one made at the highest oil bath temperature showed little difference. The original stress-strain curves for specimens under dry and "wet" conditions can be found in Appendix B.7 and B.8 respectively.

Similar tests were also run on samples made at different oil bath temperatures with the following composition: 75 g of ϵ -caprolactam, 0.75 g of polycarbonate powder, 12mmol of isobutyl-magnesium bromide (2M solution in diethyl ether). The four oil bath temperatures were: 106, 126, 146 and 164 °C. Specimens were cut into the same dimensions mentioned in Chapter 3. For each sample, 4-6 specimens were prepared and all of them were dried at 90 °C under vacuum for 24 hours before cooling to room temperature.

Figure 5.16 shows the results. Tensile properties such as tensile stress and strain at break and toughness show trends similar to those of the dry samples in Figures 5.15 (a)-(d). As the oil bath temperature increased, the three properties increased and leveled

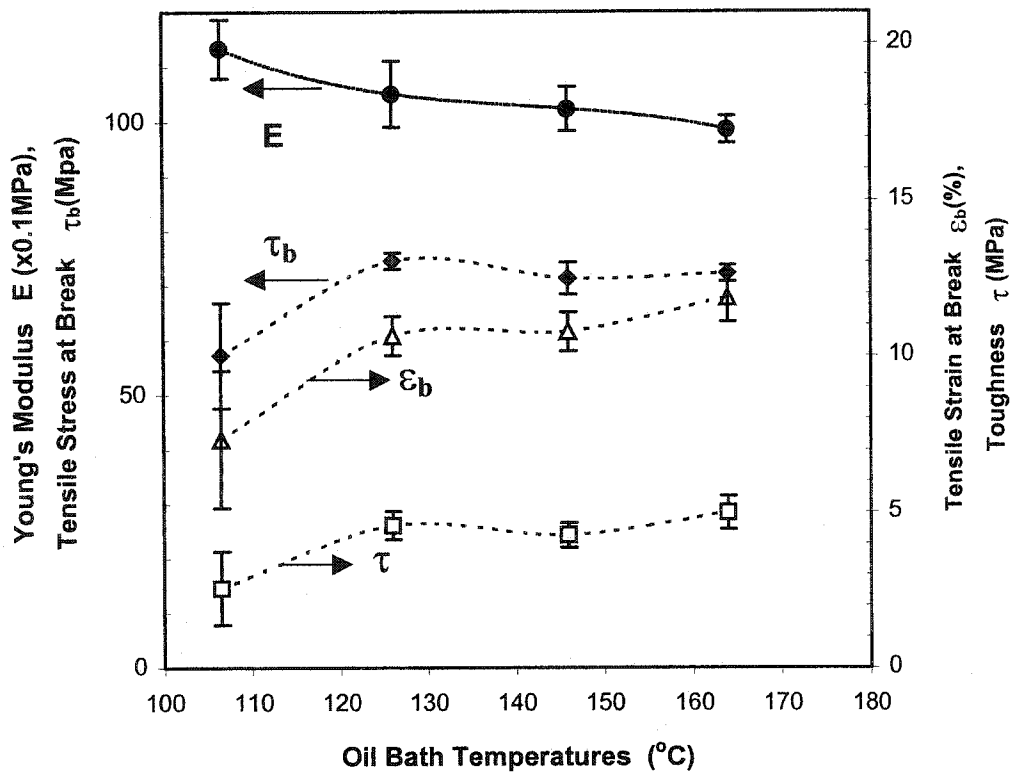


Figure 5.16. Tensile Test Results for Dry Samples Made at Different Oil Bath Temperatures (Composition: 75g ϵ -caprolactam, 0.75 polycarbonate, 12mmol isobutyl magnesium bromide)

(Note: error bars designate the range of average \pm standard deviation)

off after 126 °C. There are some differences in the Young's Modulus part where a monotonic decreasing trend was found in Figure 5.16, instead of the increasing and leveling-off trend in Figure 5.15-(a). The actual difference between the two sets of data is focused on the point where oil temperature is 110°C in Figure 5.15(a) and 106°C in Figure 5.16. The reason why this happened is uncertain, probably due to the facts that different initiator and different amount of initiator was used (which will be discussed in Chapter 6) or that there were two different drying processes involved for the two sets of samples before tensile tests. The detailed stress-strain curves can be found in Appendix B.9 (a)-(d).

5.4.6 Moisture Absorption

For the set of six samples made at different temperatures, the moisture content for “wet” samples was measured to see if the reaction temperature played a role in moisture absorption. Samples with dimension of about 10mm × 1mm × 4mm were first dried up at 70°C under vacuum for 24 hours before cooling down to the room temperature. Weight of each sample was measured before they were put into an environment of 50% R.H. until constant weight. The weight difference between the original dry sample and the “wet” sample were calculated and counted as moisture being absorbed. For each sample, at least two specimens were tested and then averaged. Results were shown in Table 5.6.

It could be found that there was a tendency between the oil bath temperature and moisture absorption. The polymer made at higher temperatures tended to absorb less moisture. This result was also reported earlier (Bai and Williams, 1999).

Table 5.6 Moisture Absorption Data from Samples Made at Different Oil Bath Temperatures (from dry to 50%R.H., room temperature)

| Oil temperature at which sample was made (°C) | Moisture Absorption (%) |
|--|----------------------------|
| 95 | 2.91 |
| 110 | 2.69 |
| 120 | 2.60 |
| 134 | 2.46 |
| 147 | 2.15 |
| 160 | 1.51 |

5.4.7 Bulk Density Measurement

As mention in 5.4.6., polymer made at lower oil bath temperatures did absorb more moisture which would in turn influence its tensile properties. The more moisture existing in the material, the more plasticizing effect would be shown (i.e. lower modulus, lower tensile strength and higher tensile strain). However, between the samples made at oil bath temperature of 95°C and 160°C, the difference in their moisture absorption was not extraordinary (2.91% vs. 1.51%), but their tensile properties were very different. Why?

Another question was: since it had been shown that polymers made at lower temperatures tended to have higher crystallinity which might lead to higher modulus and higher tensile strength for “dry” samples. But the real situation is: for samples made at 95°C and 110°C, their tensile properties (for “dry” samples) are the lowest. It was true that molecular weight and molecular structure would be influencing factors here, and another possible factor would be presence of voids that were formed during polymerization and crystallization.

Bulk density of each sample made at different temperatures was measured.

Details of measurement can be found in Chapter 3.

Figure 5.17 Shows the results of bulk density data for the six samples. It was found that the bulk density of the sample increased as the oil bath temperature (at which the polymer was made) increased up to 134 °C and after that leveled off.

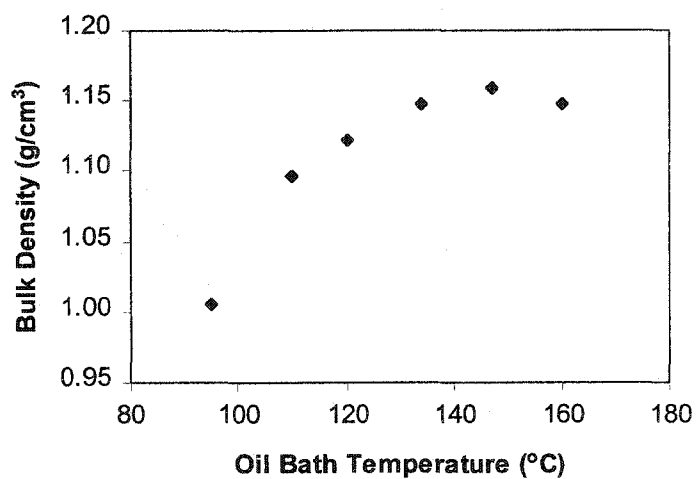


Figure 5.17 Bulk Densities of Copolymer Samples Made at Different Oil Bath Temperatures. (Measured at room temperature)

A rough estimation for copolymer density ρ (based on the assumption of additivity of properties for both amorphous and crystalline phases) was calculated by using the known densities ((Brandrup and Immergut, 1989) for amorphous nylon 6 ($\rho_{a,NY6}=1.09 \text{ g/cm}^3$), 100% crystalline nylon 6 ($\rho_{c,NY6}=1.23 \text{ g/cm}^3$ for α monoclinic) and polycarbonate ($\rho_{PC}=1.20 \text{ g/cm}^3$), and the degree of crystallinity data x_C from DSC:

$$\rho_{est} = 0.99[x_C\rho_{c,NY6} + (1 - x_C)\rho_{a,NY6}] + 0.01\rho_{PC}$$

Then the void content $V\%$ was calculated by:

$$V\% = \left(1 - \frac{\rho_{bulk}}{\rho_{est}}\right) \times 100\%$$

As the results show in Table 5.7, the void content for polymer made at lower temperatures was much higher than those made at higher temperature. This explained why samples made at these low temperatures showed very poor tensile properties.

Possible sources for the presence of voids include: volatiles and dissolved gas in the original reactive mixtures, possible side reactions and the volume shrinkage due to the process of crystallization etc. The effect of void content on the mechanical properties has been studied by Ghiorse (1993) on the carbon/epoxy laminates. It has been found that, a 2% void content increase in the range from zero to 5% may cause an approximately 20% decrease in both interlaminar shear strength and flexural strength with an approximate

10% drop in flexural modulus. Others found an onset threshold exists at about 3-4% void volume fraction. (Springer et al, 1987; Boey, 1990).

It should be mentioned that the above calculation for the void content was not a precise method, and there are many possible errors involved such as instrument error in the bulk density measurement and using $x_{C, DSC}$ in the calculation etc. However, the general trend would not change too much.

Table 5.7 Bulk Density, Estimated Density and Void Content for Samples

Made at Different Oil Bath Temperatures. (*: negative value)

| Oil temperature at which samples were made (°C) | ρ_{bulk} (g/cm ³) | $x_{\text{C,DSC}}$ (%) | ρ_{est} (g/cm ³) | V% |
|---|--|---------------------------|---|------|
| 95 | 1.006 | 46.3 | 1.153 | 12.8 |
| 110 | 1.096 | 49.1 | 1.160 | 5.5 |
| 120 | 1.122 | 43.6 | 1.152 | 2.5 |
| 134 | 1.147 | 40.3 | 1.146 | 0* |
| 146 | 1.159 | 40.8 | 1.148 | 0* |
| 160 | 1.148 | 37.2 | 1.144 | 0* |

Chapter 6 The Effect of Initiator and Activator

6.1 Why is It Important to Study the Effects of Initiator and Activator?

As discussed in Chapter 4 about the possible reaction route for the "L-L" system, the initiator could have two functions. Part of the initiator would perform its traditional function (i.e. forming a ϵ -caprolactam anion), while part would attack the polycarbonate chain to form activating species. If there is too little initiator in the reacting system, it might be consumed for the reaction with polycarbonate before it could start the chain propagation. Therefore, it is interesting to know how the amount of initiator would influence the polymerization process. In the first part of this chapter, results on the rate of the reaction, monomer conversion and inherent viscosity for polymers made at various amount of initiator will be discussed. An optimal amount of initiator will be proposed.

For the study on the role of activator, it has been well known that the amount of activator was related to the molecular weight of the final product, i.e. the more activator, the lower molecular weight of polymer. The special part of this system is that polycarbonate chain (i.e. the macro-activator) would not maintain its original length, somehow it would be scissored which would make it complicated to understand the process. Two polycarbonate samples from GE Plastics of different molecular weight (for GE-S11AP, $\bar{M}_w = 16500$; for GE-S3G100, $\bar{M}_w = 24400$ by using HDPE standard for calibration) were used to see if there is an effect of molecular weight on the copolymer

properties such as monomer conversion, molecular weight and crystallinity. Diphenyl carbonate was also used as an activator for reference as pure nylon 6. The amount of both diphenyl carbonate and polycarbonate resins was also varied to see how the properties were affected.

6.2. The Effect of Initiator

6.2.1. The Use of Grignard Reagents

Alkali and alkaline salts have been used as initiators of anionic polymerization of ϵ -caprolactam since 1941 (Joyce et al. 1941). However, sometimes Grignard reagents are preferred because of the difficulties in handling sodium or sodium lactamate due to their unstable nature. Also Stehlicek and Šebenda (1982) reported that the Grignard reagents gave higher polymerization rates than sodium caprolactamates.

Previously in our group it has been found (Sankholkar, 1996) that sodium hydride was “ineffective for the polymerization of ϵ -caprolactam in the presence of aromatic polycarbonate”. This conclusion was in accordance with the one given by Wurm et al. (1992) who found that sodium caprolactamate tends to react preferably with aliphatic polycarbonate instead of with the endocyclic carbonyl group of the activated caprolactam moiety.

A similar effect was also discussed by Mougin et al. (1993) who found that sodium caprolactamate would attack the Si-O bond of PDMS chain in synthesizing a PDMS-b-Nylon 6 copolymer with NaH as initiator and result in very low conversion of caprolactam. To avoid the cleavage of PDMS chains, an initiator with reducing

nucleophilicity was chosen, i.e. $\text{NaAlH}_2(\text{OCH}_2\text{CH}_2\text{OMe})_2$. Although a new reaction mechanism was proposed by choosing the above-mentioned initiator, it is not of my interest and out of our ability to evaluate the new mechanism. The focus was that if this initiator could be used in the “L-L” system in this research and would not break the chain of polycarbonate, then the so-produced copolymer or polymer blend might be made in a more-controlled way.

It has been mentioned briefly in Chapter 5 that pure nylon 6 can be synthesized by using N-acetyl caprolactam and Red-Al (i.e. 65%(wt) solution of sodium bis(2-methoxyethoxy) aluminum hydride [i.e. $\text{NaAlH}_2(\text{OCH}_2\text{CH}_2\text{OMe})_2$] in toluene) as activator and initiator respectively. This time in order to see if there is any chemical interaction between Red-Al and polycarbonate, two solutions were made with one containing 50 g of ϵ -caprolactam melt and 2 ml of Red-Al at 140 °C and the other containing 50g of ϵ -caprolactam melt and 2 g of dissolved polycarbonate at 140 °C. If there was no interaction between Red-Al and polycarbonate, after mixing these two solutions, the viscosity of the mixed solution would not build up unless an activator like N-acetyl caprolactam was added. However this was not what was observed. The viscosity of the mixed solution increased gradually and finally a light-yellowish solid product was formed. This indicated that unlike the system of Red-Al and PDMS, there was an interaction between Red-Al and polycarbonate. Details on using Red-Al as initiator was not further studied in this research.

Other initiators were also tried in the “L-L” system, such as LiBH_4 , NaBH_4 and $(\text{iso-Bu})_2\text{Mg}$. However, all these initiators ended up giving unsuccessful results, with either low reaction rate or low monomer conversion or both. Therefore, in this chapter only two initiators will be discussed in detail, i.e. isobutyl magnesium bromide and isobutyl magnesium chloride.

6.2.2 The Amount of Initiator

To study the effect of various amount of initiator in the “L-L” system, a series of polymerizations were conducted. The concentration of initiator (isobutyl magnesium bromide and isobutyl magnesium chloride) was changed while the other compositions were kept the same. GE-S11AP as macroactivator was used at two concentrations, i.e. 1% (w/w) and 2% (w/w). The oil bath temperature was kept at $130\text{ }^\circ\text{C}$ for all the experiments in this chapter except specifically mentioned.

6.2.2.1 Rate of Polymerization

Generally, two melt solutions were prepared under nitrogen environment: one containing 50g ϵ -caprolactam melt and certain amount of initiator (6-20 mmol); the other containing 50g ϵ -caprolactam melt and dissolved polycarbonate (1% or 2%). After two clear solutions were formed, they were mixed together under nitrogen. The whole mixture was under vigorous stirring (by magnetic stirrer) up to a certain point when the solution was too viscous to be stirred. The time from the start of the mixing to the viscous point was recorded as t_s (s stands for solidification) and would be used as indication of

the rate of polymerization. The reproducibility of t_s was checked by repeating some of the polymerization for two or three times. It was found that the results were consistent, for a reaction with t_s of 2.5 minutes, the difference between individual runs was within 10 seconds.

Figure 6.1 shows the results of t_s value vs. the concentration of initiators for 1%(w/w) and 2%(w/w) of GE-S11AP polycarbonate. It can be seen that, at 1% concentration of polycarbonate, for both iso-Bu-MgCl and iso-Bu-MgBr there is sharp change of t_s at 8 mmol. When the amount of initiator is lower than 8 mmol, the rate of polymerization is very low; even after one hour, the magnetic stirrer is still movable indicating that the polymer chain was not long enough. When the amount of initiator is higher than 8 mmol, the rate of polymerization does not change much for both initiators. However there is still some slight difference between the two initiators. For example, for iso-Bu-MgBr, as its amount increases from 8 mmol to 14 mmol, the value of t_s almost keeps the same at around 3.4 minutes; while for iso-Bu-MgCl, as its amounts changes from 8 mmol to 12 mmol, t_s decreases from 6.5 minutes to 2.5 minutes and stays the same at 14 mmol.

For 2% concentration of polycarbonate, similar trend can be found. The rate of polymerization is much higher when the amount of initiator reaches 16 mmol. It only takes 1 minute for the reactive mixture to solidify for both 16 mmol and 18 mmol of iso-Bu-MgBr. It seems that a certain ratio between initiator and activator has to be reached in order for the polymerization to proceed fast. For 1% polycarbonate, the amount of

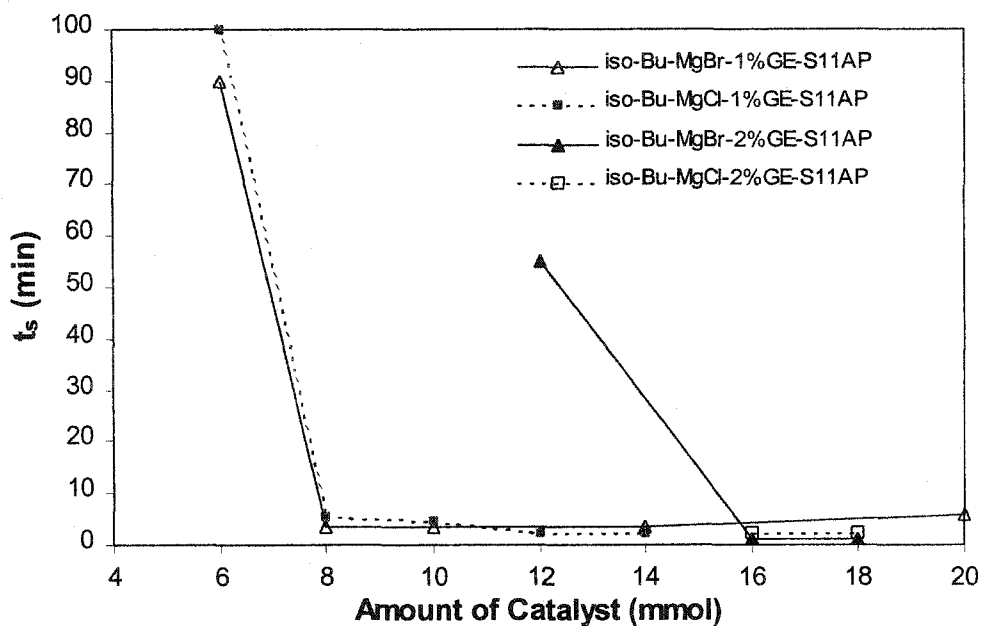


Figure 6.1. The Effect of Amount of Initiators on Rate of Polymerization.

[Composition: 100 g ϵ -caprolactam/1%(w/w) or 2% (w/w) GE-S11AP/various amounts of iso-BuMgCl or iso-Bu-MgBr; Temperature: 130°C]

initiator has to be above 8 mmol; for 2% polycarbonate, the amount of initiator has to be above 16 mmol. Therefore the ratio of initiator over polycarbonate must be higher than 8 mmol/g for both concentrations of polycarbonate.

Ueda et al. (1996) showed that in their system (150°C, ethylene magnesium bromide as initiator, N-acetyl caprolactam as activator), polymerization rate increased with the increase of initiator concentration. This is also what we found for our system at initiator concentration up to 14 mmol with 1% polycarbonate. However it should be noted that at very high concentration of initiator (e.g. 20 mmol of iso-Bu-MgBr), the value of t_s increases to 6 minutes. The reason may be attributed to the fact that with a lot of extra initiator in the reaction system, there will be more scission of polycarbonate chains (i.e. more chain starter). In this way, it will end up with lower molecular weight. This is supported by the solution viscosity data which will be discussed later in this chapter.

6.2.2.2. Monomer Conversion

For the same series of polymers mentioned in 6.2.2.1, the water-extractable content data for each sample was also measured and compared. Since there are mainly monomer caprolactam and oligomer in the water-extractable content, the information on monomer conversion can be obtained. Figure 6.2 shows the results of monomer conversion.

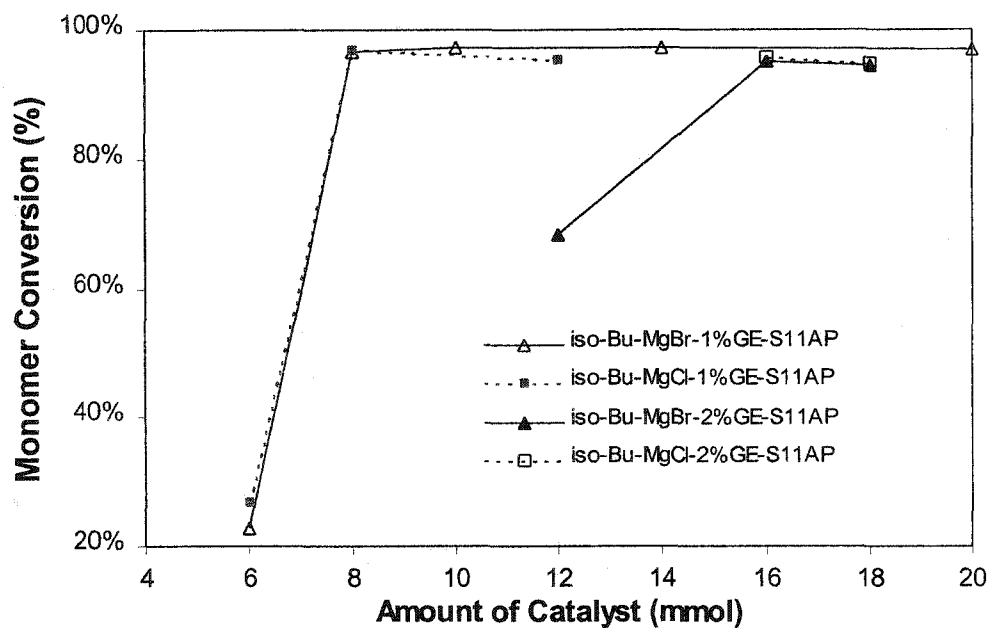


Figure 6.2. The Effect of Amount of Initiators on Monomer Conversion.

[Composition: 100 g ϵ -caprolactam/1%(w/w) or 2% (w/w) GE-S11AP/various amounts of iso-BuMgCl or iso-Bu-MgBr; Temperature: 130°C]

Similar to what was found in the influence of amount of initiator on polymerization rate, there is a clear-cut influence of the amount of initiator on the final monomer conversion data. For polymers with 1% polycarbonate, when the amount of initiator (both iso-Bu-MgBr and iso-Bu-MgCl) is lower than 8 mmol, the conversion of ϵ -caprolactam is very low; when the amount of initiator is equal to or higher than 8mmol, more than 95% of monomer is converted and there is little difference between polymers made with various amounts of initiators. The same trend can be found for polymers with 2% polycarbonate: when 12mmol of iso-Bu-MgBr was used, the monomer conversion of the final polymer is low (around 69%); when the amount of initiators is higher or equal to 16mmol, the monomer conversion is higher than 94%.

6.2.2.3 Intrinsic Viscosity $[\eta]$

After the water-extraction treatment, the dry samples were dissolved into 90% formic acid (a good solvent for nylon 6) at concentration around 0.06g/dL. The viscosity measurement was conducted with a Ubbelohde Viscometer being kept in a water bath of constant temperature at 30°C.

Usually to represent the molecular dimension in certain solvent, intrinsic viscosity $[\eta]$ was used. For each sample, $[\eta]$ could be obtained from the y-intercept of plot η_{sp}/C vs. C or $\ln\eta_{rel}/C$ vs. C at concentration equal to zero. Both methods are somewhat time-consuming because several points needed to be measured to draw the plot. The method of Solomon and Ciuta (1962) involved just one single point by using the following equation:

$$[\eta] = \frac{\sqrt{2(\eta_{SP} - \ln \eta_{rel})}}{C}$$

$$\eta_{SP} = \frac{t}{t_0} - 1 = \eta_{rel} - 1$$

here C is the concentration of the solution (in g/dL), η_{SP} and η_{rel} represent specific viscosity and relative viscosity respectively, t and t_0 are the flow time to pass through the capillary for the solution and pure solvent respectively.

To verify the above equation, seven samples were used. First, for each sample, four solutions of different concentrations were prepared and $[\eta]$ was obtained by the multi-point method. Then, for the same sample, $[\eta]$ was calculated based on Solomon-Ciuta equation where η_{SP} and η_{rel} values were taken at concentration of 0.06g/dL. The comparison between the two methods on seven samples is shown in Figure 6.3.

From Figure 6.3, it can be seen that there is some difference between the $[\eta]$ values from two methods (the $[\eta]$ from single-point method is slightly higher than that from multi-point method). However, all of the points are pretty close to the dotted line where two of them are supposed to be equal to each other. Therefore, for the rest of this chapter, the one-point method will be used to calculate $[\eta]$ value.

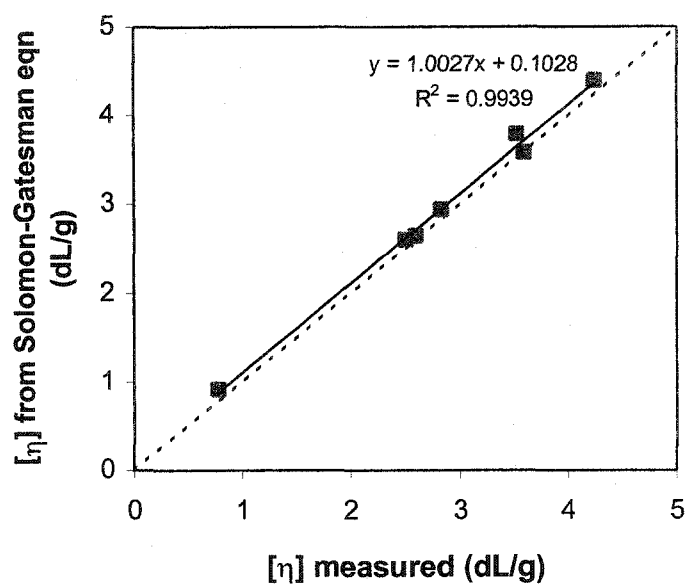


Figure 6.3. Comparison of $[\eta]$ Values from Two Different Methods.

(Solid line represents linear trendline; Dotted line represents the case where two $[\eta]$ s equal to each other)

The intrinsic viscosity data for polymers made at various amount of initiators are shown in Figure 6.4. It is obvious that the intrinsic viscosity (implicitly the molecular weight of the nylon 6 block in the final product) is greatly influenced by the amount of initiator. At a low concentration of initiator (e.g. 6 mmol for 100 g polymer with 1% polycarbonate, 12 mmol for 100 g polymer with 2% polycarbonate), the intrinsic viscosity is very low. As the amount of initiator increases in the reactive mixture, the intrinsic viscosity value increases. However, when more and more initiator is in the reactive mixture, the intrinsic viscosity levels off and decreases slowly with the increase of initiator concentration. This is somehow different from the results of Ueda et al. (1996) where there was no dependence of molecular weight \bar{M}_w on the concentration of initiator. Careful comparison between systems used in this research and Ueda's leads to the factor that the system used in this research is more complicated. In the system used in this research, initiator was used to form caprolactamate anion which would be consumed in both chain propagation and interacting with polycarbonate to form activating species. If the concentration of initiator is not sufficient, the caprolactamate anion would be used up solely in interacting with polycarbonate, and there would not be enough anion for chain propagation. This would lead to a final product with low monomer conversion and low molecular weight (like the one with 6 mmol initiator/100 g caprolactam/1 g polycarbonate). On the other hand, when the concentration of initiator is too much, there

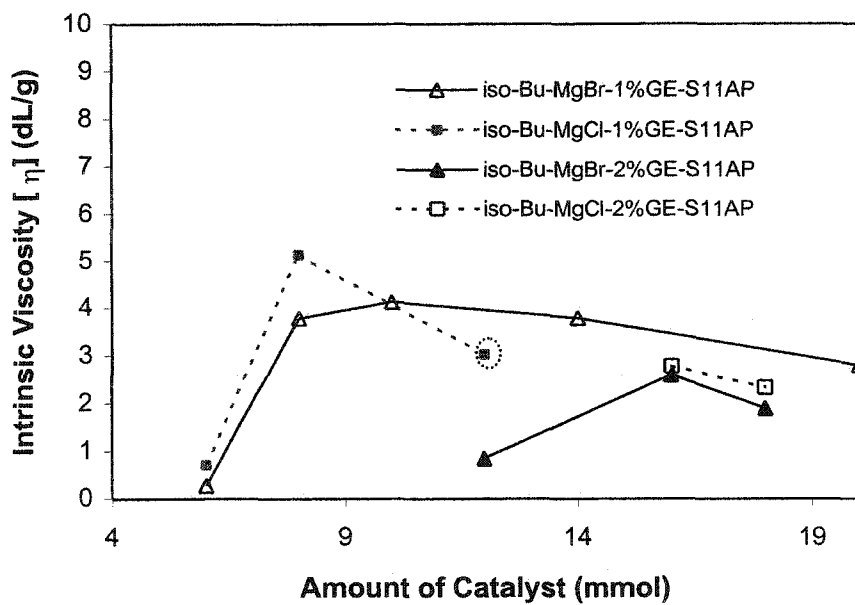


Figure 6.4. The Effect of Amount of Initiators on Intrinsic Viscosity.

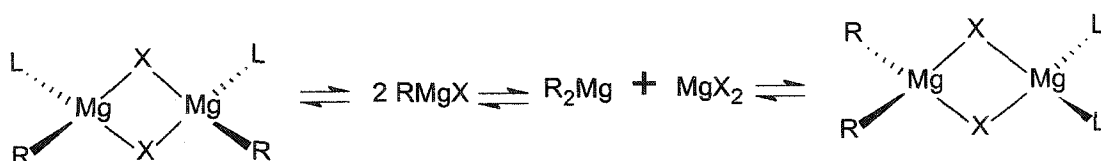
[Composition: 100 g ϵ -caprolactam/1%(w/w) or 2% (w/w) GE-S11AP/various amounts of iso-BuMgCl or iso-BuMgBr; Temperature: 130°C]

would be more interactions between initiator and polycarbonate. Thus more activating species would be formed and this would lead to low molecular weight for nylon 6 block.

Therefore, in terms of rate of polymerization, monomer conversion and molecular weight, there is an optimal ratio between the initiator and polycarbonate, i.e. *8mmol of initiator/g of polycarbonate*.

6.2.3 Comparison between iso-Bu-MgBr and iso-Bu-MgCl

The composition of Grignard reagents in solvent is complicated. The classic Schlenk (1929) equilibrium gives a simplified description of Grignard composition as following:



where L represents solvent molecule with donor properties. The factors that affect the above equilibrium (i.e. the reactivity of Grignard reagent) include: temperature, solvent and amount and type of R and X etc. (Elschenbroich and Salzer, 1992). For the systems used in this study, the only difference between the two Grignard reagents is the type of halide while solvent and temperature were kept the same. Therefore if there are differences in properties such as rate of polymerization, monomer conversion and so on, it could be attributed to the different initiating activity the two Grignard reagents.

By comparing the curves corresponding to iso-Bu-MgBr and iso-Bu-MgCl in Figures 6.1, 6.2 and 6.4, the following can be found: (1). At relatively low concentration of initiator (≤ 10 mmol for 100 g caprolactam/1% polycarbonate, ≤ 18 mmol for 100 g caprolactam/2% polycarbonate), the reaction with iso-Bu-MgBr shows higher reaction rate (shorter time of t_s) than that with iso-Bu-MgCl. For the reaction system with 1% polycarbonate, when the concentration of initiator is higher than 12 mmol (for reactive mixture with 1% polycarbonate), the rate of polymerization for the ones with iso-Bu-MgCl is faster than that with iso-Bu-MgBr. (2). In terms of monomer conversion, there is not much difference between the two initiators; they show similar trends. (3). In terms of intrinsic viscosity, for both systems with 1% and 2% polycarbonate, the ones with iso-Bu-MgCl (dotted lines) show higher intrinsic viscosity than those with iso-Bu-MgBr (solid lines). There is one exception which will be discussed in the next paragraph. More data on the two initiators will be shown and discussed in Section 6.3 together with the effects of various polycarbonates.

For the sample made at composition (12 mmol iso-Bu-MgCl/100 g ϵ -caprolactam/1 g polycarbonate), there is a big drop on its $[\eta]$ value in Figure 6.4. It was marked with a dotted circle. The reason is: when it was dissolved into 90% formic acid, there was lots of gel formation that could not be completely dissolved. After filtration and drying, it was found that the weight concentration of gel is around 18.3%. Because of the special situation of cross-linking for this composition, this $[\eta]$ value may not be used to compare with the others.

6.3 The Effect of Activators

Activator is sometimes called chain-initiator, because according to the well-accepted mechanism for the anionic polymerization of ϵ -caprolactam, the propagation of the polymer (i.e. nylon 6) chain will start from the activator. Therefore, by changing the amount of activator with a fixed amount of monomer, it is expected that the molecular weight of the final polymers would be different. The higher the concentration of the activator, the lower the molecular weight for the polymer. This is the theoretical derivation. However, in the system used in this thesis, it is a bit complicated with the joining of polycarbonate chains. Will the polymers made with polycarbonate show the same trend in various properties as those of pure nylon 6s?

In this part, the effect of activators on various properties of the final polymers will be studied. Polycarbonate samples of different molecular weight (GE-S3G100 and GE-S11AP) were used. Their molecular weight information can be found in Chapter 3. For comparison, diphenyl carbonate (DPC) was also chosen as activator by a small molecule. By varying the concentration of DPC, theoretically pure nylon 6s with different molecular weight were produced. For each kind of activator, three concentrations were chosen, i.e. 0.2%, 1%, 2% (w/w).

For each sample, 100g ϵ -caprolactam was used. Temperature of the oil bath was controlled isothermally at 130°C for polycarbonates and 150°C for DPC (the rate of polymerization was too slow for DPC at 130°C). Both iso-Bu-MgBr and iso-Bu-MgCl were used as initiators: for DPC and GE-S11AP, iso-Bu-MgBr was used; while for GE-

S11AP and GE-S3G100, iso-Bu-MgCl was used. As discussed in 6.2, the amount of initiator used for each concentration of activator is listed in Table 6.1.

The properties which will be discussed include: rate of polymerization (t_s); monomer conversion; intrinsic viscosity; melt viscosity and degree of crystallinity etc.

Table 6.1. Amount of Initiators Used for Various Concentrations of Activators

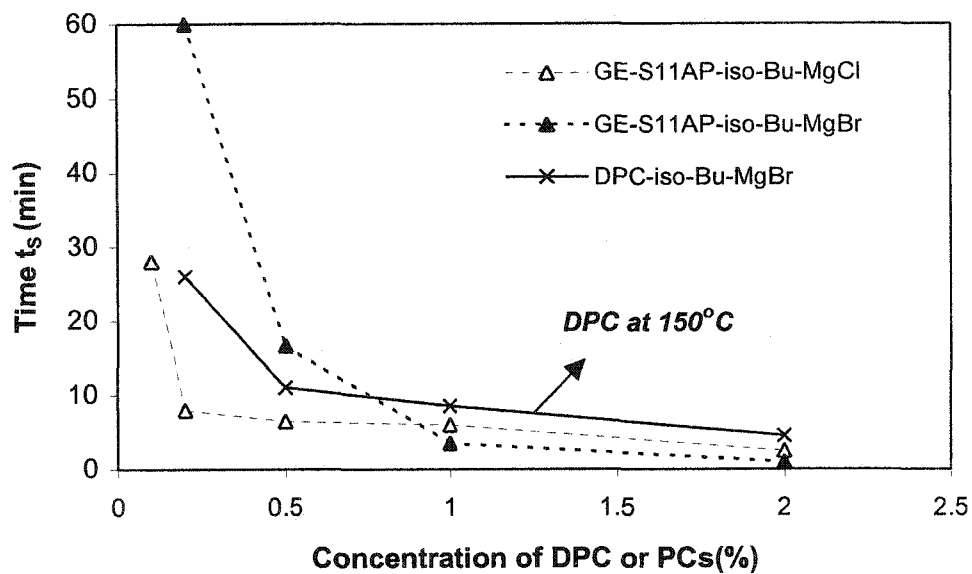
| Concentration of Activators (%w/w) (for DPC, GE-S3G100 and GE-S11AP) | Amount of Initiators Used in Polymerization (mmol/100g ϵ -caprolactam) |
|--|---|
| 0.1 –1 | 8 |
| 2 | 16 |

6.3.1. Rate of Polymerization

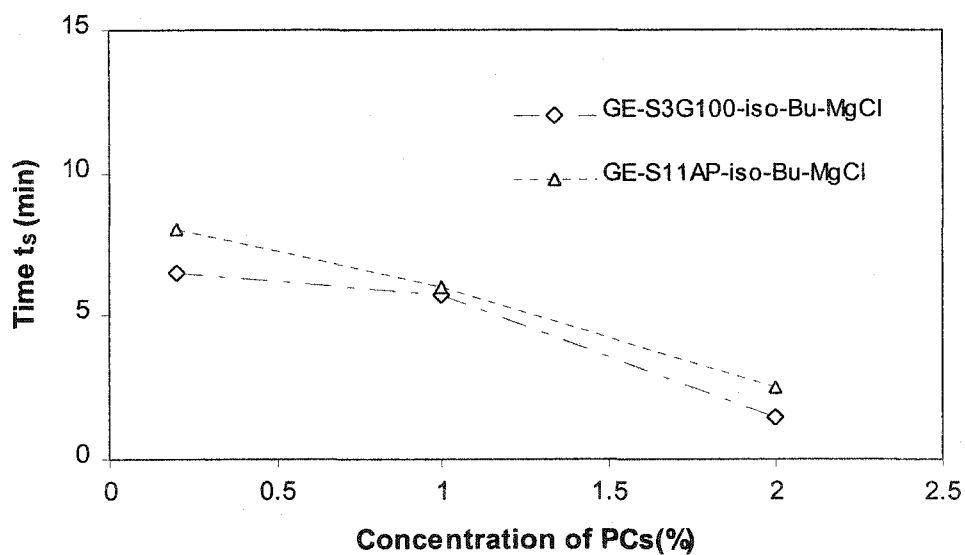
The time t_s between the start of mixing two reactive melt solutions to the point when the magnetic stirrer can barely move was used to represent the rate of polymerization. Results are shown in Figure 6.5-(a) and (b). All systems showed a similar trend, i.e. the higher the concentration of activator (either DPC or polycarbonates), the faster the rate of polymerization.

It needs to be mentioned that, in Figure 6.5-(a), some values of t_s for DPC (e.g. at concentration of 0.2% and 0.5%) are smaller than those for GE-S11AP polycarbonate. This does not mean that these reacting mixtures with DPC have higher rate of polymerization, because the group of t_s data with DPC was measured at 150°C instead of 130°C for the polycarbonates. In fact, the systems with either polycarbonate showed higher rate of polymerization than the ones with DPC. Attempts have been made to make polymers at various concentration of DPC at 130°C, it was not successful due to the very long t_s measured. Although by switching oil bath temperature from 130°C to 150°C, the reaction kinetics would be changed. Since DPC was used as reference to show the trend for the case of pure nylon 6, no absolute comparison between DPC and polycarbonates was needed.

Figure 6.5-(a) also showed the differences between two initiators (i.e. iso-Bu-MgBr and iso-Bu-MgCl) with the same kind of polycarbonate (i.e. GE-S11AP) used. At



(a)



(b)

Figure 6.5 Plot on Rate of Polymerization vs. Activator Concentration
 (a). with DPC (iso-Bu-MgBr), GE-S11AP (both iso-Bu-MgBr and iso-Bu-MgCl);
 (b) with GE-S11AP and GE-S3G100 (iso-Bu-MgCl)

0.2% and 0.5% concentration of GE-S11AP, the systems containing iso-Bu-MgCl have a higher rate of polymerization; while at 1% and 2% concentration of GE-S11AP, the systems containing iso-Bu-MgBr show a higher rate of polymerization.

In Figure 6.5-(b), the difference between two polycarbonate samples (of different molecular weight) was compared by using the same initiator (iso-Bu-MgCl). It can be seen that, with the same initiator, there was not much difference on rate of polymerization. The t_s values for GE-S3G100 were slightly lower than those for GE-S11AP at corresponding concentration. It has been known that GE-S3G100 has higher molecular weight and narrower MWD than GE-S11AP. However, a conclusion still cannot be made about how the MW and MWD play a role in the rate of polymerization.

6.3.2. Monomer Conversion

In Figure 6.6, monomer conversion data are plotted against concentration of various activators with two initiators.

Generally, it can be seen that for each activator used, monomer conversion was high, with all values above 95%. There was not much difference between different activators. For systems using polycarbonates, the values of monomer conversion at concentration of 2% seem to be lower than those at 0.2% and 1%. This might be due to the faster reaction kinetics at higher concentration like 2%. As shown in Figure 6.5-(a) and (b), with 2% polycarbonate in the reactive mixture, the t_s value can be as low as 1 minute. This means that the reaction mixture becomes viscous very fast, some part of the

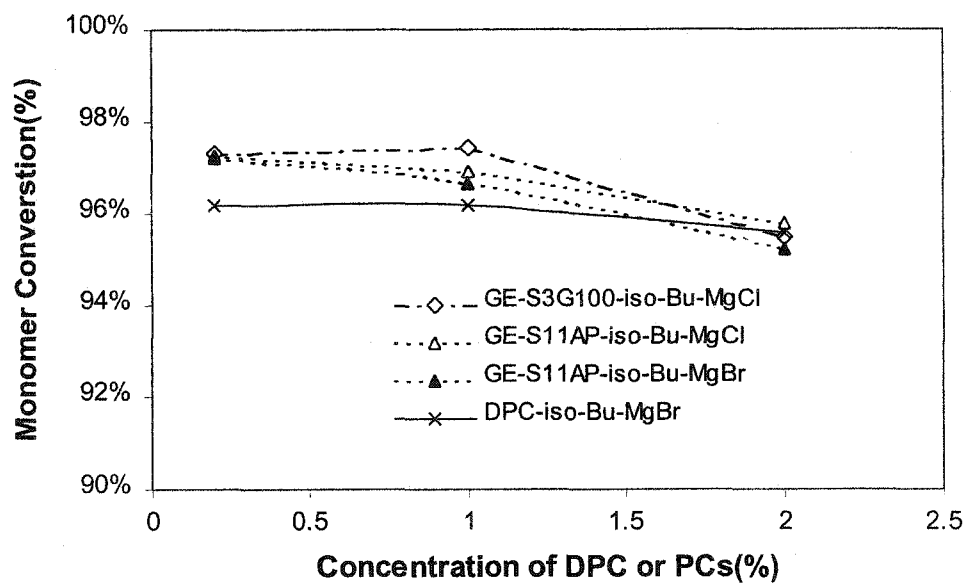


Figure 6.6. Results of Monomer Conversion vs. Concentration of Various Activators (DPC or PCs with two initiators)

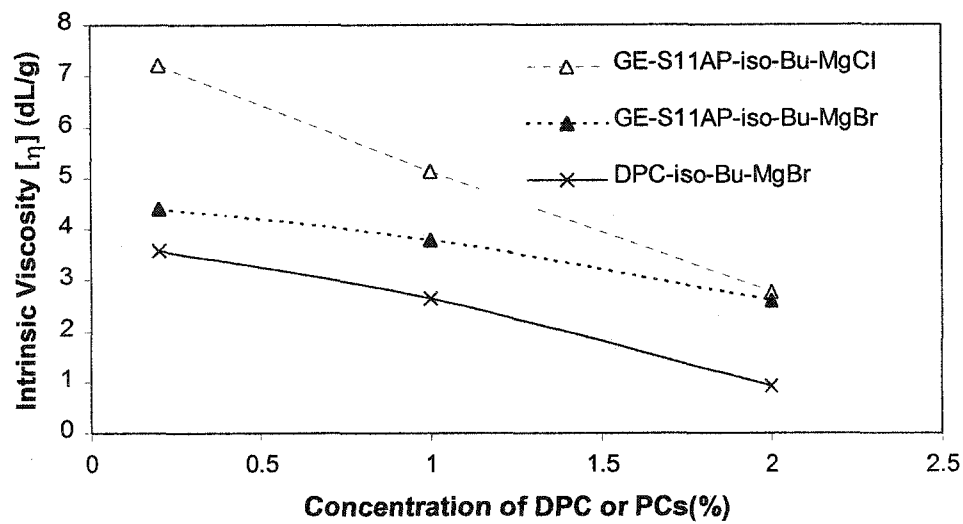
monomer might be trapped in the middle and cannot be accessed by activating reagent due to the viscous hindrance. In this way, the amount of unreacted monomer might be high.

6.3.3. Intrinsic Viscosity

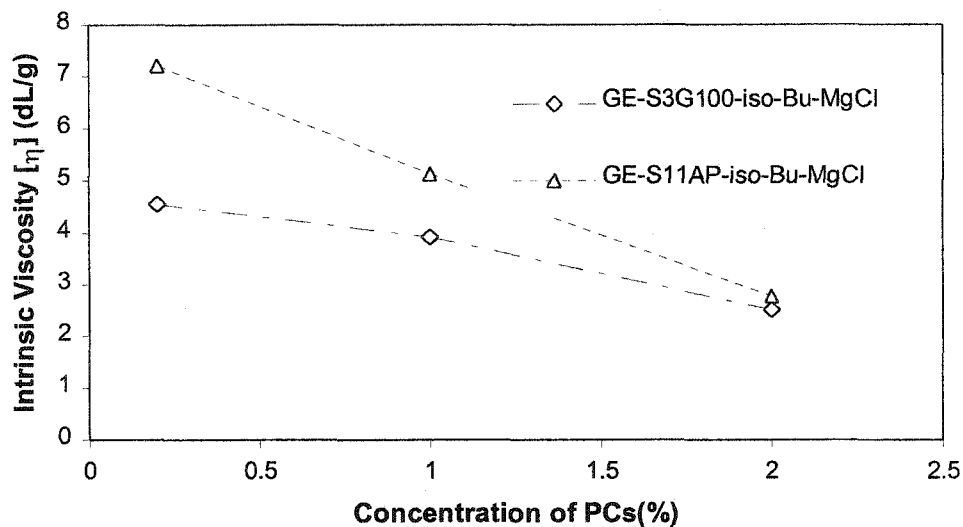
The intrinsic viscosity data versus concentration of various activators are shown in Figures 6.7-(a) and (b) with two initiators used. In Figure 6.7-(a), comparisons are between the pure nylon 6s with DPC as activator at three levels of concentration (iso-Bu-MgBr as initiator), copolymers with GE-S11AP polycarbonate as activator at the same three concentrations (both iso-Bu-MgBr and iso-Bu-MgCl as initiators respectively). In Figure 6.7-(b), the effect of two different polycarbonate activators was compared by using same initiator iso-Bu-MgCl.

The general trend is: as the concentration of activator (either DPC or PCs) in the reactive mixture increases, the intrinsic viscosity tends to decrease. This suggests that: the more activator used, the shorter nylon 6 chain formed. Since the number of polymer chains (nylon 6 chains) is related to the amount of activator used, the smaller amount of activator would lead to higher molecular weight of nylon 6.

In Figure 6.7-(a), both products with polycarbonates showed higher $[\eta]$ than those of pure nylon 6 with DPC as activator at various concentrations. Taking into consideration that at each concentration (weight percentage) of activator the molar



(a)



(b)

Figure 6.7 Plot of Intrinsic Viscosity $[\eta]$ vs. Activator Concentration
 (a). with DPC (iso-Bu-MgBr), polycarbonate GE-S11AP (both iso-Bu-MgBr and iso-Bu-MgCl); (b) with the two polycarbonates GE-S11AP and GE-S3G100 (iso-Bu-MgCl)

concentration of DPC is much higher than that of polycarbonate, it seems reasonable that at each concentration the molecular weight of nylon 6 made from DPC is lower than the molecular weight of "nylon 6 block" in the copolymer made from polycarbonate.

Also in Figure 6.7-(a), the use of iso-Bu-MgBr and iso-Bu-MgCl was compared by using the same polycarbonate GE-S11AP at various concentrations. Generally the copolymers made from iso-Bu-MgCl have higher $[\eta]$ values than those from iso-Bu-MgBr. The difference between the two was much higher at lower concentration (e.g. 0.2%) than higher concentration (e.g. 2%). At 2% concentration, there is not much difference between the two products. This might suggest that, at 0.2% concentration of GE-S11AP, the molecular size of copolymer made from iso-Bu-MgCl in 90% formic acid was much larger than that of copolymer made from iso-Bu-MgBr; at 2%, the molecular size of the two in 90% formic acid are close. The cause of this difference may come from the use of initiators with different nucleophilicity. For example, at 0.2%, there are many more activating chains for the start of propagation in the system with iso-Bu-MgBr than in the system with iso-Bu-MgCl (due to the different extent of interaction between initiators and polycarbonate), this leads to the lower molecular weight of nylon 6 part in the copolymer using iso-Bu-MgBr. On the other hand, at 2%, the number of chains to start the propagation for the two systems may be close to each other, therefore the molecular weights of nylon 6 blocks in the two systems are similar.

In Figure 6.7-(b), with the same initiator (iso-Bu-MgCl), the $[\eta]$ values from GE-S11AP were higher than those from GE-S3G100 over all three concentrations. The difference between the two polycarbonates was much higher at lower concentration (e.g.

0.2%) than at higher concentration (e.g. 2%). This might be caused by the use of polycarbonate with different MW and MWD. By using 0.2% GE-S3G100 which has higher MW, the molecular size of the polymer in 90% formic acid was much smaller than that made from 0.2% GE-S11AP. This indicates that there are many more initial chains to start propagation in the system with 0.2% GE-S3G100 than in the one with 0.2% GE-S11AP. One possibility is that there are more interactions between the initiator and GE-S3G100. If this held true, then the MW of polycarbonate block in the final copolymer would be smaller. How can we prove this possibility right or wrong?

6.3.4. Complex Melt Viscosity

Dynamic complex viscosities of each polymer melt (both pure nylon 6s and nylon 6 copolymers) were measured and compared. Unlike the $[\eta]$ which is used in 6.3.3 as rough indicator of molecular weight of nylon 6 block in the copolymer, complex melt viscosity η^* is a value which reflects the melt states of the copolymers including both nylon 6 block and polycarbonate block in the copolymer.

RMS 800 was used for the measurement with a disk and plate fixture. A dynamic frequency sweep was run from 0.1 rad/s to 100 rad/s with 1% strain amplitude. For polymer samples made with DPC and GE-S11AP by using iso-Bu-MgBr, measurements were done at temperature of 240°C; while for the others, temperature of 250°C was used (note: T_m is around 220°C). The complex viscosity η^* at 0.1 rad/s (close to the limit η_0) was picked to compare among various samples.

For the linear chain of pure nylon 6, with no influence from polycarbonate block, its zero-shear rate viscosity η_0 could be related to its viscosity-average molecular weight M_v in a power-law equation as follows:

$$\eta_0 = kM_v^a$$

where k and a are constants (generally $a = 1$ for low molecular weight, and 3.4 for high molecular weight). On the other hand, the intrinsic viscosity of pure nylon 6 is also related to the molecular weight by the Mark-Houwink equation:

$$[\eta] = KM_v^A$$

where K and A are also constants. Therefore, for a linear homopolymer, there is certain relation between its zero-shear melt viscosity η_0 and intrinsic viscosity:

$$\eta^* \leftrightarrow \eta_0 \leftrightarrow M_v \leftrightarrow [\eta]$$

By plotting η^* against $[\eta]$ for linear-chain polymers of different molecular weights on a semi-log plot, a straight line is expected. For pure nylon 6 made at various concentrations of DPC, η^* vs. $[\eta]$ is plotted in Figure 6.8. Clearly a straight line is shown on this semi-log plot.

If the effect of polycarbonate blocks in the copolymer was taken into consideration, there would be some difference from the pure nylon 6. For example, if one nylon 6 homopolymer and one copolymer of nylon 6-polycarbonate have same $[\eta]$ values (in 90% formic acid), since in 90% formic acid polycarbonate does not contribute much to the $[\eta]$ value which represents the molecular size of polymer (either homopolymer or

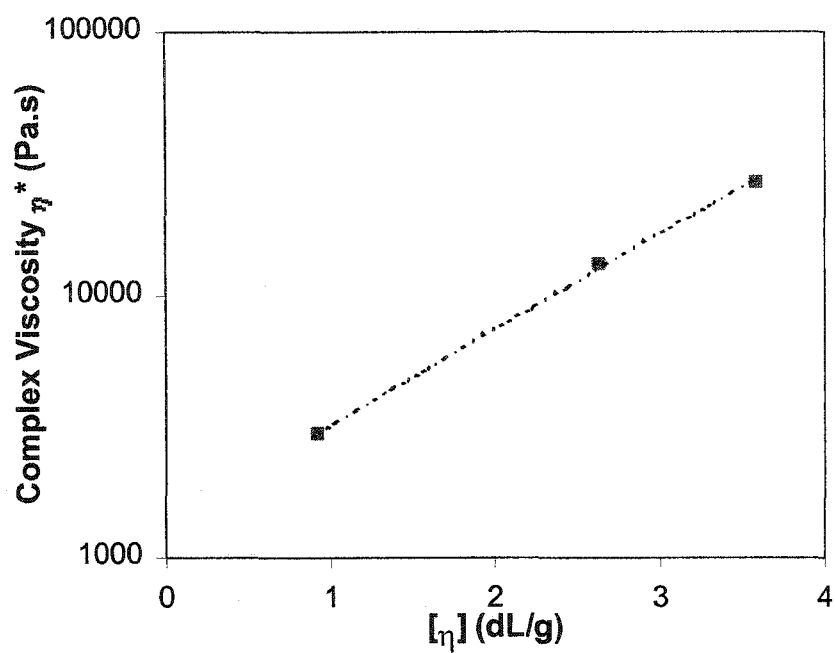


Figure 6.8 Plot of η^* versus $[\eta]$ for Nylon 6s Made from Various Concentrations of DPC.

copolymer) in the solvent, roughly the length of nylon 6 chain for both nylon 6 homopolymer and copolymer might be close to each other. On the other hand, in the melt state, the polycarbonate block in the copolymer would contribute to the melt viscosity of the sample. In this way, in a η^* vs. $[\eta]$ plot for copolymer, the points for the copolymer would not form a straight line relation, instead, they would deviate positively from the straight line obtained for pure nylon 6. Figure 6.9 shows the results for the copolymers made from different polycarbonate of various amounts. The straight line for pure nylon 6 was also included for reference at 240°C.

It is clear that, with the inclusion of polycarbonate, samples show deviations from the one for homopolymers. And the extent of deviation is different if different initiators and polycarbonates of various concentrations were used. In Figures 6.10(a)-(c), the correlation between the complex melt viscosity η^* and various concentrations of polycarbonates were shown.

In Figure 6.10-(a) for the system using GE-S3G100 polycarbonate and iso-Bu-MgCl as initiator, the complex melt viscosity η^* increased monotonically with the concentration of GE-S3G100 even though the chain length of nylon 6 block decreased monotonically with the concentration of GE-S3G100 (from Figure 6.7-(b)). This might suggest that the chain length of PC block increases as the concentration of polycarbonate increases, in this way the melt viscosity has an increasing tendency. As it can be seen from the top plot of Figure 6.9, the point corresponding to 2% GE-S3G100 (the solid diamond at top-left corner) showed the most deviation from the straight dotted line.

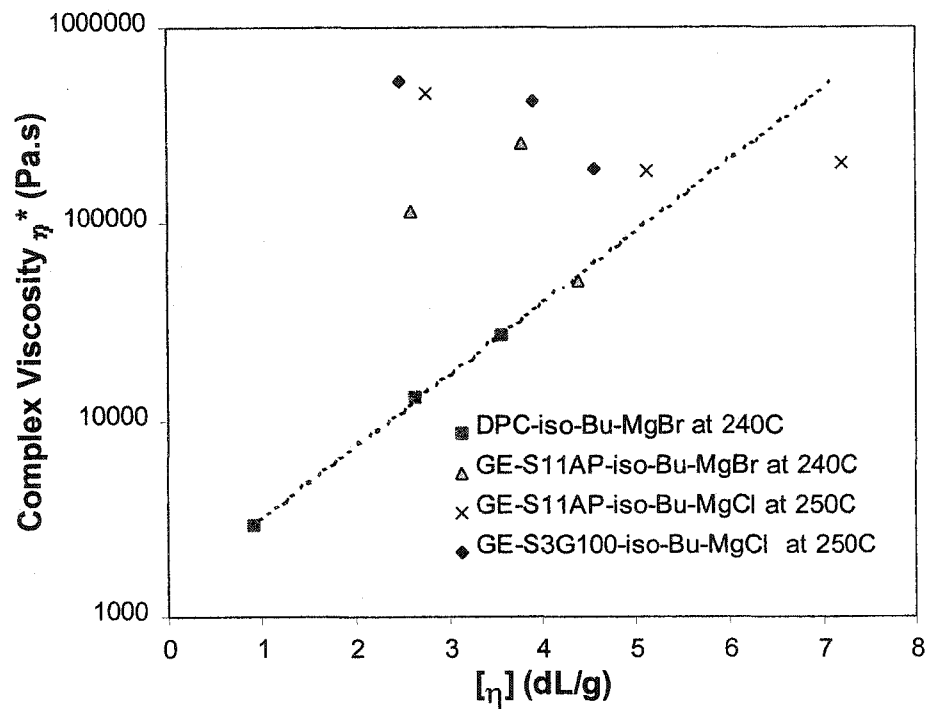
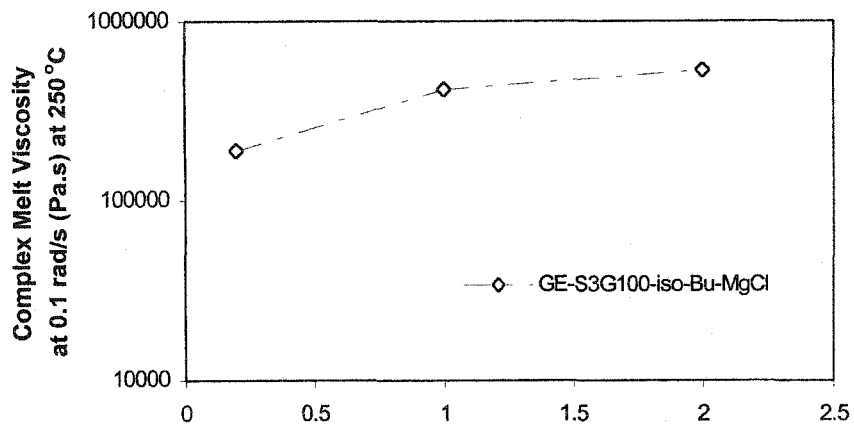
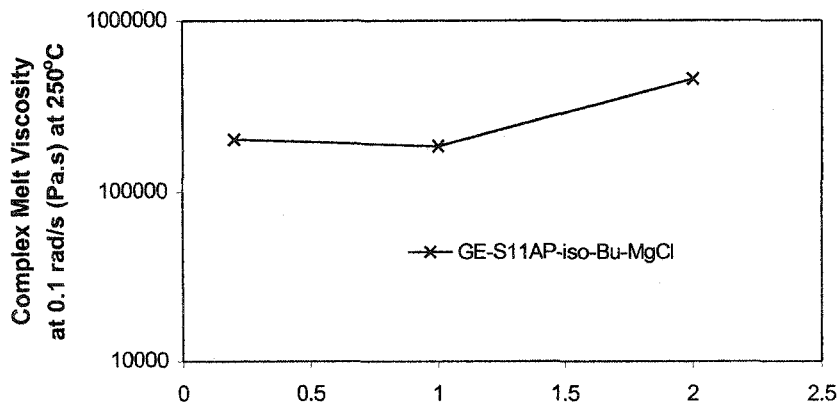


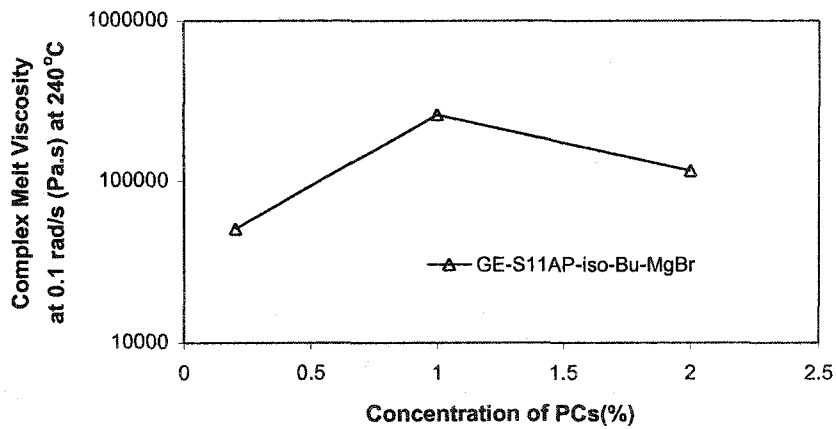
Figure 6.9. Plot of η^* versus $[\eta]$ for All Samples at Various Concentrations of DPC or Polycarbonates.



(a)



(b)



(c)

Figure 6.10 Plots of η^* versus Polycarbonate Concentrations

- (a). for GE-S3G100 polycarbonate and iso-Bu-MgCl;
- (b). for GE-S11AP polycarbonate and iso-Bu-MgCl;
- (c). for GE-S11AP polycarbonate and iso-Bu-MgBr.

In Figure 6.10-(b) for the system using GE-S11AP polycarbonate and iso-Bu-MgCl as initiator, the trend is not monotonic. Between 1% and 2% polycarbonate concentration, there is an increase of η^* with increase of concentration. This can be explained by the same reason in last paragraph, i.e. the chain length of polycarbonate block for 2% concentration is longer than that for 1% which in turn leads to higher η^* . However, the one corresponding to 0.2% concentration of GE-S11AP showed higher η^* than that of 1%. Possibly this is due to the contribution of the very long nylon 6 chain in 0.2% concentration (with $[\eta]$ around 7.2 dL/g).

In Figure 6.10-(c) for the system using GE-S11AP polycarbonate and iso-Bu-MgBr as initiator, in Figure 6.10-(c) there is another trend. Between 0.2% and 1%, the η^* value increases due to the increase of polycarbonate chain length. However, at 2% concentration, the η^* value decreased which is probably due to the shorter chain length of nylon 6 block.

If the effect of different polycarbonate was to be studied, it could be found that, between GE-S11AP and GE-S3G100 (by using the same iso-Bu-MgCl as initiator), GE-S3G100 would lead to longer chain length of polycarbonate block (Figure 6.9) and shorter chain length of nylon 6 block (from Figure 6.7-(b)) than those of GE-S11AP at each corresponding concentration.

If the effect of different initiators was to be studied, it could be found that, between iso-Bu-MgCl and iso-Bu-MgBr (by using the same GE-S11AP polycarbonate), iso-Bu-MgCl tended to give a longer chain length of nylon 6 block (Figure 6.7-(a)) and longer chain length of polycarbonate block (Figure 6.9).

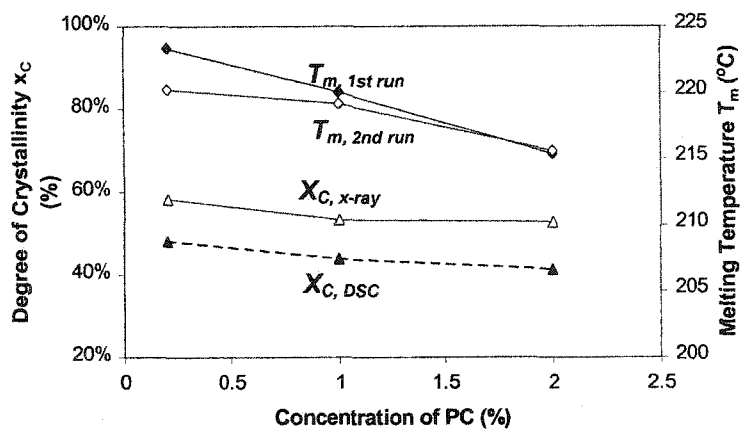
6.3.5. Melting Temperature and Degree of Crystallization

As discussed in 6.3.4, when different polycarbonates and initiators were used in the “L-L” system, the resulted polymers would show different chain length for both nylon 6 and polycarbonate blocks. This in turn would influence the process of crystallization. As it is known, due to the special feature of anionic polymerization route (the reaction temperature was below the crystallization temperature of nylon 6), the polymer would tend to crystallize after a certain length of nylon 6 was produced. If polycarbonate exists in the reaction system, it might act as nuclei or impurities to influence the process of crystallization. Therefore, by using different polycarbonates in various amounts, the nascent final products might show differences in melting temperature T_m and degree of crystallinity x_C .

6.3.5.1 DSC Results

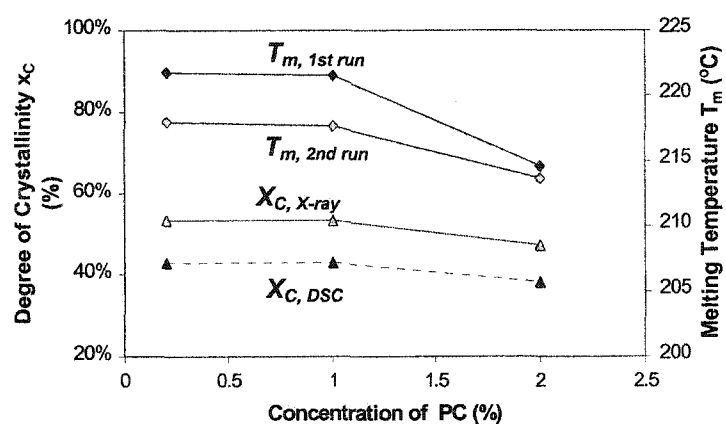
DSC was used to obtain the information on T_m and heat of fusion ΔH_f from the first and second heating scans. For each sample, two individual runs were conducted to get average values for T_m and ΔH_f . Then ΔH_f was used to calculate the weight fraction crystallized x_C value. Another way to get x_C data was through X-ray. The details on calculating x_C by X-ray were described in Chapter 5. Results are shown in Figure 6.11 (a)-(d).

For polymers (Figure 6.11-(a)-(c)) made from *polycarbonates* (PC) with different initiators, the followings are found: (1). For each sample, the T_m value from the



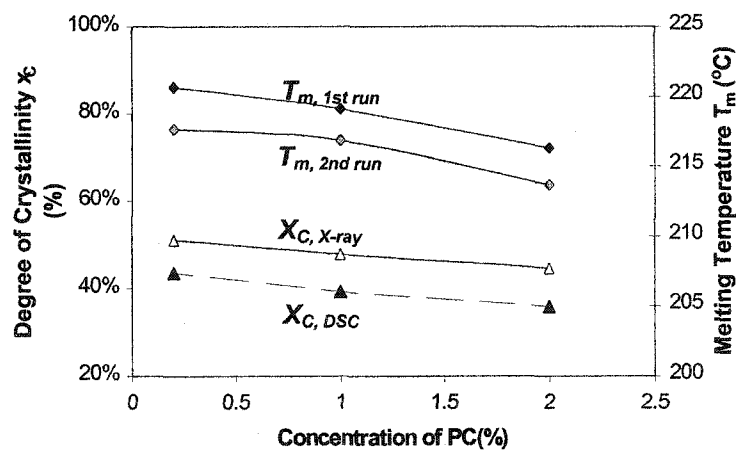
(a)

GE-S11AP
/iso-Bu-MgBr



(b)

GE-S11AP
/iso-Bu-MgCl



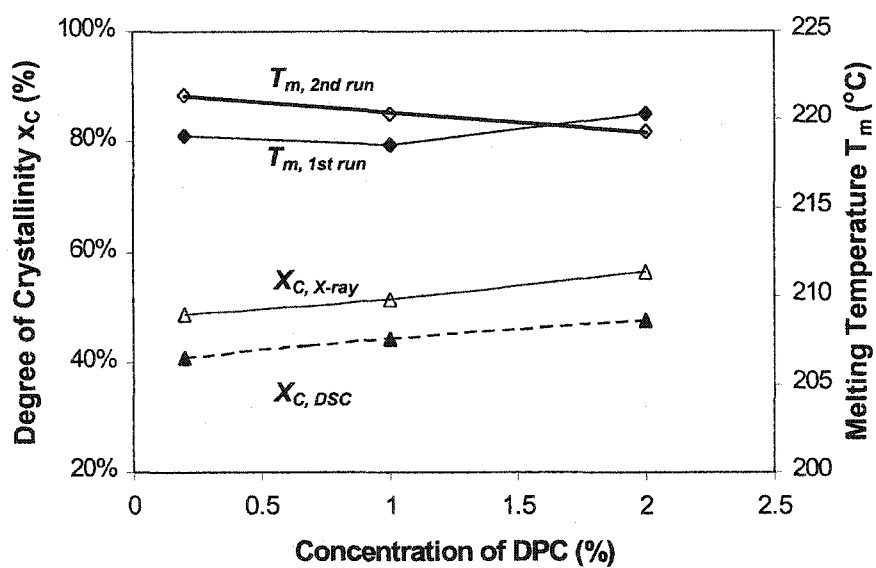
(c)

GE-S3G100
/iso-Bu-MgCl

Figure 6.11-(a)-(c). Data of Degree of Crystallinity x_C and Melting Temperatures T_m s versus Concentration of Polycarbonates with Different Initiators.

first heating is higher than that for the second heating, due to different thermal history that samples went through; (2). The melting temperature T_m from the first heating run $T_{m,1st}$ and the second heating $T_{m,2nd}$ showed the same trend with concentration of polycarbonate; (3). As concentration of polycarbonate increases, T_m tends to decrease. This could be caused by the existence of polycarbonate. With more polycarbonate chains in the reactive system, the crystallization of nylon 6 would be less perfect, the effect of melting temperature depression would be stronger which lead to lower T_m and x_C . (4) The x_C data from both DSC and X-ray are not quite the same, with the x_C from X-ray always higher than that from DSC. However, both data showed the same trend with the change of PC concentration, i.e. as concentration of polycarbonate increases, the degree of crystallinity decreases.

The results for pure nylon 6 samples by using DPC as activator are shown in Figure 6.11-(d). The trends for T_m and x_C are quite different from the ones for the copolymers. The melting temperature from the first heating scan, $T_{m,1st\ run}$, increases with the increase of DPC concentration, so does the degree of crystallinity x_C . This is exactly opposite to what was found for the copolymers. There have been reports that, by using various amount of small molecule activator (like trialkylsilylcaprolactam, Mateva et al., 1995), the degree of crystallinity and melting temperature decreased with the increase of that activator. However, that is not the situation met here. A possible explanation is: there are lots of factors which can influence the process of crystallization of certain polymers. Among them there are the effect of diluents or impurities, the effect of



(d)
DPC
/iso-Bu-MgBr

Figure 6.11-(d). Data of Degree of Crystallinity x_C and Melting Temperatures T_m s versus Concentration of DPC.

molecular weight, and the effect of thermal history etc. Since there is no long polycarbonate chain in the system, the influence of impurity is smaller. Even if the impurity factor was considered, the resultant effect should be contrary to what is seen here. For the molecular weight, since the lower amount of activator used, the higher the molecular weight of nylon 6, the higher the melting temperature was supposed to be. Therefore molecular weight is also not the reason for the strange trend. There remains only the effect of thermal history. Due to the exothermic nature of the anionic polymerization route, the samples with different amount of DPC would experience different temperature increases throughout the whole polymerization process. There are other things to be born in mind for the system with DPC, i.e. the slower rate of polymerization (long t_s values in Figure 6.5-(a)) and the environment temperature of 150°C instead of 130°C (the temperature for better rate of crystallization for nylon 6 is around 138°C). All in all their crystallization process would be influenced. Actually after checking the data on the melting temperature on the second heating scan $T_{m, 2nd run}$, it becomes clear how the thermal history could change the crystallization information. The second heating scan was done after each sample was cooled at 10°C/min from the melt state (when any previous thermal history would be destroyed). Thus each sample would share similar thermal history before the second heating scan. As it was shown in Figure 6.11-(d), the $T_{m, 2nd run}$ did show decreases as the concentration of DPC increases. Also for samples with 0.2% and 1% DPC, their $T_{m, 1st run}$ values were even lower than their $T_{m, 2nd run}$ values (about 2 °C difference). This indicates that the thermal history in samples made at 0.2% and 1% concentration of DPC would not favor their crystallization process

compared with the one with 2% DPC and other copolymers. The detailed DSC thermograms for all samples are available in Appendix C.1.

6.3.5.2 X-ray Results

From X-ray diffraction data, not only can the information on degree of crystallinity be obtained, but also the relative amount of the two crystal structures existed in nylon 6 chains (i.e. α and γ crystal structures). Table 6.2 lists the final results from the X-ray data analysis.

For the copolymers made with polycarbonates at different concentration, the α structure was the major crystal structure in the as-is copolymers. The amount of γ crystal was very small. However, for the nylon 6s made with DPC as activator, the situation is different. At concentration of 0.2% and 1%, the amount of γ crystal was quite large, almost one order of magnitude higher than the data for the one with 2% DPC and other copolymers. Similar result was obtained with sample using 0.5% DPC. Compared with other samples, the polymers made with low concentration of DPC (i.e. 0.2%-1%) showed different X-ray diffraction patterns. In Figure 6.12, the X-ray results for polymers made with various concentrations of DPC were plotted. It can be found that for nylon 6 with 0.2% and 1% DPC, there are reflections at 2θ around 22.4° which is evidence for the existence of γ form while the more stable α form could be found at 2θ around 20° and 23.6° . The existence of the large amount of γ form in the samples made with low concentrations of DPC (i.e. 0.2%-1%) could explain why they showed lower melting

Table 6.2 X-Ray Results for Polymers Made from DPC and PCs at Various Concentrations with Different Initiators.

| Activator Type and Amount | | Crystalline Peak Area (%) | | | Amorphous Area (%) |
|---------------------------|-------------------|----------------------------------|--------------------|-------|--------------------|
| Type | Concentration (%) | α structure (200+002+202) | γ structure | Total | |
| GE-S11AP /iso-Bu-MgBr | 0.2 | 54.91 | 3.29 | 58.20 | 41.80 |
| | 1 | 48.29 | 4.88 | 53.17 | 46.83 |
| | 2 | 51.50 | 1.19 | 52.69 | 47.31 |
| GE-S11AP /iso-Bu-MgCl | 0.2 | 50.37 | 3.05 | 53.42 | 46.58 |
| | 1 | 48.36 | 4.95 | 53.31 | 46.69 |
| | 2 | 46.04 | 1.06 | 47.10 | 52.90 |
| GE-S3G100 /iso-Bu-MgCl | 0.2 | 49.25 | 1.90 | 51.15 | 48.85 |
| | 1 | 43.40 | 4.45 | 47.85 | 52.15 |
| | 2 | 41.46 | 3.14 | 44.60 | 55.40 |
| DPC /iso-Bu-MgBr | 0.2 | 38.03 | 10.69 | 48.72 | 51.28 |
| | 1 | 36.22 | 15.30 | 51.53 | 48.47 |
| | 2 | 54.80 | 1.60 | 56.40 | 43.60 |

temperatures on their first heating scan. It has been reported that the melting points of α and γ structures are about 256°C and 228°C respectively (Puffr, R. et al. 1991). Therefore, for a polymer with a mixture of α and γ forms, if the amount of γ form is higher, then the melting temperature of the polymer is expected to be lower. The X-ray patterns for the rest of the samples can be found in Appendix C.2.

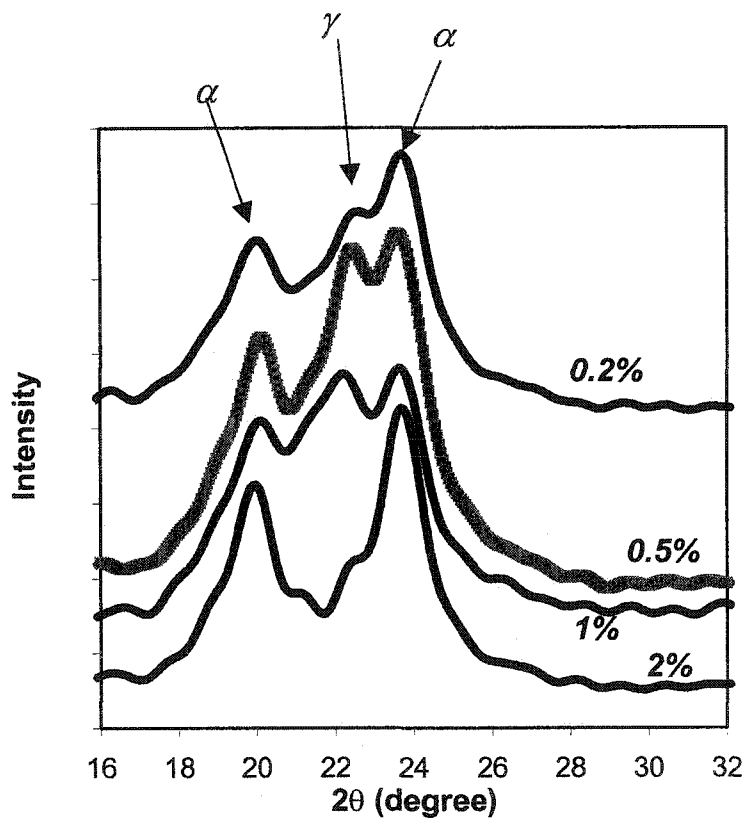


Figure 6.12. X-ray Diffraction Patterns for Nylon 6s Made with DPC at Various Concentrations.

Chapter 7 Conclusions and Future Work

7.1 Conclusions

This thesis consists of three major studies including: firstly, synthesis of a polymer through anionic ring-opening polymerization of ϵ -caprolactam with the presence of Bisphenol-A polycarbonate, then characterization on the so-produced polymeric material; secondly, the effect of environmental temperature during polymerization was investigated and correlated with various properties of the final products; thirdly, the influence of initiator and activator were studied; the type and amount of initiator and activator were varied to obtain optimal value in terms of rate of polymerization, monomer conversion and intrinsic viscosity. For each part, conclusions will be listed separately.

From Chapter 4 (synthesis and characterization), the following conclusions can be obtained:

(1). Comparison between “L-S” and “L-L” methods was made based on tensile tests (for specimens conditioned at 44%RH) and DSC results. It was found that the particle size of polycarbonate in “L-S” method did play an important role in determining the final properties. The smaller particle size of polycarbonate, the better tensile stress and strain at break and toughness in the “L-S” samples. The “L-L” data anchored the trend while representing an imaginary limit of particle size of zero.

(2). It has been proved that there is interaction between polycarbonate and Grignard reagent. The essential activating specie in the "L-L" system is formed from the reaction between ϵ -caprolactam anion and polycarbonate.

(3). Diphenyl carbonate (DPC) was chosen for a model polymerization to produce homopolymer nylon 6 successfully. FTIR was used to compare among homopolymer nylon 6 (by using 1% DPC), copolymer of nylon 6-polycarbonate (with 1% polycarbonate) and commercial nylon 6. Characteristic FTIR spectroscopy for nylon 6 was found for all samples with little difference, indicating that a nylon 6 part (in the form of blocks in the copolymer) dominates in the final product. On the other hand, ^1H and ^{13}C NMR were run on solutions of trifluoroacetylated copolymer in deuterated chloroform, and evidence on the existence of nylon 6-polycarbonate copolymer was found. A possible reaction route was then proposed.

(4). The copolymer was characterized in terms of solubility and thermal stability. It was found that the copolymer (with 1% PC) showed better thermal stability than the homopolymer of nylon 6 (made from 1% DPC).

(5). Morphological study of the in-situ copolymer of nylon 6/polycarbonate was studied. A single phase morphology was found. Comparison was made with the in-situ reactive blend of nylon 6 and polystyrene where a two-phase morphology typical of immiscible polymer blends was found. Melt blends of nylon 6 and polycarbonate were also prepared at two levels of concentrations (i.e 2% and 10% w/w). The influence of mixing time was also studied. SEM indicated in general a morphology of polycarbonate particles dispersed into a continuous nylon 6 phase for every sample. For the blend with

10% polycarbonate, particle size of polycarbonate decreased significantly with mixing time; while for the blend with 2% polycarbonate, the polycarbonate particle size did not show a similar trend.

From Chapter 5 (the effect of reaction temperature), six different oil bath temperatures were used in this study. The composition of the reactive mixture mostly used in this chapter was: 75 g ϵ -caprolactam/ 0.75 g polycarbonate (from SPP)/ 10 mmol isobutyl magnesium chloride. The following conclusions can be obtained:

(1). Due to the exothermic nature of the polymerization, the actual temperature of the reactive mixture did not stay the same as the environmental temperature, instead it started increasing after the reaction started and reached a maximum value and then decreased. The actual temperature of core point during the polymerization was measured for four different initial environmental temperatures. The rate of polymerization was slower for the one at lower initial environmental temperature for which it took a longer time to reach its maximum temperature. The temperature increase between the maximum and the initial ones varied from 40°C to 56°C (for the composition of 75 g ϵ -caprolactam/0.75 g SPP polycarbonate/12 mmol isobutyl magnesium bromide) when different initial temperatures (from 105°C-164°C) were used.

(2). Homogeneity analysis was done on both the “scale-up” sample (250 g) and the small sample. For the “scale-up” sample, tensile tests were run on specimens selected from different locations within the sample. No significant trend for the tensile properties with relation to various locations was found, indicating good uniformity and the success

of the scale-up process. For the small-sized sample, $[\eta]$ values along the radial direction were measured and compared. Although the one from the center location showed a slightly higher $[\eta]$ value than the ones from other locations, the range between the highest and the lowest was still narrow with the ratio between the highest and the lowest not exceeding 1.12.

(3). Monomer conversion has been measured by both a water-extraction method and a GC-MS method. It was found that the monomer conversion did not change much when different oil bath temperatures were used for polymerization, remaining above 96%.

(4). The intrinsic viscosity in 90% formic acid at room temperature for samples increased when the oil bath temperature for polymerization increased from 95 °C to 134 °C, indicating an increase in molecular weight of the nylon 6 block in the copolymer. Gel was formed at higher temperature such as 147 °C and 160 °C which may be caused by side reactions when temperature reached to a certain level.

(5). Complex melt viscosity η^* and modulus G^* at 250 °C for samples were measured. It was found that η^* and G^* increased when the oil bath temperature for polymerization increased. This may be caused partly from the molecular weight increase (at 110, 120 and 134 °C) and partly from the formation of gel (at 147 °C and 160 °C). There is little dependence of η^* and G^* on molecular weight under intensive shearing (at higher frequency the difference of η^* and G^* between samples became less).

(6). The degree of crystallinity for samples made at different temperatures showed a decreasing trend as the oil bath temperature for polymerization increased. This

conclusion has been reached by both DSC analysis and X-ray diffraction methods. Within the temperature range studied in this chapter, α structure is the main crystal form in all nascent samples, while the amount of γ structure is minimal except the one made at oil bath temperature of 160 °C. There is no significant trend for the influence of reaction temperature on the melting points of the nascent polymers.

(7). The void content inside samples increased greatly when the oil bath temperature for polymerization was below 120 °C. This led to the increasing moisture absorption and decreasing bulk density when the oil bath temperature for polymerization decreased. In tensile tests, for samples pre-conditioned in 50% R.H., because of the higher moisture absorption in samples made at lower oil bath temperatures (95 °C, 110 °C), moisture acted as plasticizer to cause more reduction (compared with the same sample under dry condition) on tensile stress at break and Young's Modulus and longer tensile strain at break.

(8). For tensile results on dry samples, two sets of data have been obtained. For tensile stress and strain at break and toughness, both groups of data showed the same trends, that is, as the oil bath temperature for polymerization increased, tensile stress and strain at break and toughness tended to increase and leveled off after 134 °C and 125 °C respectively. There is some difference on the Young's Modulus data between these two. One showed a monotonic decrease with increasing oil bath temperature, while the other showed an increase at lower range of oil bath temperature and leveling off after 120 °C was reached.

In Chapter 6 the effects of activator and initiator were studied. Iso-Bu-MgBr and iso-Bu-MgCl were used as initiators. Two polycarbonates and diphenyl carbonate were used as activators. The oil bath temperature was kept at 130 °C for all polymerization with polycarbonates and 150 °C for DPC.

(1). By varying the concentration of initiator while keeping the other composition the same, polymers were synthesized while the rate of polymerization (in terms of solidification time) for each polymerization process was recorded; for each sample, its monomer conversion and intrinsic viscosity (in 90% formic acid at room temperature) were measured. An optimal initiator concentration was found for systems containing both 1% and 2% concentration of GE-S11AP polycarbonate (in 100 g ϵ -caprolactam), i.e.

$$\frac{\text{mmol of initiator}}{\text{mass of GE - S11AP}} = 8 \text{ mmol/g}$$

Below this ratio, the rate of polymerization was slow, monomer conversion was very low and molecular weight (in terms of $[\eta]$) of the final product was very low too. Above this ratio, the following were found: the rate of polymerization did not change much for the systems using iso-Bu-MgBr, while for systems using iso-Bu-MgCL the solidification time decreased slightly with more initiator used; monomer conversion was high and changed little afterwards; the intrinsic viscosity value reached to a maximum value at this ratio and decreased a little bit afterwards.

(2). Different type and different concentration of polycarbonate or DPC were studied. The following results were found:

- a. For the rate of polymerization in all samples, the higher concentration of polycarbonates or DPC, the faster the rate of polymerization proceeded. The systems using polycarbonates showed higher rate of polymerization than those using DPC. When same initiator iso-Bu-MgCl was used, the rate of polymerization for samples using GE-S3G100 (higher MW) was faster than those using GE-S11AP (lower MW) over three concentration levels.
- b. For monomer conversion, at all concentration levels of activator (either DPC or polycarbonates), high monomer conversion (above 95%) can be reached. Generally monomer conversion for samples made at 2% concentrations showed higher water-soluble content than samples made at 0.2% and 1% concentrations. This may be related to the viscous hindrance caused by the fast kinetics at 2% concentration.
 - a. For the intrinsic viscosity in 90% formic acid, polymers made by both polycarbonates and DPC showed decreased $[\eta]$ with the increase of activator concentration. When iso-Bu-MgCl was used as initiator, the $[\eta]$ for the samples using GE-S11AP were higher than those using GE-S3G100 over all three concentrations, indicating longer nylon 6 chains obtained for samples using GE-S11AP.
- d. For the melt complex viscosity η^* , the effect of polycarbonate was studied. For linear homopolymer nylon 6 such as the one made by using DPC as activator, the melt complex viscosity showed a straight line with regard to intrinsic viscosity (i.e. molecular weight of nylon 6) on a semi-log plot. With different polycarbonate and

various amounts of polycarbonates involved, the trend for η^* with regard to $[\eta]$ differed because of the different chain length of polycarbonate incorporated into the final copolymer. Under the assumption of block copolymer, it could be derived that by using the same iso-Bu-MgCl, the samples containing GE-S3G100 would have longer polycarbonate chain and shorter nylon 6 chain compared with those containing GE-S11AP polycarbonate.

(3). For the comparison between two initiators iso-Bu-MgBr and iso-Bu-MgCl, one polycarbonate was used, i.e. GE-S11AP, at various concentrations. The following results were found:

- a. For the rate of polymerization, at lower concentration of GE-S11AP (0.2% and 0.5%), the systems containing iso-Bu-MgCl had higher rate of polymerization than the ones containing iso-Bu-MgBr; at higher concentration of GE-S11AP (1% and 2%), the systems containing iso-Bu-MgBr showed higher rate of polymerization.
- b. For the intrinsic viscosity $[\eta]$, polymers using iso-Bu-MgCl have higher values than those using iso-Bu-MgBr. The difference between the two systems is much higher at low concentration (e.g. 0.2%) of GE-S11AP than at high concentration (e.g. 2%).
- c. For the melt complex viscosity η^* , the samples using iso-Bu-MgCl always had higher values of η^* than those using iso-Bu-MgBr. Under the assumption of block copolymer, the samples using iso-Bu-MgCl tend to have longer polycarbonate (here GE-S11AP) chain and longer nylon 6 chain than those using iso-Bu-MgBr.

(4). For the degree of crystallinity, both X-ray and DSC analysis showed the same results even though the one from X-ray was always about 7-11% higher than the value from DSC for the exactly same sample. For all samples using polycarbonates (either GE-S11AP or GE-S3G100), there is a decrease of degree of crystallinity when more polycarbonate was used. The data for samples using DPC showed an opposite trend which could result from the different thermal history those samples experienced. The samples using DPC at lower concentration (0.2%, 0.5% and 1%) also showed much higher amount of γ structure while the sample with DPC at 2% and other samples all showed mainly α crystal structures.

(5). For the melting temperatures, the samples using polycarbonates always showed higher T_m during the first heating run than the one at the second heating run. There is a decreasing trend of melting temperature with the increase of polycarbonate amount. The samples using DPC showed the different trend for all melting temperatures from first heating run; the existence of the γ structure is the probable cause for the low melting temperature in first heating.

7.2 Future work

There are several subjects of interest for future work.

It has been intended to study the special adhesion at interface between glass fiber and the nylon 6/polycarbonate copolymer in glass-fiber reinforced composites. In fact, some composites have been made, and SEM pictures have been taken to study the fracture surface. It has been found that there was more adhesion for samples made at

higher reaction temperature than at lower temperature. Also it has been found that the samples containing more polycarbonate showed more adhesion than those containing less. All the SEM microscopy pictures can be found in Appendix D, together with the bare glass fibre for comparison. However, quantitative results could not be obtained. It is of interest to find a way to do such measurements in the future.

Since nascent samples were loaded into RMS 800 for the melt viscosity measurements, it is unclear as to what extent did the existence of void influence the final results of complex melt viscosity and other rheological data. More studies need to be conducted on this subject.

It is of interest to have more mechanical property measurements such as abrasion resistance test, impact test and so on.

References

Akkapeddi, M. K., Dege, G. J., Gallagher, T. D. and Walsh, M. S., "Some Mechanistic Aspects of the Anionic Block Copolymerization of Caprolactam and Polyether Diols", *Polym. Prepr.*, **27**(1), 177-178 (1986).

ASTM D 638-95, "Standard Test Method for Tensile Properties of Plastics", Annual Book of ASTM Standards, **Vol. 08.01**, 45-65 (1995).

ASTM D 2857-95, "Standard Practice for Dilute Solution Viscosity of Polymers", Annual Book of ASTM Standards, **Vol. 08.02**, 149-153(1995).

Baer, M., "Multiphase Core/Shell Polymers", U. S. Patent 4,306,040 (1981).

Bai, J. and Williams, M.C., "Temperature Effects on the Anionic Polymerization of ϵ -Caprolactam with the Presence of Polycarbonate", *49th CSCHE Conference*, Saskatoon, Canada, Oct.3-7, 1999.

Blazen, M. and Potin, P., "Anionic Polymerization of Lactams in an Extruder with Controlled Output Rate", U. S. Patent 4,067,861 (1978).

Boey, F. Y. C., "Reducing the Void Content and its Variability in Polymeric Fibre Reinforced Composite Test Specimens Using a Vacuum Injection Moulding Process", *Polym. Test.*, **9**, 363-377 (1990).

Brandrup, J. and Immergut, E. H., "Polymer handbook", 3rd edition, Wiley, New York (1989)

Chen, Y. and Chen, A. S., "Bulk Anionic Copolymerization of ϵ -Caprolactam in the Presence of Macroactivators Derived from Polypropylene Glycol", *J. Appl. Polym. Sci.*, **47**, 1721-1729 (1993).

Chorvath, I., Mertens, M. D. M., van Geenen, A. A., van Schijndel, R. J. G., Lemstra, P. J. and Meijer, H. E. H., "ACS Symposium Series 696: Applications of Anionic Polymerization Research", 267-290, The American Chemical Society, Washington, DC (1998).

Coleman, M. M., Lichkus, A. M. and Painter, P.C., "Thermodynamics of Hydrogen Bonding in Polymer Blends. 3. Experimental Studies of Blends involving Poly(4-vinylphenol)", *Macromols.*, **22**(2), 586-595 (1989).

Cortazar, M., Eguiazabal, J. I. and Iruin, J. J., "A Calorimetric Study of the Interchange Reactions in Bisphenol A Polycarbonate/Nylon-6 Blends", *Br. Polym. J.*, **21**, 395-397 (1989)

Coutinho, F. M. B. and Sobrinho, A. A. B., "Thermal and Mechanical Properties of Some Caprolactam-Poly(Propylene Oxide) Block Copolymers", *Eur. Polym. J.*, **27**(1), 105-108 (1991).

Davenport, R., Riepl, J. and Sasano, T., "CEH Marketing Research Report: Nylon Resins", Chemical Economics Handbook – SRI International (2001).

Duangchan, A., "Glass Fibre and Nylon 6: an Advanced Composite Material", M. Sc. thesis, University of Alberta (1994).

Elschenbroich, Ch. and Salzer, A., "Organometallics: A Concise Introduction", 43-44, VCH Publishers Inc., New York, USA, 2nd edition, 1992.

Foldi, V. S. and Campbell, T. W., "Preparation of Copoly(carbonate/urethane) from Polycarbonates", *J. Polym. Sci.*, **56**, 1-9 (1962).

Frisch, K. C., Ashida, K., van Derloos, J. L. M. and van Geenen, A. A., "Reaction Injection Molding Process and Reaction Injection Molded Products", U. S. Patent 4,582, 879 (1986).

Frunze, T. M., Shleifman, R. B., Belavtseva, E. M., Genin, Ya. V., Volkova, T. V., Kotelnikov, V. A., Radchenko, L. G., Davtyan, S. P., Kurashev, V. V. and Tsvankin, D. Ya., "Kinetic Studies of Structure Formation During Anionic Adiabatic Polymerization of ϵ -Caprolactam", *J. Polym. Sci. Polym. Phys. Ed.*, **18**(7), 1523-1532 (1980).

Frunze, T. M., Shleifman, R. B., Godovskii, Yu. K., Genin, Ya. V., Volkova, T. V., Kotelnikov, V. A., Kurashev, V. V., Davtyan, S. P. and Tsvankin, D. Ya., "Effect of Conditions of Synthesis on Kinetics of Structure-Formation of Polycaproamide During Anionic Adiabatic Polymerization", *Polym. Sci. U.S.S.R.*, **23**(10), 2545-2554 (1981).

Gabbert, J. D., Garner, A. Y. and Hedrick, R. M., "Process for the Preparation of Nylon Block Polymers", U.S. Patent 4,590,243 (1986).

Gaitskell, J. N., Herring, J. M., Williams, I.G., "Polyamides-Development of Mechanical Properties by Glass Fibre Reinforcement, Mineral Filling and Rubber Toughening", *Polimery*, **29**(10-12), 432-434 (1984).

Gattiglia, E., Turturro, A. and Pedemonte, E., "Blends of Polyamide 6 with Bisphenol-A Polycarbonate. I. Thermal Properties and Compatibility Aspects", *J. Appl. Polym. Sci.*, **38**, 1807-1818 (1989).

Gattiglia, E., Turturro, A., Pedemonte, E. and Dondero, G., "Blends of Polyamide 6 with Bisphenol-A Polycarbonate. II. Morphology-Mechanical Properties Relationships", *J. Appl. Polym. Sci.*, **41**, 1411-1422 (1990).

Gattiglia, E., Turturro, A., Lamantia, F. P. and Valenza, A., "Blends of Polyamide 6 and Bisphenol-A Polycarbonate. Effects of Interchange Reactions on Morphology and Mechanical Properties", *J. Appl. Polym. Sci.*, **46**, 1887-1897 (1992).

Gardlund, Z. G. and Bator, M. A., "In Situ Polymerization of Nylon-Polyurea Block Copolymers. I. Synthesis and Characterization", *J. Appl. Polym. Sci.*, **40**, 2027-2035 (1990).

Ghiorse, S.R., "Effect of Void Content on the Mechanical Properties of Carbon/Epoxy Laminates", *SAMPE Qlty.*, 1, 54-59 (1993).

Gonzalez-de los Santos, E A., Rodriguez, A. S. L., Gonzalez, M. J. L. and Corral, F. S., "Starlike Nylon 6/Polyurethane Block Copolymers by Reaction Injection-Molding Process (RIM)", *J. Appl. Polym. Sci.*, **80**, 2483-2494 (2001).

Hall, W. L. and Humphrey Jr., J. S., "Method of Coating a Polycarbonate Substrate with Galss", U. S. Patent 4,190,681(1980).

Hathaway, S. J. and Pyles, R. A., "Functionalized Thermoplastic Polymers, Blends Prepared therefrom, and Methods for Preparing Blends", U. S. Patent 4,732,934 (1988).

Hergenrother, W. Z. and Ambrose, R. J., "Block Polymers from Isocyanate-Terminated Intermediates. II. Preparation of Butadiene- ϵ -Caprolactam and Styrene- ϵ -Caprolactam Block Copolymer", *J. Polym. Sci. Polym. Chem. Ed.*, **12**, 2613-2622 (1974).

Hodek, R. B. and Seiner, J. A., "Property Enhancement of Anionically Polymerized Nylon with Dual Initiators", U. S. Patent 4,501,821 (1985).

Horiuchi, S., Matchariyakul, N., Yase, K., Kitano, T., Choi, H. K. and Lee, Y. M., "Compatibilizing Effect of a Maleic Anhydride Functionalized SEBS Triblock Elastomer through a Reaction Induced Phase Formation in the Blends of Polyamide 6 and Polycarbonate: 1. Morphology and Interfacial Situation", *Polymer*, **37** (14), 3065-3078 (1996).

Horiuchi, S., Matchariyakul, N., Yase, K., Kitano, T., Choi, H. K. and Lee, Y. M., "Compatibilizing Effect of a Maleic Anhydride Functionalized SEBS Triblock Elastomer through a Reaction Induced Phase Formation in the Blends of Polyamide 6 and Polycarbonate: 2. Mechanical Properties", *Polymer*, **38** (1), 59-78 (1997).

Hornsby, P. R., Tung, J. F. and Tarverdi, K., "Characterization of Polyamide 6 Made by Reactive Extrusion. I. Synthesis and Characterization of Properties", *J. Appl. Polym. Sci.*, **53**, 891-897 (1994).

Hornsby, P. R. and Tung, J. F., "Microstructure Characterization of PA-6/PP Blends Formed during Reactive Extrusion of ϵ -Caprolactam", *Plast. Rubber Compos. Process. Appl.*, **24** (2), 69-77 (1995).

Hu, G. H., Cartier, H. and Plummer, C., "Reactive Extrusion: Toward Nanoblends", *Macromols.*, **32**, 4713-4718 (1999).

Huggins, M. L., "The Viscosity of Dilute Solutions of Long-Chain Molecules. IV. Dependence on Concentration", *J. Am. Chem. Soc.*, **64**, 2716-2718 (1942).

Iobst, S. A. and Garner, D. P., "Reaction Injection Moulding Behaviour of Nylon 6 and 612 Polyether Block Copolymers", *Eng. Plas. (UK)*, **5**(1), 14-30 (1992).

Jacobi, E., Schuttenberg, H. and Schulz, R. C., "A New Method for Gel Permeation Chromatography of Polyamides", *Makromol. Chem. Rapid Commun.*, **1**(6), 397- 402 (1980).

Joyce, R.M. and Ritter, D.M., "Process for Making Polymeric Materials", U.S. Patent 2,251,519 (1941).

Khanna, Y.P., Han, P. K. and Day, E. D., "New Developments in the Melt Rheology of Nylons: I: Effect of Moisture and Molecular Weight", *Polym. Eng. Sci.*, **36**(13), 1745-1754 (1996).

Khoury, F., "Fibrillar Structure of Sphrulites in Poly(hexamethylene adipamide)", *J. Polym. Sci.*, **26**, 373-379 (1957).

Kim, Y. H., Akiyama, S. and Matsuda, A., "Chemical Reactions and Morphology of Polycarbonate/Nylon Alloys with Poly(allyl-co-maleic anhydride) as Compatibilizers", *Kobunsh. Ronbun.*, **53** (3), 169-175 (1996).

Kohan, M. I., "Nylon Plastics", 63-63, John Wiley & Sons Inc., USA, 1973.

Kye, H. and White, J. L., "Continuous Polymerization of Caprolactam in a Modular Intermeshing Co-rotating Twin Screw Extruder Integrated with Continuous Melt Spinning of Polyamide 6 Fiber. Influence of Screw Design and Process Conditions", *J. Appl. Polym. Sci.*, **52**(9), 1249-1262 (1994).

Levita, G., "Ternary Blends in the Toughening of Epoxy Resins", *Polym. Compos.*, **8** (3), 141-148 (1987).

Li, N.H. and Williams, M.C., "Synthesis of a Compatibilizer for Blends of Polycarbonate and Nylon 6 by Ring-Opening of Two Cyclic Monomers", *CSCHE Annual Conference*, Calgary, AB, October 1995.

Magill, J.H., "Crystallization of Polyamides II-Nylon 6 and Nylon 66", *Polymer*, **6**(7), 367-371 (1965).

Malkin, A. Ya., Ivanova, S. L., Frolov, V. G., Ivanova, A. N. and Andrianova, Z. S., "Kinetics of Anionic Polymerization of Lactams. (Solution of Non-Isothermal Kinetic Problems by the Inverse Method)", *Polymer*, **23**, 1791-1800 (1982).

Mateva, R., Delev, O. and Kaschieva, E., "Structure of Poly(ϵ -Caprolactam) Obtained in Anionic Bulk Polymerization", *J. Appl. Polym. Sci.*, **58**, 2333-2343 (1995).

Mateva, R., Petrov, P., Rousseva, S., Dimitrov, R. and Zolova, G., "On the Structure of Poly- ϵ -Caprolactams, Obtained with bifunctional N-Carbamyl Derivatives of Lactams", *Eur. Polym. J.*, **36**, 813-821 (2000).

Montaudo, G., Puglisi, C. and Samperi, F., "Exchange Reactions Occurring through Active Chain Ends: Melt Mixing of Nylon 6 and Polycarbonate", *J. Polym. Sci, Part A: Polym. Chem.*, **32**, 15-31 (1994).

Montaudo, G., Puglisi, C., Samperi, F. and Lamantia, F. P., "Synthesis of AB and ABA Block Copolymers as Compatibilizers in Nylon 6/Polycarbonate Blends" *J. Polym. Sci.: Part A: Polym. Chem.*, **34**, 1283-1290 (1996).

Moskala, E. J., Howe, S. E., Painter, P. C. and Coleman, M. M., "On the Role of Intermolecular Hydrogen Bonding in Miscible Polymer Blends", *Macromols.*, **17**(9), 1671-1678 (1984).

Moskala, E. J., Varnell, D. F. and Coleman, M. M., "Concerning the Miscibility of Poly(vinyl phenol) Blends – Fourier-Transform IR Study", *Polymer*, **26**(2), 228-234 (1985).

Mougin, N., Rempp, P. and Gnanou, Y., "New Activating Agents for the Anionic Polymerization of Lactams", *Macromols.*, **25**, 6739-6743 (1992).

Mougin, N., Rempp, P. and Gnanou, Y., "Synthesis and Characterization of Polysiloxane-Polyamide Block and Graft Copolymers", *J. Polym. Sci.: Part A: Polym. Chem.*, **31**, 1253-1260 (1993).

Nelson, W.E., "Nylon Plastics Technology", Butterworth (Publishers) Inc., Boston, Mass. (1976).

Ning, X. and Ishida, H., "RIM-Pultrusion of Nylon 6 and Rubber-Toughened Nylon 6 Composites", *Polym. Eng. Sci.*, **31**(9), 632-637 (1991).

Ongemach, G.C. and Moody, A.C., "Determination of Caprolactam Monomer Content in Nylon 6 Extractables by Gas Chromatography", *Anal. Chem.*, **39**(8), 1005-1007 (1967).

Paul, D. R. and Newman, S., "Polymer Blends", Academic Press, New York, USA, 1978.

Petit, D., Jerome, R. and Teyssie, Ph., "Anionic Block Copolymerization of ϵ -Caprolactam", *J. Polym. Sci., Polym. Chem. Ed.*, **17**, 2903-2916 (1979).

Puffr, R. and Kubanek, V., "Lactam-Based Polyamides, Vol. 1: Polymerization Structure", CRC Press, Boca Raton, Florida, page 187(1991).

Reimschuessel, H. K., "Nylon 6: Chemistry and Mechanisms", *J. Poly. Sci.: Macromol. Rev.*, **12**, 6-139 (1977).

Reinking, K. et al., "Process for the Continuous Production of Polyamide Sections or Profiles", U. S. Patent 3,634,574 (1972).

"Resin 2001", *Mod. Plas.*, **78**(2), 43 (2001).

Ricco, L., Russo, S., Orefice, G. and Riva, F., "Anionic Poly(ϵ -caprolactam): Relationships among conditions of Synthesis, Chain Regularity, Reticular Order, and Polymorphism", *Macromols.*, **32**, 7726-7731 (1999)

Sankholkar, Y., "Copolymers of Nylon 6 and Polycarbonate as Matrices for Advanced Composite Materials", M. Sc. thesis, University of Alberta (1996).

Schlack, P., "Preparation of Polyamides", U.S. Patent 2,241,321 (1941).

Schlenk, W. and Schlenk, W. Jr., "The Constitution of the Grignard Magnesium Derivatives", *Ber.*, **62B**, 920-924 (1929).

Šebenda J., "Anionic Ring-opening Polymerization: Lactams", *Comprehensive Polymer Science: the Synthesis, Characterization, Reactions & Applications of Polymers, Vol. 3: Chain Polymerization Part I*, 511-530 (1989).

Sekiguchi, H. and Coutin, B., "Polymerizability and Related Problems in the Anionic Polymerization of Lactams", *J. Polym. Sci., Polym. Chem. Ed.*, **11**, 1601-1614 (1973).

Seo, S. W. and Ha, W. S., "Synthesis and Characterization of Poly(ether urethane) – Nylon 6 Block Copolymer", *J. Appl. Polym. Sci.*, **48**, 833-843 (1993).

Shah, D., "In-situ Molding of Glass Fibre/Nylon 6 Composites: Studies in the Development of Composite Properties by Surface-Modification of Glass Fibre", M. Sc. thesis, University of Alberta (1996).

Solomon, O. F. and Ciuta, I. Z., "Determination of the Intrinsic Viscosity of Polymer Solutions by a Single Point Viscosity Measurement", *J. Appl. Polym. Sci.*, **6** (24), 683-686 (1962).

Springer, G.S., Tang, J. M. and Lee, W. I., "Effects of Cure Pressure on Resin Flow, Voids, and Mechanical Properties", AFWAL TR 87-4058, U.S. Air Force Wright-Patterson Aeronautics Laboratory, July 1987.

Stehlicek, J. and Šebenda, J., "Block Copolymers of ϵ -Caprolactam and Oxirane Prepared by the Activated Anionic Polymerization of ϵ -Caprolactam", *Eur. Polym. J.*, **18**, 535-540 (1982).

Turi, E. A., "Thermal Characterization of Polymeric Materials", 745-820, Academic Press, Inc., San Diego, USA, 1997.

Udipi, K., "Rubber Modified Reaction Moldable Nylon-6 Compositions", U. S. Patent 4,994,524 (1991).

Udipi, K., Dave, R. S., Kruse, R. L. and Stebbins, L. R., "ACS Symposium Series 696: Applications of Anionic Polymerization Research", 255-266, The American Chemical Society, Washington, DC (1998).

Ueda, K., Yamada, K., Nakai, M., Matsuda, T., Hosoda, M. and Tai, K., "Synthesis of High Molecular Weight Nylon 6 by Anionic Polymerization of ϵ -Caprolactam", *Polym. J.*, **28** (5), 446-451(1996).

Valenza, A., Lamantia, F. P., Gattiglia, E. and Turturro, A., "Reactive Blending of Polyamide 6 and Polycarbonate", *Intern. Polym. Process. IX*, **3**, 240-245 (1994).

VanBuskirk, B. and Akkapeddi, M. K., "Anionic Polymerization and Graft Copolymerization of Caprolactam in an Extruder", *Polym. Prepr.*, **29**, 567-570 (1988).

Van Geenen, A. A. M. and Kerssemakers, A. M. W., "Process for the Preparation of Nylon Block Copolymer", European Patent 0613917 A1(1994).

Wade, L. G. Jr., "Organic Chemistry", Prentice-Hall Inc., Englewood Cliffs, New Jersey, USA, 1987.

Wichterle, O., "On Caprolactam Polymerization", *Makromol. Chem.*, **35**, 174-182 (1960).

Yn, M. S. and Ma, C. C. M., "Poly(ϵ -Caprolactam)-Poly(Butadiene-co-Acrylonitrile) Block Copolymers. I. Synthesis, Characterization, Mechanical Properties, and Morphology", *J. Appl. Polym. Sci.*, **53**, 213-224 (1994).

Wurm, B., Keul, H. and Hocker, H., "Synthesis of Alternating Copolymers of 2,2-Dimethyltrimethylene Carbonate and ϵ -Caprolactam via Insertion of ϵ -Caprolactam into Poly(2,2-dimethyltrimethylene carbonate)", *Macromols.*, **25**, 2977-2984 (1992).

Zhang, Y., "Synthesis and Characterization of Nylon 6-b-aramid-b-Nylon 6 Copolymers", Ph.D. thesis, The University of Akron (1998).

Appendix A Supplement to Chapter 4

Table A-1a. Tensile Test Result

Sample Identification: **DD (copolymer with 1% PC by "L-L" method)**
 Test Date: Monday, January 25, 1999
 Test Method Number: 3
 Interface Type: 8500
 Crosshead Speed: 1.0000 mm/min
 Sampling Rate: 5 pts/secs
 Temperature: 22 degree C
 Humidity (%): 50
 Specimen G.L.: 10.15 mm

| Specimen No. | Modulus (AutoYoung) (MPa) | Stress at Auto.Break (MPa) | %Strain at Auto.Break (%) | Toughness (MPa) |
|--------------|---------------------------|----------------------------|---------------------------|-----------------|
| 1 | 1157.1 | 72.8 | 7.8 | 3.2 |
| 2 | 1096.4 | 78.4 | 9.2 | 4.5 |
| 3 | 1151.8 | 75.3 | 7.9 | 3.4 |
| 4 | 1086.5 | 78.2 | 10.5 | 5.3 |
| Mean | 1122.9 | 76.2 | 8.9 | 4.1 |
| S.D. | 36.6 | 2.6 | 1.3 | 0.99 |

Table A-1b. Tensile Test Result

Sample Identification: **AA [polymer by "L-S" method with 1% PC (<80µm)]**
 Test Date: Monday, January 25, 1999
 Test Method Number: 3
 Interface Type: 8500
 Crosshead Speed: 1.0000 mm/min
 Sampling Rate: 5 pts/secs
 Temperature: 22 degree C
 Humidity (%): 50
 Specimen G.L.: 10.15 mm

| Specimen No. | Modulus (Auto.Young) (MPa) | Stress at Auto.Break (MPa) | %Strain at Auto.Break (%) | Toughness (MPa) |
|--------------|----------------------------|----------------------------|---------------------------|-----------------|
| 1 | | Excluded | | |
| 2 | 1143.5 | 71.4 | 9.0 | 3.4 |
| 3 | 1232.0 | 76.9 | 8.6 | 4.0 |
| 4 | 1182.7 | 75.9 | 8.8 | 4.2 |
| Mean | 1186.1 | 74.7 | 8.8 | 3.85 |
| S.D. | 44.3 | 2.9 | 0.21 | 0.41 |

Table A-1c. Tensile Test Result

Sample Identification: **CC [polymer by "L-S" method with 1% PC (80-200 μ m)]**
 Test Date: Monday, January 25, 1999
 Test Method Number: 3
 Interface Type: 8500
 Crosshead Speed: 1.0000 mm/min
 Sampling Rate: 5 pts/secs
 Temperature: 22 degree C
 Humidity (%): 50
 Specimen G.L.: 10.15 mm

| Specimen No. | Modulus (AutoYoung) (MPa) | Stress at Auto.Break (MPa) | %Strain at Auto.Break (%) | Toughness (MPa) |
|--------------|---------------------------|----------------------------|---------------------------|-----------------|
| 1 | 1235.6 | 70.5 | 8.1 | 3.4 |
| 2 | 1202.8 | 71.3 | 8.6 | 3.7 |
| 3 | 1256.0 | 70.8 | 8.5 | 3.6 |
| 4 | 1102.1 | 71.6 | 8.3 | 3.6 |
| Mean | 1199.1 | 71.1 | 8.4 | 3.57 |
| S.D. | 68.3 | 0.49 | 0.21 | 0.11 |

Table A-1d. Tensile Test Result

Sample Identification: **GG [polymer by "L-S" method with 1% PC (200-400 μ m)]**
 Test Date: Monday, January 25, 1999
 Test Method Number: 3
 Interface Type: 8500
 Crosshead Speed: 1.0000 mm/min
 Sampling Rate: 5 pts/secs
 Temperature: 22 degree C
 Humidity (%): 50
 Specimen G.L.: 10.15 mm

| Specimen No. | Modulus (AutoYoung) (MPa) | Stress at Auto.Break (MPa) | %Strain at Auto.Break (%) | Toughness (MPa) |
|--------------|---------------------------|----------------------------|---------------------------|-----------------|
| 1 | | Excluded | | |
| 2 | 1218.3 | 63.2 | 7.6 | 2.88 |
| 3 | 1122.7 | 62.9 | 7.2 | 2.38 |
| 4 | 1143.5 | 62.3 | 6.8 | 2.50 |
| Mean | 1161.5 | 62.8 | 7.19 | 2.59 |
| S.D. | 50.2 | 0.46 | 0.42 | 0.26 |

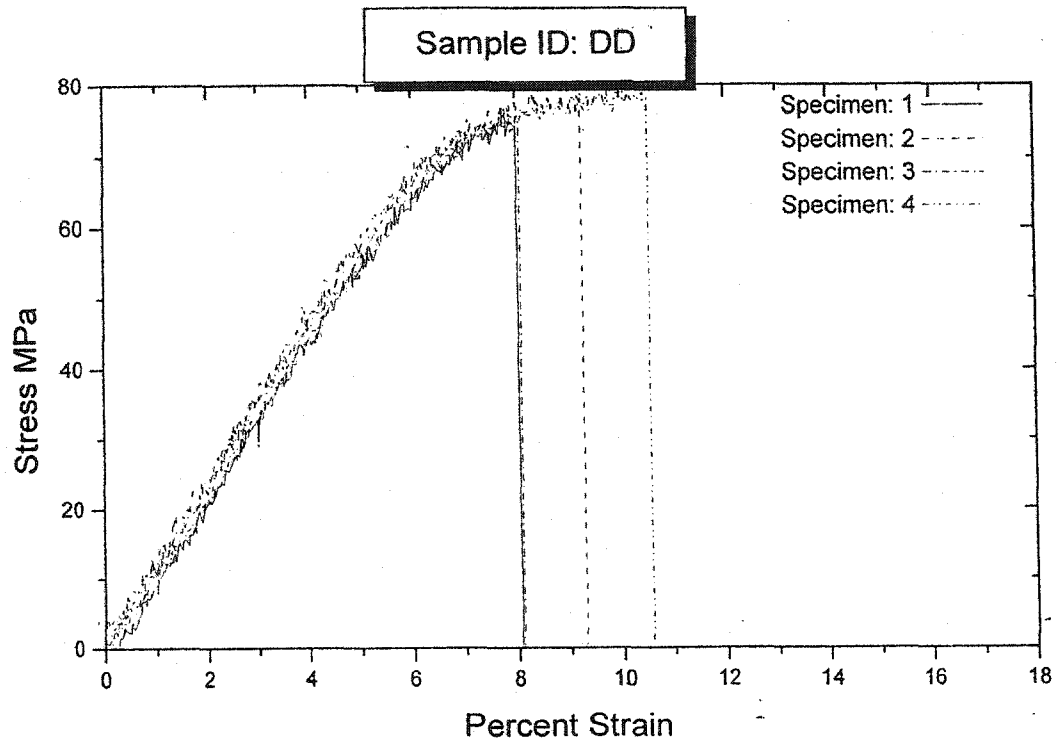


Figure A.1a. Stress-Strain Curves
for **DD** (copolymer with 1% PC by "L-L" method, 1998-12-01)

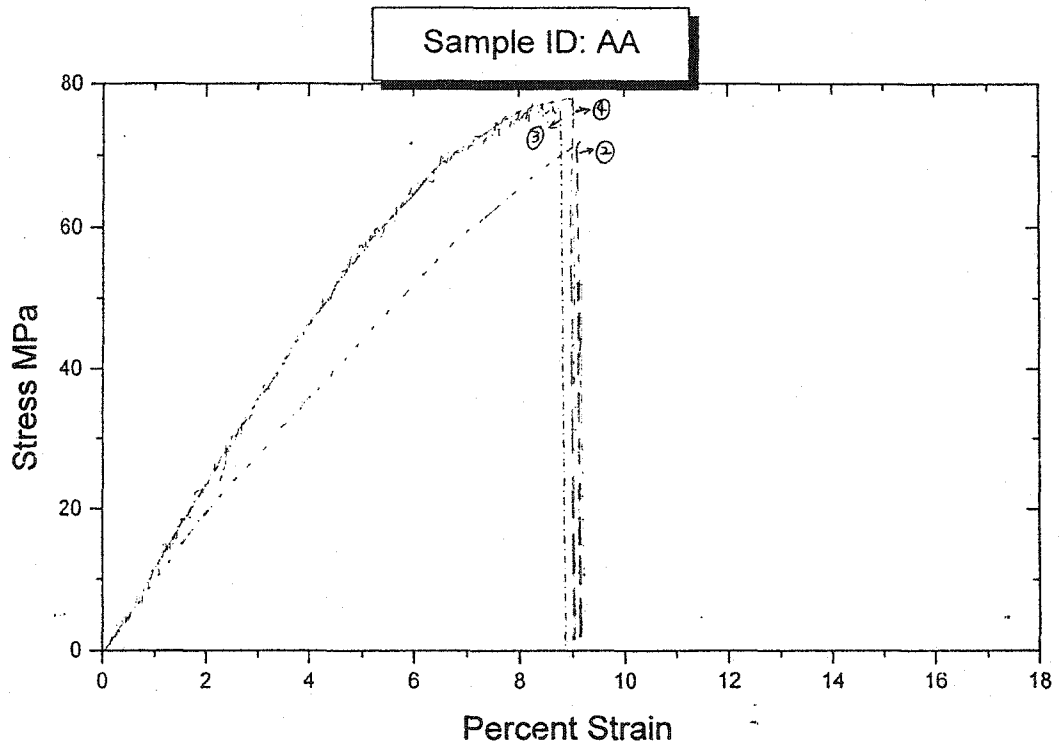


Figure A.1b. Stress-Strain Curves
for **AA** [polymer by "L-S" method with 1% PC (<math><80\mu\text{m}</math>), 1998-11-23]

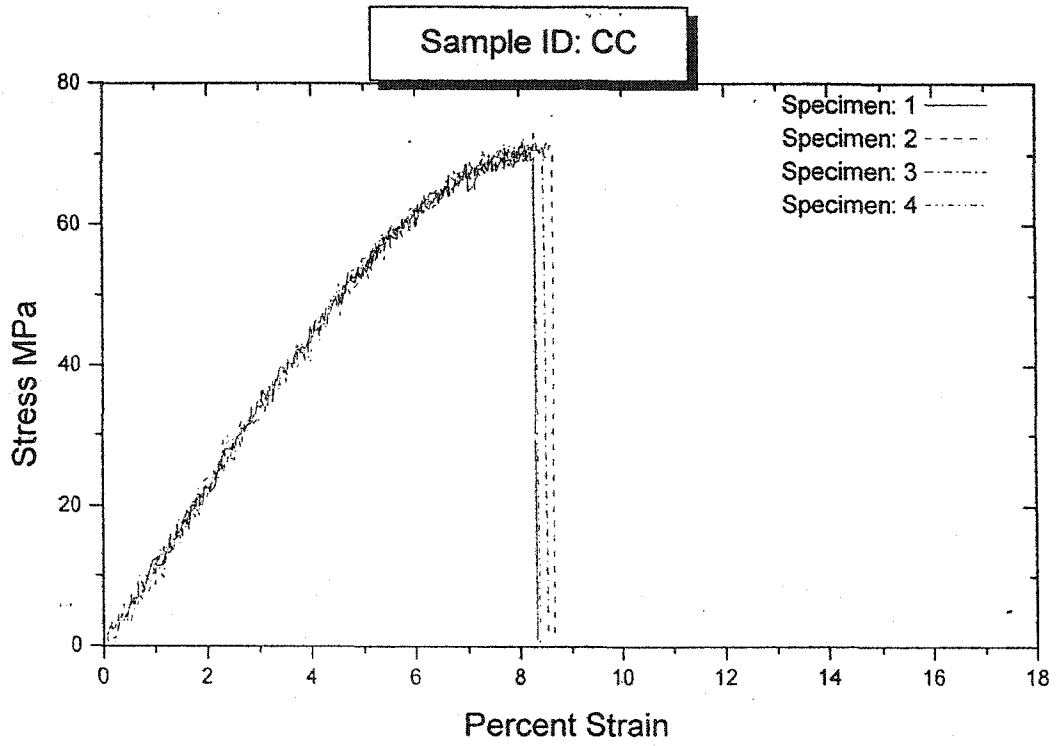


Figure A.1c. Stress-Strain Curves
 for CC [polymer by "L-S" method with 1% PC (80-200 μ m), 1998-11-18]

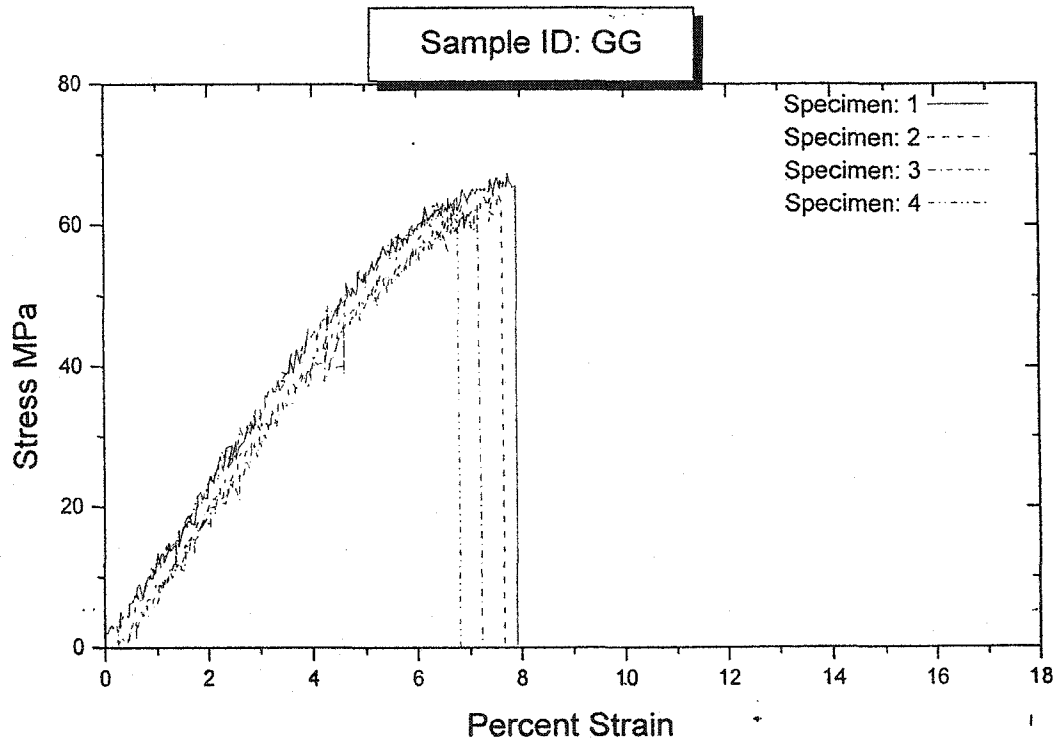


Figure A.1d. Stress-Strain Curves
 for GG [polymer by "L-S" method with 1% PC (200-400 μ m), 1998-11-19]

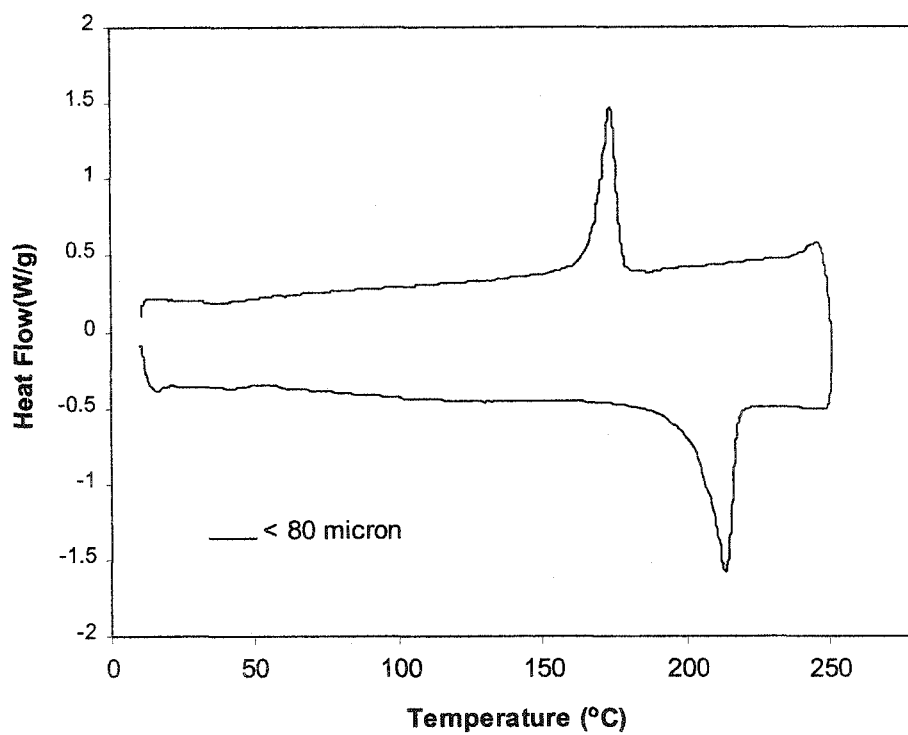


Figure A.2 DSC Heating and Cooling Curves for "L-S" Sample with "<80 micron" PC
(Scan rate: 10°C/min, nitrogen)

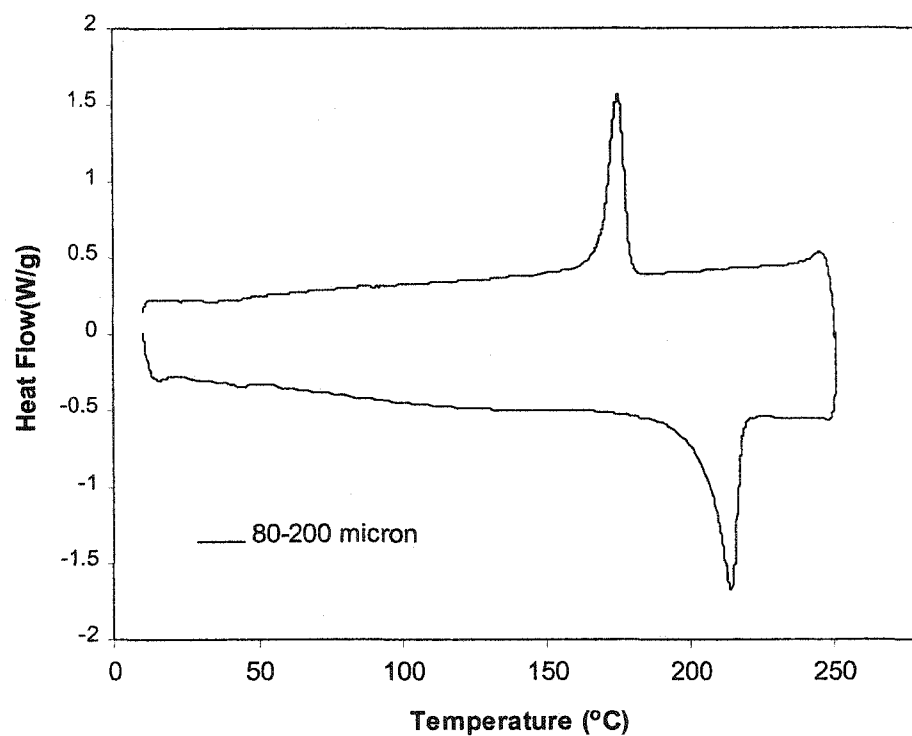


Figure A.3 DSC Heating and Cooling Curves for “L-S” Sample with “80-200 micron”
PC (Scan rate: 10°C/min, nitrogen)

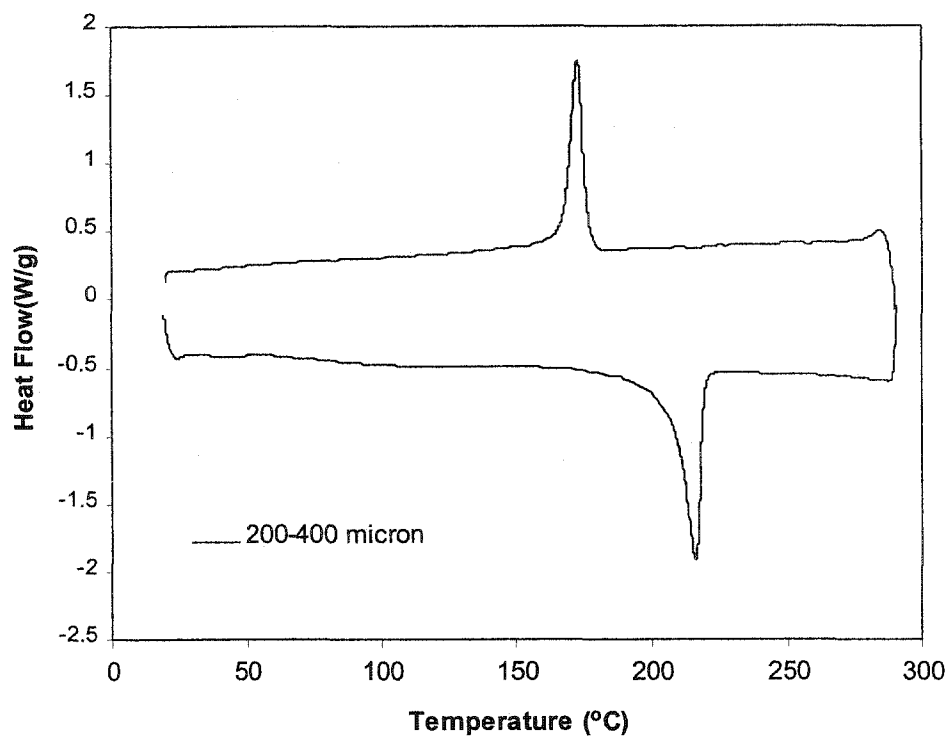


Figure A.4 DSC Heating and Cooling Curves for “L-S” Sample with “200-400 micron” PC (Scan rate: 10°C/min, nitrogen)

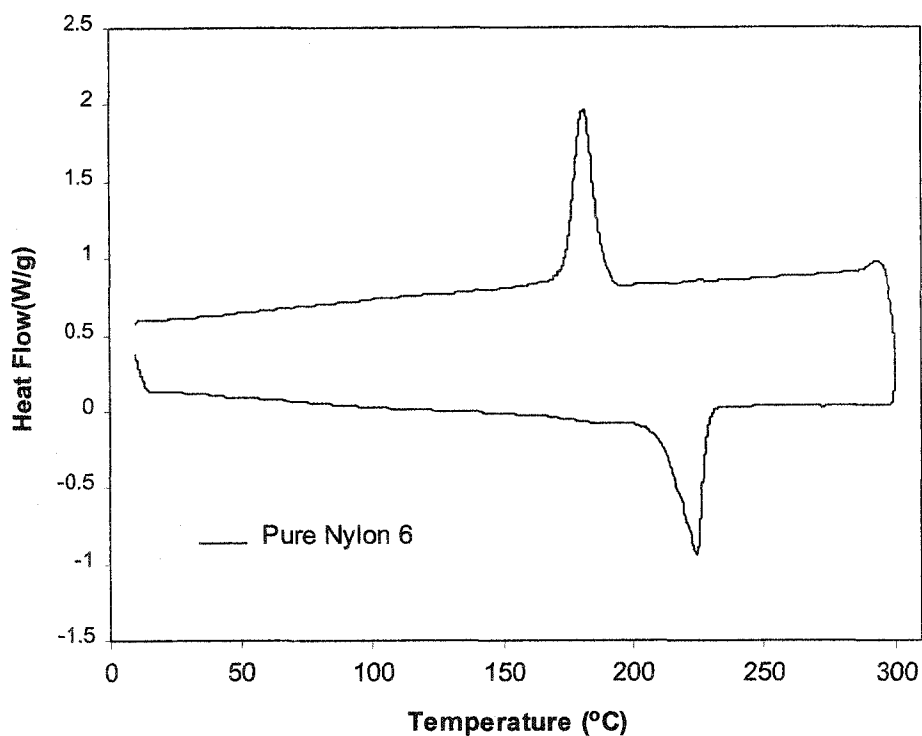


Figure A.5 DSC Heating and Cooling Curves for Pure Nylon 6 Pellets
(Scan rate: 10°C/min, nitrogen)

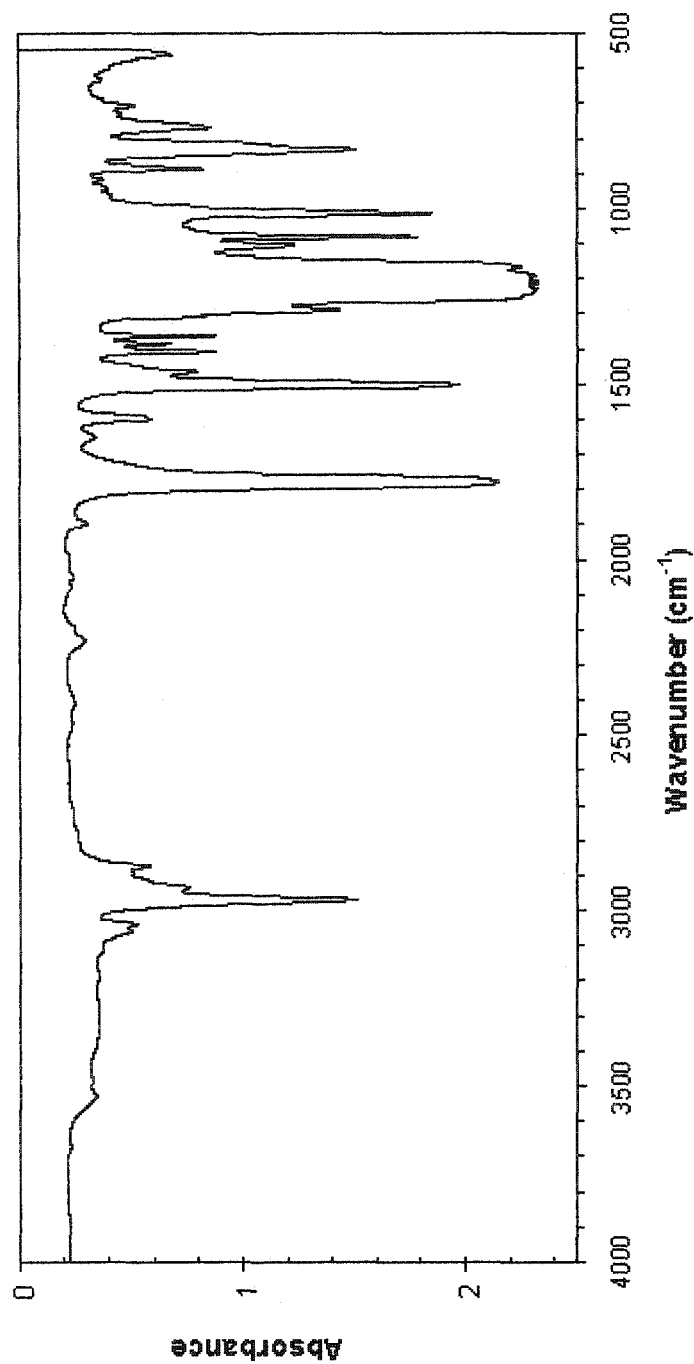


Figure A.6 FTIR Spectrum of Polycarbonate Powder

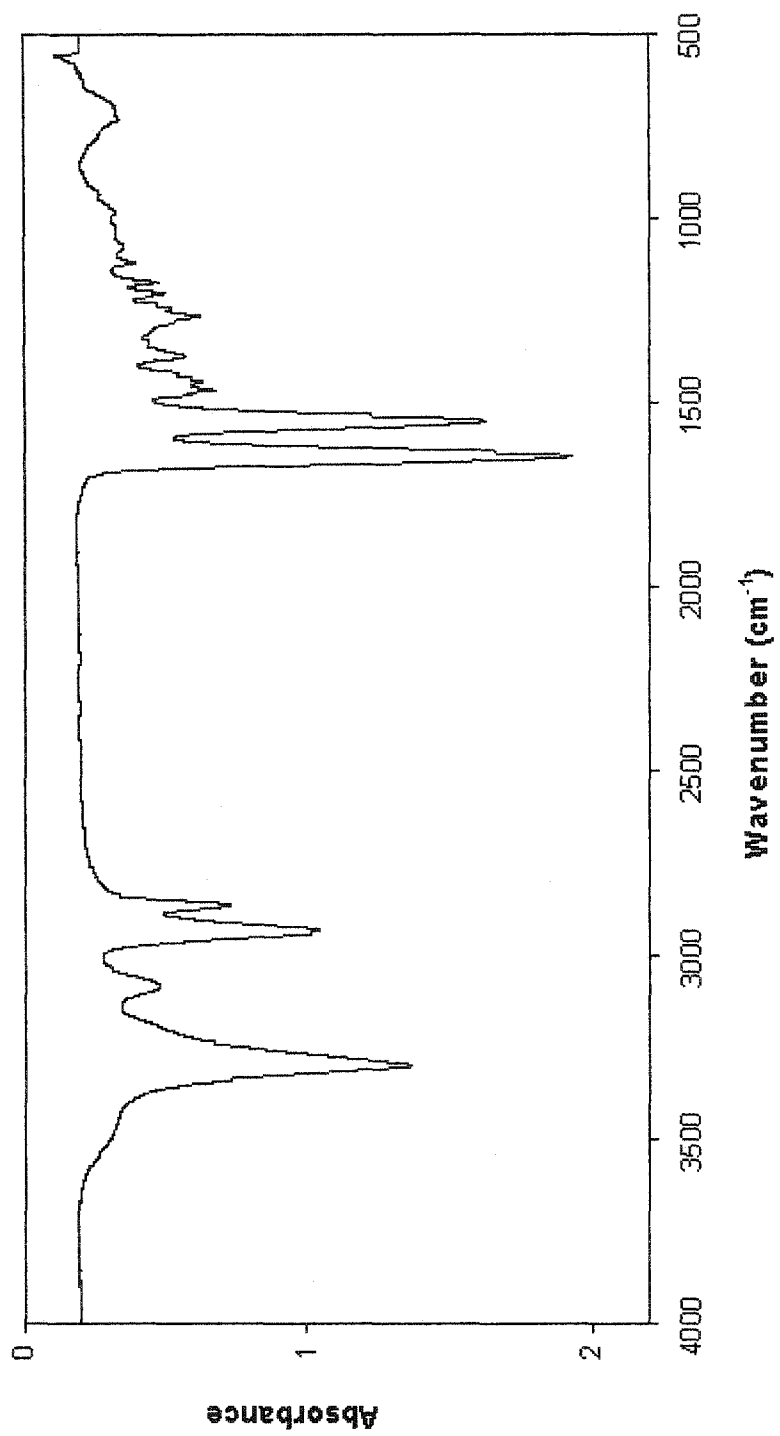


Figure A.7 FTIR Spectrum of Nylon 6 Made from 0.1% Diphenyl Carbonate

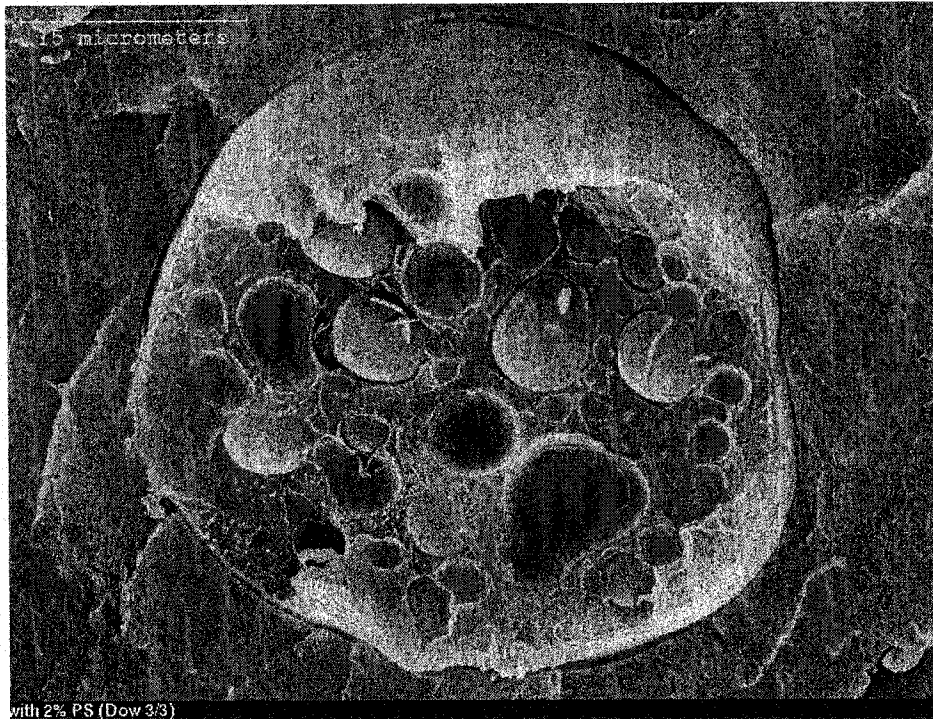
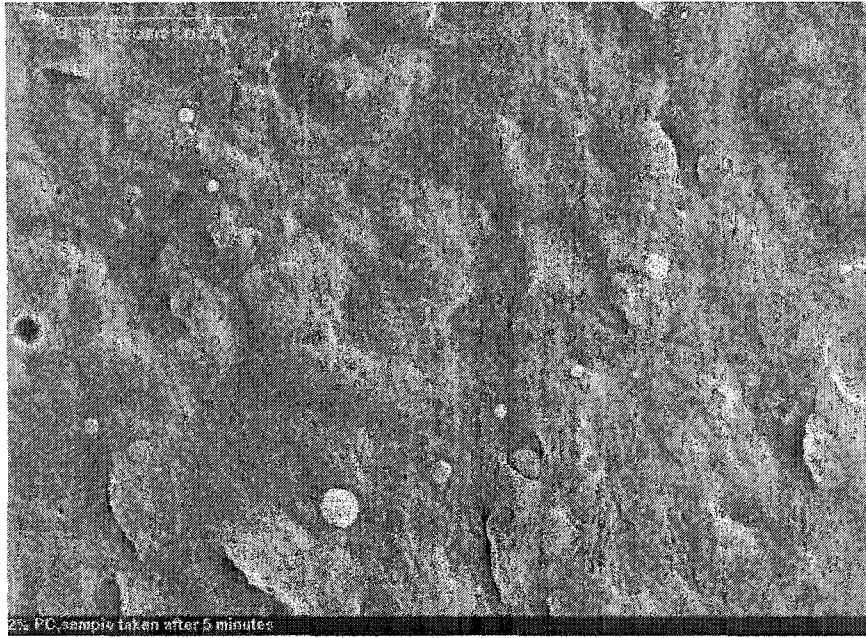


Figure A.8 SEM Image of Nylon 6/PS (2%wt) *in-situ* Reactive Blend



(a)



(b)

Figure A.9 (a) & (b) SEM Images of Nylon 6/Polycarbonate Melt Blend (with 2% Polycarbonate) after Mixing for 5 minutes (at different magnifications)

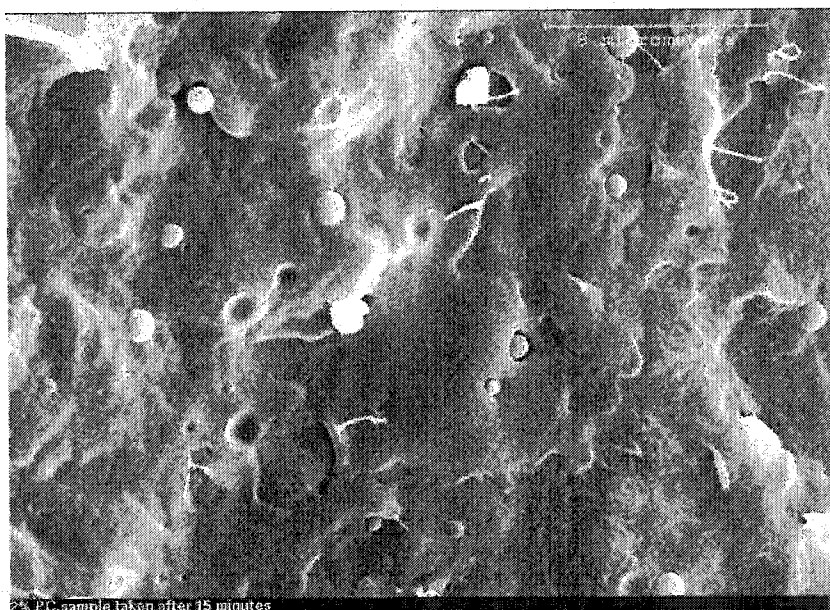


(a)



(b)

Figure A.10 (a) & (b) SEM Images of Nylon 6/Polycarbonate Melt Blend (with 2% Polycarbonate) after Mixing for 10 minutes (at different magnifications)



(a)



(b)

Figure A.11 (a) & (b) SEM Images of Nylon 6/Polycarbonate Melt Blend (with 2% Polycarbonate) after Mixing for 15 minutes (at different magnifications)

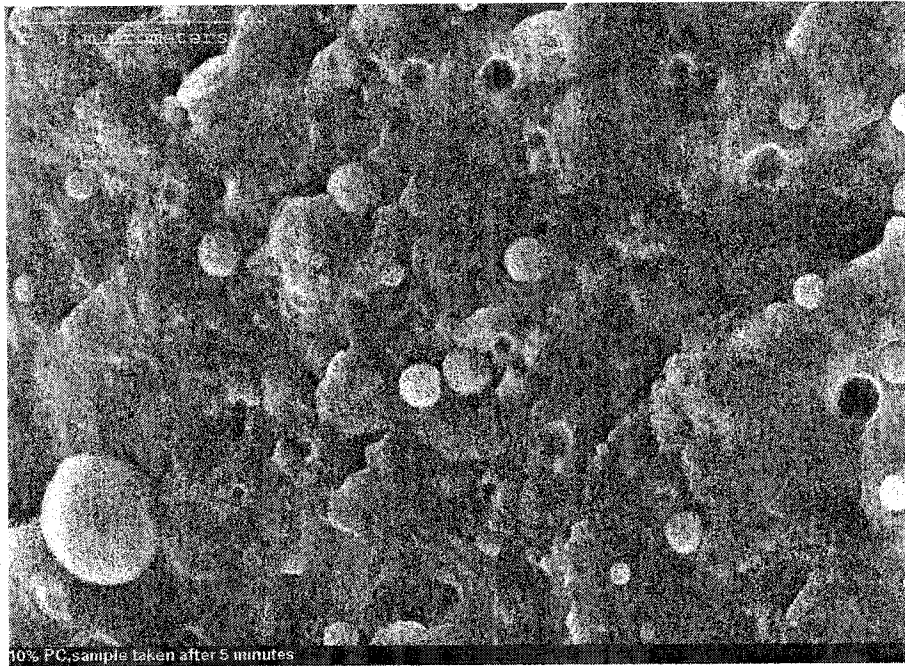


Figure A.12 SEM Image of Nylon 6/Polycarbonate Melt Blend (with 10% Polycarbonate) after Mixing for 5 minutes

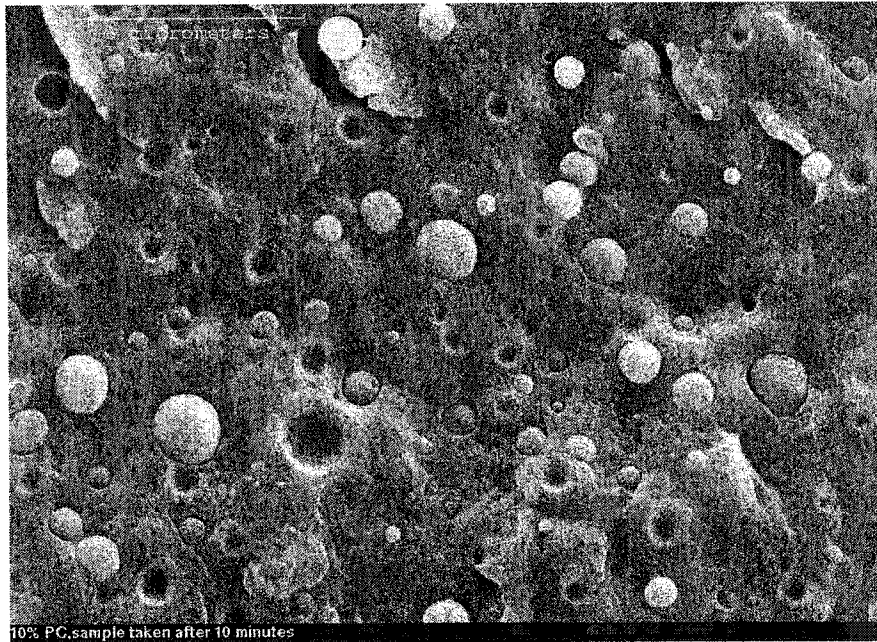
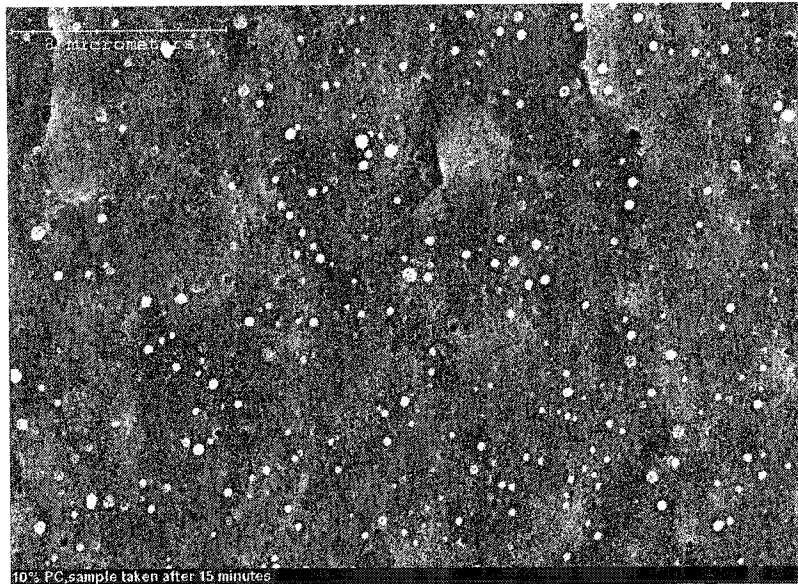
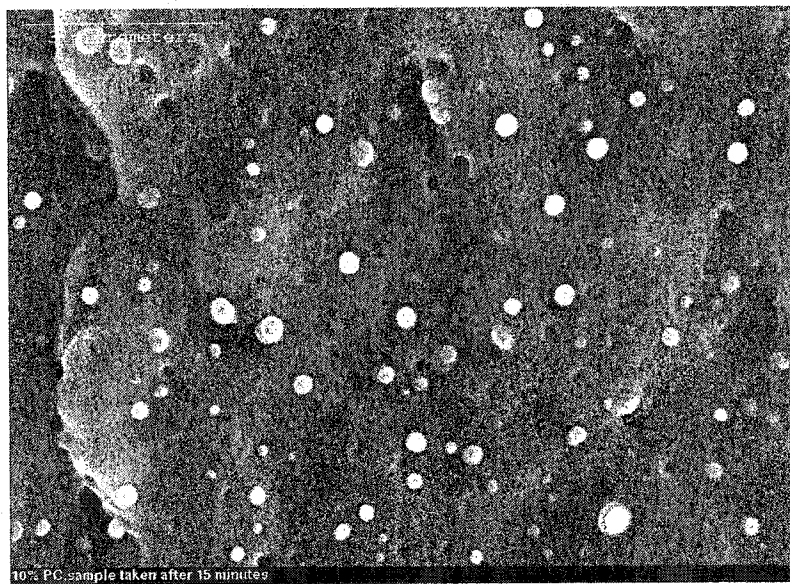


Figure A.13 SEM Image of Nylon 6/Polycarbonate Melt Blend (with 10% Polycarbonate) after Mixing for 10 minutes



(a)



(b)

Figure A.14 (a) & (b) SEM Pictures of Nylon 6/Polycarbonate Melt Blend (with 10% Polycarbonate) after Mixing for 15 minutes (at different magnifications)

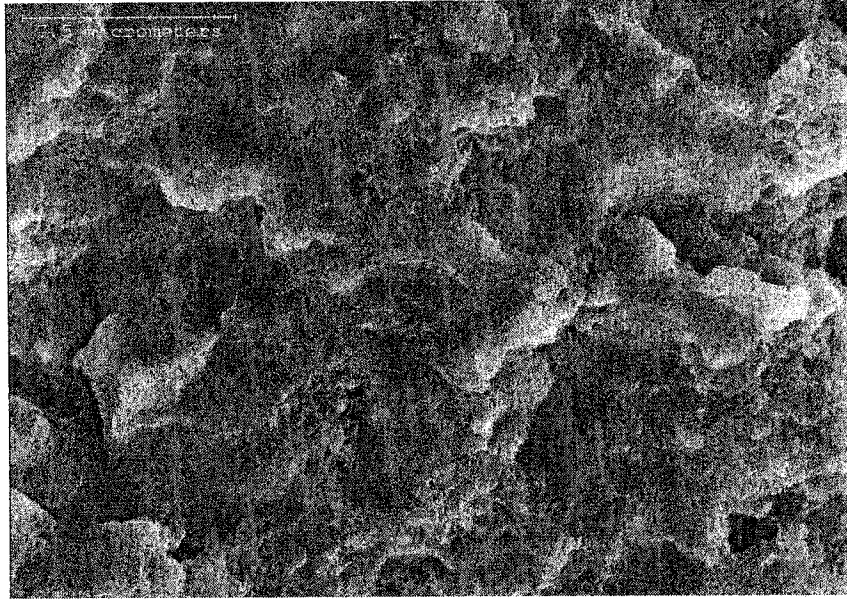


Figure A.15. SEM Image of Copolymer with 2%wt Polycarbonate

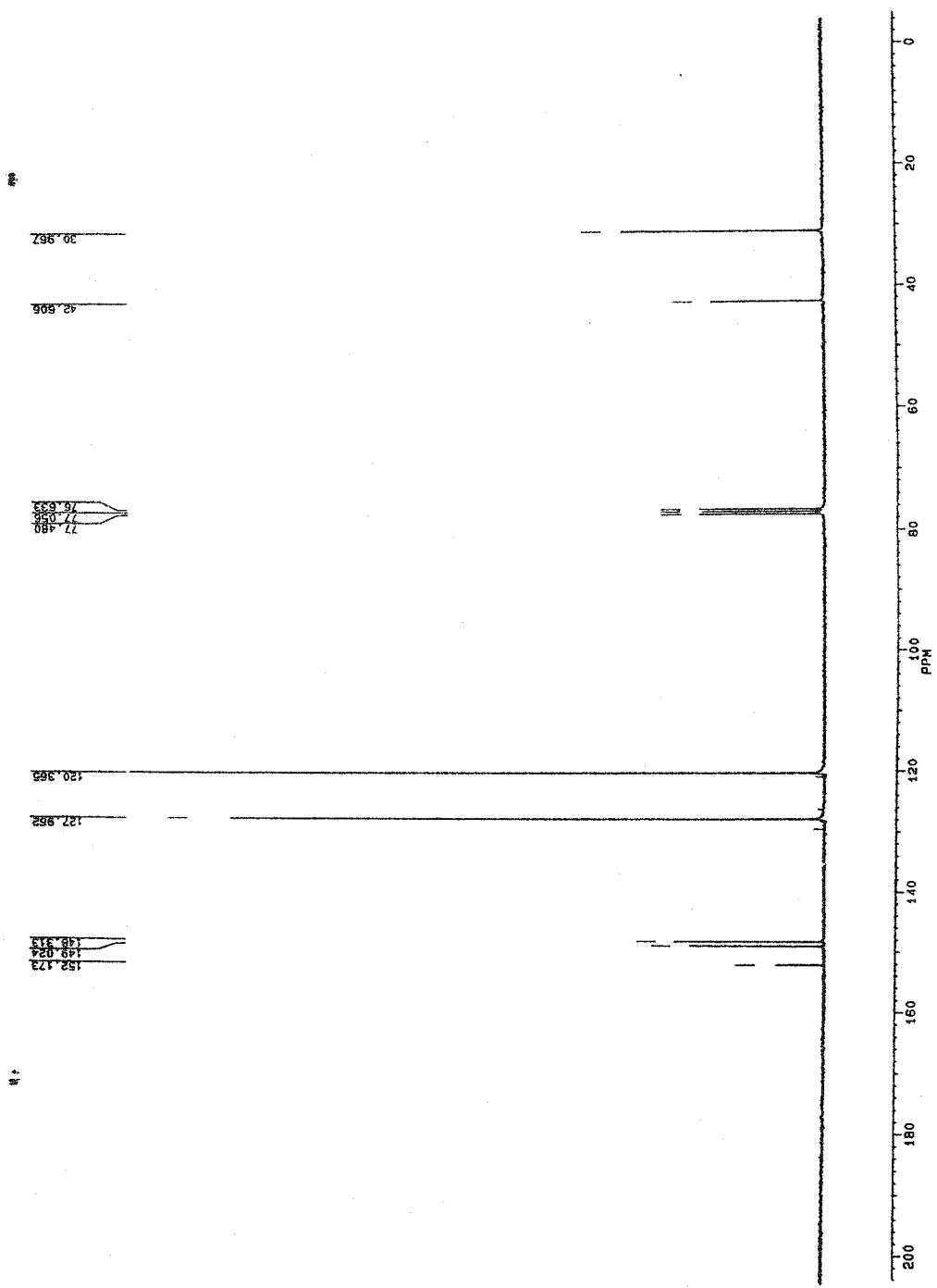


Figure A.16 ^{13}C NMR spectrum of Polycarbonate in CDCl_3

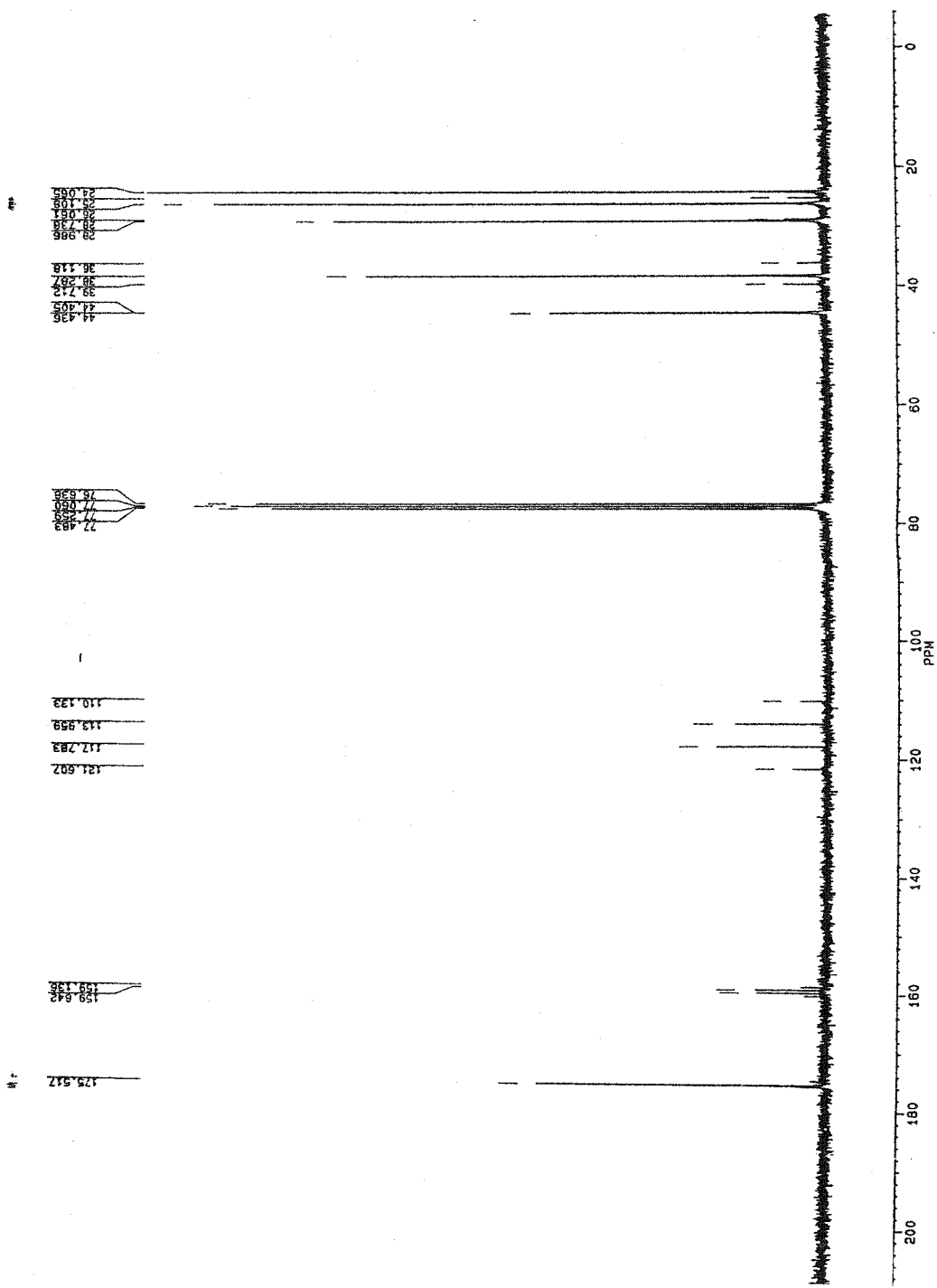


Figure A.17 ^{13}C NMR spectrum of trifluoroacetylated Nylon 6 in CDCl_3

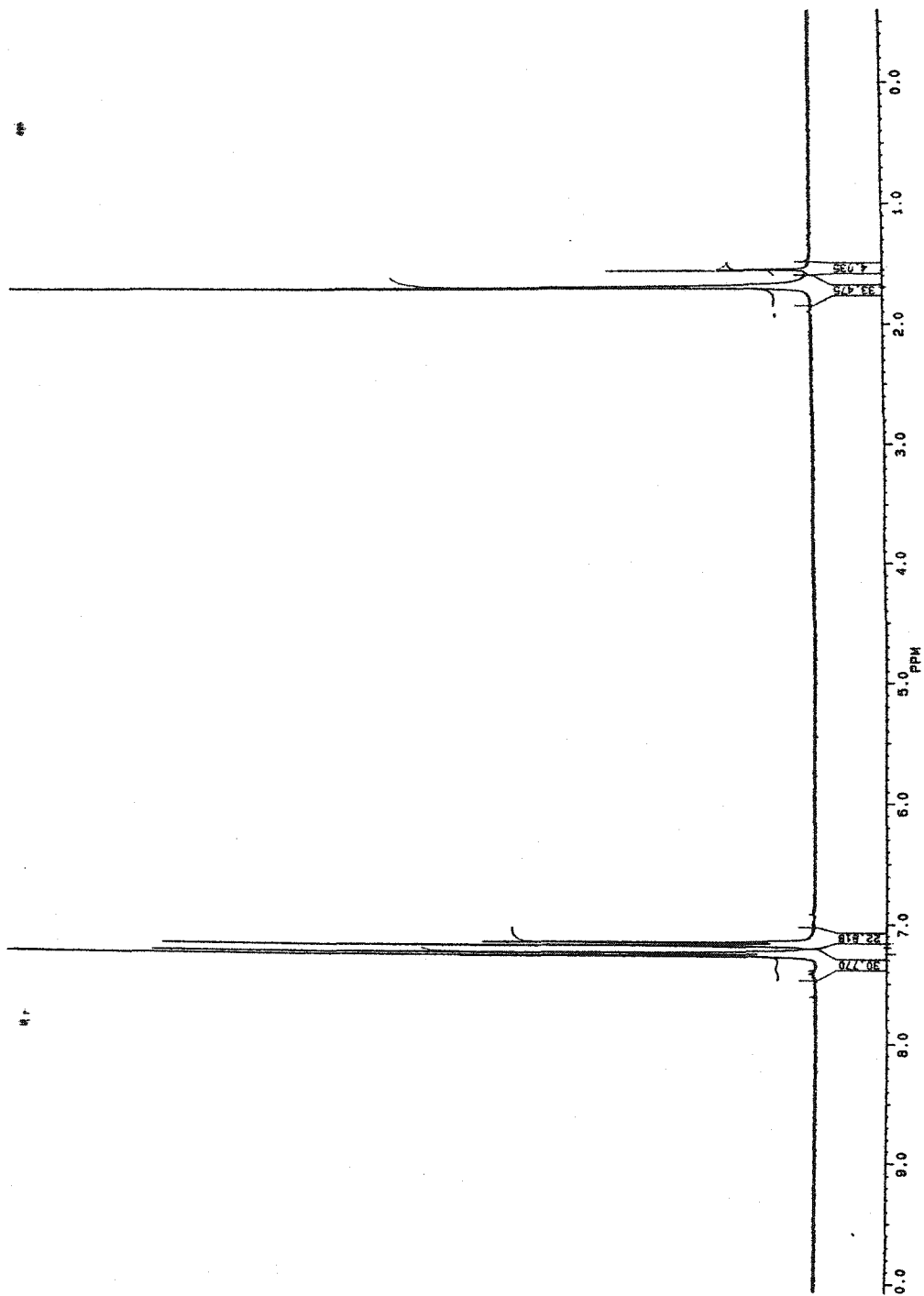


Figure A.18 ^1H NMR spectrum of Polycarbonate in CDCl_3

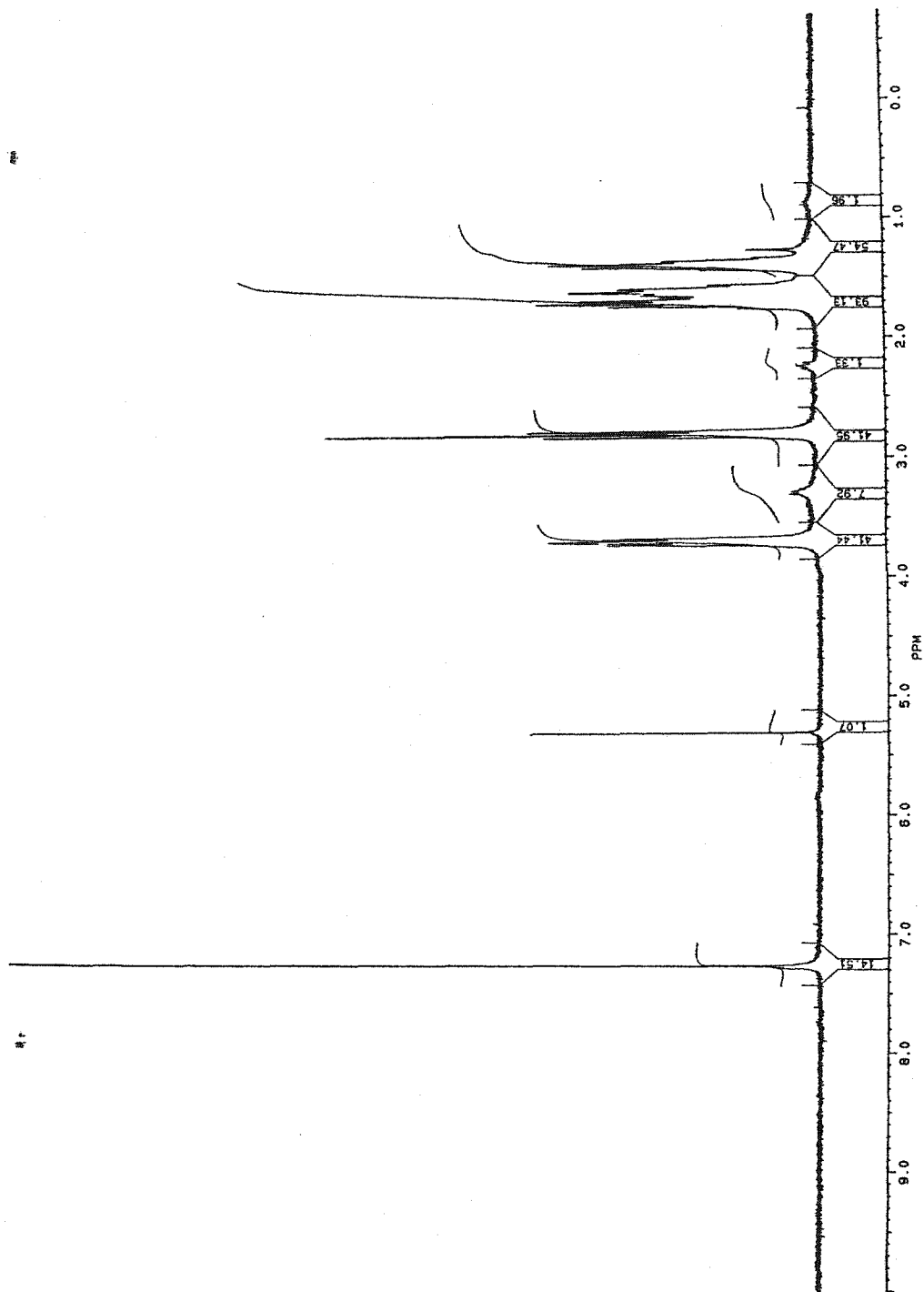


Figure A.19 ^1H NMR spectrum of trifluoroacetylated Nylon 6 in CDCl_3

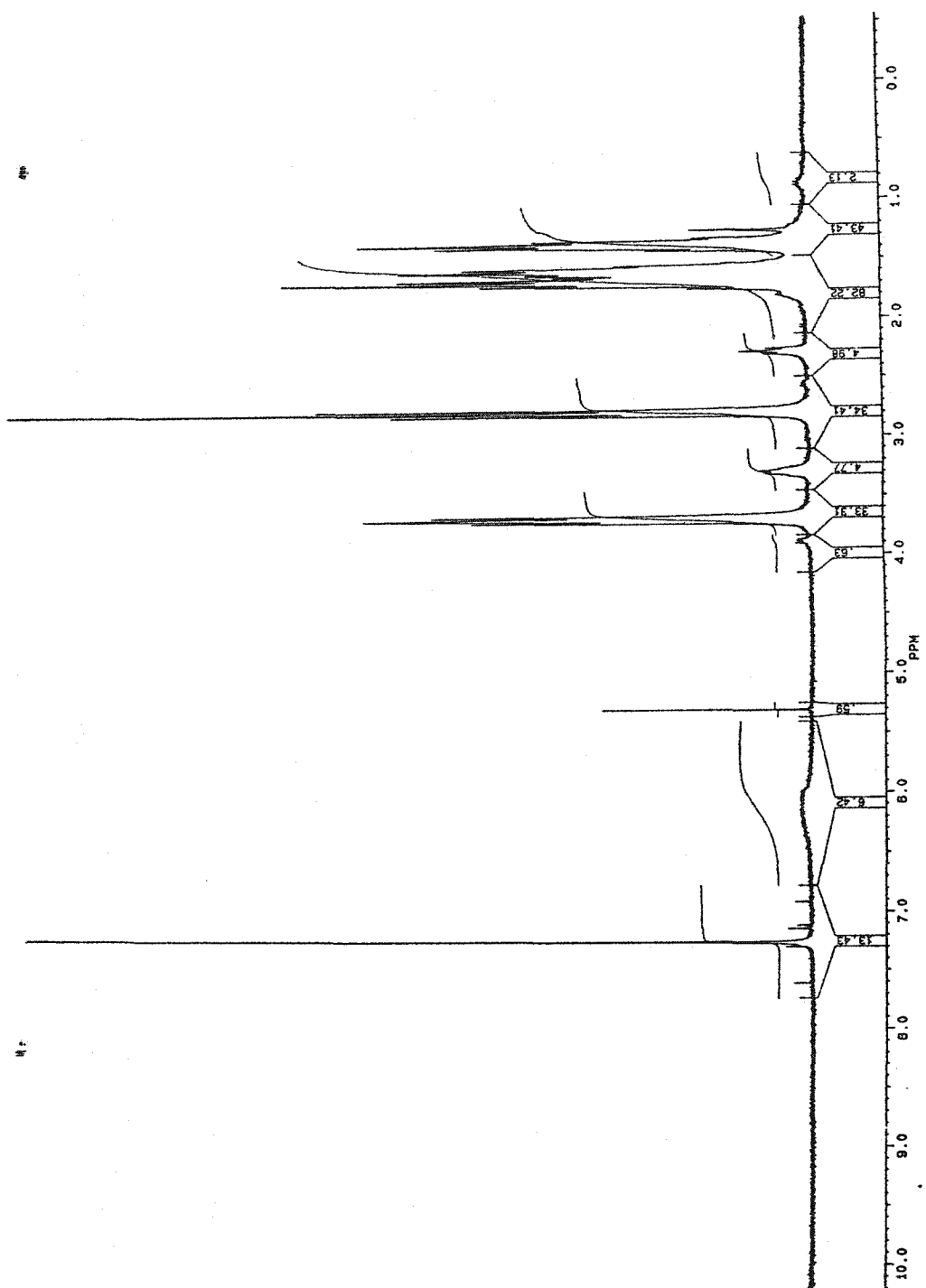


Figure A.20 ^1H NMR spectrum of trifluoroacetylated copolymer (with 2% PC) in CDCl_3

Appendix B Supplement to Chapter 5

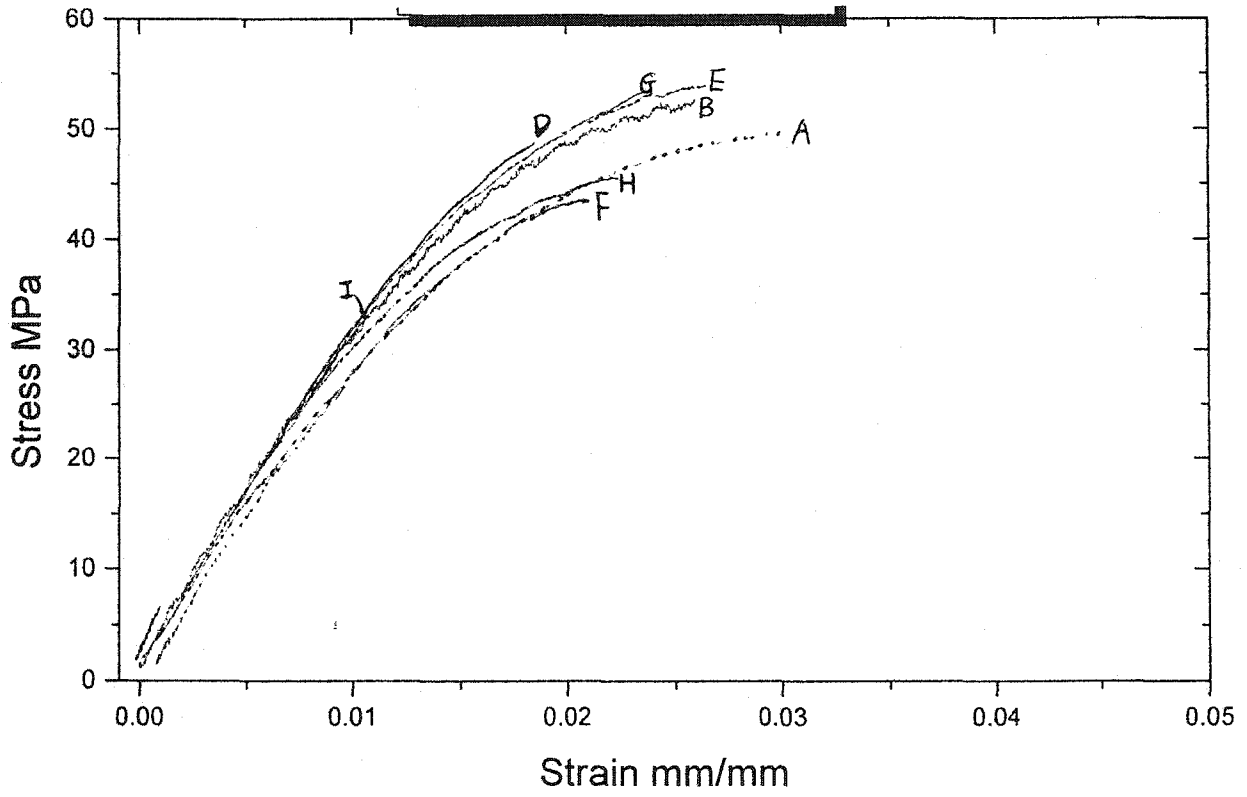
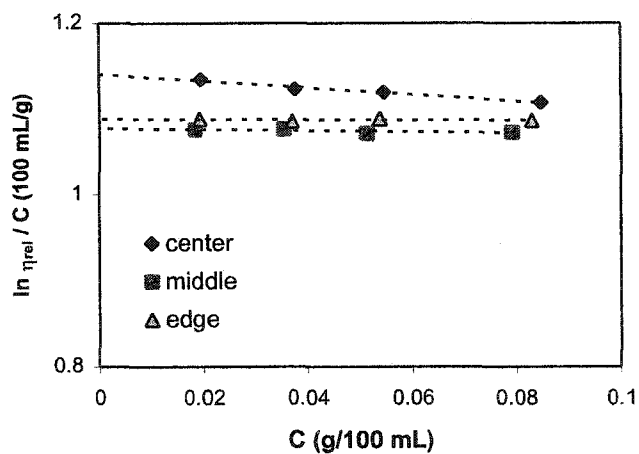
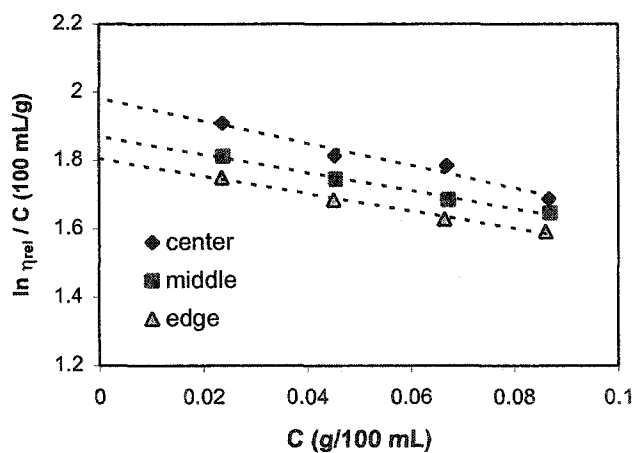


Figure B.1 Tensile stress-strain curves for specimens from the “Scale-up” sample



(a)



(b)

Figure B.2 (a) & (b). Plots of $\ln \eta_{rel}/C$ versus C

- (a). Nylon 6 made by using isobutyl magnesium chloride as initiator (100g ϵ -caprolactam/1ml N-acetyl caprolactam/3mmol isobutyl magnesium chloride);
- (b). Nylon 6 made by using Red-Al as initiator (100g ϵ -caprolactam/1ml N-acetyl caprolactam/3mmol Red-Al).

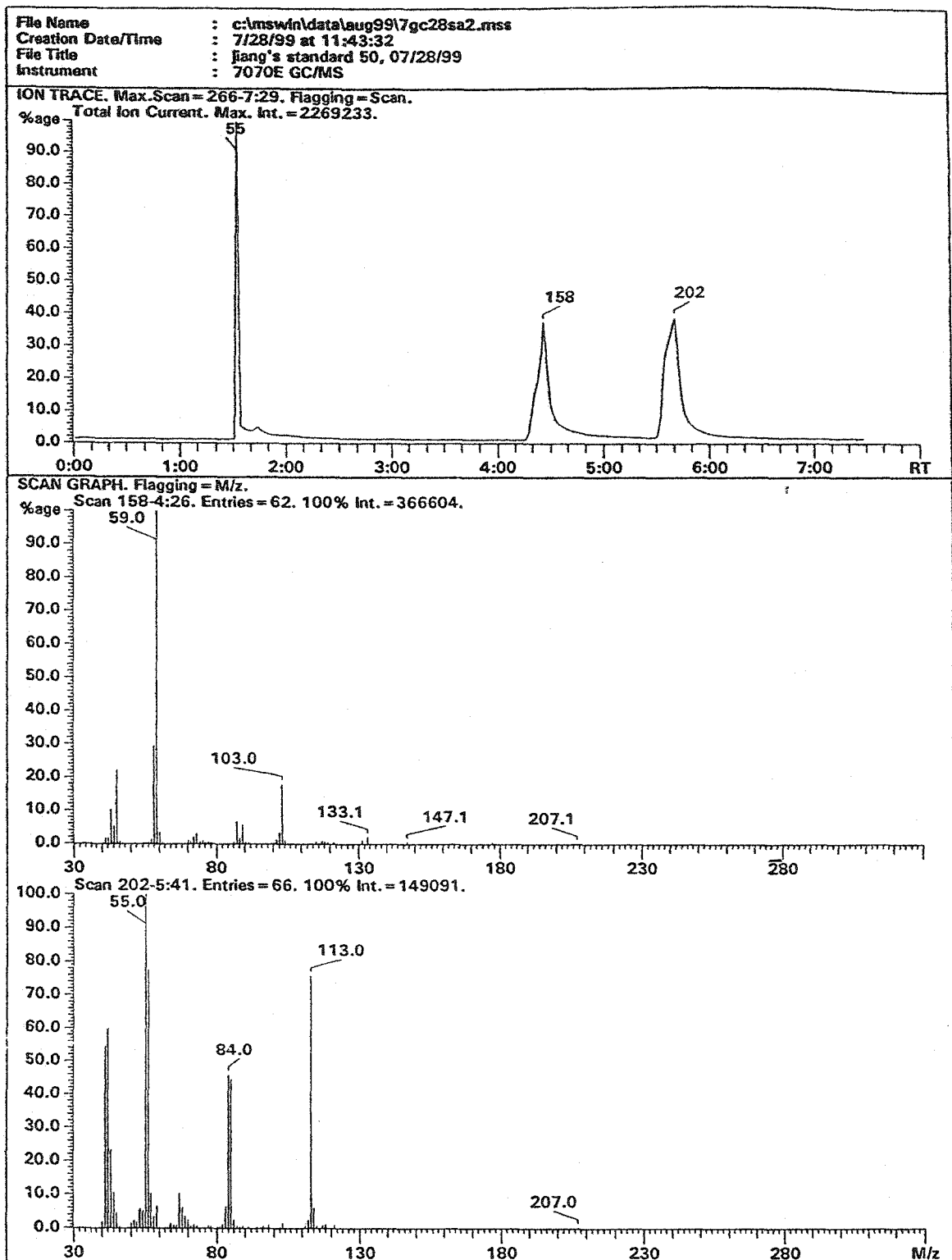


Figure B.3-(a1). GC-MS result for 0.0523g/100mL standard solution (run 1).

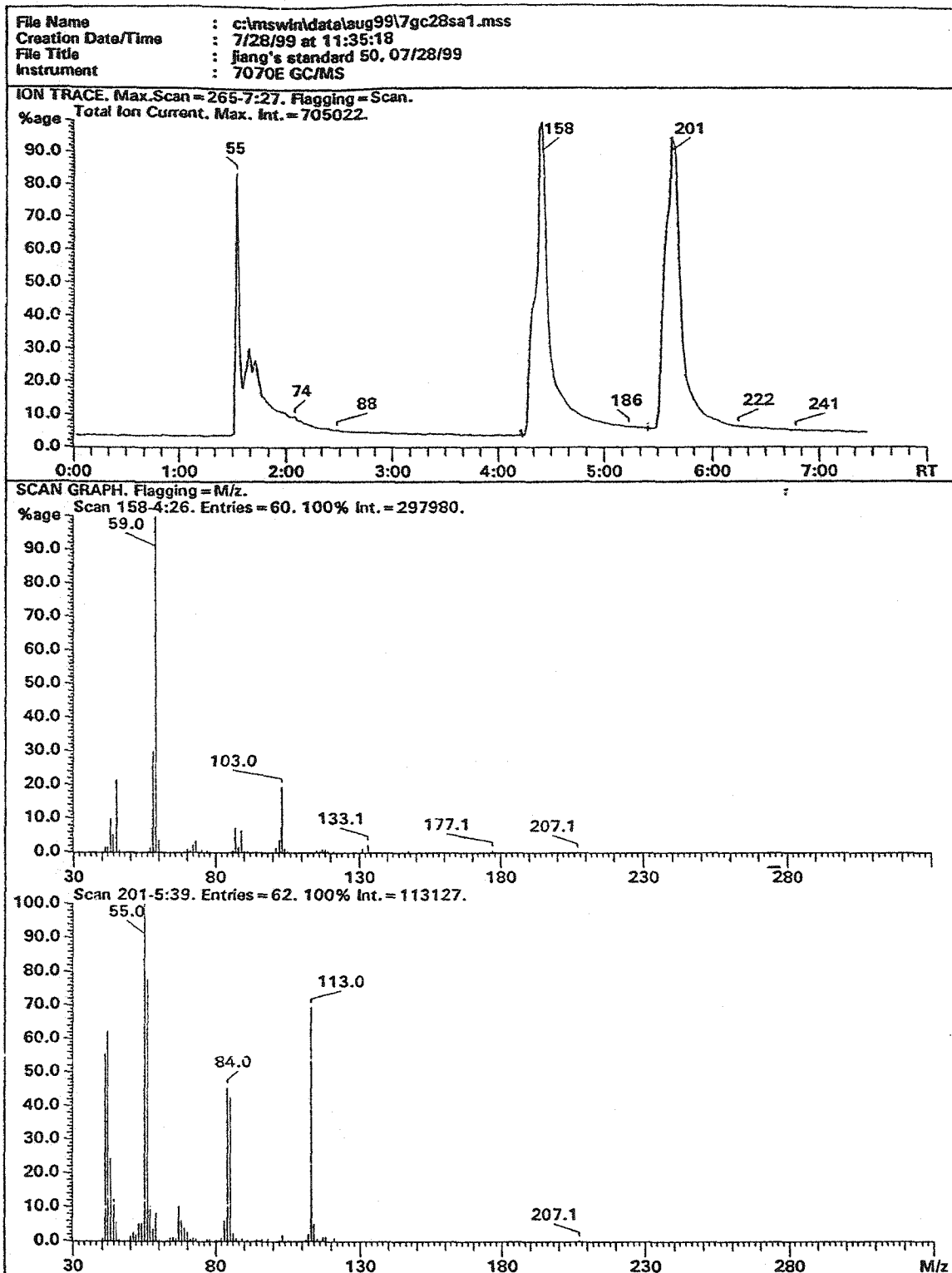


Figure B.3-(a2). GC-MS result for 0.0523g/100mL standard solution (run 2).

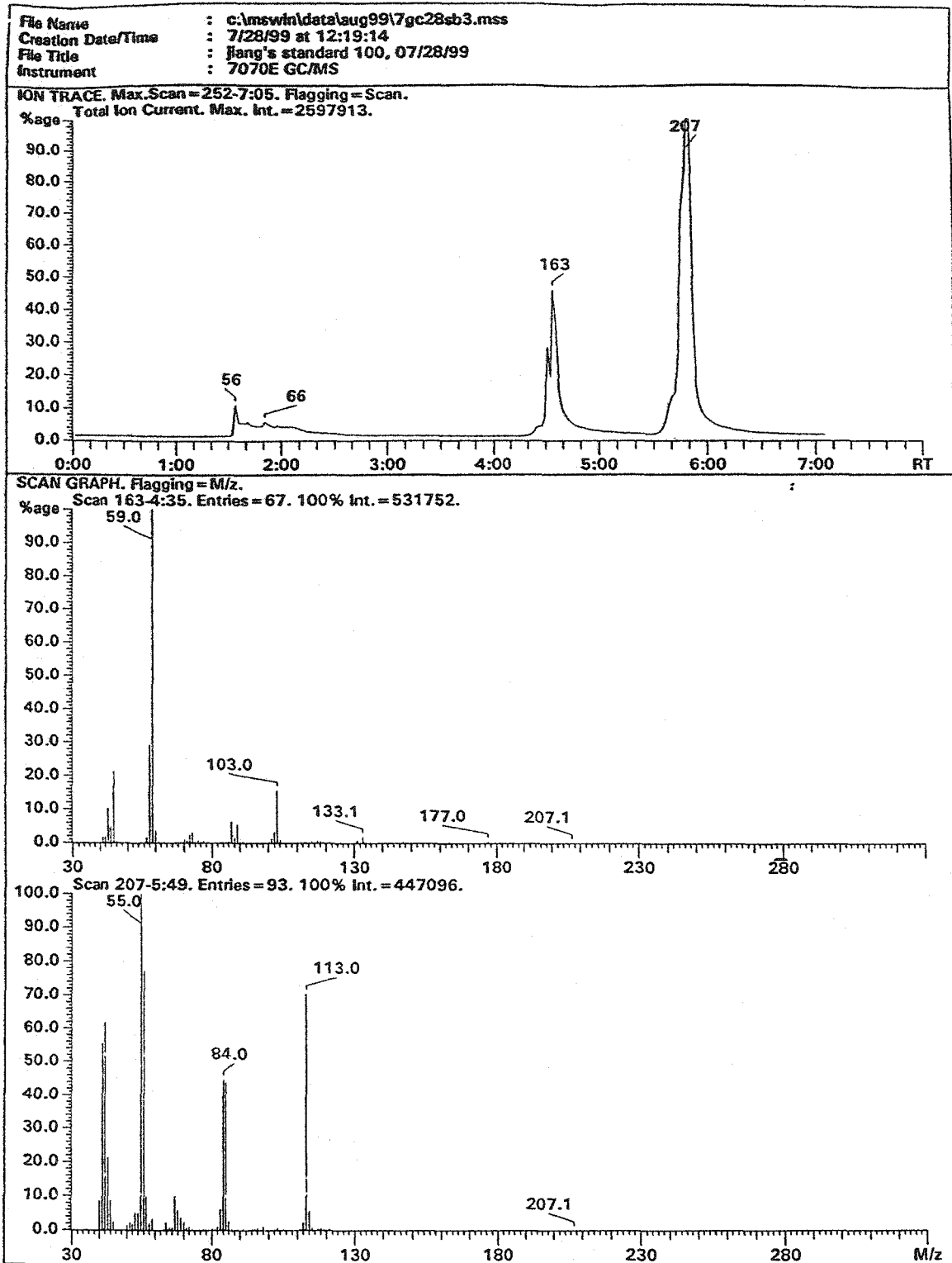


Figure B.3-(b1).GC-MS result for 0.1028g/100mL standard solution (run 1)

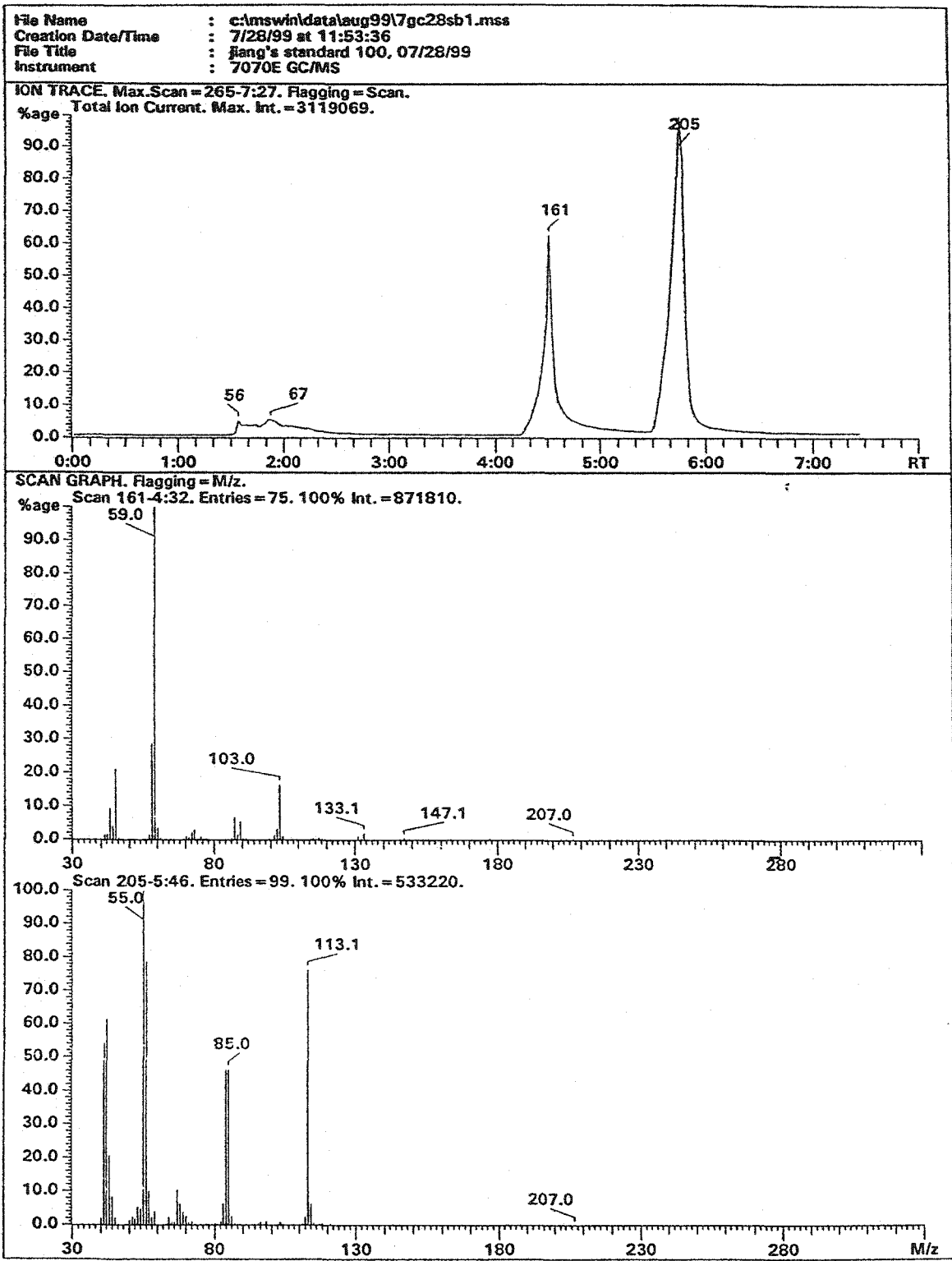


Figure B.3-(b2). GC-MS result for 0.1028g/100mL standard solution (run 2)

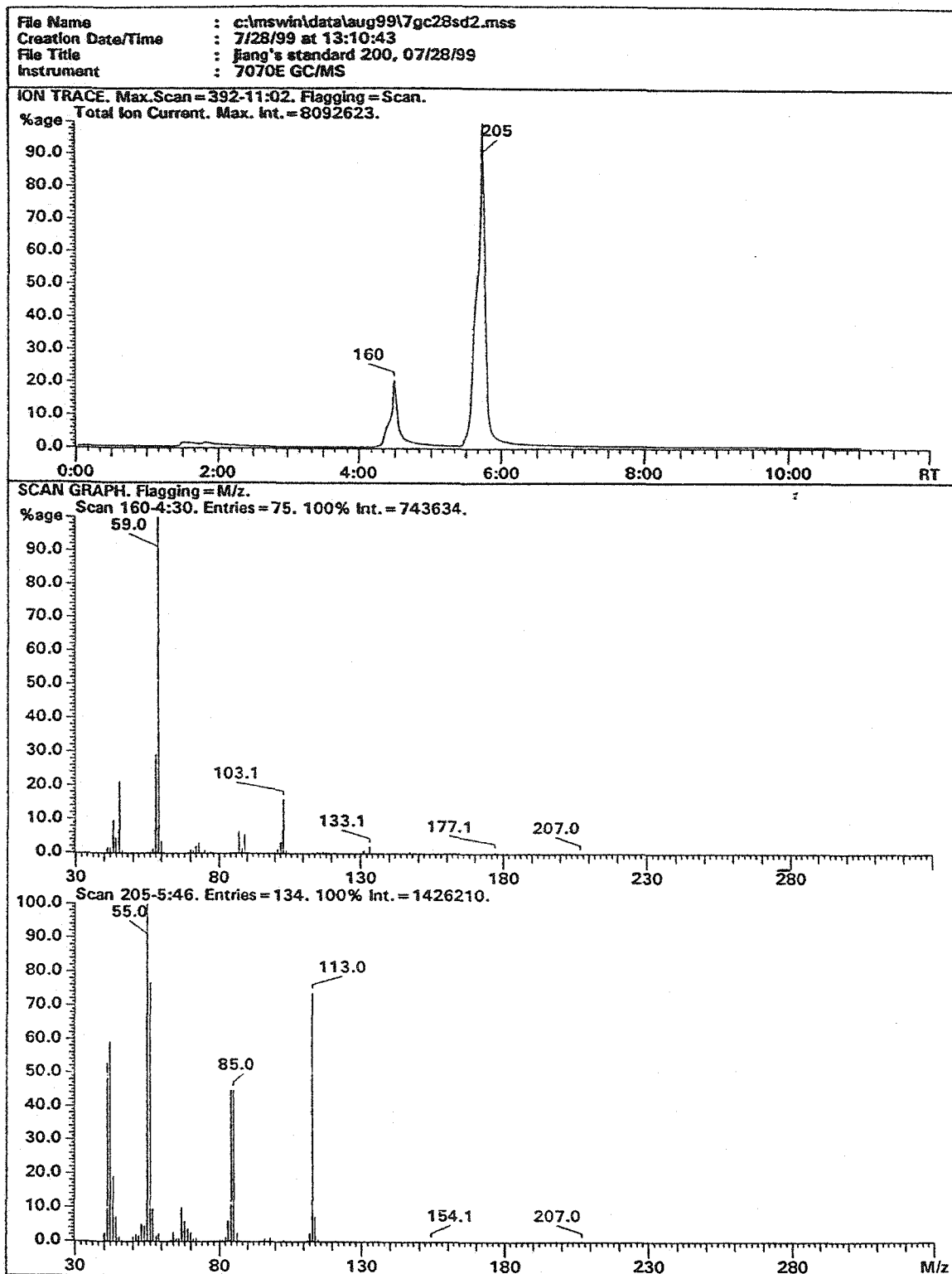


Figure B.3-(c1). GC-MS result for 0.2162/100mL standard solution (run 1).

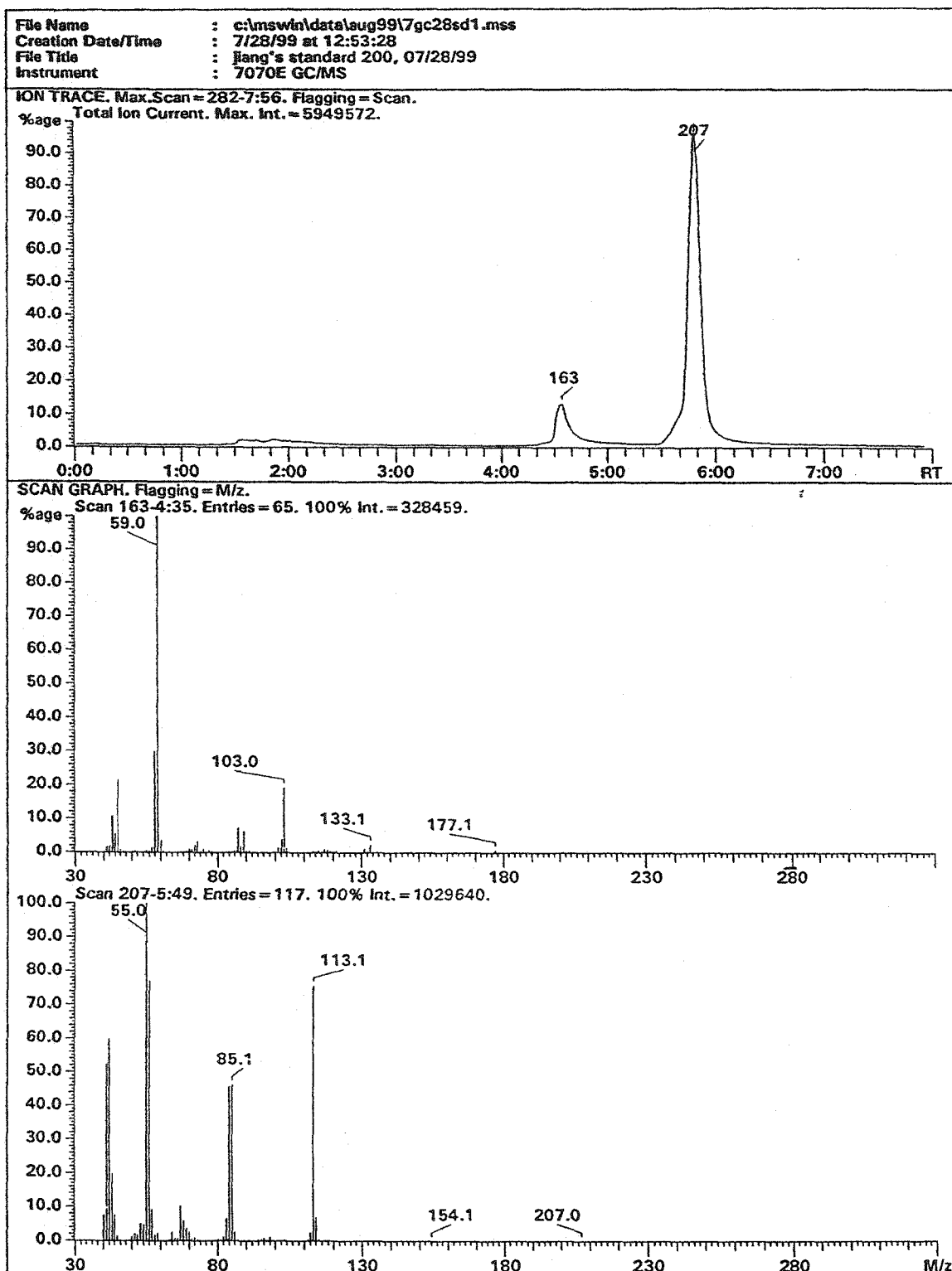


Figure B.3-(c2). GC-MS result for 0.2162/100mL standard solution (run 2).

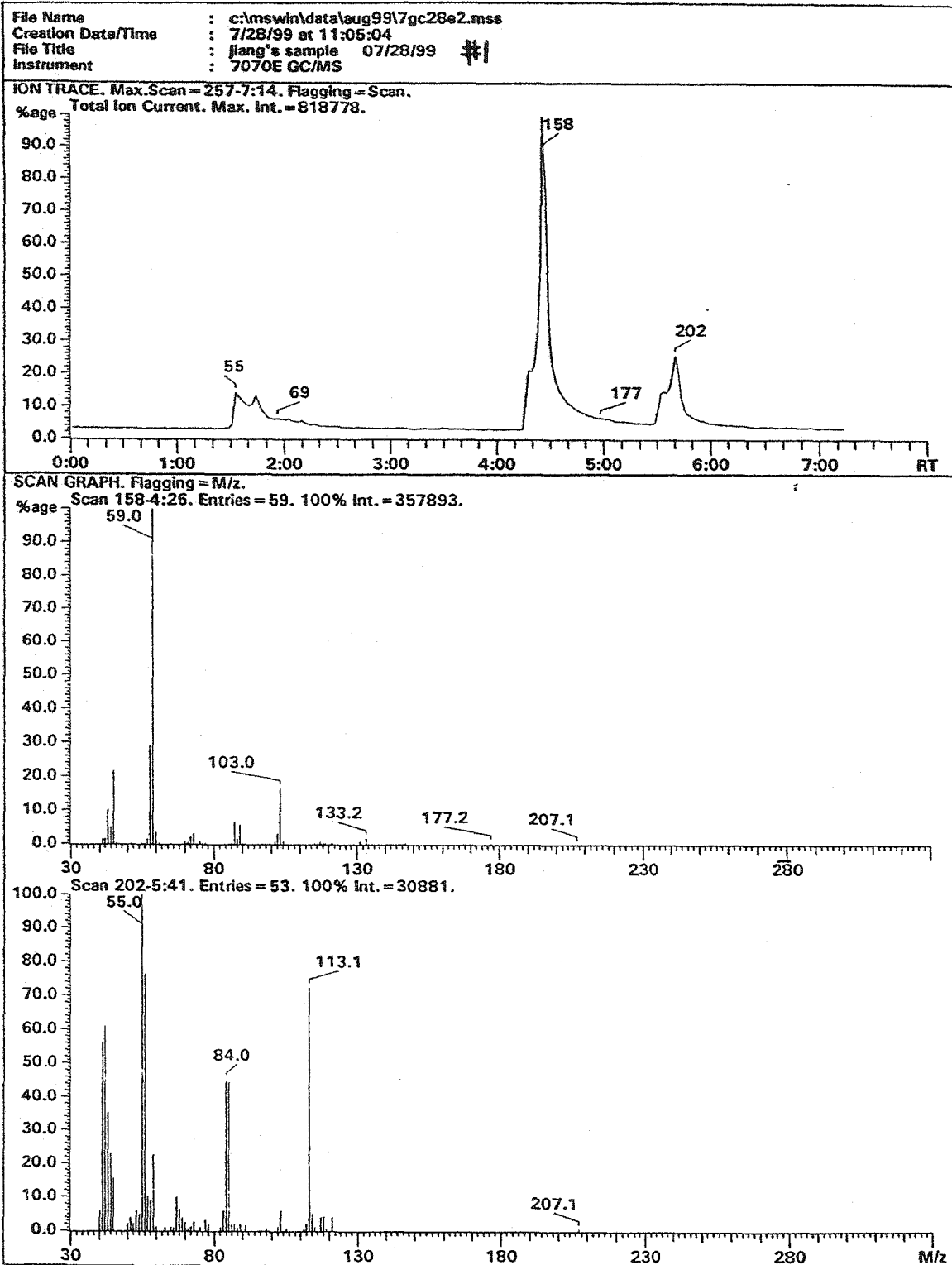


Figure B.4-(a1). GC-MS result for sample #1 (run1).

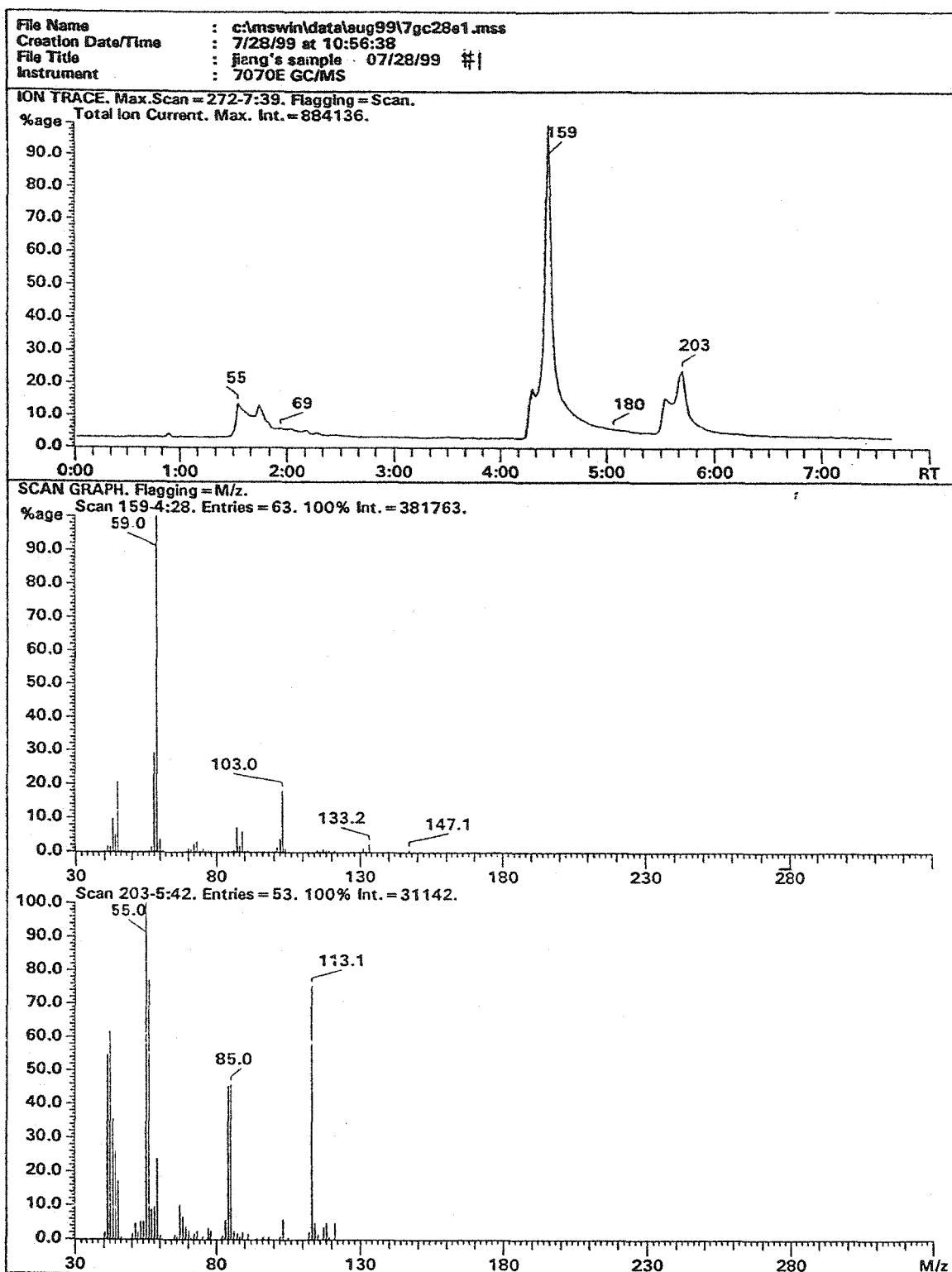


Figure B.4-(a2). GC-MS result for sample #1 (run2).

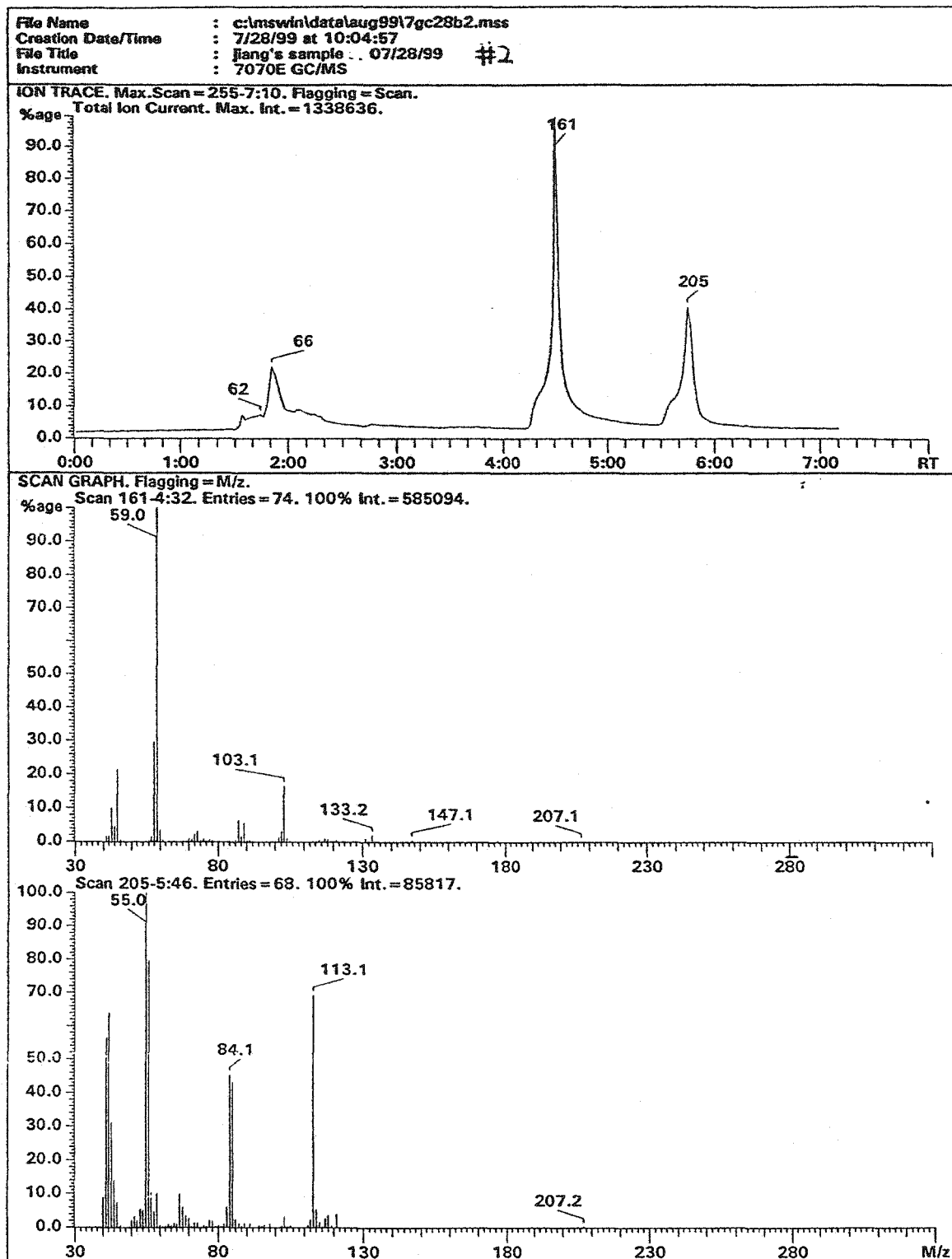


Figure B.4-(b1). GC-MS result for sample #2 (run1).

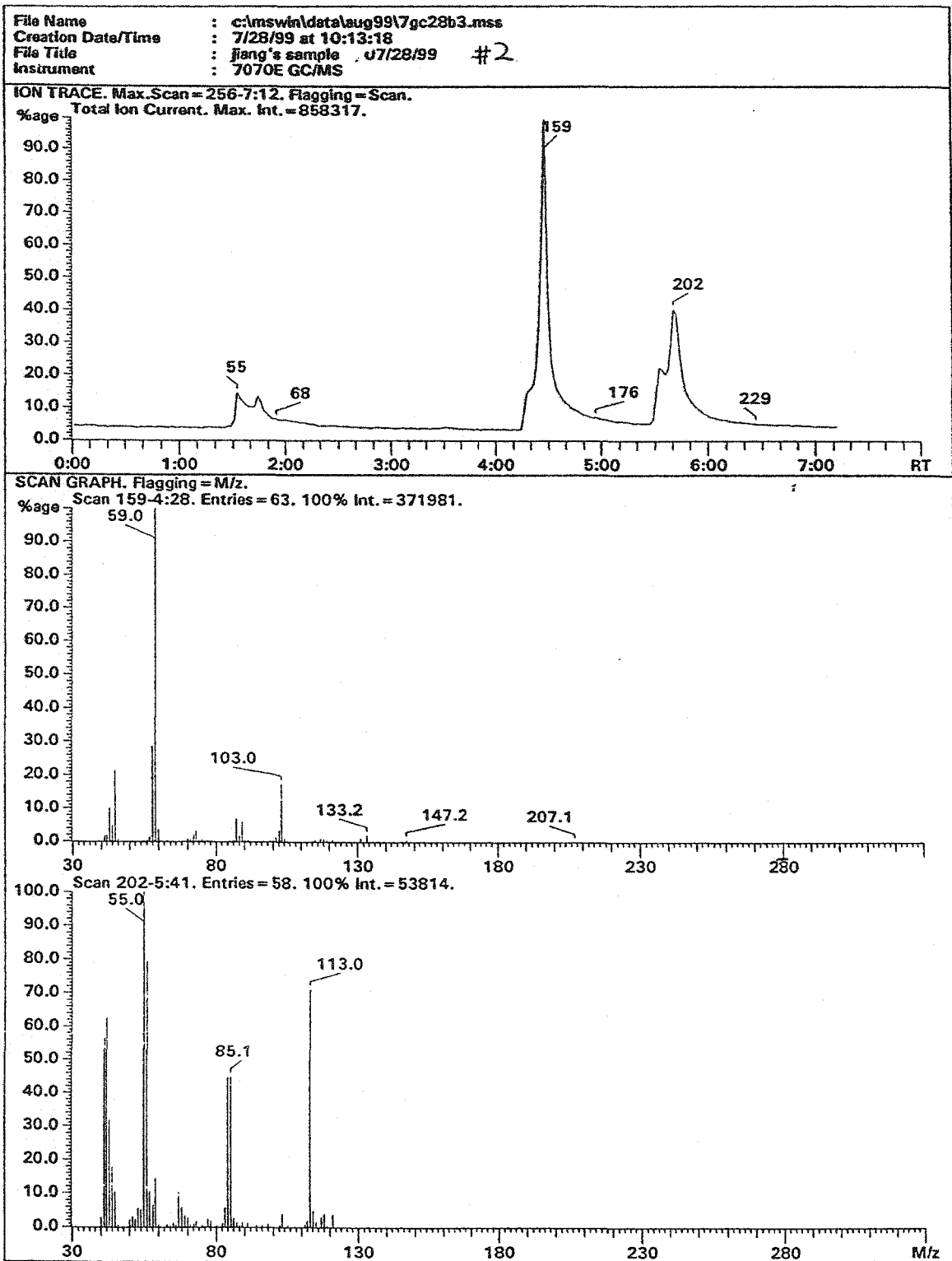


Figure B.4-(b2). GC-MS result for sample #2 (run2).

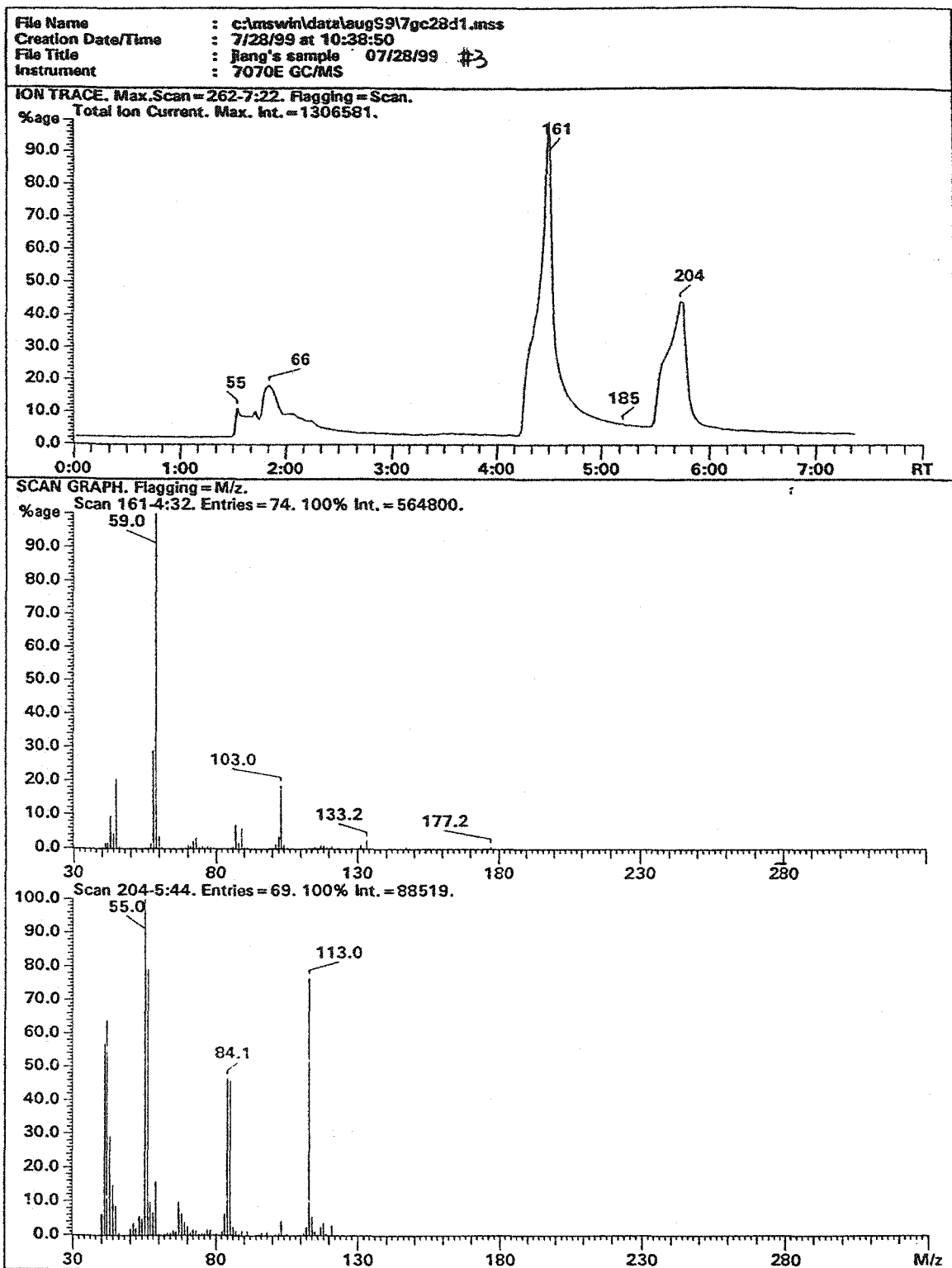


Figure B.4-(c1). GC-MS result for sample #3 (run1).

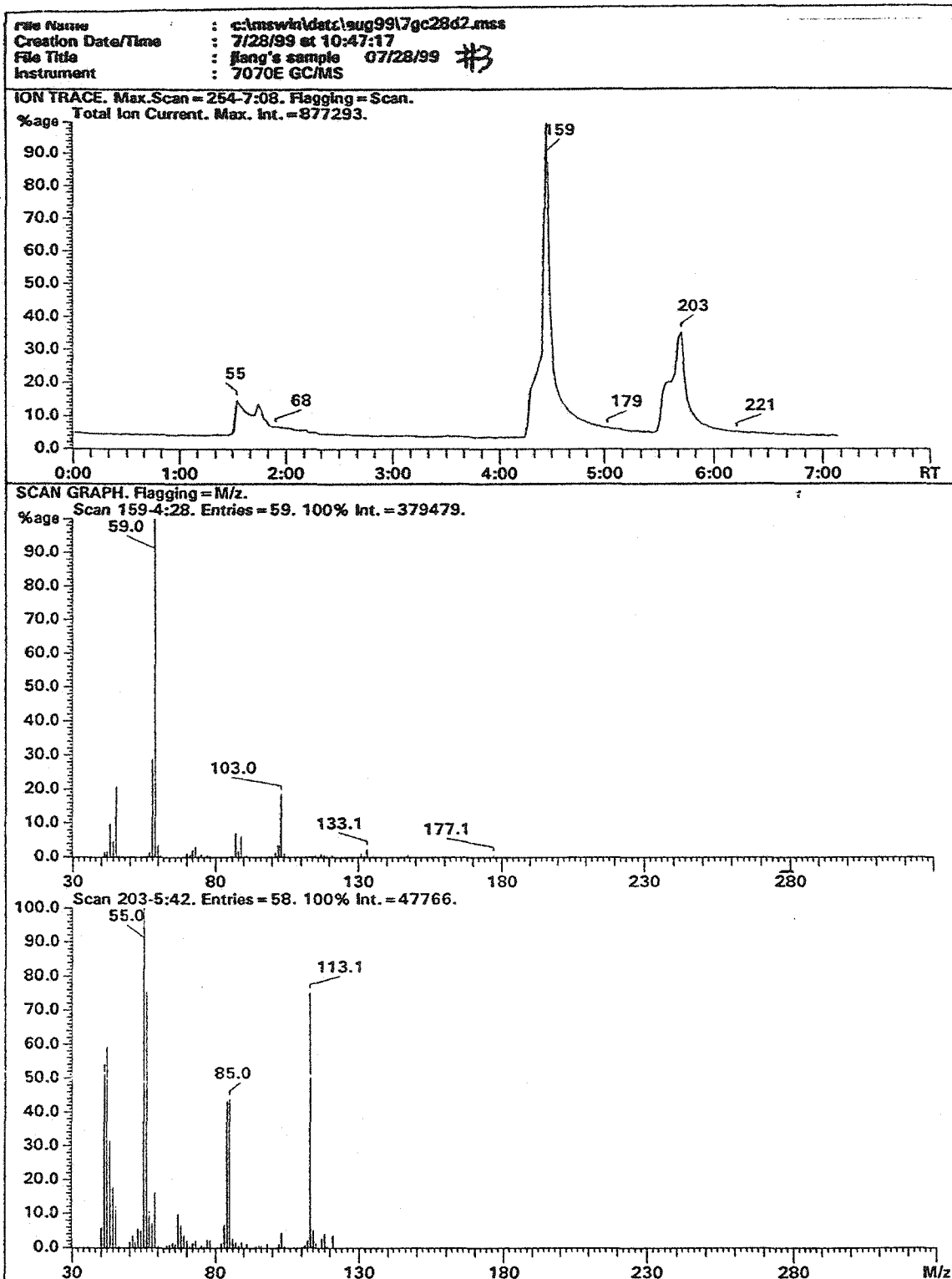


Figure B.4-(c2). GC-MS result for sample #3 (run2).

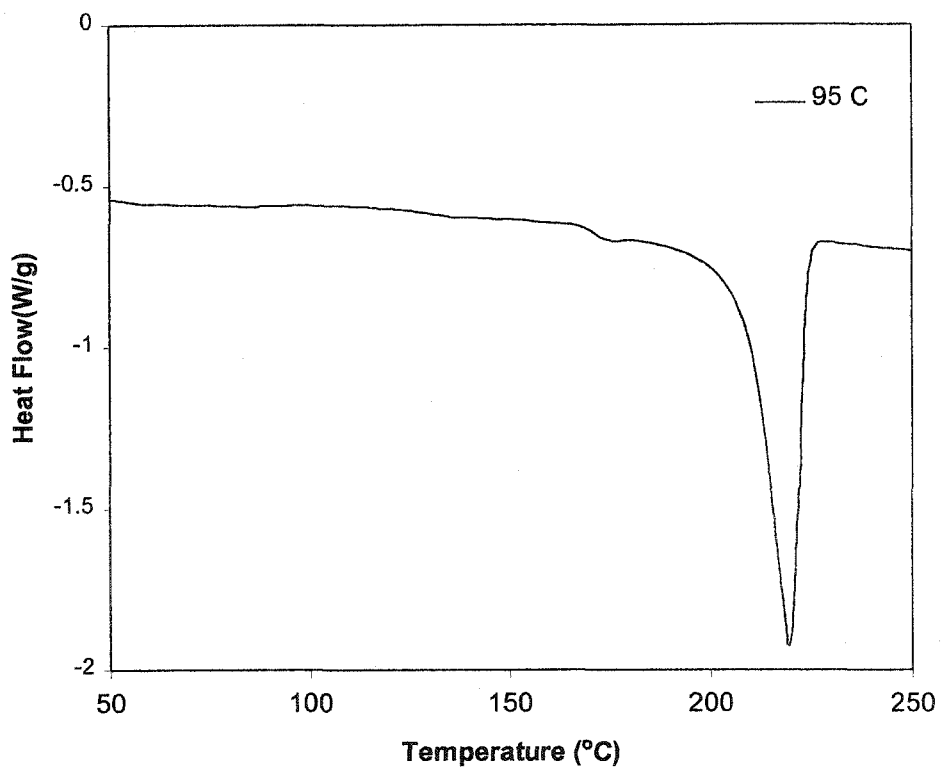


Figure B.5-(a). DSC thermogram for sample made at T_{oil} of 95°C
(10°C/min, first heating scan, nitrogen)

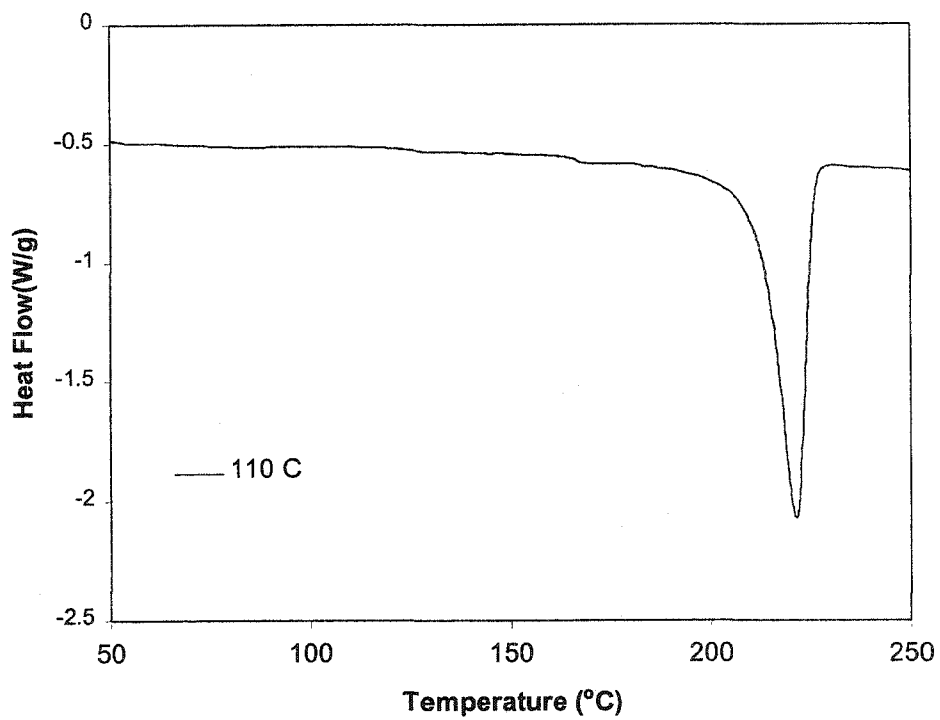


Figure B.5-(b). DSC thermogram for sample made at T_{oil} of 110°C
(10°C/min, first heating scan, nitrogen)

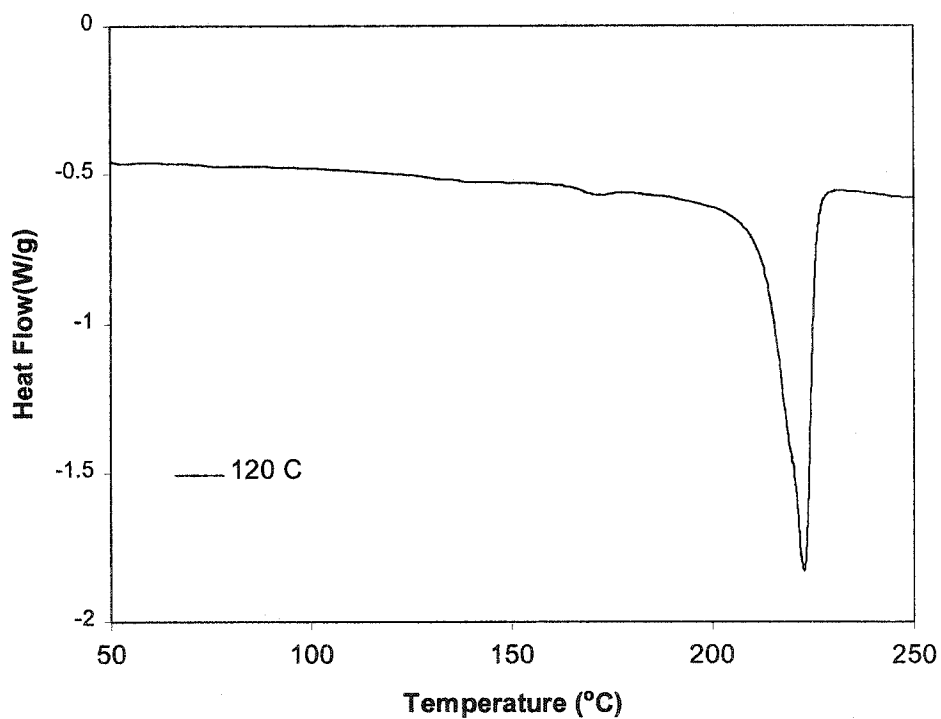


Figure B.5-(c). DSC thermogram for sample made at T_{oil} of 120°C (10°C/min, first heating scan, nitrogen)

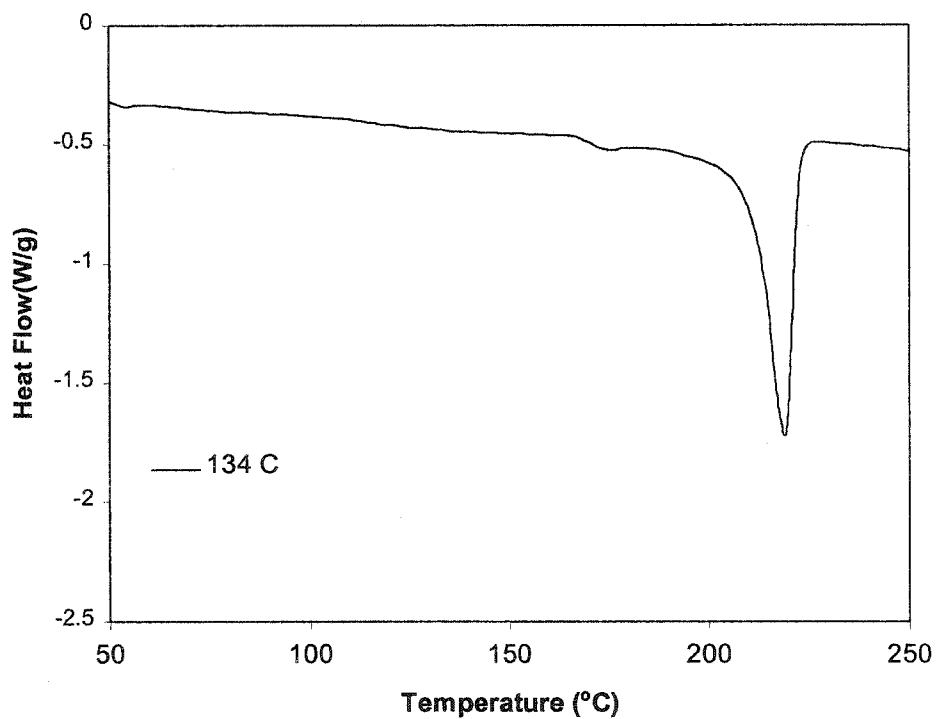


Figure B.5-(d). DSC thermogram for sample made at T_{oil} of 134°C
(10°C/min, first heating scan, nitrogen)

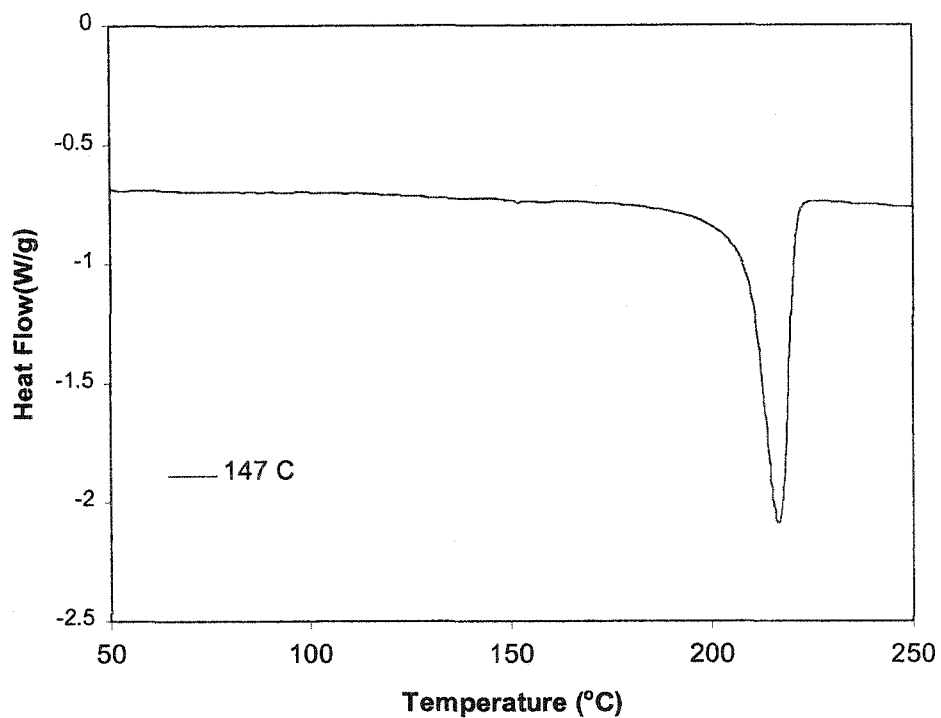


Figure B.5-(e). DSC thermogram for sample made at T_{oil} of 147°C
(10°C/min, first heating scan, nitrogen)

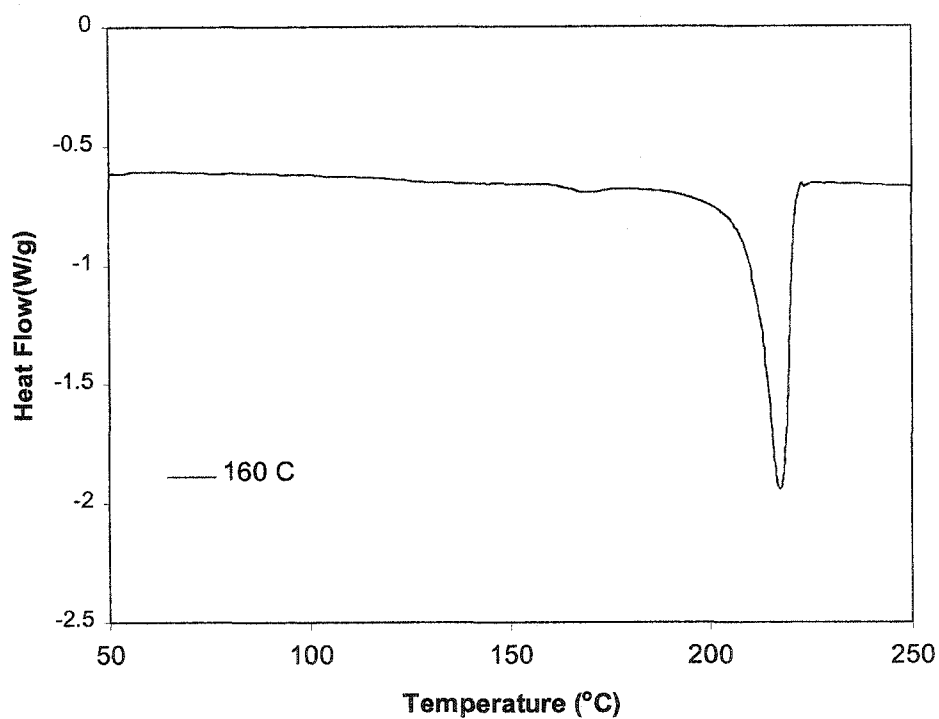


Figure B.5-(f). DSC thermogram for sample made at T_{oil} of 160°C (10°C/min, first heating scan, nitrogen)

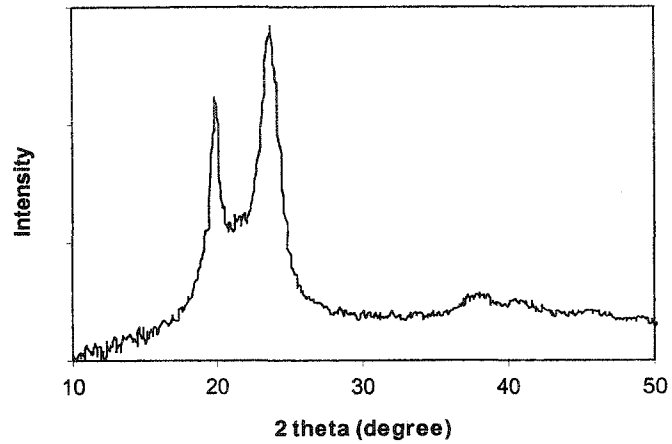


Figure B.6-(a) X-Ray diffraction pattern for sample made at oil bath temperature of 95°C.

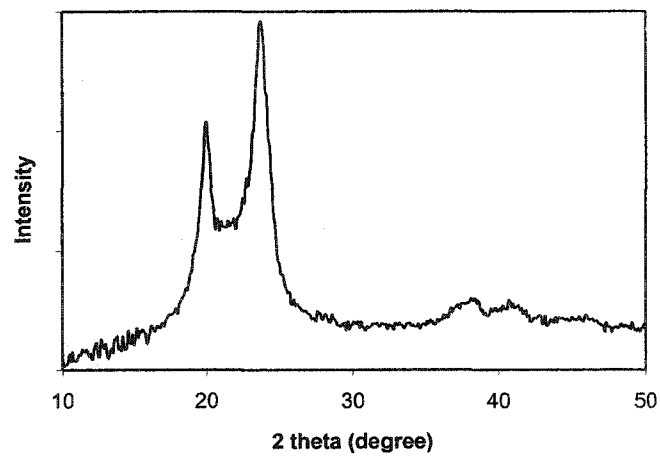


Figure B.6-(b) X-Ray diffraction pattern for sample made at oil bath temperature of 110°C.

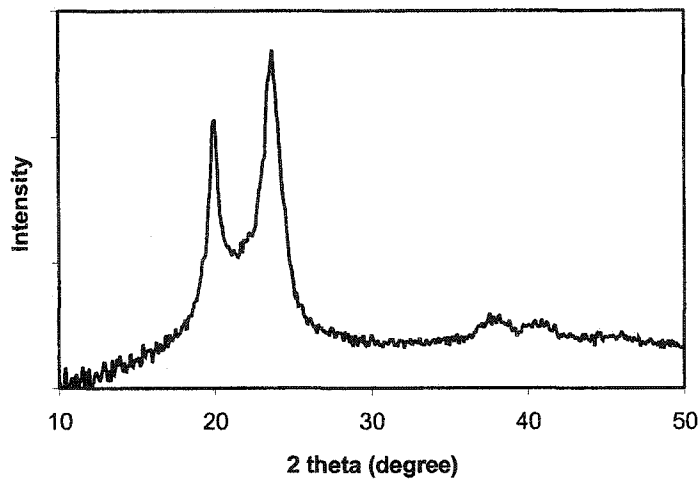


Figure B.6-(c) X-Ray diffraction pattern for sample made at oil bath temperature of 120°C.

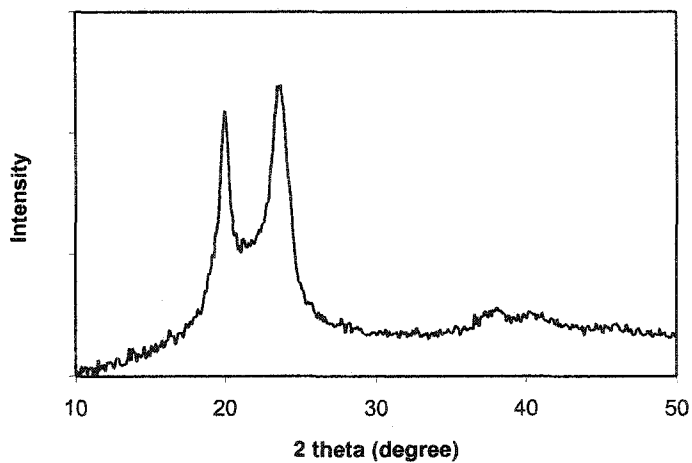


Figure B.6-(d) X-Ray diffraction pattern for sample made at oil bath temperature of 134°C.

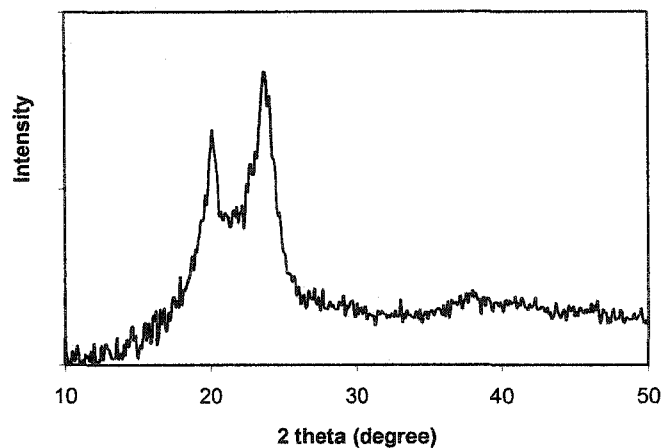


Figure B.6-(e) X-Ray diffraction pattern for sample made at oil bath temperature of 147°C.

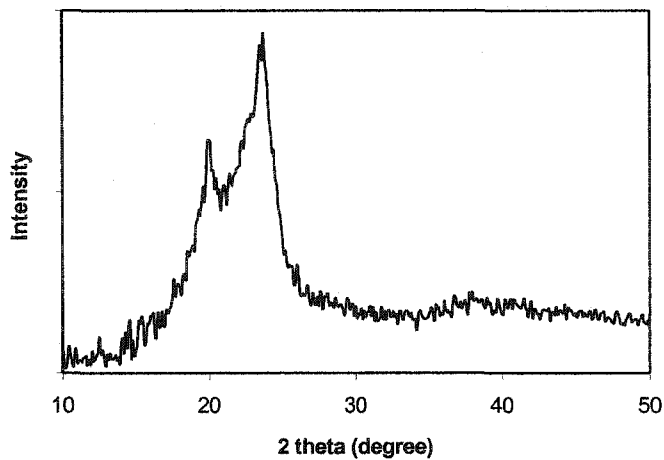


Figure B.6-(f) X-Ray diffraction pattern for sample made at oil bath temperature of 160°C.

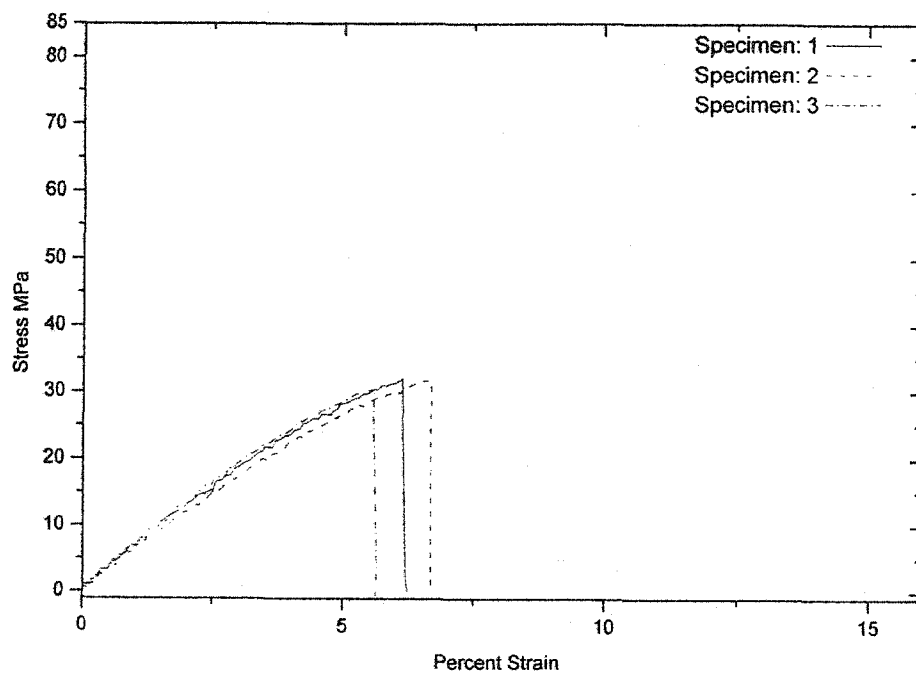


Figure B.7-(a). Tensile test results for "dry" specimens from sample made at 95°C.
 (75g ϵ -caprolactam/0.75 polycarbonate(SPP)/10mmol isobutyl magnesium chloride)

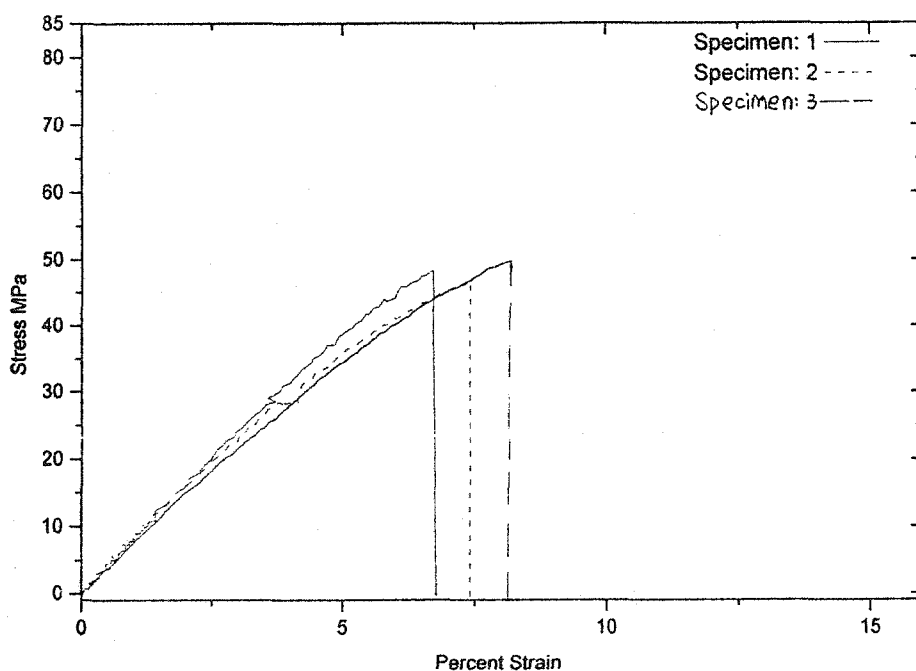


Figure B.7-(b). Tensile test results for "dry" specimens from sample made at 110°C.
 (75g ϵ -caprolactam/0.75 polycarbonate(SPP)/10mmol isobutyl magnesium chloride)

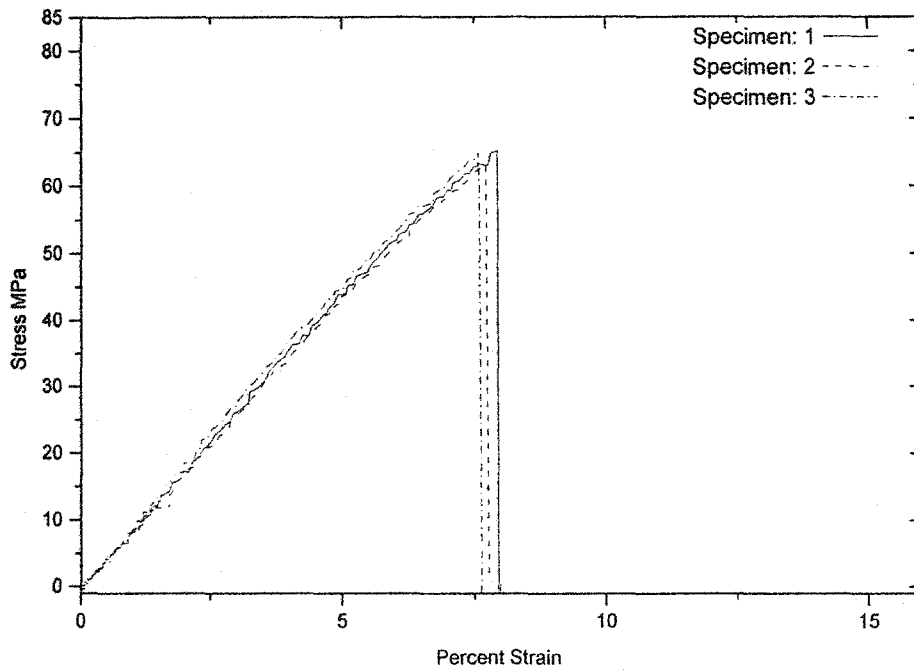


Figure B.7-(c). Tensile test results for "dry" specimens from sample made at 120°C.
 (75g ϵ -caprolactam/0.75 polycarbonate(SPP)/10mmol isobutyl magnesium chloride)

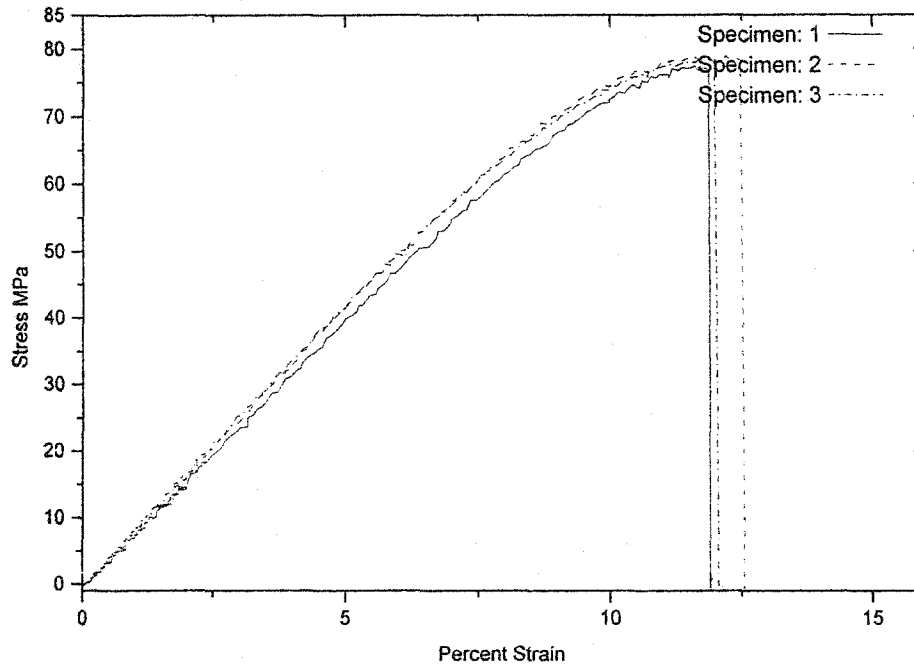


Figure B.7-(d). Tensile test results for "dry" specimens from sample made at 134°C.
 (75g ϵ -caprolactam/0.75 polycarbonate(SPP)/10mmol isobutyl magnesium chloride)

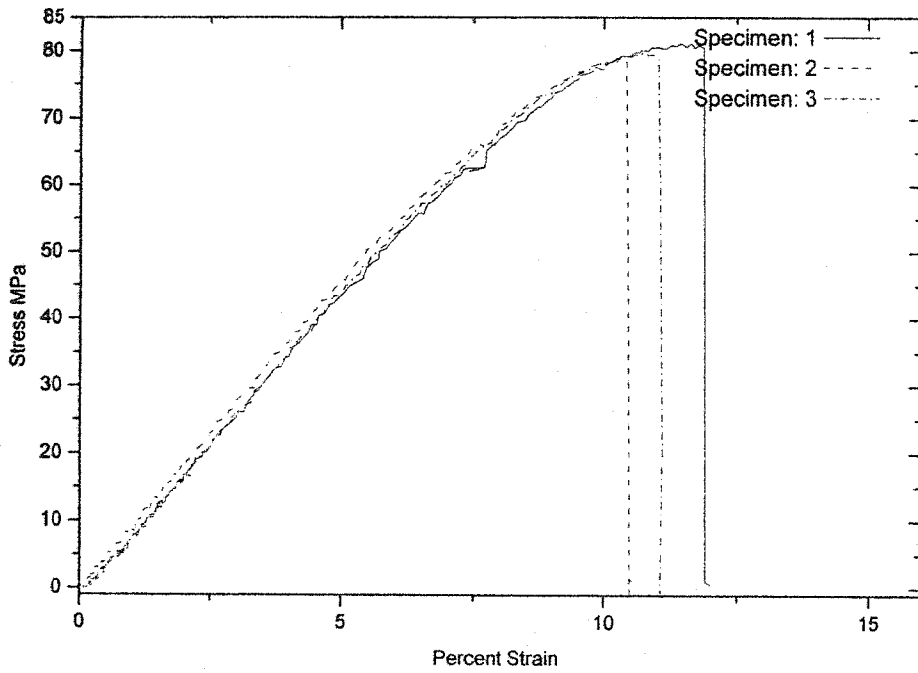


Figure B.7-(e). Tensile test results for "dry" specimens from sample made at 147°C.
 (75g ϵ -caprolactam/0.75 polycarbonate(SPP)/10mmol isobutyl magnesium chloride)

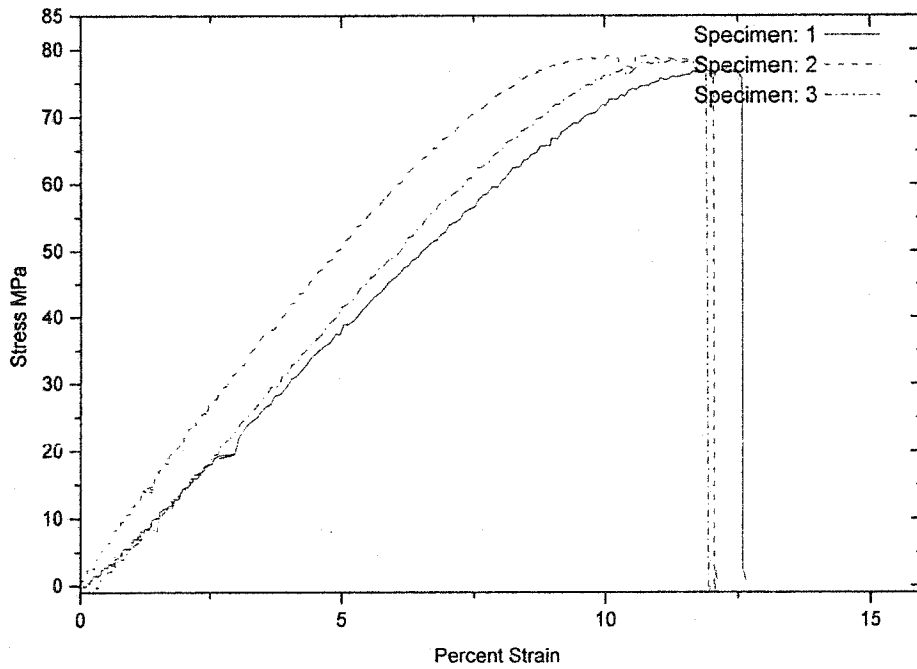


Figure B.7-(f). Tensile test results for "dry" specimens from sample made at 160°C.
 (75g ϵ -caprolactam/0.75 polycarbonate(SPP)/10mmol isobutyl magnesium chloride)

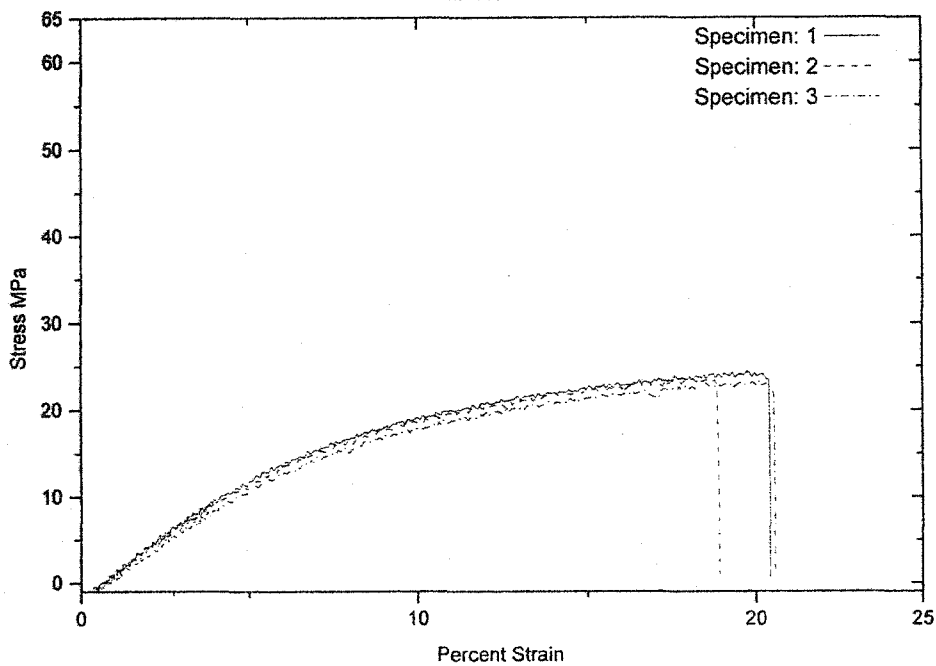


Figure B.8-(a). Tensile test results for "wet" specimens from sample made at 95°C.
 (75g ϵ -caprolactam/0.75 polycarbonate(SPP)/10mmol isobutyl magnesium chloride)

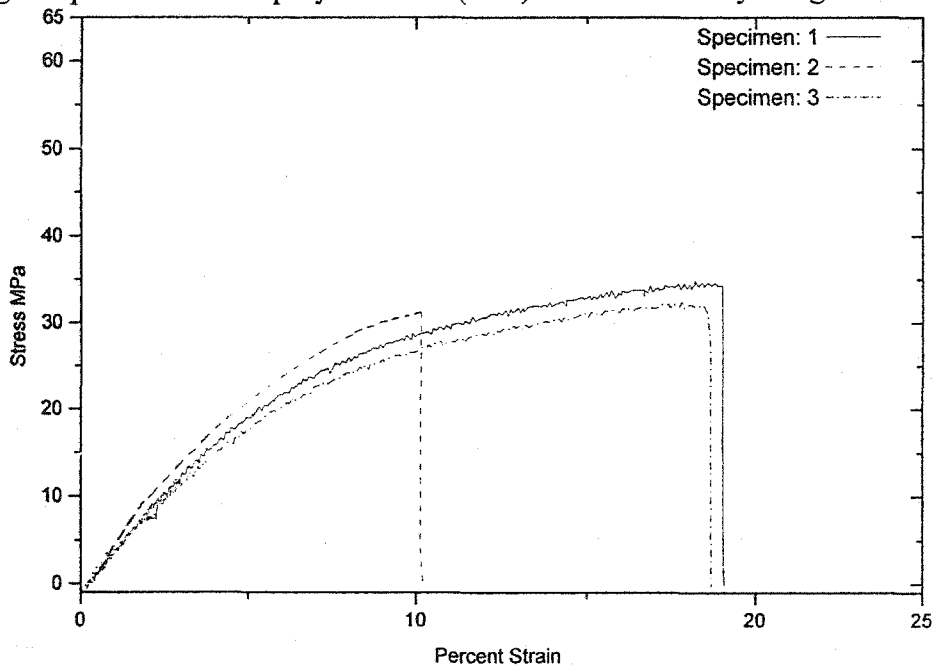


Figure B.8-(b). Tensile test results for "wet" specimens from sample made at 110°C.
 (75g ϵ -caprolactam/0.75 polycarbonate(SPP)/10mmol isobutyl magnesium chloride)

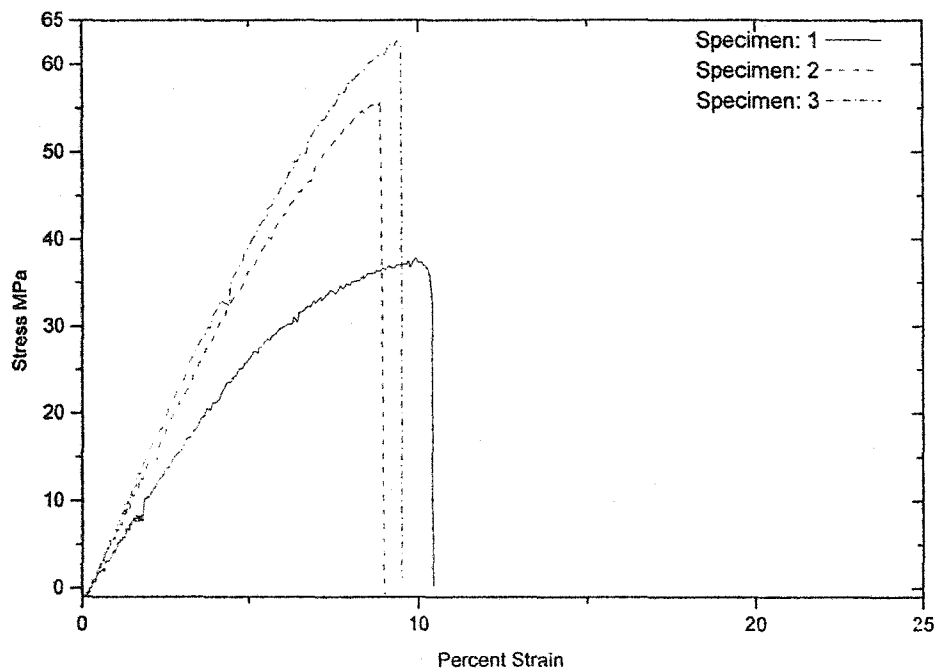


Figure B.8-(c). Tensile test results for "wet" specimens from sample made at 120°C.
 (75g ϵ -caprolactam/0.75 polycarbonate(SPP)/10mmol isobutyl magnesium chloride)

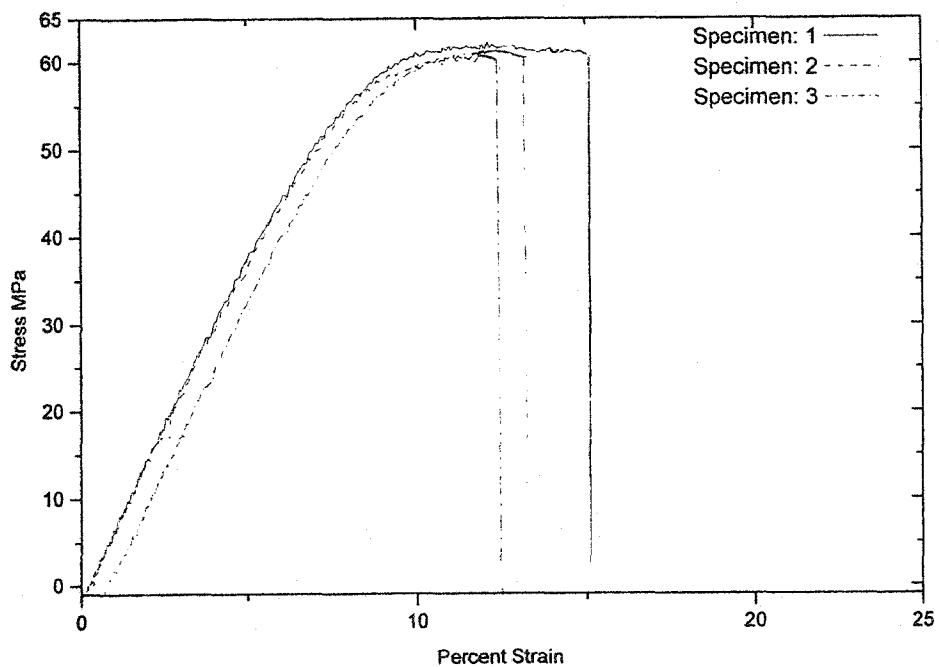


Figure B.8-(d). Tensile test results for "wet" specimens from sample made at 134°C.
 (75g ϵ -caprolactam/0.75 polycarbonate(SPP)/10mmol isobutyl magnesium chloride)

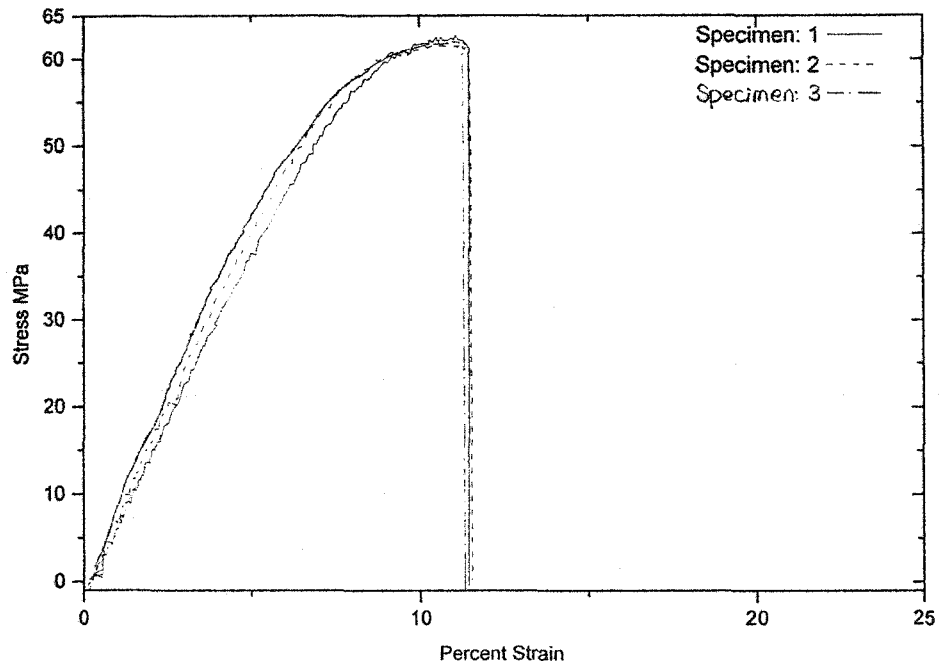


Figure B.8-(e). Tensile test results for "wet" specimens from sample made at 147°C.
 (75g ϵ -caprolactam/0.75 polycarbonate(SPP)/10mmol isobutyl magnesium chloride)

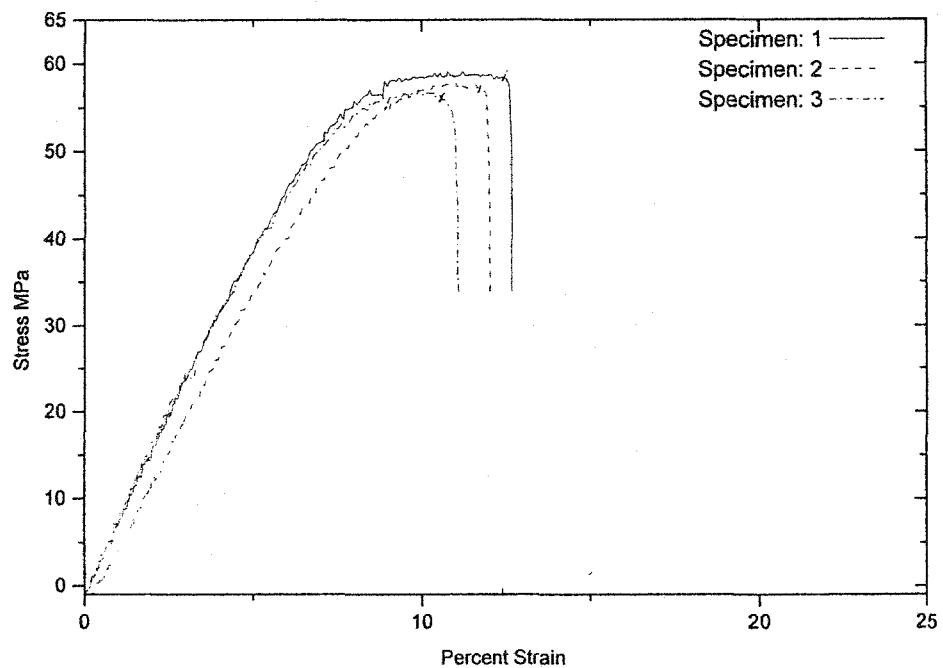


Figure B.8-(f). Tensile test results for "wet" specimens from sample made at 160°C.
 (75g ϵ -caprolactam/0.75 polycarbonate(SPP)/10mmol isobutyl magnesium chloride)

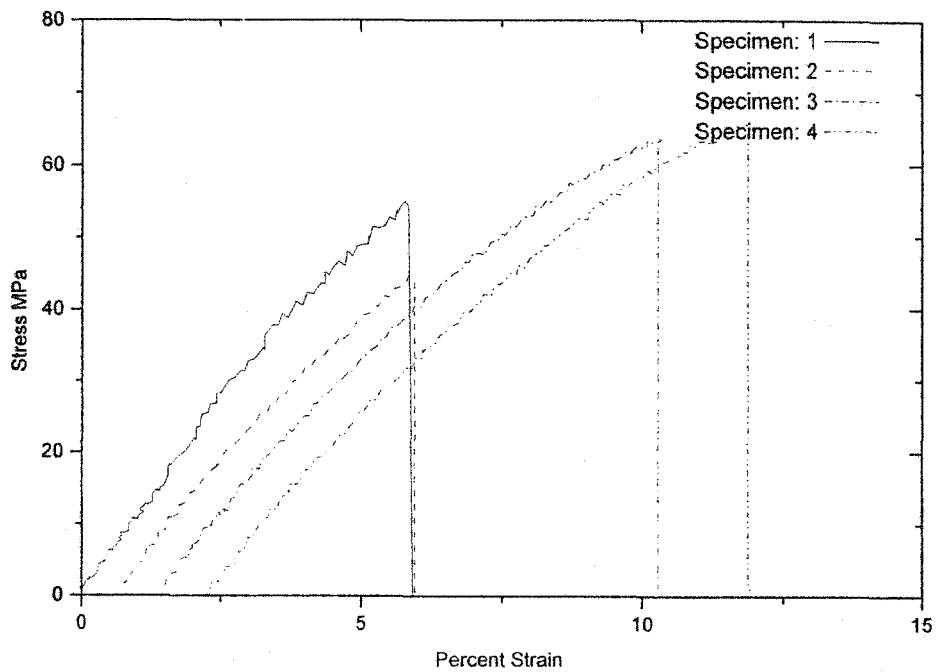


Figure B.9-(a). Tensile test results for "dry" specimens from sample made at 106°C.
 (75g ϵ -caprolactam/0.75 polycarbonate(SPP)/12mmol isobutyl magnesium bromide)

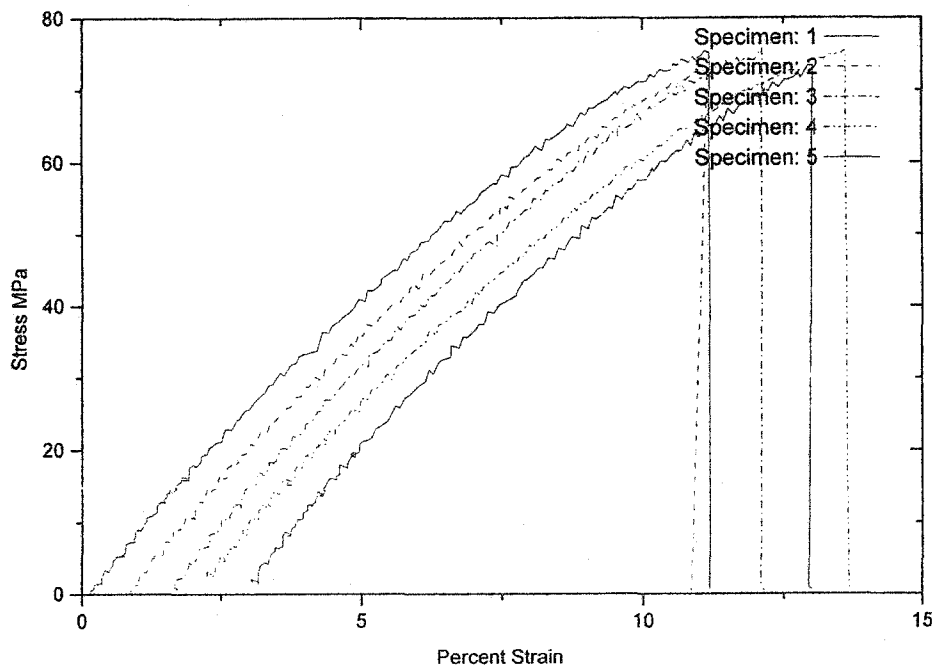


Figure B.9-(b). Tensile test results for "dry" specimens from sample made at 126°C.
 (75g ϵ -caprolactam/0.75 polycarbonate(SPP)/12mmol isobutyl magnesium bromide)

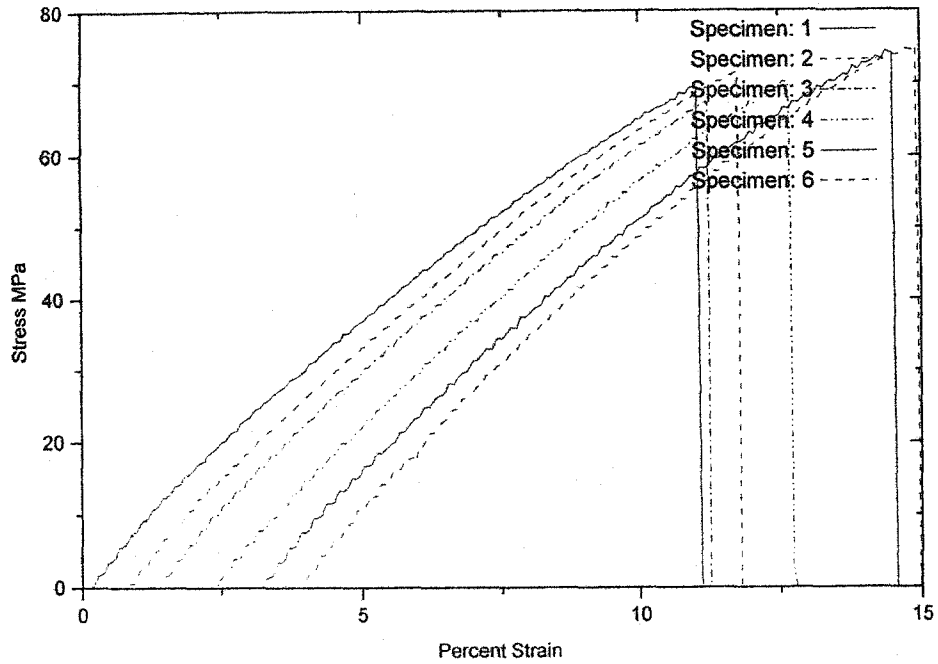


Figure B.9-(c). Tensile test results for "dry" specimens from sample made at 146°C.
 (75g ϵ -caprolactam/0.75 polycarbonate(SPP)/12mmol isobutyl magnesium bromide)

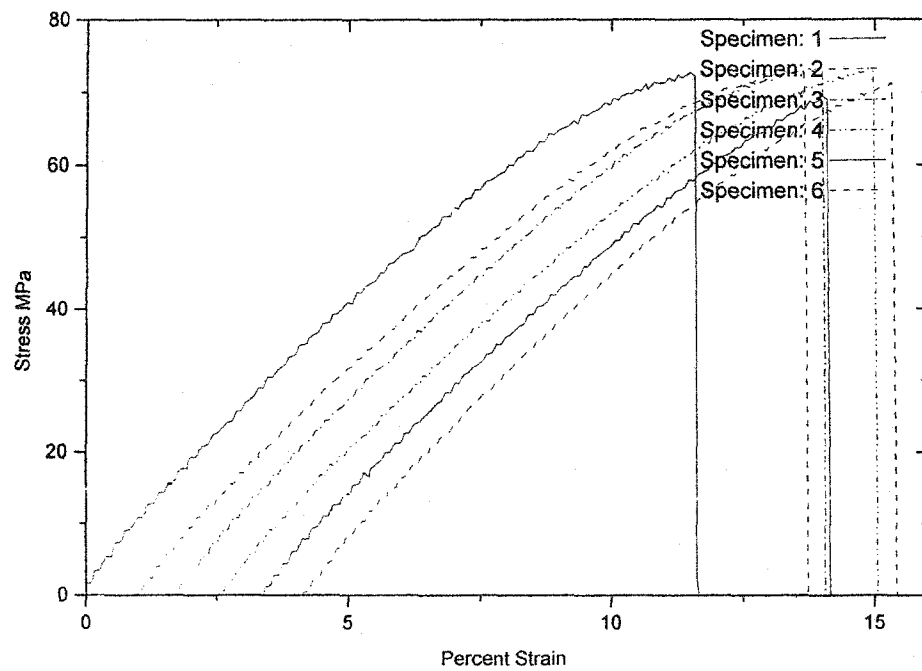


Figure B.9-(d). Tensile test results for "dry" specimens from sample made at 164°C.
 (75g ϵ -caprolactam/0.75 polycarbonate(SPP)/12mmol isobutyl magnesium bromide)

Appendix C Supplement to Chapter 6

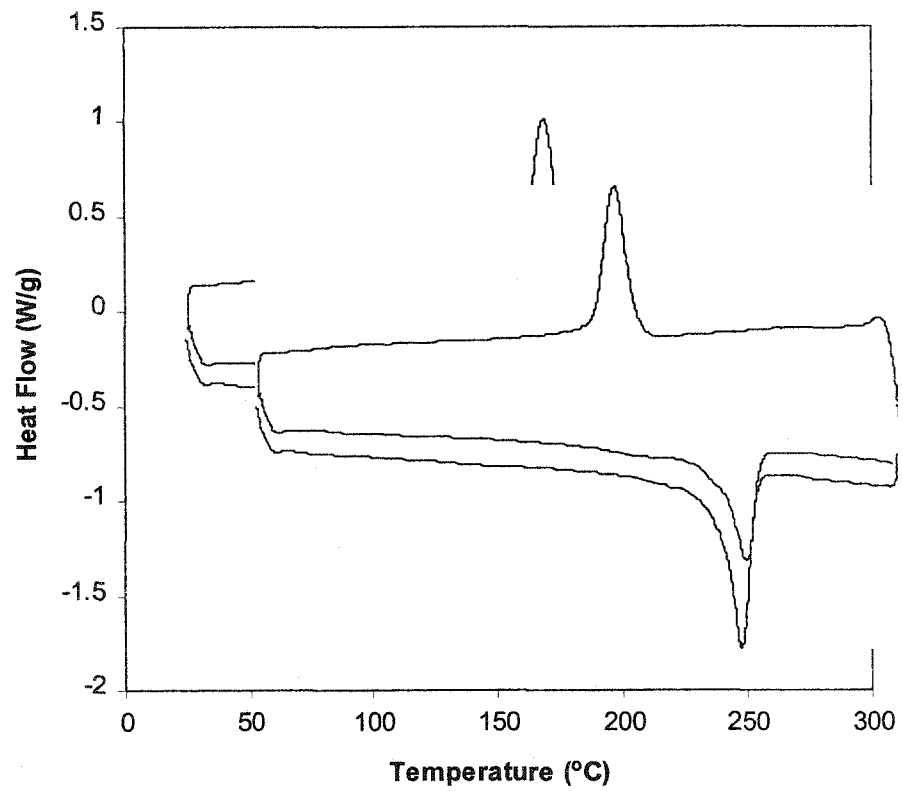


Figure C.1-(a). DSC thermogram for pure nylon 6 made from 0.2% wt DPC (10°C/min, nitrogen)

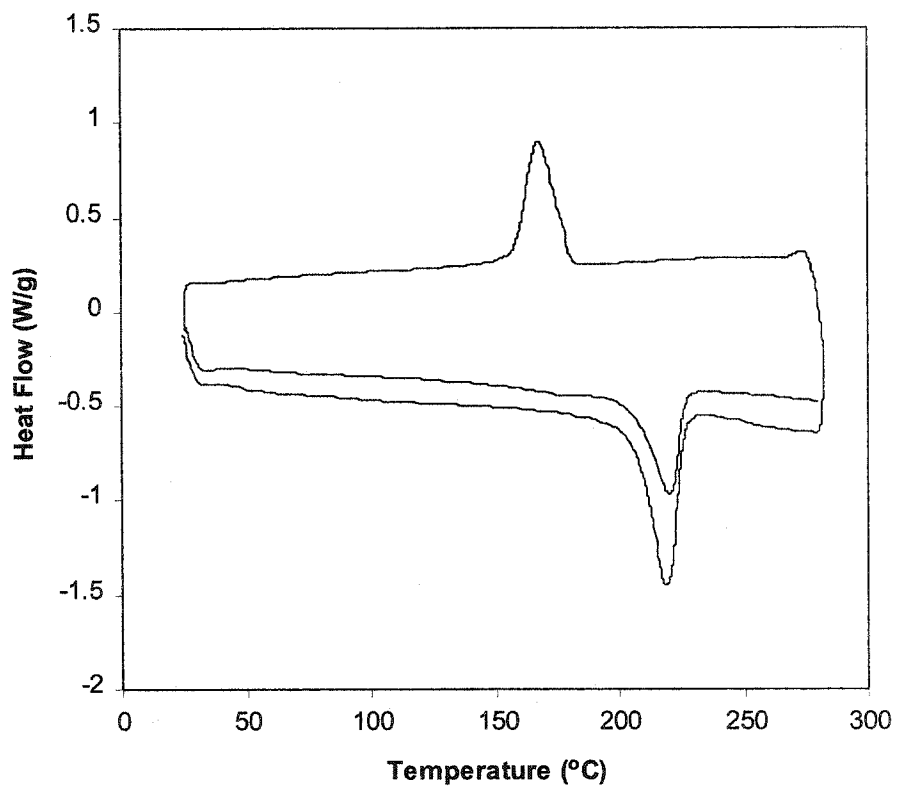


Figure C.1-(b). DSC thermogram for pure nylon 6 made from 1% wt DPC
(10°C/min, nitrogen)

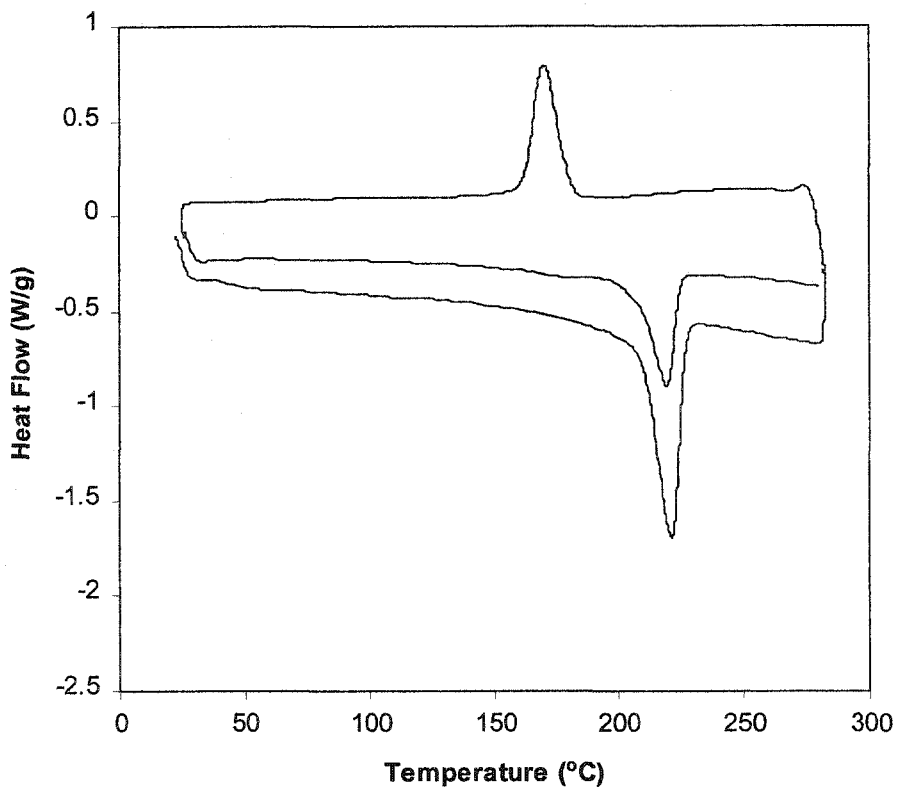


Figure C.1-(c). DSC thermogram for pure nylon 6 made from 2% wt DPC
(10°C/min, nitrogen)

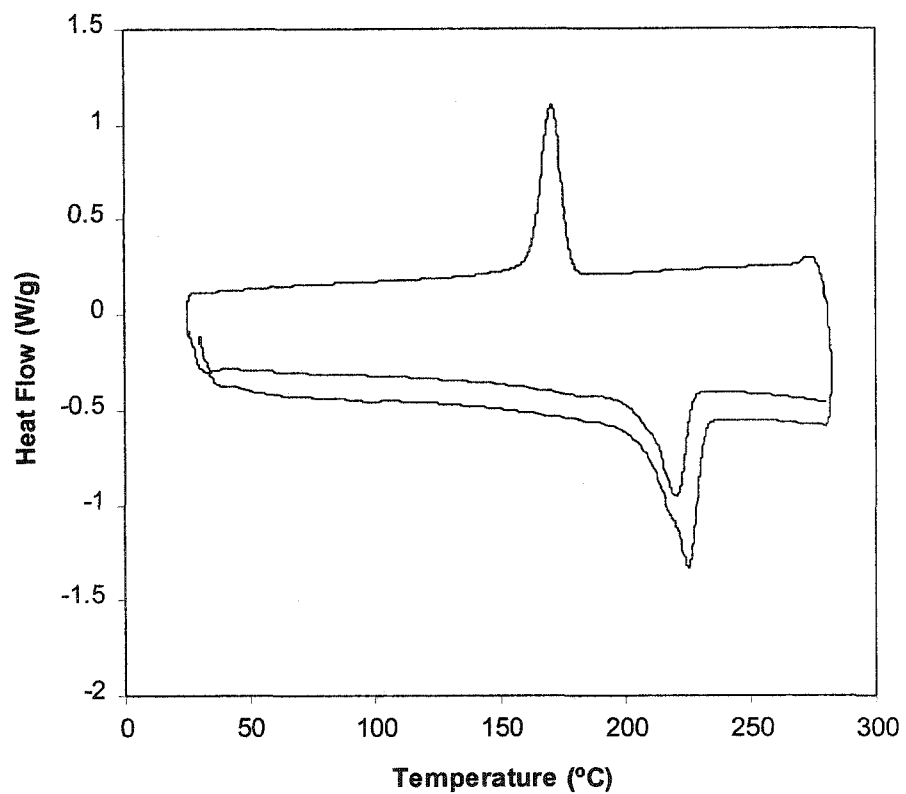


Figure C.1-(d). DSC thermogram for copolymer made from 0.2% wt GE-S11AP (with iso-Bu-MgBr). (10°C/min, nitrogen)

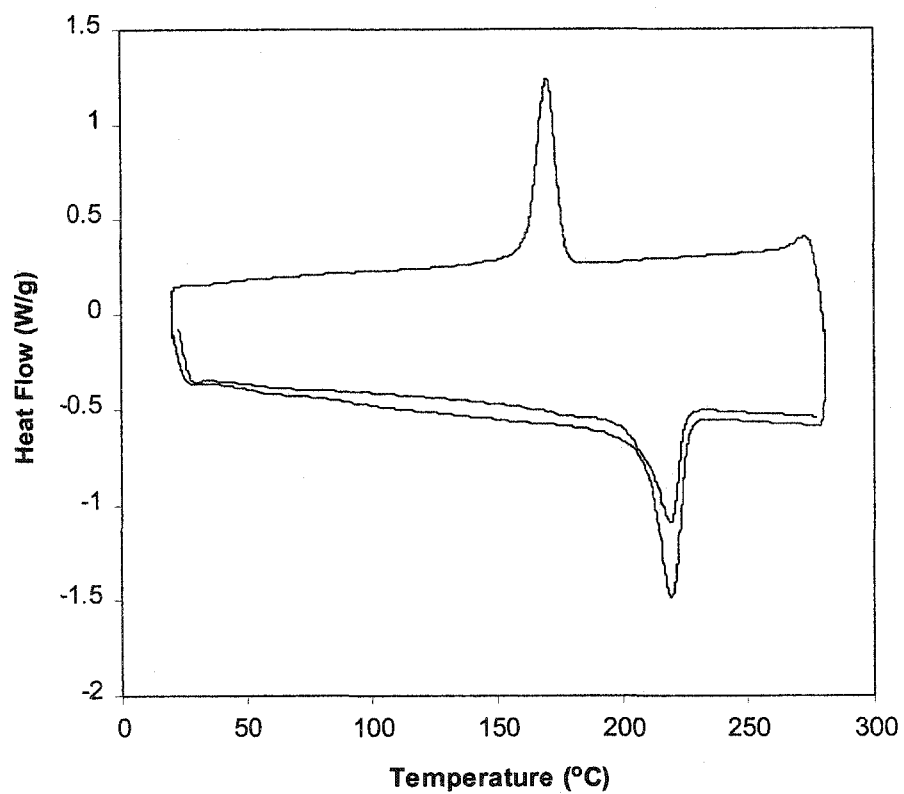


Figure C.1-(e). DSC thermogram for copolymer made from 1% wt GE-S11AP (with iso-Bu-MgBr). (10°C/min, nitrogen)

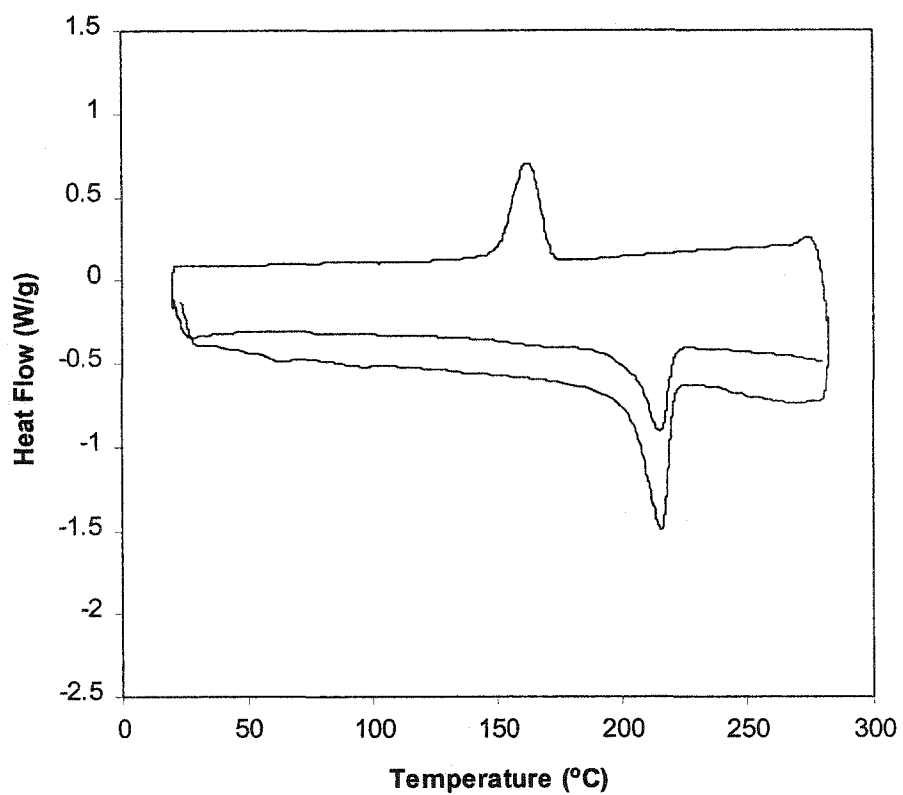


Figure C.1-(f). DSC thermogram for copolymer made from 2% wt GE-S11AP (with iso-Bu-MgBr). (10°C/min, nitrogen)

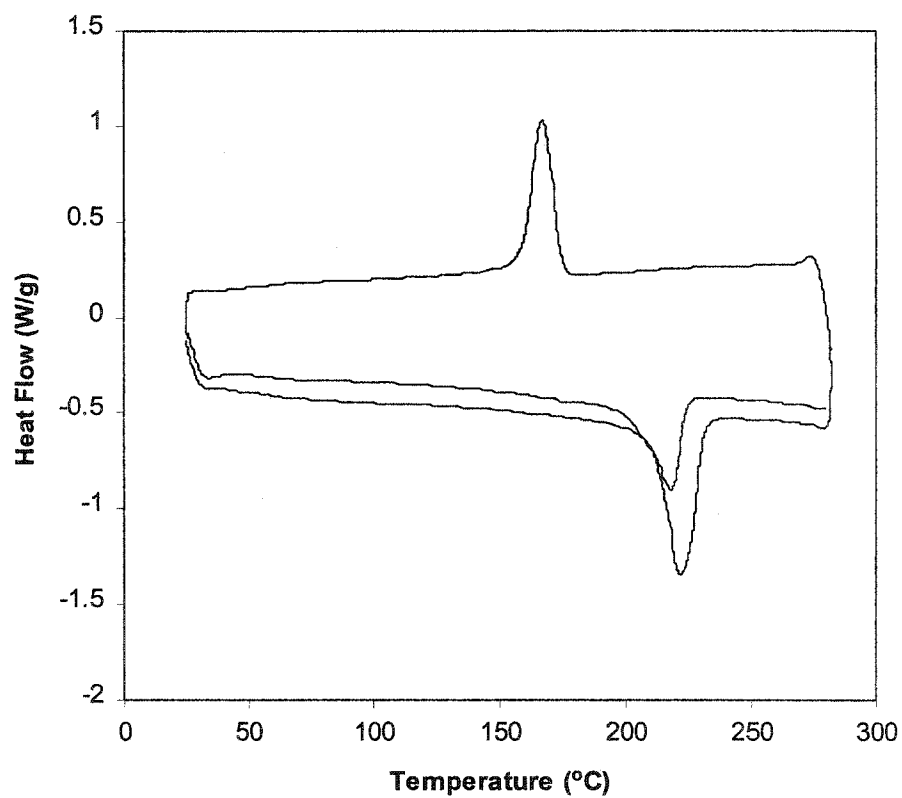


Figure C.1-(g). DSC thermogram for copolymer made from 0.2% wt GE-S11AP (with iso-Bu-MgCl). (10°C/min, nitrogen)

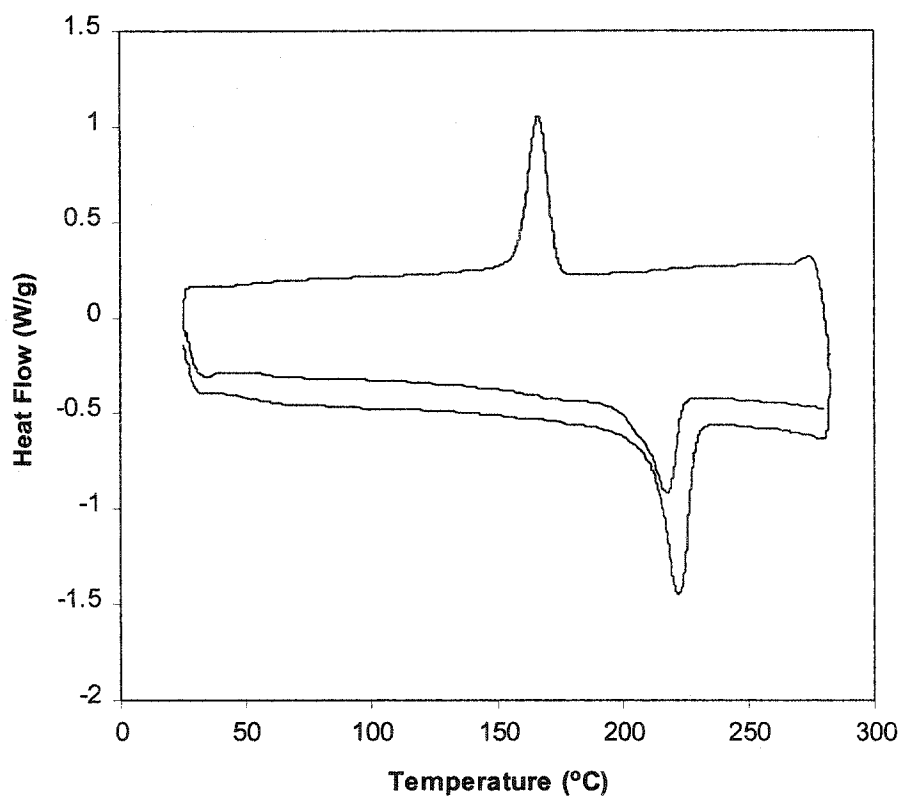


Figure C.1-(h). DSC thermogram for copolymer made from 1% wt GE-S11AP (with iso-Bu-MgCl). (10°C/min, nitrogen)

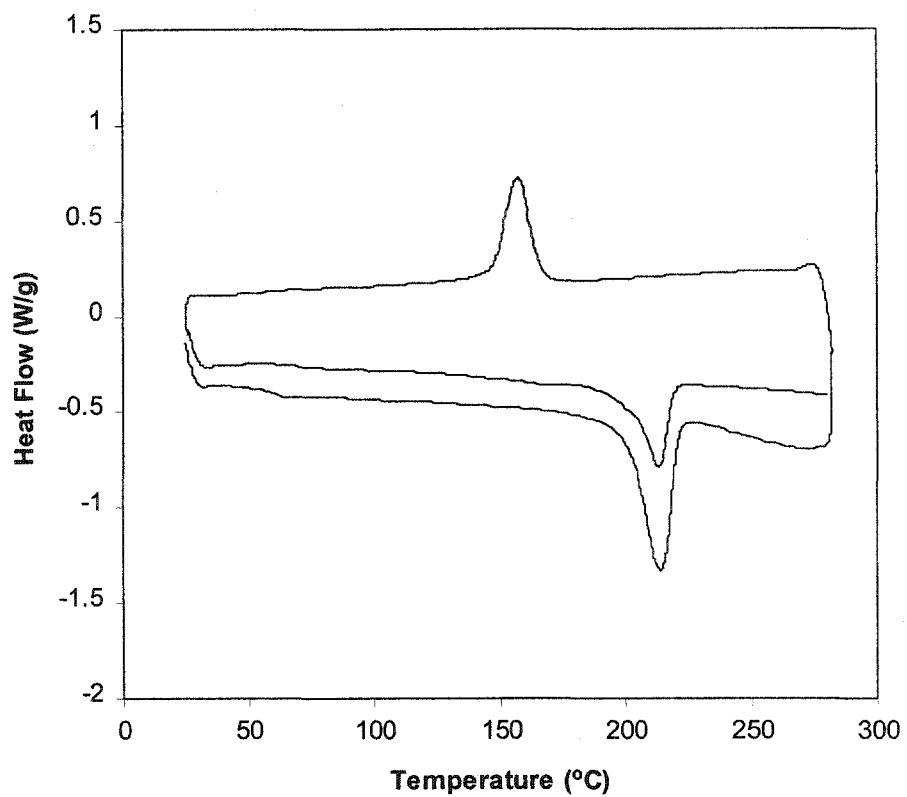


Figure C.1-(i). DSC thermogram for copolymer made from 2% wt GE-S11AP (with iso-Bu-MgCl). (10°C/min, nitrogen)

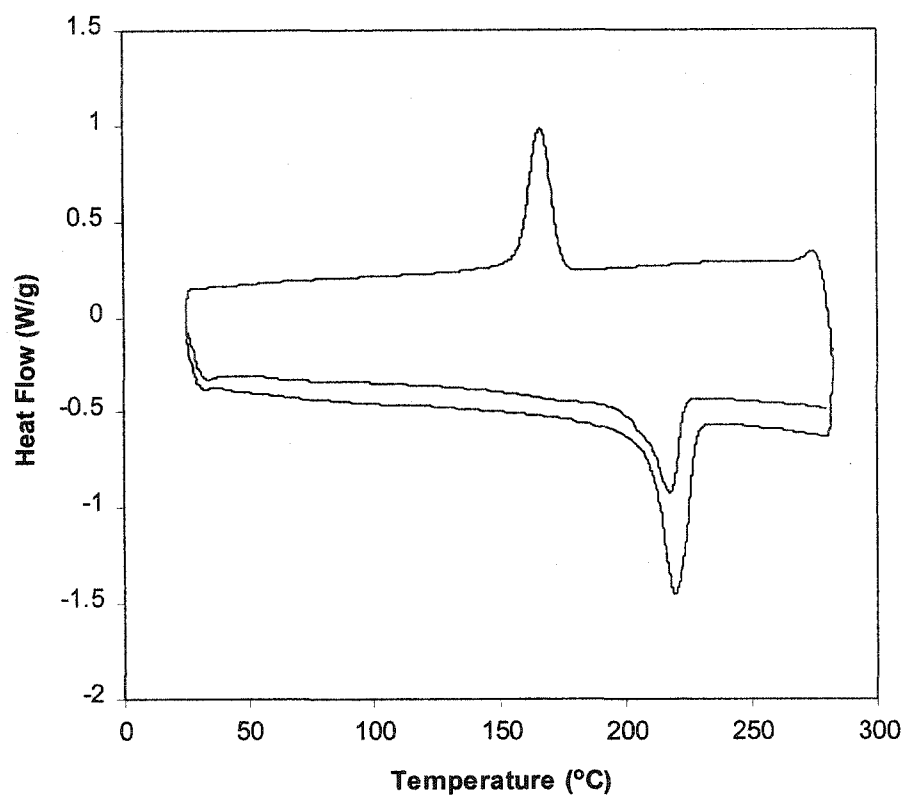


Figure C.1-(j). DSC thermogram for copolymer made from 0.2% wt GE-S3G100 (with iso-Bu-MgCl). (10°C/min, nitrogen)

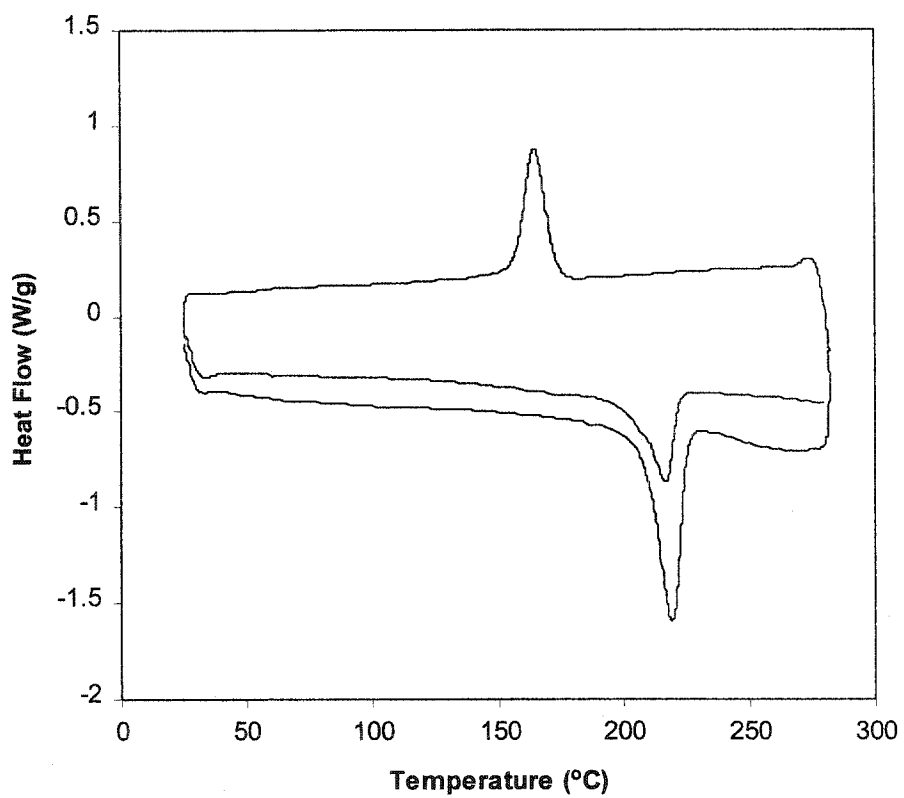


Figure C.1-(k). DSC thermogram for copolymer made from 1% wt GE-S3G100 (with iso-Bu-MgCl). (10°C/min, nitrogen)

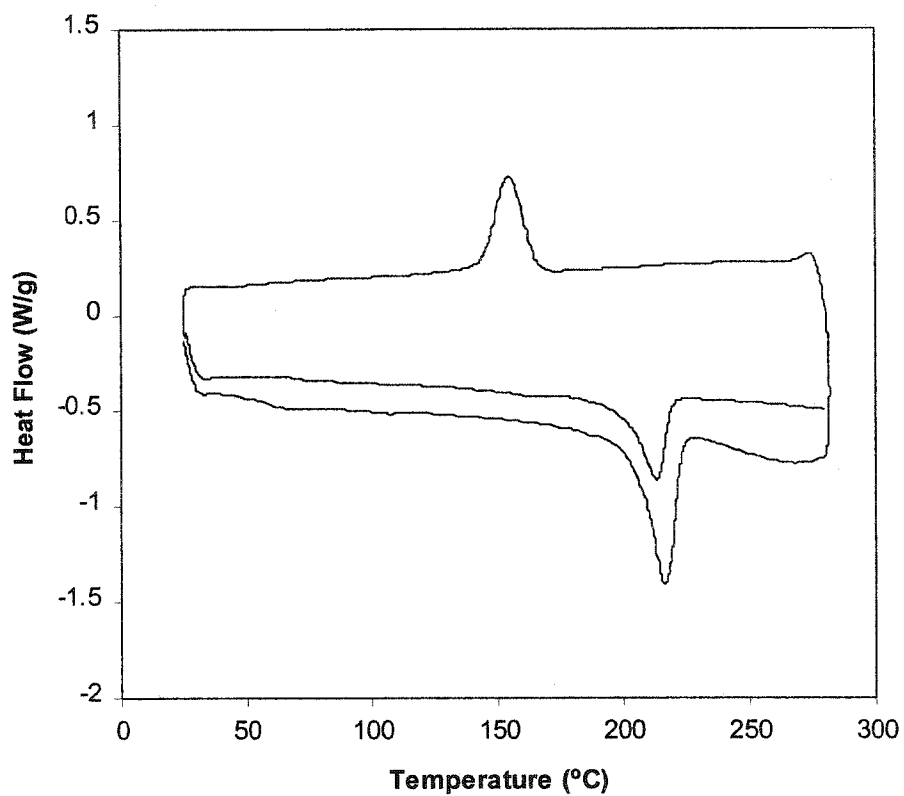


Figure C.1-(l). DSC thermogram for copolymer made from 2% wt GE-S3G100 (with iso-Bu-MgCl). (10°C/min, nitrogen)

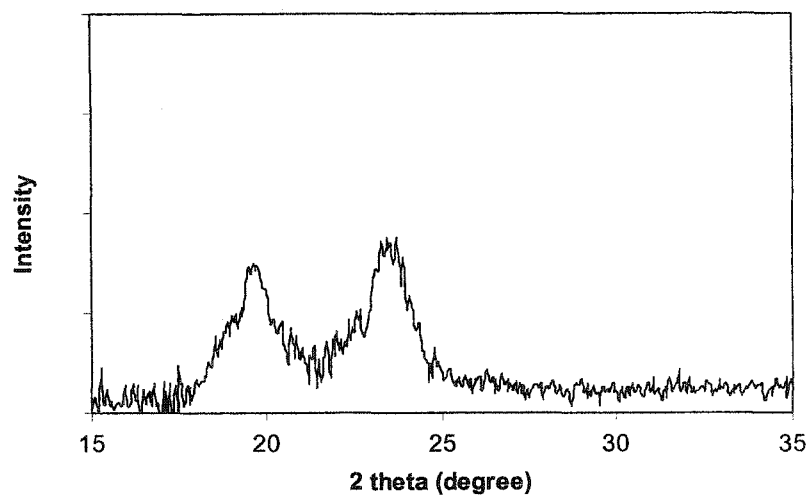


Figure C.2-(a) X-Ray diffraction pattern for copolymer made from 0.2%wt GE-S11AP (with iso-Bu-MgBr).

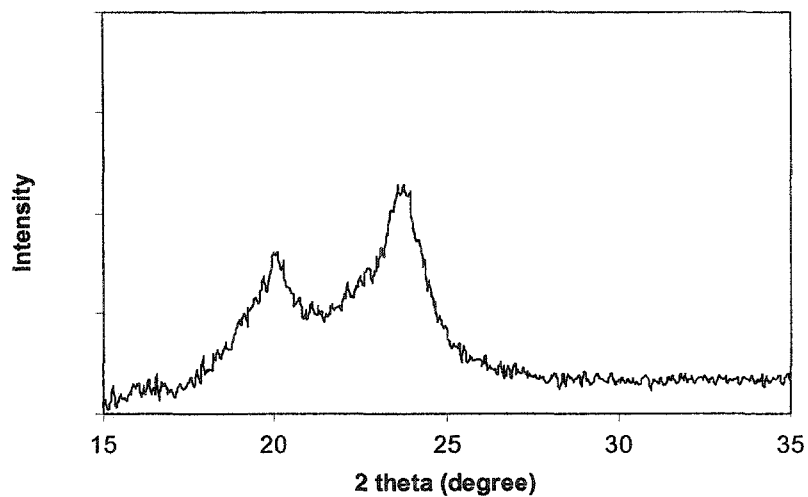


Figure C.2-(b) X-Ray diffraction pattern for copolymer made from 1%wt GE-S11AP (with iso-Bu-MgBr).

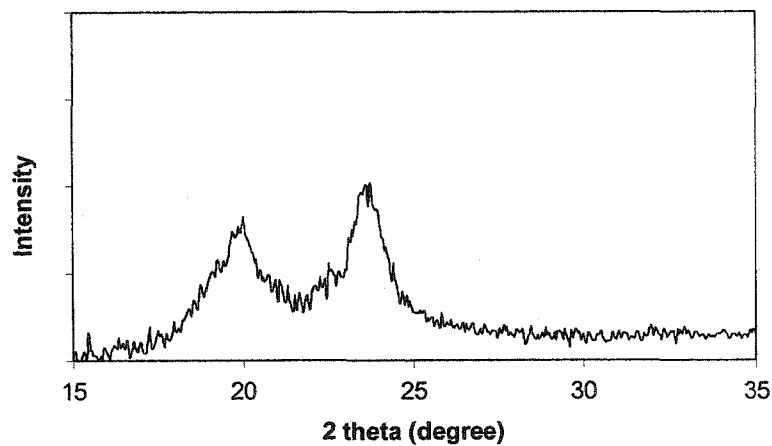


Figure C.2-(c) X-Ray diffraction pattern for copolymer made from 2%wt GE-S11AP (with iso-Bu-MgBr).

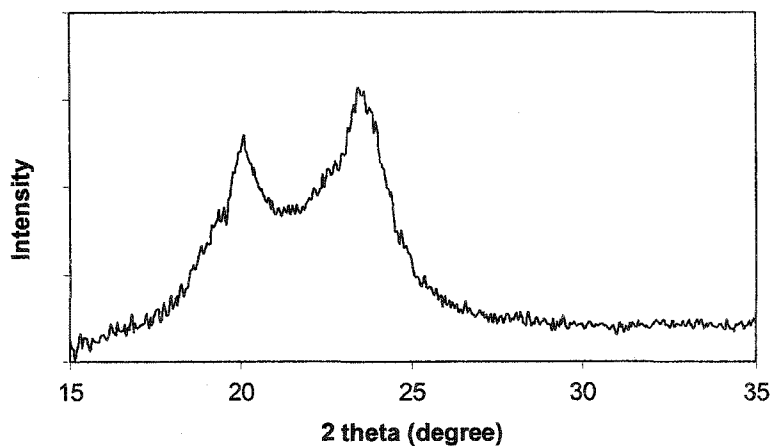


Figure C.2-(d) X-Ray diffraction pattern for copolymer made from 0.2%wt GE-S11AP (with iso-Bu-MgCl).

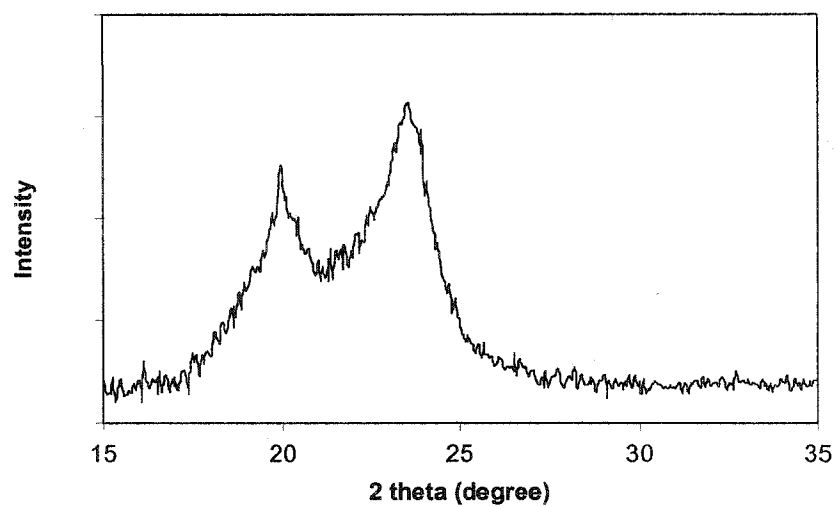


Figure C.2-(e) X-Ray diffraction pattern for copolymer made from 1%wt GE-S11AP (with iso-Bu-MgCl).

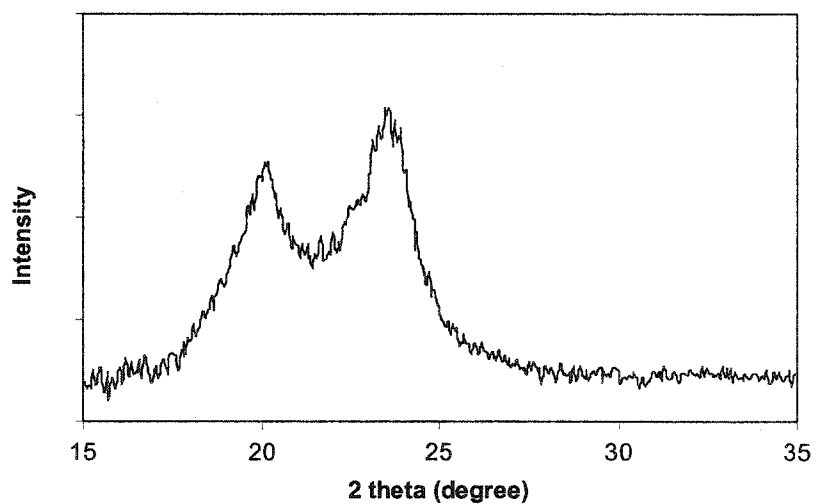


Figure C.2-(f) X-Ray diffraction pattern for copolymer made from 2%wt GE-S11AP (with iso-Bu-MgCl).

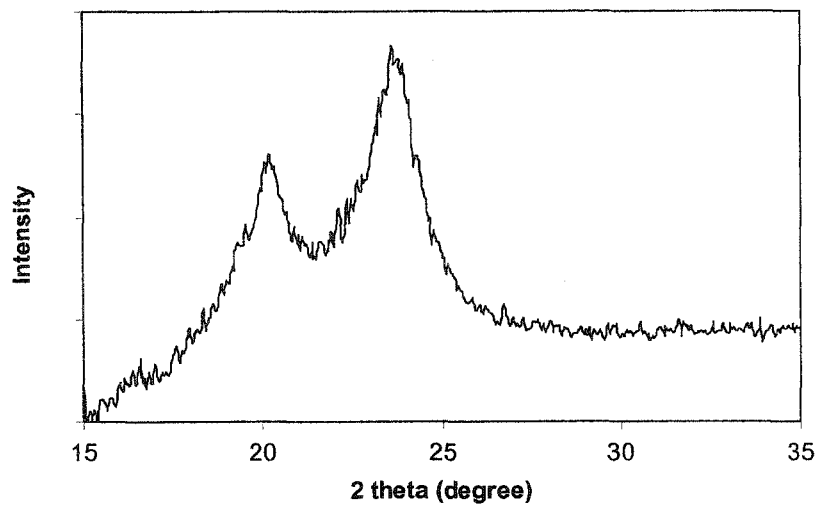


Figure C.2-(g) X-Ray diffraction pattern for copolymer made from 0.2%wt GE-S3G100 (with iso-Bu-MgCl).

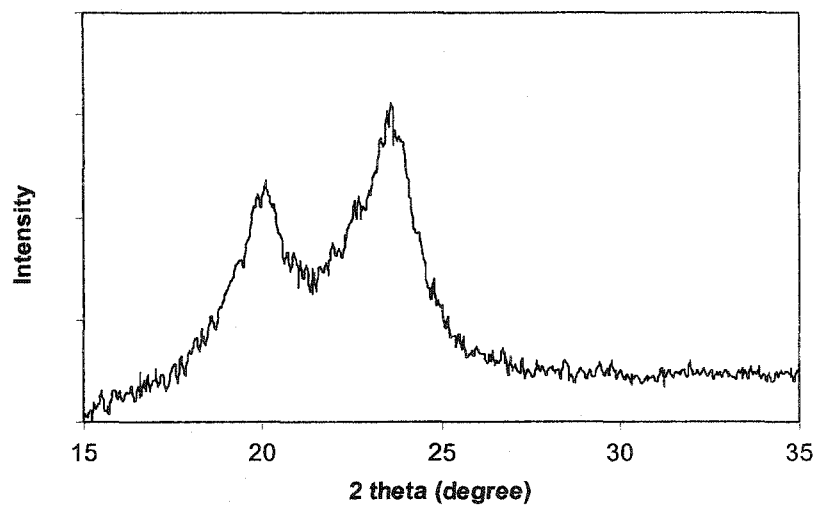


Figure C.2-(h) X-Ray diffraction pattern for copolymer made from 1%wt GE-S3G100 (with iso-Bu-MgCl).

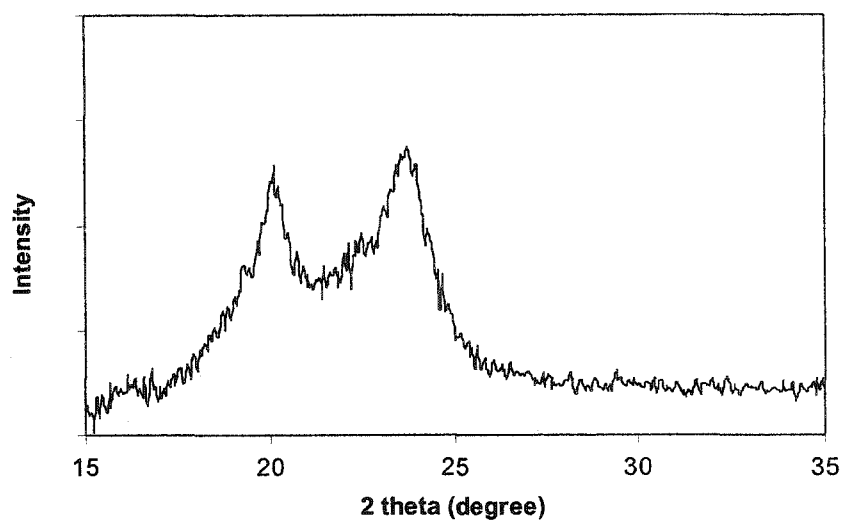
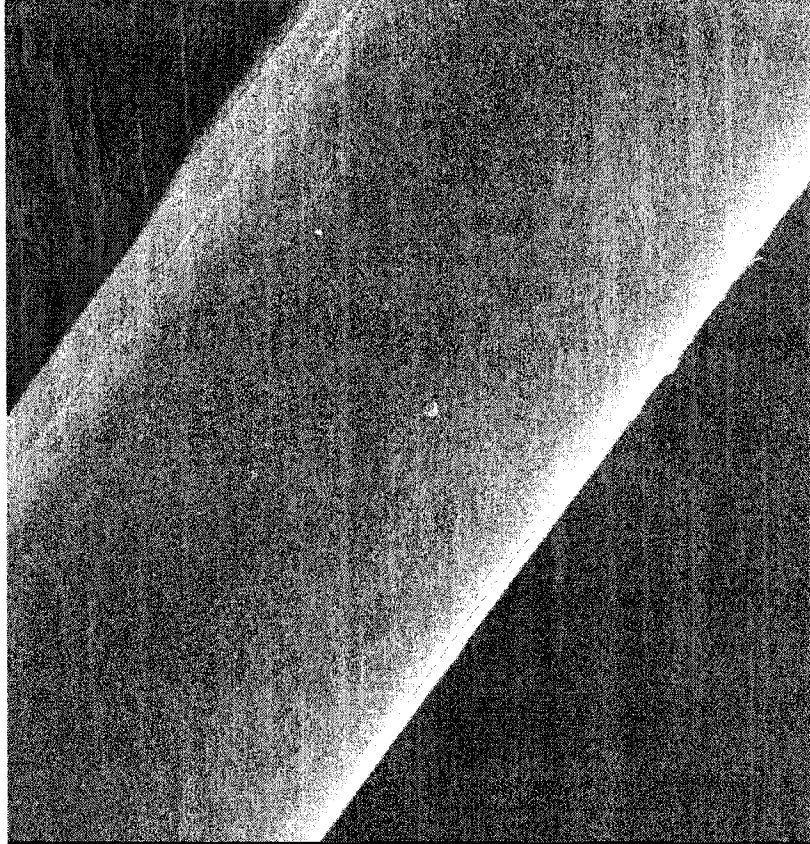


Figure C.2-(i) X-Ray diffraction pattern for copolymer made from 2%wt GE-S3G100 (with iso-Bu-MgCl).

Appendix D Supplement to Chapter 7



1 μm
—

Figure D.1 SEM image of bare glass fibre.

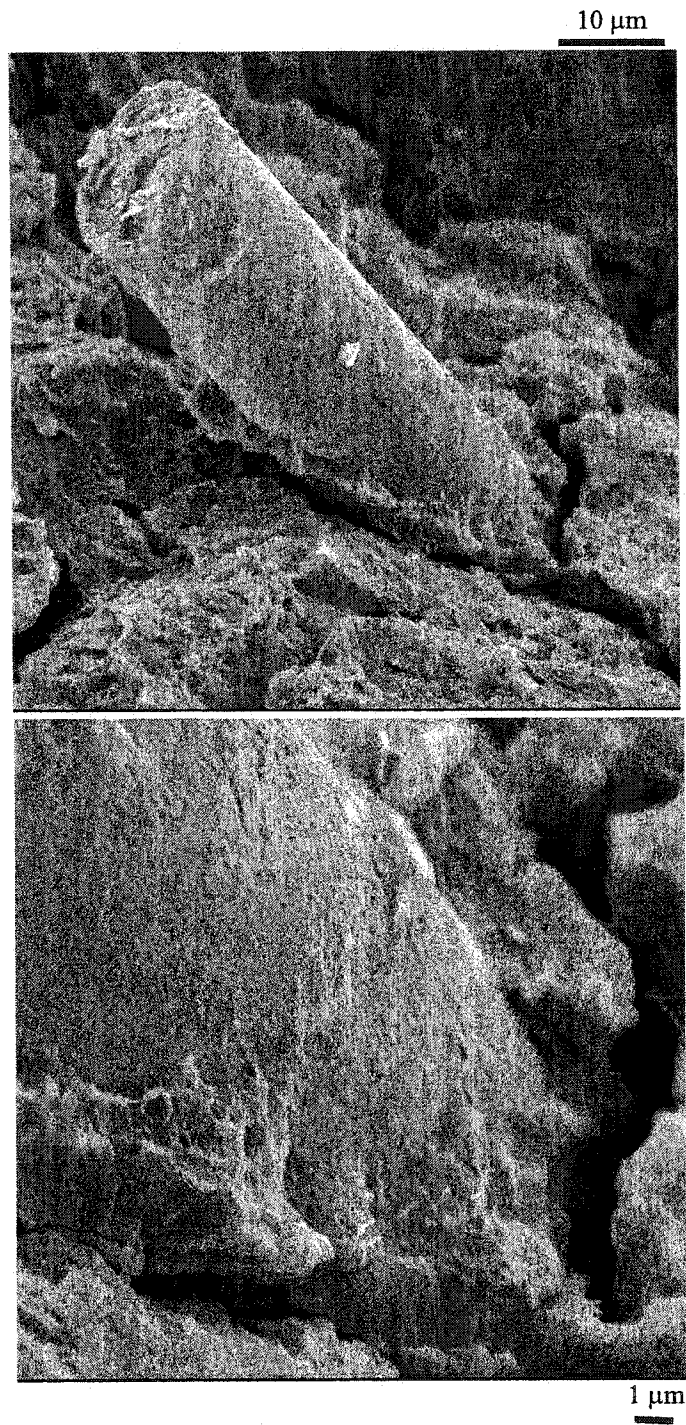


Figure D.2 SEM images of fractured surface for glass-fiber reinforced composite made at 100 °C oil bath temperature (at different magnifications)

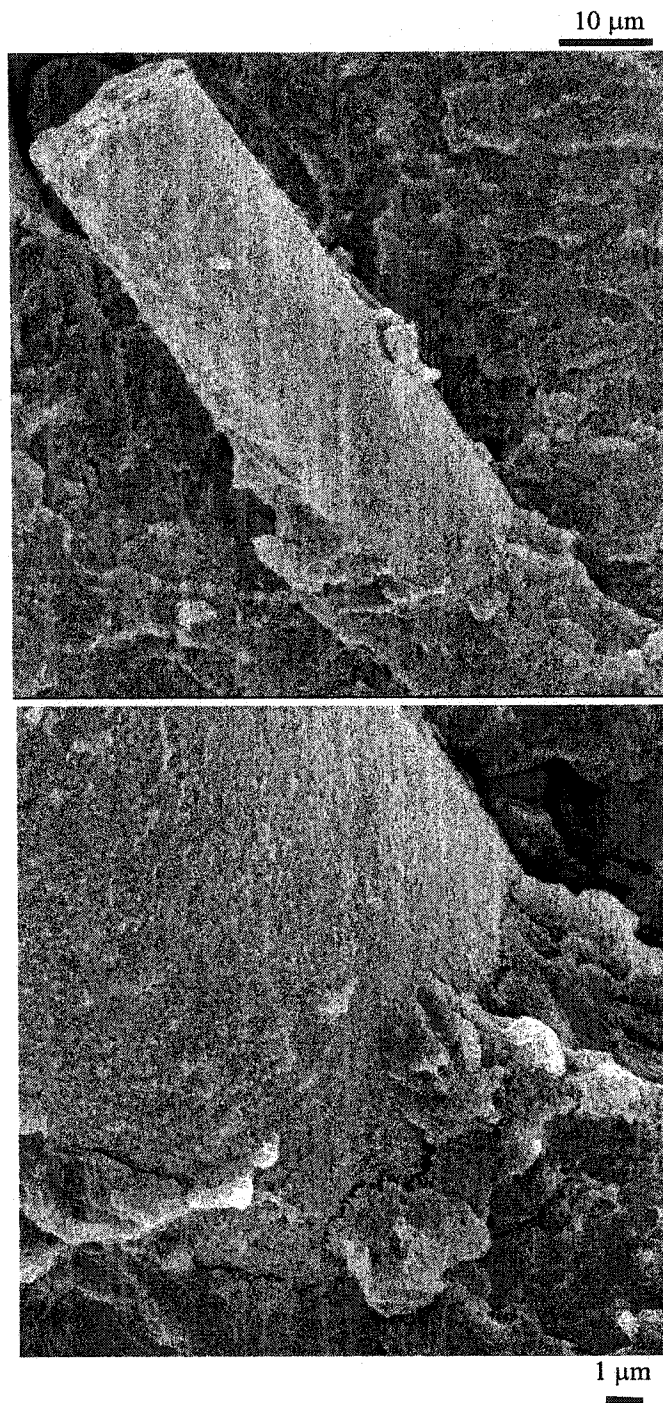


Figure D.3 SEM images of fractured surface for glass-fiber reinforced composite made at 117 °C oil bath temperature (at different magnifications)

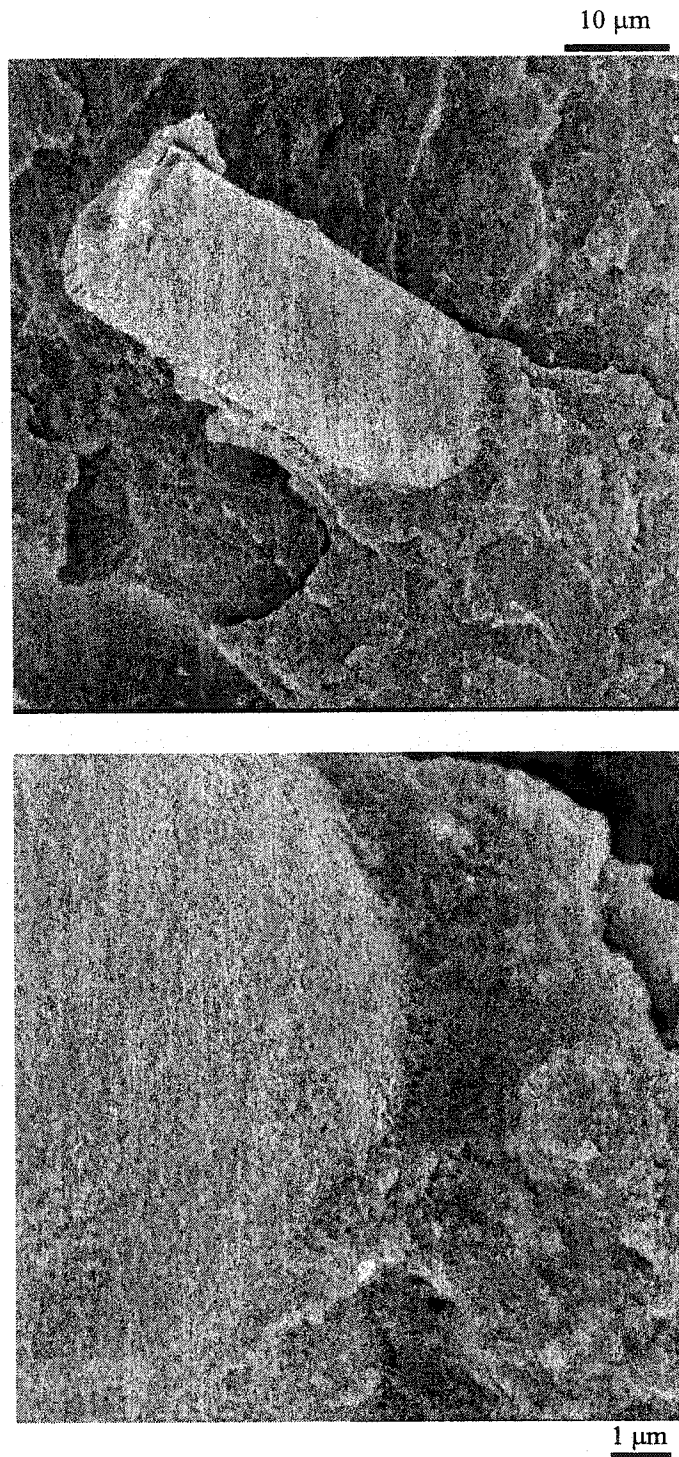
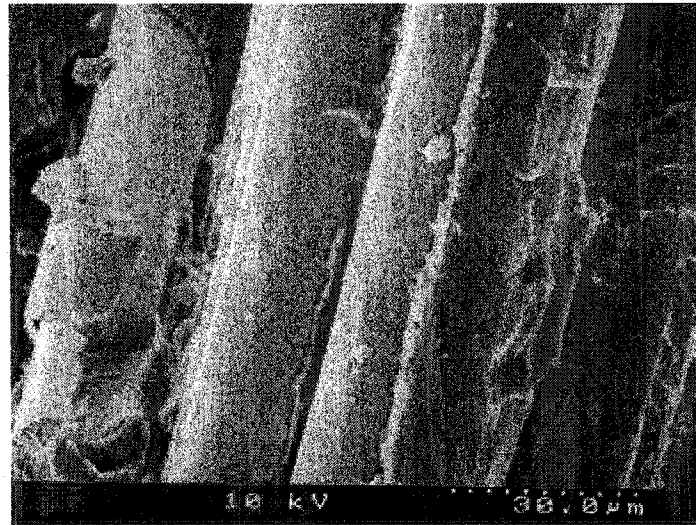


Figure D.4 SEM images of fractured surface for glass-fiber reinforced composite made at 133 °C oil bath temperature (at different magnifications)



(a)



(b)

Figure D.5 SEM images of glass-fiber reinforced composites containing polycarbonate (SPP) at concentration of: (a). 0.1%; (b). 1%. (Both were made at environmental temperature 170°C)